Fakultät für Maschinenwesen
Lehrstuhl für Flugsystemdynamik

Event-based Risk Quantification in Flight Data Analysis

Max Butter

Vollständiger Abdruck der von der Fakultät für Maschinenwesen

der Technischen Universität München

zur Erlangung des akademischen Grades eines

Doktor-Ingenieurs (Dr.-Ing.) genehmigten Dissertation.

Vorsitzender:	Prof. Dr. phil. Klaus Bengler
Prüfer der Dissertation:	1. Prof. Dr.-Ing. Florian Holzapfel
	2. Prof. Dr.-Ing. Manfred Hajek
	3. Prof. Dr.-Ing. Robert Luckner

Die Dissertation wurde am 21.09.2018 bei der Technischen Universität München eingereicht und durch die Fakultät für Maschinenwesen am 16.02.2019 angenommen.

Risk comes from not knowing what you're doing.

Warren Buffett

Danksagung

Die Idee zu der vorliegenden Arbeit entstand im Laufe vieler Jahre meiner Tätigkeit als Pilot und Spezialist für Flugsicherheit. Auslöser war das Forschungsprojekt SAMSYS, das vor knapp einer Dekade ins Leben gerufen wurde und dessen Zielsetzung es war, die Flugsicherheit zu verbessern. Auch wenn diese Dissertation erst begonnen wurde, nachdem das Projekt bereits beendet war, so wurden dennoch die Grundlagen dafür innerhalb der Projektphase geschaffen. Während der Erstellung dieser Arbeit bin ich einigen Menschen begegnet, die mich unterstützt haben oder es überhaupt erst ermöglicht haben, dass ich die Arbeit erstellen konnte, und bei denen ich mich an dieser Stelle besonders bedanken möchte.

An erster Stelle möchte ich mich bei Florian Holzapfel bedanken, der meine Dissertation betreut und begleitet hat. Ich möchte mich darüber hinaus besonders bei Prof. Hajek und Prof. Luckner bedanken, die als Zweit- bzw. Drittprüfer fungiert haben, sowie bei Prof. Bengler, der sich bereit erklärt hat, den Vorsitz zu übernehmen.

Mein besonderer Dank gilt meiner Familie, zuallererst meiner Frau Andrea Rosa, aber auch meinen Söhnen Paul und Oskar, die nicht nur alle Höhen und Tiefen dieser Arbeit miterlebt haben, sondern die vor allem geraume Zeit auf mich verzichten mussten.

Bedanken möchte ich mich auch bei Jürgen Steinberg und Manfred Müller, die das Forschungsprojekt SAMSYS ins Leben gerufen und betreut haben und damit die Grundlage für meine Arbeit geschaffen haben.

Besonders danken möchte ich auch Jochen Mickel, der mich durchgehend zu der Arbeit motiviert hat und mit dem ich über Jahre sehr viele interessante Diskussionen zum Thema Risiko geführt habe.

Ich möchte mich auch bei meiner Kollegin Ariane Winterfeldt bedanken, die sich stets mit großem Engagement bemüht hat, die hohe Qualität der zugrundeliegenden Flugdaten aufrechtzuerhalten.

Ein weiterer Dank gilt meinen Kollegen Alfred Ringlstetter und Heinz Liebminger, die mich fachlich und organisatorisch unterstützt haben.

Auch meinem Vater Ulrich Butter möchte ich danken. Ich habe mit ihm viele interessante Gespräche zu physikalischen Modellen geführt. Zwar nicht fachlich, aber moralisch wurde ich von meiner Mutter Rosmarie Butter unterstützt, bei der ich mich ebenfalls bedanken möchte.

Weiterer Dank gilt Ludwig Drees, Chong Wang, Nadine Gissibl und David Löbl, die ich im Rahmen des Forschungsprojekts kennengelernt habe und die mich entweder fachlich oder organisatorisch bei der Erstellung der Arbeit weitergebracht haben.

Heppenheim, September 2018 Max Butter

Abstract

The requirement to implement a Safety Management System in aviation currently leads to a change from compliance-based regulation towards performance-based regulation. This requires an objective way to evaluate the safety performance. Safety is the absence of risks beyond an acceptable level. Using accident rates is not appropriate due to the low numbers. Hence, the measurement of safety performance nowadays usually relies either on counting precursor events, often without a distinct reference to safety, or on expert judgement, which is rather subjective. This makes it difficult to compare different events or categories and allocate resources effectively to reduce the associated risks.

In this thesis, a comprehensive methodology for the evaluation of a risk level by means of Flight Data Analysis is presented. This methodology enables a quantitative determination of a risk level for potential accident scenarios of each individual flight in hindsight. The methodology is based on two aspects, the aircraft state and the environmental conditions. The aircraft state in conjunction with the environmental conditions may contain a potential safety risk.

While the aircraft state can be derived from the recorded flight data for an individual flight, the environmental conditions have to be derived from a model. A common approach of how to model the environmental conditions is not possible, because of the different nature of potential safety events. The development of such a model is divided into four different categories to cover the whole range of possible risk scenarios.

These categories are based on a physical, a system, a pilot, and a correlation model of the environmental conditions. The physical model is based on the flight dynamical relationship between the aircraft and the environmental conditions, derived from flight data. The system model is a mathematical model of an alert system, based on the requirements specification. The pilot model is based on human interaction under certain conditions, derived from external studies. The correlation model is based on the relationship between flight data and additional sources of information.

Selected examples of typical safety events to prove the above models are landing overrun, pilot induced collision during a Traffic Collision Avoidance System alert, and injury due to turbulence encounter.

For verification of the safety risk determination method, a large number of simulations with randomly distributed environmental conditions is performed. The simulation results show a high degree of coincidence with recorded numbers of real accidents, which have occurred in the past.

The new data-driven methodology is a major contribution to an objective way to evaluate the risk level in aviation.

Übersicht

Die Verpflichtung, ein Sicherheitsmanagementsystem in der Luftfahrt einzuführen, führt derzeit zu einem Wechsel von einer richtlinienbasierten hin zu einer leistungsbasierten Regulierung. Dies erfordert eine objektive Bewertung der Flugsicherheit. Sicherheit ist die Abwesenheit von inakzeptablen Risiken. Die Verwendung von Unfallzahlen ist aufgrund der geringen Anzahl nicht zielführend. Daher beruht die Messung der Sicherheit heute in der Regel entweder auf der Zählung von Vorläuferereignissen, oft ohne eindeutigen Bezug zur Sicherheit, oder auf einem subjektiv geprägten Expertenurteil. Dies macht es schwierig, verschiedene Ereignisse oder Kategorien zu vergleichen und in der Konsequenz Ressourcen gezielt einzusetzen, um die damit verbundenen Risiken zu reduzieren.

In dieser Arbeit wird eine umfassende Methodik zur Bewertung eines Risikoniveaus mittels Flugdatenanalyse vorgestellt. Diese Methodik ermöglicht die quantitative Bestimmung eines Risikoniveaus für verschiedene Unfallszenarien eines einzelnen Fluges in der Nachbetrachtung. Die Methodik basiert auf zwei Aspekten, dem Zustand des Flugzeugs und den Umgebungsbedingungen. Der Zustand des Flugzeugs in Verbindung mit den Umgebungsbedingungen kann ein potentielles Sicherheitsrisiko beinhalten.

Während der Zustand des Flugzeugs aus den aufgezeichneten Flugdaten für einen einzelnen Flug abgeleitet werden kann, müssen die Umgebungsbedingungen aus einem statistischen Modell abgeleitet werden. Ein allgemeingültiger Ansatz zur Modellierung der Umgebungsbedingungen ist aufgrund der Bandbreite möglicher Sicherheitsereignisse nicht möglich. Die Entwicklung eines solchen Modells ist in vier verschiedene Kategorien unterteilt, um die gesamte Bandbreite möglicher Risikoszenarien abzudecken.

Diese Kategorien basieren auf einem physikalischen Modell, einem Systemmodell, einem Pilotenmodell und einem Korrelationsmodell der Umgebungsbedingungen. Das physikalische Modell basiert auf der flugdynamischen Beziehung zwischen dem Flugzeug und den Umgebungsbedingungen, abgeleitet aus Flugdaten. Das Systemmodell ist ein mathematisches Modell eines technischen Sicherheitssystems, das dazu entwickelt wurde, einen Unfall in letzter Instanz zu verhindern. Das Pilotenmodell basiert auf menschlicher Interaktion unter bestimmten Bedingungen, abgeleitet aus internen oder externen Studien. Das Korrelationsmodell basiert auf der Beziehung zwischen Flugdaten und zusätzlichen Informationsquellen.

Ausgewählte Beispiele für typische Sicherheitsereignisse, die die oben genannten Modelle belegen, sind das Überschießen der Landebahn, vom Piloten verursachte Kollisionen während einer Warnung des Kollisionswarnsystems TCAS und Verletzungen aufgrund von Turbulenzen.

Zur Überprüfung der vorgestellten Methode wird eine Vielzahl von Simulationen von verschiedenen Zuständen des Flugzeugs und den Umgebungsbedingungen durchgeführt. Die

Simulationsergebnisse resultieren in einer hohen Übereinstimmung mit tatsächlichen Unfallzahlen.

Die neue datengetriebene Methodik kann somit als wichtiger Beitrag zu einer objektiven Risikobewertung in der Luftfahrt gesehen werden.

Content

List of Figures

List of Tables

Abbreviations

AB	Autobrake
ABV	Above
ACAS	Airborne Collision Avoidance System
ACI	Airports Council International
ADC	Air Data Computer
ALIM	Altitude Limit
ALoS	Acceptable Level of Safety
ALT	Altitude
AMC	Acceptable Means of Compliance
APP	Approach
ARMS	Aviation Risk Management Solutions
ALARP	As Low as Reasonably Possible
ARINC	Aeronautical Radio Incorporated
ASR	Air Safety Report
ATC	Air Traffic Control
AVBL	Available
BADA	Base of Aircraft Data
BFU	Bundesstelle für Flugunfalluntersuchung
BLW	Below
BPD	Brake Pedal Deflection
CANSO	Civil Air Navigation Services Organization
CAS	Collision Avoidance System
CDF	Cumulative Probability Distribution Function
CFIT	Controlled Flight into Terrain
CFM	Joint venture of General Electric and Snecma, Manufacturer of CFM56 Engine
CFTT	Controlled Flight Towards Terrain
CLR	Clear
CPA	Closest Point of Approach
CSR	Confidential Safety Report
DEN	IATA code of Denver Airport
DFDR	Digital Flight Data Recorder
DFL	Dataframe Layout
DHL	DHL International GmbH
DMOD	Distance Modification
EAFDM	European Authorities Coordination group on Flight Data Monitoring
EASA	European Aviation Safety Agency
EASp	European Aviation Safety Plan 2014-2017

EC	European Commission
ECAST	Safety Management System and Safety Culture Working Group, Component of European Strategic Safety Initiative (ESSI)
ED	Executive Director
EFIS	Electronic flight instrument system
EMS	Event Measurement System
ENV	Environmental Factor
ESC	Event Severity Classification
ERC	Event Risk Classification
ERCS	European Risk Classification Scheme
ESRA	European Safety and Reliability Association
ESREL	European Safety and Reliability Conference
EU	European Union
EUROCONTROL	European organization for the safety of air navigation
FAA	Federal Aviation Administration
FDA	Flight Data Analysis
FDAP	Flight Data Analysis Program
FDAU	Flight Data Acquisition Device
FDM	Flight Data Monitoring
FDMP	Flight Data Monitoring Program
FDR	Flight Data Recorder
FH	Flight Hours
FL	Flight Level
FODA	Flight Operations Data Analysis
FOQA	Flight Operations Quality Assurance
FRA	IATA code of Frankfurt Rhein Main airport
FSF	Flight Safety Foundation
FT	Feet
GE	General Electric
GEV	Generalized Extreme Value Distribution
GM	Guidance Material
GPWS	Ground Proximity Warning System
GS	Ground Speed
HMD	Horizontal Miss Distance
HUM	Human Factor
IAE	International Aero Engines
IATA	International Air Transport Association
ICAO	International Civil Aviation Organization
IFALPA	International Federation of Air Line Pilots' Associations
IFR	Instrument Flight Rules

IR-OPS	Implementing Rules - Operations
ISSG	Industry Safety Strategy Group
LAX	IATA Code of Los Angeles International Airport
LOC-I	Loss of Control Inflight
MAC	Midair Collision
MDF	Miss Distance Filter
METAR	Meteorological Aerodrome Report
MHz	Megahertz
MIT	Massachusetts Institute of Technology
MITRE	U.S. non-profit company, emerged from Massachusetts Institute of Technology
MOTNE	Meteorological Operational Telecommunications Network Europe
MQAR	Mini-QAR
N1	Engine Speed of the Fan
NASA	National Aeronautics and Space Administration
ND	Navigation Display
NLR	Nationaal Lucht- en Ruimtevaartlaboratorium, National Aerospace Laboratory of Netherlands
NM	Nautical Miles
NMAC	Near Midair Collision
NTSB	National Transportation Safety Board
OQAR	Optical Quick Access Recorder
ORG	Organizational Factor
ORO	Organisation Requirements for Air Operations
PC	Personal Computer
PCMCIA	Personal Computer Memory Card International Association
PFD	Primary Flight Display
POT	Peak Over Threshold Method
PQAR	Personal Computer Memory Card International Association Quick Access Recorder
QAR	Quick Access Recorder
RA	Resolution Advisory
RAC	Resolution Advisory Complement
RMS	Root Mean Square
ROPS	Runway Overrun Protection System
RPM	Revolutions Per Minute
RPTG	Reporting
RTCA	Radio Technical Commission for Aeronautics
RU	Risk Unit
RWY	Runway

SA	Safety Assurance
SARPs	Standards and Recommended Practices
SD	Standard Deviation
SFO	IATA code of San Francisco Airport
SL	Sensitivity Level
SMM	ICAO Safety Management Manual / Doc 9859
SMS	Safety Management System
SOP	Standard Operating Procedure
SPI	Safety Performance Indicator
SRB	Safety Review Board
SRM	Safety Risk Management
SSFDR	Solid State Flight Data Recorder
SSP	State Safety Program
STBY	Standby
STCA	Short Term Conflict Alert
TA	Traffic Advisory
TAS	True Airspeed
TAU	Horizontal time threshold
TCAS	Traffic Collision and Avoidance System
TDZ	Touchdown Zone
TEC	Technical Factor
TOPA	TCAS Operational Performance Assessment
TVTHR	Vertical Time Threshold
UAS	Undesired Aircraft State
U.S.	United States
USD	US Dollars
VFR	Visual Flight Rules
VKO	IATA airport code for Moscow Vnukovo Airport
VMD	Vertical Miss Distance
VOR	Very High Frequency Omni Directional Radio Range
VRC	Vertical Resolution Complement
VSI	Vertical Speed Indicator
WPS	Words per Second
WQAR	Wireless Quick Access Recorder
XPDR	Transponder
XPNDR	Transponder
ZTHR	Altitude Threshold

Nomenclature

Chapter 2

Latin Small Letters		
Symbol	**Explanation**	**Units**
r_{Ev}	Data acquisition rate	-

Chapter 5

Greek Letters		
Symbol	**Explanation**	**Units**
γ	Runway slope	deg
μ	Friction coefficient	-
μ	Mean value	-
μ	Location parameter (distribution parameter)	-
μ_a	Available friction coefficient	-
$\mu_{nx,diff}$	Mean value of the difference between measured deceleration and calculated deceleration $n_{x,diff}$	-
μ_r	Required friction coefficient	-
μ_{r_max}	Maximum required friction coefficient during landing	-
μ_{roll}	Rolling resistance coefficient	-
μ_{thr}	Friction coefficient at threshold thr	-
ρ	Air density	kg/m^3
θ	Deflection angle of reverse thrust	deg
σ	Standard deviation	-
σ	Scale parameter (distribution parameter)	-
$\sigma_{nx,diff}$	Standard deviation of the difference between measured deceleration and calculated deceleration $n_{x,diff}$	-

Latin Capital Letters		
Symbol	**Explanation**	**Units**
C_D	Drag coefficient	-
C_L	Lift coefficient	-
C_R	Runway condition	-
D	Aerodynamic drag	N
F_1	Thrust force of hot engine section	N
F_2	Thrust force of engine fan section	N

$F(x)$	Cumulative probability at x	-
L	Aerodynamic lift	N
N_{55}	Number of measurements within a brake pedal deflection-interval between 52.5 degrees and 57.5 degrees	-
N_{65}	Number of measurements within a brake pedal deflection-interval between 62.5 degrees and 67.5 degrees	-
N_O	Number of runway overruns, evaluated by Monte Carlo method	-
N_R	Number of landings used to evaluate the distribution of μ_{r_max}	-
N_{R0}	Number of landings where μ_{r_max} is greater than 0	-
R	Remaining runway distance from actual position to the physical runway end	m
S	Reference wing area	m^2
V_A	Aerodynamic speed (calibrated airspeed)	m/s
V_G	Ground speed	m/s
V_W	Longitudinal wind component	m/s
X	Engine reverse thrust	N

Latin Small Letters		
Symbol	**Explanation**	**Units**
a	Scale parameter (distribution)	-
b	Shape parameter (distribution)	-
d_a	Available deceleration	m/s^2
d_r	Equivalent constant deceleration required to stop the aircraft at the runway end	m/s^2
d_{r_max}	Maximum value of d_r during landing	m/s^2
g	Constant of gravity	m/s^2
k	Shape parameter (distribution parameter)	-
m	Aircraft mass	kg
$n_{x,data}$	Measured longitudinal load factor	-
$n_{x,diff}$	Difference between measured longitudinal load factor $n_{x,data}$ and calculated longitudinal load factor $n_{x,calc}$	-
$n_{x,diff95}$	95% of the absolute values of the difference between measured longitudinal load factor $n_{x,data}$ and calculated longitudinal load factor $n_{x,calc}$ are equal or lower than $n_{x,diff95}$	-
$n_{x,calc}$	Calculated (simulated) longitudinal load factor	-
p	Probability	-
p_{thr}	Proportion of friction values used for the Peak Over Threshold method	-
r	Random number	-
t	Time	s

t_b	Point in time at begin of braking	s

Chapter 6

Greek Letters		
Symbol	**Explanation**	**Units**
Δ_t^i	Target vertical rate (advised rate) for the own aircraft i, calculated at time t	feet/min
$\Delta_t^i(down)$	Target vertical rate for the projected down-sense for the own aircraft i, calculated at time t	feet/min
$\Delta_t^i(up)$	Target vertical rate for the projected up-sense for the own aircraft i, calculated at time t	feet/min
$\tau_{h,RA}$	Horizontal alert threshold, also called *TAU*	s
$\tau_{h,t}^{ik}$	Time to Closest Point of Approach (CPA), *tau*	s
$\tau_{h\_mod,t}^{ik}$	Modified Time to Closest Point of Approach (CPA), *modified tau*	s
$\tau_{PositiveRA}$	Duration of the current Positive RA	s
τ_{RA}^i	Actual alert threshold of the own aircraft i	s
$\tau_{z,RA}^i$	Vertical alert threshold for the own aircraft i	s
$\tau_{z,t}^{ik}$	Time until the own aircraft i and the intruder aircraft k are at the same altitude, calculated at time t, *vertical tau*	s

Latin Capital Letters		
Symbol	**Explanation**	**Units**
A_c	Required altitude separation	feet
A_{mod}	Modification of the intended separation at the Closest Point of Approach (CPA) for a Vertical Speed Limit	feet
CV	Coefficient of Variation	-
CV_{req}	Required Coefficient of Variation	-
N_i	Expected number of midair collisions induced by TCAS	-
N_0	Expected number of midair collisions without TCAS	-
N_u	Expected number of midair collisions, which cannot be resolved by TCAS	-
$NMAC_h$	Horizontal Near Midair Collision	-
P	Vector of pilot responses used for the Monte Carlo method	-
R_{TCAS}	Risk ratio of TCAS	-
T	TCAS RA type, see Table 6-4	-
T_t^i	TCAS RA type of the own aircraft i at time t	-
$T_{m,t}^i$	Modified TCAS RA type of the own aircraft i at time t	-

T^u	Observed TCAS RA type of the own aircraft i at the start of the Flight Data Analysis event	-
V	Vector of vertical rates used for the Monte Carlo method	feet/min
X	Vector of altitudes used for the Monte Carlo method	feet

Latin Small Letters		
Symbol	**Explanation**	**Units**
a^i	Projected up-sense separation at the Closest Point of Approach (CPA), calculated by the own aircraft i	feet
a_s	Additional load factor of trajectory change used for the pilot model	g
b^i	Projected down-sense separation at the Closest Point of Approach (CPA), calculated by the own aircraft i	feet
c_t^i	Crossing flag for the own aircraft i, calculated at time t	-
c_{thr}	Crossing threshold	feet
d_s	Delay used for the pilot model	s
i	Own aircraft	-
k	Intruder aircraft	-
m^i	Flag indicating the TCAS equipment status of the own aircraft i and whether the Mode S address is lower than that of the intruder aircraft	-
mod^i	Flag whether any modification has been conducted for aircraft i	-
n_{NMAC}	Number of vertical Near Midair Collisions (NMACs) during a Monte Carlo method	-
n_{req}	Number of required simulations for a Monte Carlo method	-
n_S	Number of simulations during a Monte Carlo method	-
p	Probability	-
$p_{NMAC,z}$	Probability of a Near Midair Collision (NMAC), only vertical component	-
$\hat{p}_{NMAC,z}$	Estimated probability of a Near Midair Collision (NMAC), only vertical component	-
q_t^i	Flag whether the vertical separation at the Closest Point of Approach (CPA) is sufficient, calculated for the own aircraft i at time t	-
r	Random number	-
rev^i	Flag whether a reversal RA is active for aircraft i	-
s_t^i	Selected sense of the own aircraft i at time t	-
t	Time	s
t_c	Time of assumed change in vertical rate until target rate is achieved	s
t_d	Time of delay until assumed reaction	s
t_s	Time of assumed maneuver with target rate established	s

u_t^i	Intent message of the own aircraft i at time t	-
$v_{h,t}^{ik}$	Relative horizontal velocity between the own aircraft i and the intruder aircraft k at time t	NM/s
v_{s_m}	Target vertical rate during a "Maintain Vertical Speed"-RA	feet/min
v_{s_n}	Target vertical rate during a Negative Corrective RA	feet/min
v_{s_p}	Assumed vertical rate according to the distribution of the pilot model	feet/min
$v_{z,0}$	Vertical rate at the start of the TCAS RA	feet/min
$v_{z,t}^i$	Vertical rate of the own aircraft i at time t	feet/min
$v_{z,t}^{ik}$	Relative vertical rate between the own aircraft i and the intruder aircraft k at time t	feet/min
$x_{z,t}^{ik}$	Relative altitude between the own aircraft i and the intruder aircraft k at time t	feet
$x_{h,t}^{ik}$	Horizontal distance between the own aircraft i and the intruder aircraft k at time t	NM
$x_{z,t}^i$	Altitude of the own aircraft i at time t	feet
$x_{z,t+LO}^i$	Altitude of the own aircraft i, which would be achieved with a level off, using an assumed standard reaction, calculated at time t	feet
$x_{z,t}^{ik}$	Altitude difference between aircraft i and aircraft k at time t	feet

Chapter 7

Greek Letters		
Symbol	**Explanation**	**Units**
μ	Location parameter (distribution parameter)	-
σ	Scale parameter (distribution parameter)	-

Latin Capital Letters		
Symbol	**Explanation**	**Units**
R	Coefficient of determination	-

Latin Small Letters		
Symbol	**Explanation**	**Units**
n_z	Load factor	-
k	Shape parameter (distribution parameter)	-
$n_{z,diff}$	Maximum difference between the maximum and minimum load factor within a sliding window	-
$n_{z,dmax}$	Turbulence level, maximum value of $n_{z,diff}$ during the whole flight	-

p	Probability	-
t	Time	s
t_{a0}	Timepoint 60 seconds after the aircraft gets airborne	s
t_{a1}	Timepoint 60 seconds prior to the last touchdown of the aircraft	s

1 Introduction

1.1 Background and Motivation

The hull loss rate in civil aviation has significantly been reduced during the recent decades even though the air traffic has continuously increased [1]. The transition from a fragile system towards an ultra-safe system in terms of accident probability was achieved through several eras with a different focus on safety, as shown in Figure 1-1.

In the beginning of the increasingly widespread commercial aviation, the handling of accidents started in a solely reactive way by learning the lessons from accident investigations. Safety deficiencies have mainly been related to technical factors and technological failures. An improvement in technology led to a gradual decline in the accident rate in this era [2].

A notable enhancement in safety could be achieved since the 1970s by major technological advances and enhancements in safety regulations. The aviation system slowly shifted towards a safe system by focussing on human factor issues. Human error had been identified as a major factor in aviation accidents, however, at this time focussing mainly on the individual without considering the operational and organizational context. Incidents, which are precursors of an accident, have been taken into consideration. The investigation of incidents as a proactive tool was evolving as a new method for further safety enhancement [2].

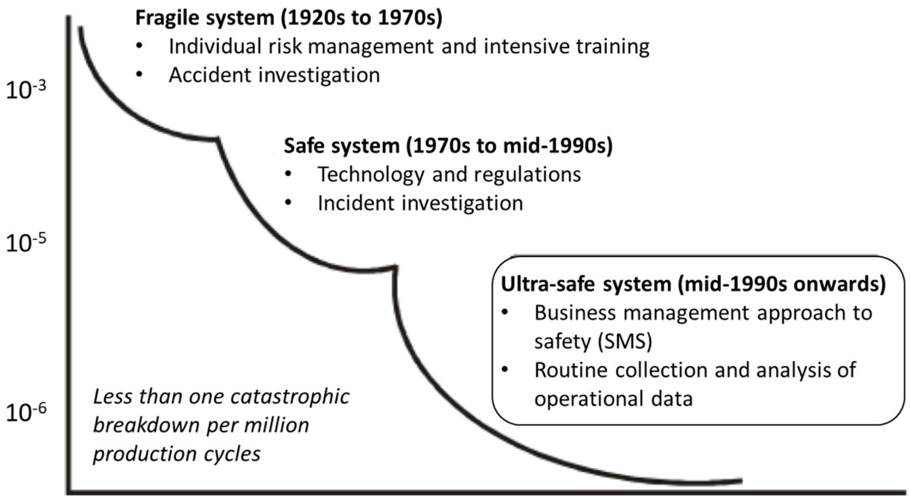

Source: René Amalberti

Figure 1-1 Evolution of ultra-safe systems, as cited in [3]

Starting from the mid-1990s, it became more and more evident that human behaviour is strongly influenced by the environment in which the individual is operating. Following this perception, the step forward towards an ultra-safe system, lowering the accident rate to a value below one accident per million flights, became possible by viewing safety from a systemic perspective. This was achieved by also encompassing organizational factors, which have a large influence in human behaviour [2]. However, focusing on organizational factors is only possible if all organizations, which are involved in the air transport system, become an integral part of safety management.

While the trend of fatal accidents outside the scope of the European Aviation Safety Agency (EASA) is still decreasing, the rate of fatal accidents within the EASA member states has remained nearly constant at a very low level for the last decade [4], see Figure 1-2. In fact, for this region a certain stagnation in the number of fatal accidents can be observed. Since the European Commission aims for an accident rate of less than one accident per ten million commercial flights until the year 2050 [5], in combination with an expected further growth in commercial air traffic, adequate means have to be implemented to further reduce the number of accidents.

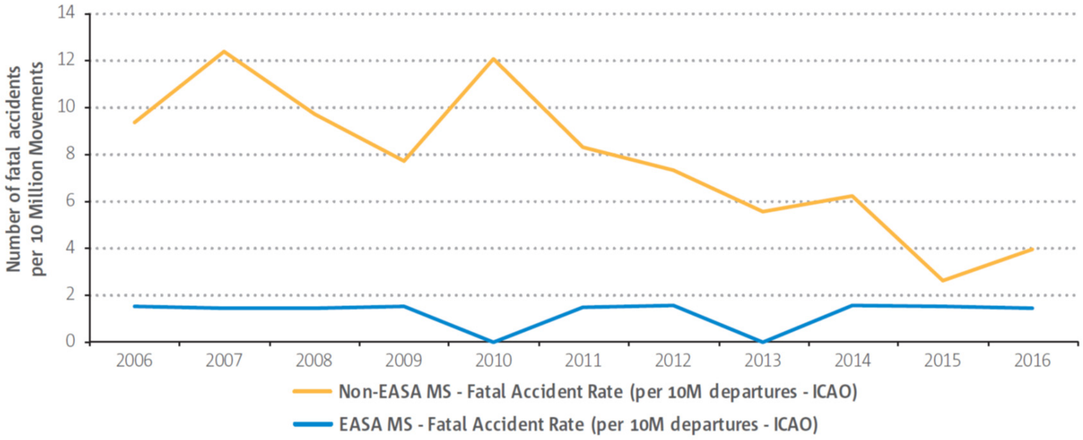

Figure 1-2 Airline fatal accident rate for EASA member states and non-EASA member states, from 2006 to 2016 [4]

The air traffic system reached a point, where more regulation would not have further improved the overall safety level [6]. The complexity of the air traffic system was at a level, at which more regulations might even have had an adverse effect on safety, since newly implemented rules might be contradictory to already existing ones [7]. Other means to improve safety had to be implemented.

At this point, the International Civil Aviation Organization (ICAO) launched the concept of a Safety Management System (SMS) in aviation [8], adapted from other high-risk industry branches[1], where certain experience with these systems had already been gained. A Safety Management System is a structured approach to manage safety within an organization [2]. Even though the elimination of accidents is the highest goal, ICAO, accepting the fact that the aviation system will never be completely free of risks, suggested that safety should be managed towards an acceptable level of risk. This becomes possible by the identification of unacceptable risks and the management of those risks towards an acceptable level by means of adequate risk controls. Within the scope of the EASA, a Safety Management System is mandatory for all airlines since the year 2012 [9].

A Safety Management System shifts responsibility towards the organizations by managing their risks on their own, instead of a solely regulatory approach. The affected organizations include airlines, air traffic control units, airport authorities, training organizations, and maintenance organizations. This means a transition from the traditional compliance-based prescriptive scheme towards a performance-based approach, where safety responsibilities are partly transferred from the authorities more towards the companies. The companies have to find a way how to achieve the required safety performance standards. It should be noted that there are no common requirements of how to achieve the safety performance standards, which fit the needs for all organizations [10].

In the context of a Safety Management System, where the management of safety is a key element, the old wisdom, that *"you can't manage what you don't measure"*, becomes particularly important. Since accidents in aviation are rare, accident statistics are not adequate to measure the safety. Sources for safety performance measurement are the data received by the operations, e.g. reports or flight data. It is a challenge to transform this operational data, which might be incomplete and biased, into a quantified risk picture, reflecting the safety performance of the organization in an objective way [10].

1.2 Related Work

ICAO proposes to measure the safety performance by the use of incident or safety event rates, which are considered as precursors of accidents [2]. According to the Safety Management Manual/Doc 9859 of ICAO, for the initial setup the mean value of the respective rate is taken as a reference, and any deviation above a certain threshold, e.g. one or two standard deviations above the mean value, is used as an alarm threshold. The goal is to reduce the rate over time by a certain amount. This approach consists of a simple count of events in relation to the number of flights, without considering the content of the event [10]. An example given by ICAO is the

[1] A Safety Management System had already been implemented in the nuclear-, chemical- and the oil-industry at that time

voluntary hazard report rate, where the number of reports is focused on, rather than the content of the respective report [2].

Since the focus in this thesis is on risk evaluation based on Flight Data Analysis (FDA), it is important to describe the state-of-the-art of safety performance measurement by means of flight data. The European Authorities coordination group on Flight Data Monitoring[2] (EAFDM), a voluntary partnership between EASA and the National Aviation Authorities of EASA member states, published a set of "standardized FDM-based indicators" based on Flight Data Analysis [11]. These indicators are more specific than the examples given by ICAO, and they refer to the operational safety issues, which have been identified in the European Aviation Safety Plan (EASp) 2012-2015 [12], e.g. runway excursions or midair collisions. The intention of those indicators is to provide relevant indicators for common operational risks, and support operators to detect potentially unsafe situations and assess their severity.

Safety events of the same type are differentiated in terms of severity, depending on the exceedance of the respective parameters. Even though this method enables a certain comparison of the severity between events of the same type, no quantification about how close the event was to an accident, nor a comparison of events of different types is possible, since no common risk classification is used.

The traditional approach to Flight Data Analysis uses non-compliance with flight manual limits and deviations from Standard Operating Procedures (SOPs) or good airmanship to generate a safety event [13]. In many cases there is no clear distinction between non-compliance and risk. Even though, non-compliance may contain a certain risk level, it still depends on additional factors which might not be taken into consideration. E.g. an unstable approach event indicates non-compliance to SOPs, but the actual risk with respect to a potential runway excursion especially depends - besides the energy situation of the aircraft - on the runway length and the runway condition. However, the latter conditions are usually not taken into account [14]. Sometimes the thresholds of the non-compliance event do not even match the respective operator's SOPs, since the event algorithms have been generically developed by the FDA software manufacturer to fit the needs of an average airline [15].

A method, which focuses on the risk of an event rather than just counting the number of events, was developed by the Aviation Risk Management Solutions (ARMS) working group[3] [16]. Since this method is based on a common risk metric, independent from the type of event, a

[2] Flight Data Analysis is sometimes referred to as Flight Data Monitoring (FDM)

[3] The ARMS working group was set up to develop a new and better methodology for Operational Risk Assessment. The primary target group for the methodology is airlines. The industry working group consisted mainly of safety practitioners from airlines [16].

comparison between the different risks of events becomes possible. This enables the measurement of safety instead of counting the number of events, whose relationship to safety is difficult to estimate.

The ARMS method is solely based on expert estimation. In simple terms, the expert estimates how many barriers had still been in place to prevent an accident scenario, i.e. how close the event was to an accident. For the first time, it became possible to compare the risk levels of different events and prioritize the safety work, i.e. to manage safety.

Nisula described the event risk classification based on the ARMS method in the context of the requirements of safety performance measurement [10]. The ARMS method is primarily aimed for the risk assessment of safety reports, i.e. single events. The evaluation of the overall risk of an occurrence category, which results from the sum of all events within this category, is difficult, since the number of unreported events is usually unknown [7].

Mickel adapted the ARMS method for the use with Flight Data Analysis, where the number of non-recorded flights is known [7]. Therefore, an evaluation of the overall risk level becomes possible. In combination with a refined risk metric, this adapted method enables the generation of measurable trends of safety performance and to identify safety issues. Since the risk level of each FDA event has to be estimated by a safety expert, not all events can be processed due to limited human resources. The focus of the safety work has to remain on events with higher risk levels, based on a preliminary evaluation of exceedances. Thus, the portion of the overall risk, which cannot be covered by this method, is still unknown [17].

Van Es et al. developed a landing overrun risk index, which is based on risk ratios rather than absolute risk. Risk ratios indicate the factor by which the risk increases under defined circumstances in comparison to a reference condition, where all risk factors are absent [14]. Selected risk factors for landing overrun have been evaluated in a study of runway overruns, conducted by the NLR Air Transport Safety Institute a few years earlier [18]. In this study, factors like excessive approach speed, significant tailwind, high on threshold, long landing or wet/flooded runway as well as non-precision approaches have been identified as factors, which increase the risk of an overrun. Besides the identification of those risk factors, a quantification in terms of risk ratio has been conducted in this study, e.g. a long landing increases the risk of a landing overrun by a factor of 55. To avoid double counting of risk factors, correlations between the respective risk factors had to be eliminated, e.g. a non-precision approach increases the probability that an approach is high on threshold. Since a landing overrun correlates especially with the runway length, this factor had to be incorporated, which has not been considered in the previous study. A certain limitation regarding the quantification of data results from the fact that the decision, whether or not a certain risk factor is considered, is based on discrete trigger thresholds. Therefore, either the respective risk factor is incorporated in the risk index or rejected.

The landing overrun risk index results in a relative risk, which is based on the reference landing without all risk factors. Since the risk of such a reference landing itself cannot be quantified, only relative risk levels are used. Moreover, since the index is not based on a common risk metric, the results cannot be compared with other accident categories.

A data-driven method to evaluate the probability of an accident was recently developed by Drees [19]. This method is based on a physical model of a runway overrun scenario. Several key aspects related to the landing phase are parametrized and correlated with each other, e.g. headwind, flare distance, begin of braking or approach speed deviation. This parametrized model enables the simulation of a 'typical' landing, derived by real flight data, which might not even contain any overrun, and thus, enables the evaluation of the probability of a landing overrun. The method also allows the variation of certain parameters and therefore, enables a prediction of the effects of these variations on the accident probability. Also, failures of technical equipment of the aircraft during landing can be incorporated in the simulation and therefore be quantified. Other scenarios have also been taken into consideration with this method, e.g. tail strike and hard landing during flare [20,21].

Mickel also developed a data-driven method to evaluate the risk of a landing overrun for wet runways [7]. While the probability for this scenario was derived from flight data of a major European airline, the severity was estimated from external accident statistics. The method is based on the parametrization of a "*normalized use of runway*", which is the relationship between the actually used runway length and a reference landing distance provided by the aircraft manufacturer [22]. The evaluated risk in this method depends on the buffer, which is defined as the runway portion, which is available beyond the reference, i.e. an additional safety margin in terms of landing distance. Since this method is based on an average landing depending on the buffer value, individual landings cannot be assessed and thus, risk outliers cannot immediately be identified.

Both data-driven methods, developed by Drees and Mickel, require the analysis of a set of flights. They are not capable of assessing the risk of a single safety event. This makes it difficult to measure the actual safety performance on a daily basis, and thus, to either identify safety issues affecting the current operation, or to create a safety trend, which indicates variations in the safety performance of an organization.

1.3 Mission Statement

It is therefore desirable to develop a method, which combines the evaluation of the risk level of an individual safety event with a data-driven approach based on a common risk metric. The main objective of this dissertation is to present a methodology, which

- □ enables the quantification of the risk of a safety event, gathered from (accident-free) flight data.
- □ also covers safety events with low risk, but high frequency of occurrence, which could not be reviewed and assessed by a safety expert due to the excessive number of events in combination with limited human resources, thereby also enables the estimation of those portions of the overall risk, which are not covered by expert estimation.
- □ enables a comparison between the risk levels derived by expert estimation, and an objective way to measure the event risk.
- □ identifies the risk proportion in a safety event due to non-compliance, e.g. the risk of a non-stabilized approach with regard to a certain accident scenario.
- □ describes a complex risk in the context of a single safety event.
- □ enables the evaluation of a safety trend on a daily basis.
- □ measures the safety performance of an organization.

1.4 Contributions of the Dissertation

This dissertation goes beyond the state-of-the-art in risk assessment for airlines in the following aspects:

- □ **A novel approach to quantify the risk level for defined accident scenarios of an individual flight by means of Flight Data Analysis.** The main contribution of this dissertation is the possibility to objectively assess individual risks of a single flight**.** The novelty of the presented method assumes that the **interaction between the aircraft state and the environmental conditions may contain a potential safety risk**. The aircraft state is usually controlled by the flight crew within the regulatory framework and can be derived from the recorded flight data for each point of each individual flight. The environmental conditions are more difficult to describe. Since usually not all necessary information is available, these conditions have to be derived from a statistical model. The point where the aircraft state interacts with the environmental conditions eventually defines the risk. The schematic of this novel approach can be seen in Figure 1-3.

- **Within the scope of this dissertation, a set of four different statistical models of the environmental conditions has been determined to cover the whole spectrum of risk scenarios in Flight Data Analysis:** The way how to model the environmental conditions is mainly based on the available data. The quality of the model of the environmental conditions, and thus the quality of risk evaluation, highly depends on the depth and the quality of this data. Depending on the considered risk scenario, the sources of data, which contribute to the model, may significantly vary. A common approach of how to model the environmental conditions is therefore not possible. Thus, depending on the missing data and the source, from which this missing data can be obtained, different approaches have been evaluated to develop the model of the environmental conditions:
    - If the environmental conditions can be completely derived from the flight data of a set of previous flights, a ***physical model*** of the environmental conditions can be developed by means of internal flight data.
    - If the relationship between the aircraft state and the environmental conditions is defined by the trigger threshold of an alert system, the environmental conditions can be estimated by a ***system model*** of the alert system.
    - If the environmental conditions are influenced by the behavior of (other) humans, who interact with a system, a ***pilot model*** is required to reflect this behavior. The necessary data for this model can be gathered either by internal or external studies or data analyses, respectively.
    - If the environmental conditions can only be explained by using additional data, which is not contained in the internal flight data, a ***correlation model*** between the flight data and additional sources, e.g. investigation data or reports, can be used for the evaluation of the model.

The focus of the presented risk model is on human factors and organizational factors. The reason for this is that safety management within an organization is basically limited to these factors. Technical factors are not explicitly taken into account by this risk model.

To verify the new method, three examples of accident categories have been selected, which are highly relevant to flight safety. The whole range of environmental condition models as described above are covered by these examples.

The first two examples are runway overrun during landing and risk of midair collision, which are an integral part of the European Aviation Safety Plan (EASp) 2012-2015 [12]. The third example is injury due to turbulence, which has been addressed in several Safety Reports by the International Air Transport Association (IATA) [23–25].

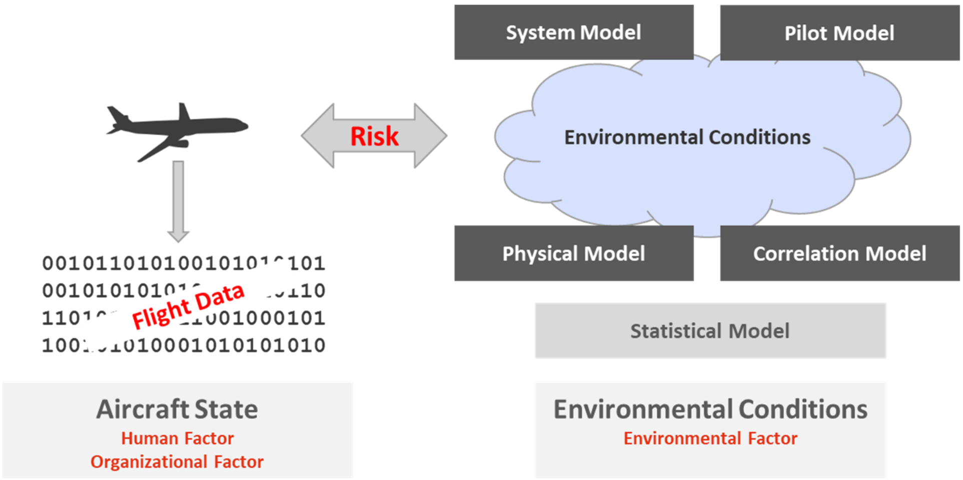

Figure 1-3 Schematic of the new approach for risk quantification: The interaction between aircraft state and environmental conditions results in a risk. While the aircraft state can be derived from flight data, the environmental conditions have to be modeled by means of a statistical model

Each of these examples contain further contributions beyond the state-of-the-art in risk management:

- □ **The risk of landing overrun is determined by a comparison between the required friction and the available friction during landing.** This novel approach enables the determination the risk of a landing overrun for each individual flight, based on a *physical model*. A flight dynamics model of the aircraft is developed to determine the minimum runway friction, which is required to stop the aircraft right at the end of the runway. This required runway friction is based on the aircraft state, i.e. velocity and remaining runway length, at the most critical point during landing for each individual flight. The environmental conditions are described by the available runway friction. They can be modelled statistically by the analysis of a large number of previous flights, from which the distribution of the available friction coefficients is derived by means of a flight dynamics model. The risk level can then be determined from the probability that the available friction is less than required.

- □ **Two novel methods have been developed and applied to determine the available friction during landing:** Even though all necessary information for the evaluation of the environmental conditions is contained in the flight data, the available friction cannot directly be measured. The available friction can only be derived from those parts of the flight data, where full brake demand was used, which is also not indicated in the data.

Only a small portion of all landings in fact allow for a measurement of the available friction. To obtain a general distribution of available friction containing all landings, adequate statistical means have to be applied.

While the first method is based on the correlation between a certain **amount of brake pedal deflection** and the respective maximum available friction, the second method is based on landings using **autobrake, where the target deceleration has not been achieved**. For the evaluation of the probability distribution of the available friction with this method, an extreme value method had to be used.

□ **A new method to estimate aerodynamical aircraft parameters during landing roll has been developed:** For the physical model of the aircraft, the respective aerodynamic aircraft parameters are required, which are not directly accessible by aircraft operators.

□ **A new method to evaluate the risk of a midair collision between two aircraft has been developed:** The Traffic Collision Avoidance System (TCAS) provides Resolution Advisories (RAs) to the flight crew if a collision is imminent. Since the reaction to this system is based on the interaction with the pilot, a wrong input is possible and thus, an *induced collision* might occur.

The new method is based on a Monte Carlo method, in which possible initial conflict geometries are evaluated, which lead to the generation of a TCAS RA, using a *system model*. A possible collision is evaluated by using an adequate *pilot model* for the assumed reaction of the intruder aircraft, combined with the recorded reaction of the own aircraft.

□ For the *system model*, **a mathematical model of the TCAS system has been developed:** This system model, based on the TCAS specification, is a balance between the necessary detail level and simplification, which is required to model the collision probability, considering the development of the conflict geometry during the encounter and, as a consequence, possible modifications of the TCAS RA.

□ **A new method to evaluate the risk of injuries due to in-flight turbulence has been developed:** While the state of the aircraft with regard to turbulence can be defined by a certain amount of vertical acceleration, the environmental conditions, which is the probability of injury depending on the turbulence intensity, can only be evaluated by *correlation* with additional information. This information can be gathered by other sources, e.g. safety reports or investigation data of incidents or accidents. Thus, the underlying model of the environmental conditions is called a *correlation model*.

Since the new method is based on algorithms rather than expert's estimation, a further important contribution has been made:

□ **Disclosure of the non-assessed part of a certain risk category:** Due to limited resources in expert estimation, not all flights can be assessed in terms of risk. Instead, the experts have to focus on the flights with supposedly higher risks. Therefore, it is not known exactly to what extent the unexamined portion contributes to the overall risk. Since the new method does not depend on the assessment by a safety expert, all flights can be evaluated.

The presented methodology is useful for airlines, as it gains insight in their safety performance of the considered accident categories. Also, resources can be used more efficiently, since the risk classification is conducted by an algorithm rather than the assessment by a safety expert. Instead, the safety experts can focus on those risks, which are not supported by flight data (e.g. bird strike) or investigate identified outliers in more depth.

Authorities may profit by the methodology, since an objective way of aggregation of risk data from different operators is possible, therefore enables the respective authority to compare the data of different organizations and create safety trends. Based on detected outliers the authorities are able to identify common safety issues, which may form the basis of Safety Action Plans in the future.

1.5 Structure of the Dissertation

This dissertation thesis consists of two parts. In the first part the fundamentals of safety management and background information are discussed. In the second part the novel approaches of how to evaluate the risk level of a safety event are presented (Figure 1-4).

After the introduction in chapter 1, the following chapter describes the pathway of an aircraft accident. It is explained, why incidents are useful as precursors of accidents. The focus is on the "organizational accident" (see chapter 2.2), which is embedded in the environment of an organization. The understanding of the development of organizational accidents forms the basis of possible interactions by the management of the organization to prevent such an accident in the future. By the identification of hazards, which are the basis of safety risks, weaknesses in the organizational structure can be identified well ahead of the occurrence of an accident. Methods are shown how to identify those hazards and how to assess the safety risks associated with these hazards. Finally, different methods how to evaluate a risk associated with a safety event are discussed, since the risk of an event forms the basis of the new methodology.

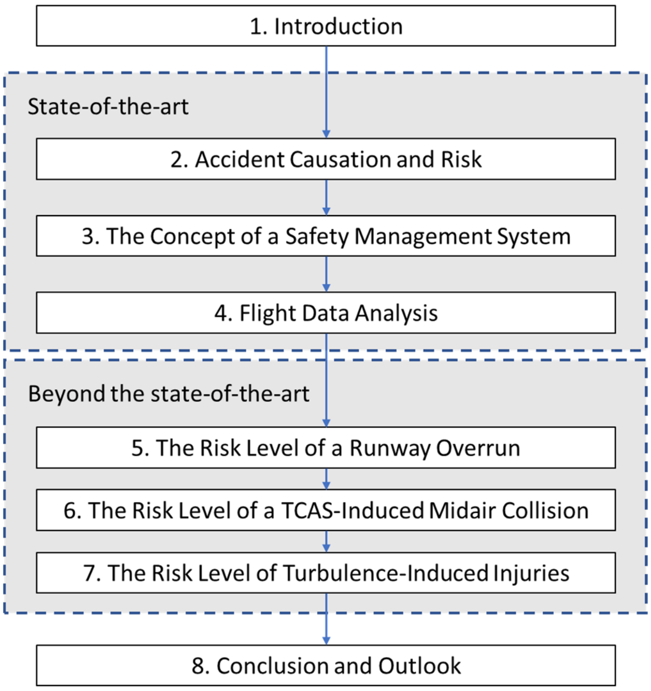
1. Introduction
State-of-the-art
2. Accident Causation and Risk
3. The Concept of a Safety Management System
4. Flight Data Analysis
Beyond the state-of-the-art
5. The Risk Level of a Runway Overrun
6. The Risk Level of a TCAS-Induced Midair Collision
7. The Risk Level of Turbulence-Induced Injuries
8. Conclusion and Outlook

Figure 1-4 Structure of this dissertation

Chapter 3 explains the requirements and the structure of a Safety Management System (SMS). The different elements of an SMS are described. A main element of an SMS is the safety assurance process, which includes the requirement to measure the safety performance.

Chapter 4 describes the requirements on elements of a Flight Data Analysis (FDA) system. FDA is a valuable source of operational information to identify hazards and measure the safety performance. A methodology how to measure safety performance is presented, which is the transition to the second part of the thesis, the novel method how to evaluate the risk level of an FDA event.

Chapters 5 through 7 describe the different risk models based on the new methodology.

In chapter 5, the risk model for the accident category runway overrun is developed by means of a **physical model**. Chapter 6 deals with the risk model of TCAS-induced midair collisions by means of a **system model** and a **pilot model**. In chapter 7, the risk model of turbulence-induced injuries is developed by means of a **correlation model**.

At the end of the dissertation, in chapter 8, a conclusion of the presented methods and an outlook is provided.

2 Accident Causation and Risk

In spite of a continuous growth in worldwide air traffic [1], the number of accidents could be steadily reduced over time, as depicted in Figure 2-1 [1]. In the early days of modern aviation industry, only little safety regulation, practical experience and engineering knowledge was available [26]. In this *technical era*, when the aviation industry emerged towards a mass transportation system, technology was rather unreliable. The focus of aviation safety was primarily on accident investigations at this time, with a clear focus on technical issues. Until the late 1960s, technological improvements, driven by the accident investigations, led to a gradual decline in aviation accident rates, accompanied by improving regulatory compliance and oversight [2].

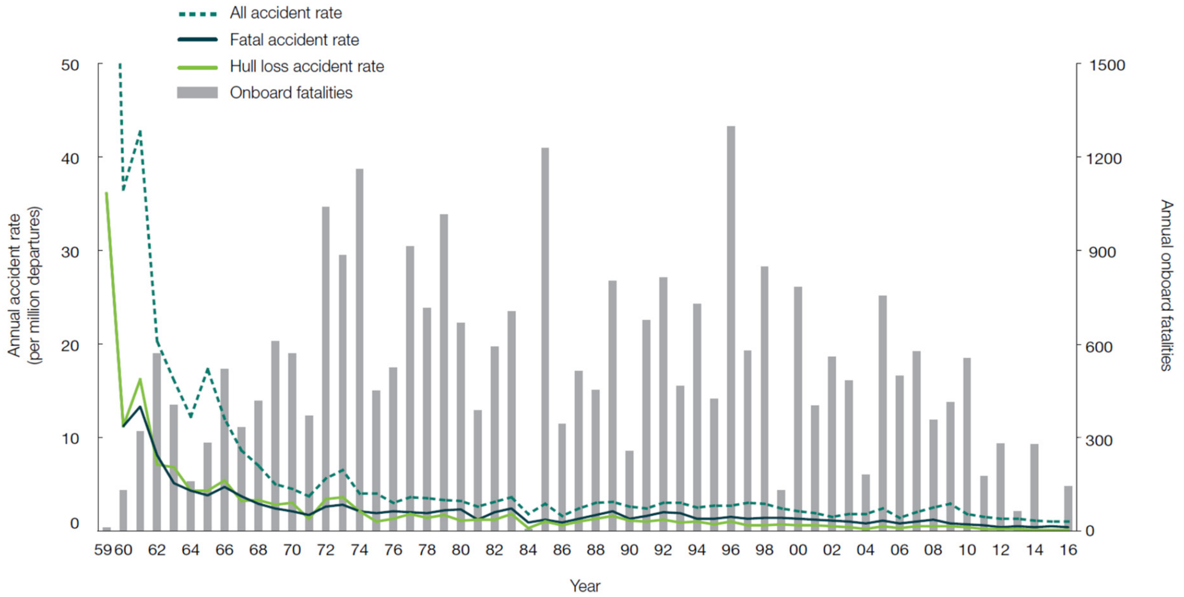

Figure 2-1 Annual aviation accident rates [1]

A further significant reduction of accident rates has been achieved in the *human factors era*, which ranged from the early 1970s to the mid-1990s, due to advances in technology as well as enhancements in safety regulations. The focus of aviation safety was extended to human factor issues. During accident investigations, the human factors issues, including the interface between man and machine, contributed to a better understanding of the pathway towards an aircraft accident. However, even though valuable resources had been invested in error mitigation, human factors recurred as an issue in accident causation [2].

A certain stagnation in accident statistics occurred due to the fact, that the focus was primarily set on the individual without considering the whole organizational context the humans have been embedded in. With focusing solely on the individual, it is not possible to eliminate the human factors issue completely. Only the recognition that individuals are influenced by factors, which origin in the complex organizational environment, could further reduce the factors contributing to an accident.

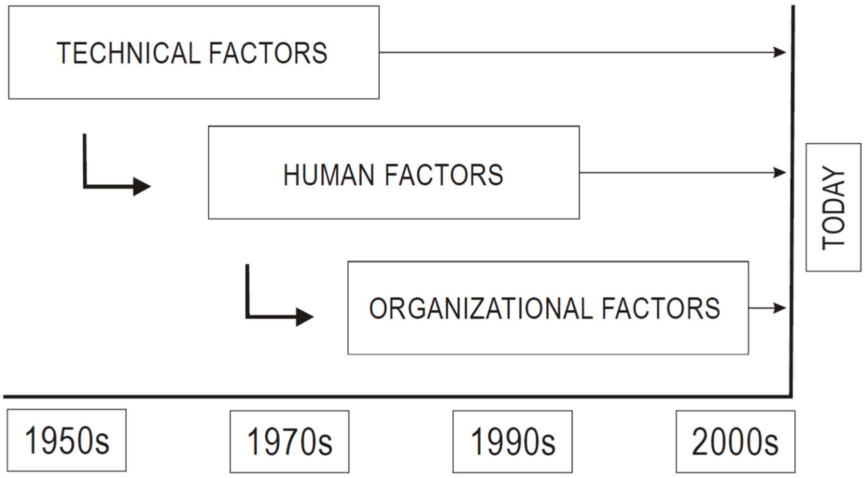

Figure 2-2 The evolution of safety [2]

In this *organizational era*, which started from the mid-1990s until today, safety was seen from a more systemic perspective, where organizational factors have been considered to contribute to an accident equivalent to human factors or technical issues. The safety community became more and more aware about the fact, that the effectiveness of risk controls is significantly influenced by the organizational culture and policies [2]. Due to the low number of accidents, the solely reactive investigation of accidents or serious incidents was not sufficient to get enough insight in actual risks anymore. Advances in computer technology enabled the processing of a huge amount of data, which could be collected during the operation of aircraft. Combined with the low number of accident investigations, this data enabled a proactive or even predictive approach in getting insight of actual risks in the operation.

Even though each approach led to a significant gain in safety, the modern air traffic system comes to a point, where better technology, more training and more efficient regulation reach their limit. Meanwhile, the system is so complex, that additional complexity due to more rules and regulations could even lead to an adverse effect in safety. At this point, ICAO realized that a shift towards more responsibility within the organizations could be the key to further reduce the accident rate in future [6].

2.1 The Relationship between Incidents and Accidents

Safety in aviation is defined as *"the state in which the possibility of harm to persons or of property damage is reduced to, and maintained at or below, an acceptable level through a continuing process of hazard identification and safety risk management"* [2]. This definition of ICAO implies that safety itself cannot be measured directly. Instead, safety is the reduction of the associated risks below a level, which is acceptable.

Even though the ultimate goal in aviation is the elimination of aircraft accidents and/or serious incidents [2], safety management is nearly impossible by focusing only on those events as the number of aircraft accidents is very low nowadays [27]. In the past, when the overall safety level has been lower, the performance of aviation safety was measured by means of accident rates. Accidents have become rare events due to increased safety [28]. In 2014 the jet aircraft hull loss rate of IATA[4] member airlines in Europe was as low as 0.15 per million flights [24]. Hence, a large operator, conducting 500,000 flights per year, would experience only one accident every 13 years in average. These numbers indicate that accident data by itself is not sufficient to develop an aviation causal risk model, even if data is aggregated over several years. Aggregation of aviation data over several years could also have an adverse effect in safety management as the involved systems, procedures, rules, regulations etc. may have changed significantly over time [27]. The combination of the continuous change of the level of safety combined with the rare occurrence of accidents makes it impossible to manage safety by using accident data only.

In certain areas, e.g. road safety, it is still possible to measure a safety performance by using high-consequence indicators. In road traffic the number of fatalities, e.g. in Germany in 2013, was 3,339. As this is – besides a continuous reduction over recent years – still a large number, it seems adequate to just use fatal accidents as a safety performance indicator, even if the number of fatalities is further reduced by down braking e.g. into months, areas of occurrence (e.g. highway, city etc.) or road user type (e.g. car occupant, bicyclist, pedestrian etc.). Because of the high number of fatalities it will even then be possible to get an immediate feedback by increase or reduction of the number of fatalities during the safety management process, e.g. if a certain countermeasure is implemented in the system [29].

Turning back to aviation safety, especially if breaking down into different accident categories, the number of fatal accidents is so low that in certain categories no single accident could be observed in certain years. However, this breakdown into different accident classes is vitally important when developing causal accident models as the contributing factors leading to an accident within the different categories are completely different and in most cases independent from the other categories [7].

[4] International Air Transport Association

If focusing for example on midair collisions as one accident category, no single fatal accident took place from 2010 to 2014, and only one non-fatal accident occurred in 2012 within the same timeframe [24]. Nevertheless, midair collision is still treated as an area of high risk in aviation indicated by recent significant events [30]. This example shows that other means of safety measurement need to be used to get a clear picture of the level of safety in aviation.

According to ICAO, an accident is "*an occurrence associated with the operation of an aircraft which [...] takes place between the time any person boards the aircraft with the intention of flight until such time as all such persons have disembarked [...], in which:*

a) a person is fatally or seriously injured [...] or

b) the aircraft sustains damage or structural failure [...] or

c) the aircraft is missing or is completely inaccessible" [31].

As accident rates are not sufficient to evaluate the level of safety, other means have to be used. In Figure 2-3 the relationship between serious accidents and possible precursors of those events can be seen in a Heinrich pyramid, introduced by H.W. Heinrich in the 1930s [32], adapted to the aviation industry by the NTSB [5] [33]. The top of the pyramid represents the low-frequency/high-consequence event, in this example a serious accident. Moving down on the pyramid, the next layers consist of lower-consequence but higher-frequency events which are less hazardous but more frequent.

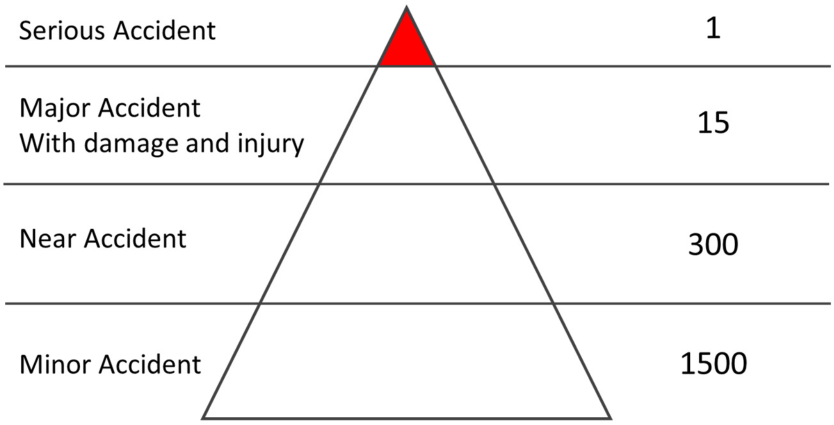

Figure 2-3 The Heinrich pyramid based on [34]

The ratio between e.g. minor incidents and serious accidents is exactly indicated with 1 by 1500 in Figure 2-3, however, other sources show a different ratio of 1 by 600 between fatal accidents and incidents [35]. This difference in ratios of the two sources may be caused by the definition

[5] National Transportation Safety Board, independent U.S. government investigative agency responsible for civil transportation accident investigation

of the different layers of the pyramid. Terms like "serious accident", "major accident", "incident" or "minor incident" have to be clearly defined, when calculating a ratio between them.

According to ICAO, an *incident* is "*an occurrence, other than an accident, associated with the operation of an aircraft which affects or could affect the safety of operation*" [31]. This definition still lacks of an exact threshold from which an occurrence affects the safety. This threshold might be defined differently, depending on the knowledge of involved people and the level of safety culture within the respective organization.

Furthermore, ICAO defines a *serious incident* as "*an incident involving circumstances indicating that there was a high probability of an accident […]*" [31]. Also, the latter definition is still not precise enough and provides some room for interpretation depending on the perspective of the respective organization.

However, the definition of a serious incident indicates, that according ICAO, there is a clear relationship between an incident and an accident, as both follow similar event paths and differ only in their outcome [27]. This is highlighted by a note in ICAO Annex 13: "*The difference between an accident and a serious incident lies only in the result*" [31].

An accident can be considered as the occurrence of a series of consecutive events causing unintentional harm [28]. Heinrich developed an accident chain model by comparing the accident with a series of lined up dominoes [32]. In this model two different immediate causes of accidents exist: unsafe acts and unsafe conditions. This model is helpful to understand that removing one of the dominoes would not cause the remaining ones to fall and thus the negative outcome would not occur. The probability that all dominoes will fall down – which would be equal to an accident in this model – will be much higher the more dominoes have fallen already. According to this model incidents are conditions, where some of the dominoes have fallen, but not all of them, so a few barriers are still existing towards the evolution of the accident. If safety performance can be expressed as the amount of dominoes that have fallen already in this model, incidents could be well considered as an indicator of safety performance.

James Reason enhanced this model by refining Heinrich's unsafe acts and unsafe conditions towards different types of possible failures that line up to create an accident [36]. Possible failures in this model are latent failures, local trigger events (environmental factors, e.g. weather) and active failures produced by individuals at the operational level, typically front-line personnel (e.g. pilots, mechanical engineers etc.). Latent failures have been created long before the accident and remain dormant until an active failure triggers their operation. They arise mainly in the managerial and organizational sphere, so these types of failures exist already within the system even before the accident sequence arises and are a delayed consequence of decisions which have been made long before the accident typically created by people who are far away from the event in time and space [2]. This describes the so-called *organizational accident*, a term, which was introduced by Reason.

2.2 Organizational Accident

The proposition of an organizational accident is the assumption that if human error contributes to an accident, the replacement of the individual who created the error would not change the safety in the long term. Instead, organizations are in control of many of the events which are elements of the potential accident chain [19,36,37].

Reason developed the "Swiss-Cheese" model [36,37], in which different layers of protections against an accident exist, comparable to slices of cheese. In an ideal world, each of the slices would be intact. However, in practice, each layer incorporates breaches of different number and size, comparable to the holes in swiss cheese. Unlike real cheese slices, these holes constantly open, close and change their positions within the slices. The holes or breaches can be generated by equipment failures, operational errors or other enabling factors. In most cases, each slice contributes in preventing an accident, except if the breaches of all layers are lined up. As a result, no remaining layer can prevent the accident, if a straight path opens through the breaches of all existing layers towards the accident. The model illustrates that complex systems like aviation are well protected by multiple layers, and thus a single failure is rarely consequential.

The holes in the defenses are caused by two reasons: Active failures and latent conditions. Latent conditions can exist in the system for a significant period of time without being detected, until an active failure is made. They possibly emerge if the breaches of the different layers have aligned due to an active failure and contribute to the accident. Latent conditions might have been incorporated in the system by poor equipment or procedural design, possibly due to a lack of safety culture in the management decision process. To prevent organizational accidents, it is essential that organizations are able to detect those latent conditions and finally mitigate them.

While the latent conditions exist in the system well before the outcome evolves, created by people on the managerial level far removed in time and space from the accident, active failures are in most cases connected to front-line personnel with an immediate outcome [2,36]. However, while active failures are often hard to predict in their specific form, latent conditions can be identified and counteracted, before the accident evolves. This is the transition from a reactive risk management towards a proactive risk management [37].

However, before active failures can trigger an accident, various defenses in the aviation system at different levels exist to prevent an accident caused solely by human error. A proactive risk management is able to establish those defenses to further decrease the probability of an accident due to fluctuating human performance or decisions. The management of an organization should aim for a system which is better able to tolerate evolving errors and contain their damaging effects [37].

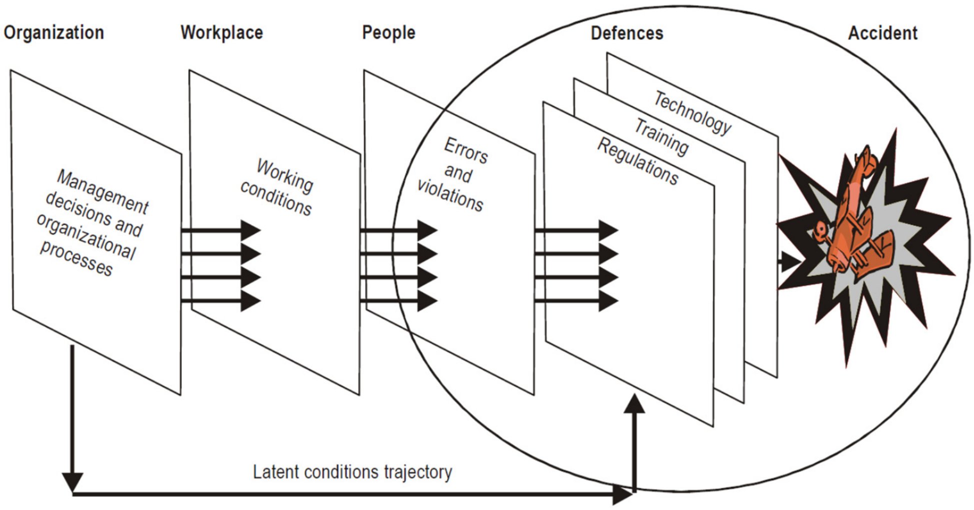

Figure 2-4 Accident causation according Reason [2,36]

Reason proposes that all accidents include a combination of latent conditions and active failures. The concept of this model can be seen in Figure 2-4 [2,19].

However, no breach, whether caused by the organization or by an individual, will on its own cause an accident. For a better understanding of this mechanism, ICAO created the diagram shown in Figure 2-5. The pathways to failure start at the top level, the organizational processes. These processes are typically controlled by management and consist of avocation of adequate resources and communication, which are the main drivers regarding safety. Furthermore, policies, planning and supervision are elements of these processes. Deficiencies in these organizational processes may trigger one of the two pathways leading to a failure or an accident.

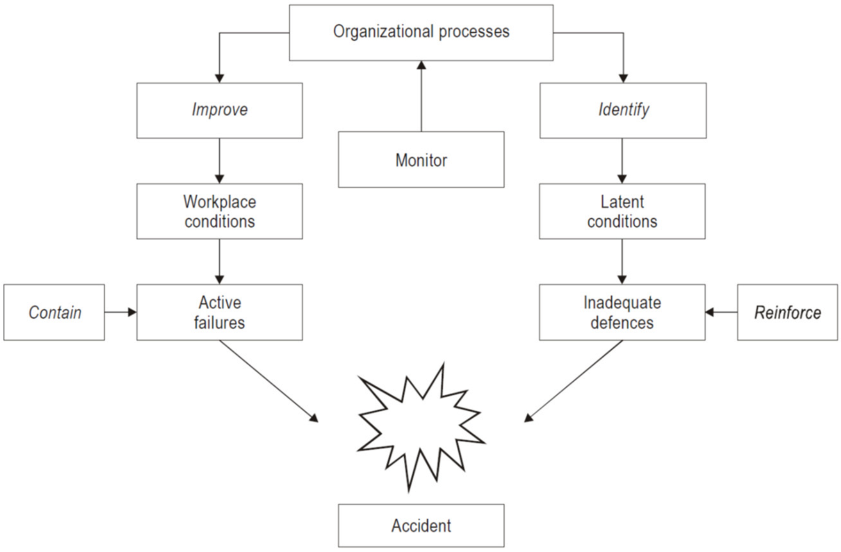

Figure 2-5 The pathways of an organizational accident [2]

The right pathway is the latent conditions pathway. If the organization is not able to identify them in time and take corrective actions, they may eventually contribute to an accident, once they become active through operational triggers. On the other hand, this pathway describes also the normalization of deviance. This describes workarounds or shortcuts by front-line personnel to cope with organizational deficiencies regarding processes or poor equipment, which is either not noticed or accepted by the management level.

The left pathway describes the workplace conditions pathways. Workplace conditions have a direct influence on human performance and decision making and therefore may contribute to human error, which finally may lead to an accident [2].

Both the model of Heinrich as well as the model of Reason, as described above, suggest that accidents and incidents within the same scenario follow at least partially similar paths [27], and hence incidents are adequate to not only gain insight in causal accident pathways, but also to provide an indication of safety performance.

During the early design of a system or part of a system, a baseline performance is defined, which is aimed for. To meet this baseline performance, the necessary resources in terms of technology, training and regulations have to be implemented. However, in the daily practice, technology may not work as intended, a lack in the interaction between man and machine may evolve, and the regulations might not be adequate in every day-to-day situation. This leads to a "drift" of actual performance from the baseline performance, also called *practical drift*, as it is a consequence of daily practice (see Figure 2-6). This practical drift occurs in every system, no matter how accurately and carefully the early system design had been conducted.

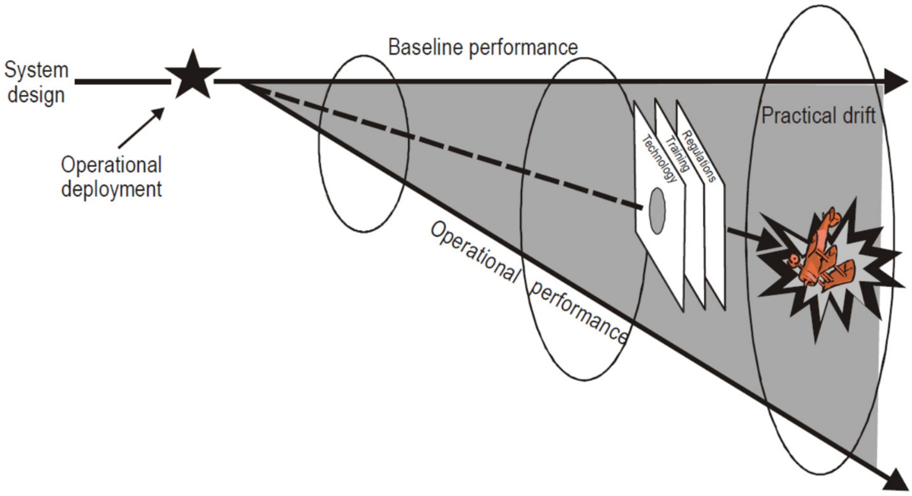

Figure 2-6 Practical drift [2]

People working in the practical environment may start to work around problems, which have not been foreseen in the design phase, deviating from procedures and developing personal strategies, which are not in accordance with the original intention of the system design. It is therefore essential, that management encourages people at the front-line to forward information about possible deviations especially at the beginning of the implementation of the system. Adequate mitigations are then necessary in order to guide the operational performance back towards the baseline performance. This is a closed loop of information and counteractions between personnel and management [2].

2.3 Active Failures

In the model of the organizational accident it is assumed, that humans are subject to possible errors. Even in the best organization, human errors can be expected. Errors are not the causes, but the consequences of systemic factors rather than the consequences of the failure of the human individual [37].

Even though in Reason's theory an active failure is an element of an organizational accident, it is still very common to blame individuals for an accident, isolating the active failure of the individual from the organizational context. This person approach ignores the fact that if the individual, who did the error, is exchanged by another person, the human error may reoccur, if the organizational circumstances will not be changed. For the risk contained in the system, nothing will change by punishing individuals for their errors. Understanding the principles of this relationship enables a more efficient risk management of an organization.

Active failures are typically the result of errors or violations of front personnel, e.g. pilots. In comparison to latent conditions, active failures lead to immediate consequences. In most cases these consequences have little impact and thus, can only be observed by the persons directly involved.

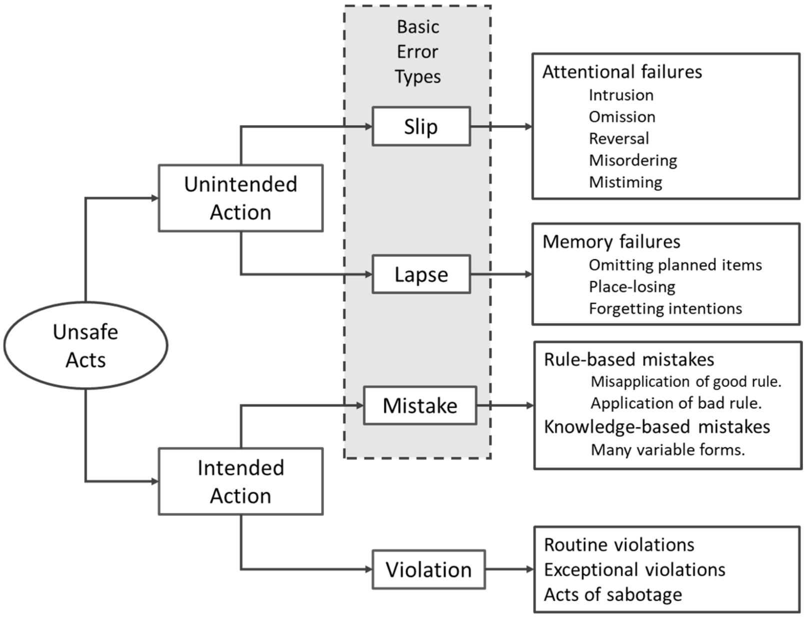

Figure 2-7 Summary of the psychological varieties of unsafe acts [36]

Figure 2-7 shows two different types of active failures: errors and violations. Both types of failures are characterized by non-compliance of operating procedures. The difference lies only in the intent.

While errors are unintentionally, violations are intentional failures [19]. According ICAO, errors can be distinguished in [2]:

- **Slips** are "*actions that do not go as planned*". For example, climbing to the wrong altitude is a slip.
- **Lapses** are "*memory failures*". For example, forgetting checklist item is a lapse.
- **Mistakes** are "*failures in the plan of action*". This means that the execution of the plan might have been correct. However, the plan was not correct and would not have led to success.

Several strategies exist to control or mitigate these errors, including [2]:

- **Reduction strategies** are aimed for the reduction or even elimination of the factors contributing to an error, e.g. improvement of ergonomic factors or reduction of environmental distractions.
- **Capturing strategies** anticipate an error and aim for the "capture" of the error to prevent any adverse consequences, e.g. use of checklists or other procedural means.
- **Tolerance strategies** accept errors to be made without resulting in any serious consequences, e.g. use of redundant systems or multiple inspection processes.

Because the human performance of the employees is affected by organizational, regulatory and environmental issues, the safety risk management has to consider organizational policies, processes and procedures, which are related to communication, scheduling of personnel and allocation of resources, and which may contribute to errors [2].

In contrast to errors, *violations* are based on intentional behavior, even though the motivation may not be malicious. An example is the deviation from a standard procedure in the conviction that it is necessary to fulfil the mission while avoiding negative consequences [2,19]. This culminates in the emergency authority of the aircraft commander in the case of an abnormal situation, where standard procedures may prevent the safe landing of the aircraft, e.g. the deviation of the standard procedures during an emergency landing of a Qantas Airbus A380 [38].

ICAO distinguishes between three categories of violations [2]:

- **Situational violations** are the result of factors that occur in a particular context, e.g. time pressure or high workload.

- **Routine violations** are deviations from intended processes or techniques within a work group. Those violations are the result of situations in which adherence to established procedures makes it difficult to complete tasks, e.g. workaround procedures, also called "drift".
- **Organizationally induced violations** are extended routine violations. They are caused or at least accepted by the organization during increased output demands in combination with safety defenses, which are ignored or stretched by the organization.

2.4 Hazards and their Analysis

A hazard is defined as "*a condition or an object with the potential to cause death, injuries to personnel, damage to equipment or structures, loss of material, or reduction of the ability to perform a prescribed function*" [2]. With regard to aviation safety risk management, the term "hazard" should focus on those conditions "*which could cause or contribute to unsafe operation of aircraft or aviation safety-related equipment, products and services*" [2].

For example, a certain wind component is not in any case a hazardous condition, as long as it constitutes as a headwind component for takeoff or landing. However, if this wind component changes to a crosswind or tailwind component, it might be a hazard, which contributes to a runway excursion.

The hazard itself should not be mixed up with a consequence. Instead, the consequence or outcome can be triggered by the hazard. There is a certain probability, that the hazard ends up in a consequence, e.g. an accident. This probability is influenced by the established mitigation measures, the recovery measures or safety barriers [2]. In general, a hazard is a condition or an object which contains a certain amount of risk, which has yet to be assessed, i.e. quantified. Thus, a hazard forms the basis of the risk assessment, which is described later.

Hazards exist at all levels of the organization. An essential part of the safety risk management process is the continuous identification of hazards, which are not yet known by the organization and, thus, are not managed yet.

Hazards can be identified by means of **internal data sources**, which contain data from the organization's operation. These data sources include:

- **Reports** are either referred to as *Air Safety Reports* (ASRs) or *Confidential Safety Reports* (CSRs). In general, employees of all domains within the organization should be able to file such reports in the aftermath of safety relevant events. ASRs are usually addressed to the management, while CSRs are confidentially sent to the safety department. Even though, the author of the report might be known by the safety department, such reports are treated confidentially towards the disciplinary system [7]. The intention is to lower the reporting threshold of the respective author, especially if own human errors have to be reported, which may contain valuable safety information. However, a systematic analysis of reports is limited due to a variable and not known rate of unreported events, depending on the respective event [7]. Reports could also be mandatory reports of specific events, submitted to the authorities.

- **Flight Data Analysis (FDA)** is the systematic collection and analysis of recorded flight data. The portion of the flight operation which is covered by the recorded flight data is usually high, and thus, enables a systematic collection of hazards. Also, the rate of unrecorded flights can be evaluated by a comparison between the number of recorded flights and the number of conducted flights. Flight Data Analysis is normally anonymous, which makes it difficult to combine the flight data with other operational data. Analysis of flight data, collected in the FDA, is the core part within the scope of this thesis, and will be described in chapters 5 to 7.
- **Safety audits** can reveal deficiencies in safety and compliance matters within the organization. Safety Audits are conducted by either an external entity or through an internal audit process.
- **Incident or accident investigations**, either conducted as an internal investigation for certain reportable events, which is in accordance with internal or regulatory requirements, or conducted by the respective authorities [2].
- Other means of internal data sources among others are: **Safety surveys**, **safety studies** (e.g. simulator studies), **safety reviews** or **feedbacks from training**.

Also, **external data sources** be included in the hazard identification process, e.g. the use of industry accident reports, state mandatory or voluntary incident reporting systems, state oversight audits or information exchange systems [2].

The hazard identification process should be an integral part of the organization’s processes and should be carried out in a structured and continuous way.

According to ICAO, three different methods for hazard identification exist [2]:

- **Reactive:** Analysis of past outcomes or events. Accident or incident analysis can be used to identify the hazards which either contributed to the event or which had been latent in the system, since accidents and incidents are indicators of deficiencies in the system.
- **Proactive:** The search for hazards in the existing processes by analysis of existing or real-time situations, using audits, evaluations or the reporting system.
- **Predictive:** Identification of potential future hazards by analyzing system processes and the environment as well as Flight Data Analysis.

Moreover, the European Commercial Aviation Safety Team (ECAST)[6] distinguishes between qualitative and quantitative methodologies for hazard identification [39]. ECAST defines quantitative methods as hazard identification from available operational data, which means that only such hazards can be identified, which are contained in past data, i.e. which have been observed by somebody already. In contrast, qualitative methodologies are based on expert knowledge, e.g. brainstorm sessions, where completely new hazards might be identified, which have previously been unknown, i.e. unimaginable hazards.

To describe hazards and their associated risks in qualitative terms, a bow tie model can be used. The bow tie model is a widely used structured methodology, which is a valuable tool in the hazard identification process [40]. Even though, the term 'bow tie' is often used to describe a diagram, which visualizes the model, it also refers to the corresponding methods used to create such a diagram [39].

The bow tie diagram shows the pathways from the causes towards the undesired event, i.e. the hazard, combined with the possible outcomes or consequences of this hazard, thus, providing the basis of a safety risk assessment. It combines a fault tree (cause) and an event tree (consequence). Since the fault tree is drawn on the left and the event tree on the right and the hazard is drawn as a "knot" in the middle, the shape of the diagram looks like a bow tie. The diagram provides a good overview of the relationship between causes, hazard and consequences as well as the safety barriers, which either prevent the hazard from occurring, or limit the effects of the hazard. It is both simple and easy to understand, even for non-specialists [40]. An example of a bow tie diagram can be seen in Figure 2-8.

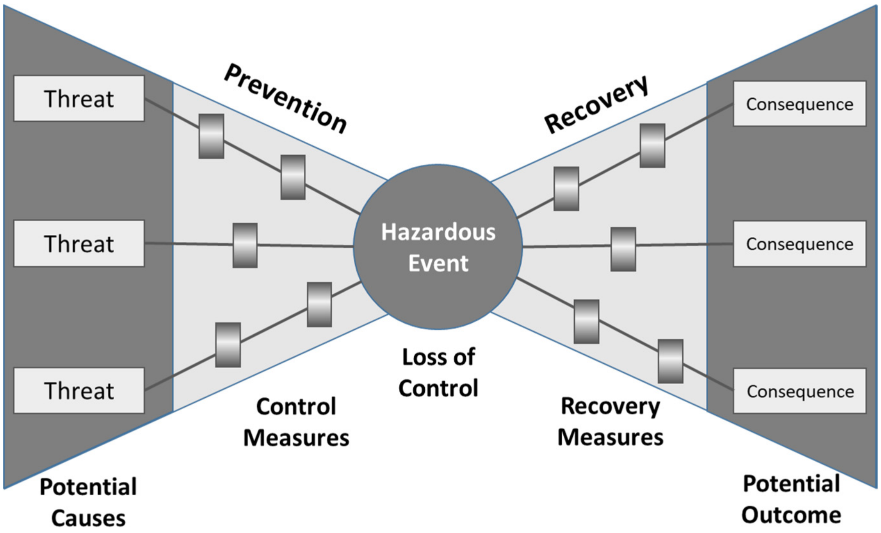

Figure 2-8 Bow tie diagram based on [40]

[6] ECAST is the European equivalent of Commercial Aviation Safety Team (CAST) in the US. In March 2016, the initiative was discontinued [124]

The bow tie methodology, also called bow tie process, is the way how the bow tie diagram is built. It consists of a structured sequence of placing the different elements in the diagram. The bow tie process may be iterative and is usually conducted by a team of safety experts. The following steps have to be conducted [40]:

Step 1: Identification of the hazard and the corresponding event

The hazard is the starting point of the diagram, where the fault tree ends and the event tree starts from. The hazard is described in form of an undesired event, in which the hazard is "released".

Step 2: Assessment of the threats

The threats are the potential causes leading to the undesired event. They are positioned on the far left of the diagram. Four different classes of threats exist: Technical factors (TEC), human factors (HUM), environmental factors (ENV) and organizational factors (ORG).

Step 3: Assessment of the consequences

The consequences are potential outcomes from the undesired event, which finally evolve from the threats through the undesired event. They are positioned on the far right of the diagram.

Step 4: Assessment of the control measures

The control measures are safety barriers that potentially prevent threats from causing a hazard. In the bow tie diagram, they are located between the threat and the hazard. Three different classes of control measures exist: Technical measures (e.g. technical equipment), operational measures (e.g. training) and organizational measures (e.g. procedures).

Step 5: Assessment of the recovery measures

The recovery measures are safety barriers that can limit the chain of consequences of an event. In the bow tie diagram, they are located between the hazard and the consequence. The possible classes of recovery measures are identical to those of the control measures.

The safety barriers are measures which potentially lower the risk of the hazard. Since safety management is the management of risks towards an acceptable level, the safety barriers are an adequate means for this purpose. Safety barriers which are put in place by the safety management are also referred to as mitigation measures. It is more desirable to use control measures instead of recovery measures, since the undesired event can potentially be avoided by those safety barriers. However, since there is still a certain probability for the undesired event to occur, also adequate recovery measures should be established to milder the effect of the potential outcome. From the perspective of the overall risk, it makes no difference whether control measures or recovery measures are used to reduce the risk.

2.5 Safety Risk Assessment

The quantification of the safety risk associated to a hazard is called Safety Risk Assessment. A safety risk is "*the projected likelihood and severity of the consequences or outcome from an existing hazard or situation*" [2], and thus, is based on two components: the probability and the severity of the consequences/outcome.

2.5.1 Probability

The probability is "*the likelihood or frequency that a safety consequence or outcome might occur*" [2]. According to ICAO, the determination of the probability can be conducted by using questions like [2]:

- *Is there a history of occurrences similar to the one under consideration, or is this an isolated occurrence?*
- *What other equipment components of the same type might have similar defects?*
- *How many personnel are following, or are subject to, the procedures in question?*
- *What percentage of the time is the suspected equipment or the questionable procedure in use?*

A typical safety risk probability table, containing 5 different levels of safety risk probabilities, is provided by ICAO, as shown in Table 2-1. However, this is only an example, and can be adapted in detail and complexity to the particular needs and complexities of different organizations [2].

Table 2-1 ICAO safety risk probability table [2, Fig. 2–11]

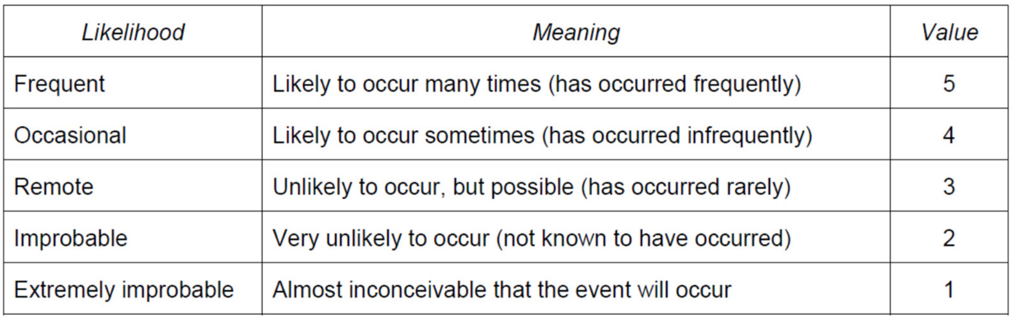

Likelihood	*Meaning*	*Value*
Frequent	Likely to occur many times (has occurred frequently)	5
Occasional	Likely to occur sometimes (has occurred infrequently)	4
Remote	Unlikely to occur, but possible (has occurred rarely)	3
Improbable	Very unlikely to occur (not known to have occurred)	2
Extremely improbable	Almost inconceivable that the event will occur	1

2.5.2 Severity

The next step is the assessment of the safety risk severity, *taking into account the potential consequences related to the hazard* [2]. Safety risk severity is defined as "*the extent of harm that might reasonably occur as a consequence or outcome of the identified hazard*" [2]. ECAST defines the terms "outcomes" and "consequences" as follows [39]:

- ***Outcome:*** *a potential end point of an accident scenario which can be assigned to a consequence severity*

- ***Consequence:*** *the degree of injuries to personnel, damage to equipment or structures, loss of material, or reduction of ability to perform a prescribed function arising from an outcome. Consequences have a magnitude that can be based on the number of fatalities or the level of damage.*

According ICAO, the severity assessment can be based on [2]:

- ***Fatalities/injury:*** *How many lives may be lost (employees, passengers, bystanders and the general public)?*
- ***Damage:*** *What is the likely extent of aircraft, property or equipment damage?*

All possible consequences related to the respective hazard should be considered, taking into account the ***worst foreseeable situation*** [2]. Table 2-2 shows an example of a safety risk severity table from ICAO, considering 5 different severity categories. As for the probability, the table can be adapted to the specific needs of the respective organization in terms of complexity.

Table 2-2 ICAO safety risk severity table [2, Fig. 2–12]

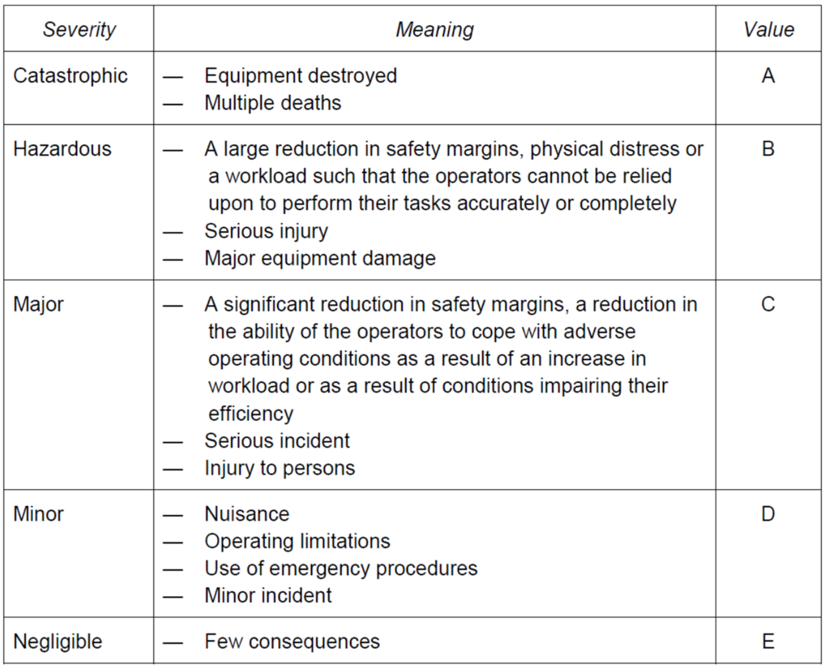

Severity	*Meaning*	*Value*
Catastrophic	— Equipment destroyed — Multiple deaths	A
Hazardous	— A large reduction in safety margins, physical distress or a workload such that the operators cannot be relied upon to perform their tasks accurately or completely — Serious injury — Major equipment damage	B
Major	— A significant reduction in safety margins, a reduction in the ability of the operators to cope with adverse operating conditions as a result of an increase in workload or as a result of conditions impairing their efficiency — Serious incident — Injury to persons	C
Minor	— Nuisance — Operating limitations — Use of emergency procedures — Minor incident	D
Negligible	— Few consequences	E

2.5.3 Safety Risk Index

After the probability and the severity have been assessed, the safety risk index can be determined by means of a so-called risk matrix. Every level of the safety risk probability table as well as every category of the safety risk severity table is contained in the risk matrix, thus, a distinct risk index is defined for every probability/severity combination by an alphanumeric designator. An example of a safety risk matrix can be seen in Table 2-3:

Table 2-3 ICAO example of a safety risk matrix [2]

Risk probability		Risk severity				
		Catastrophic A	Hazardous B	Major C	Minor D	Negligible E
Frequent	5	5A	5B	5C	5D	5E
Occasional	4	4A	4B	4C	4D	4E
Remote	3	3A	3B	3C	3D	3E
Improbable	2	2A	2B	2C	2D	2E
Extremely improbable	1	1A	1B	1C	1D	1E

The last step of the safety risk assessment is the determination of the safety risk tolerability. The index derived from the safety risk matrix is exported to the safety risk tolerability matrix, that describes the tolerability criteria for each organization. An example can be seen in Table 2-4.

Table 2-4 ICAO safety risk tolerability matrix [2]

Tolerability description	Assessed risk index	Suggested criteria
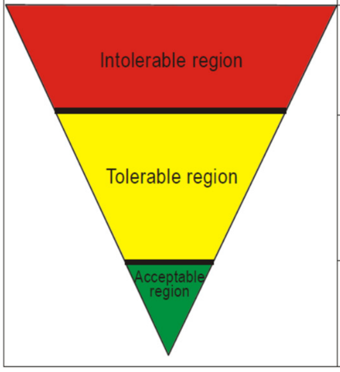	5A, 5B, 5C, 4A, 4B, 3A	Unacceptable under the existing circumstances
	5D, 5E, 4C, 4D, 4E, 3B, 3C, 3D, 2A, 2B, 2C, 1A	Acceptable based on risk mitigation. It may require management decision.
	3E, 2D, 2E, 1B, 1C, 1D, 1E	Acceptable

Depending on the region, where the safety risk falls into, different measures are necessary to deal with the risk [2], see also the alternate safety risk tolerability matrix, as shown in Table 2-5:

- If the safety risk is within the intolerable region, the organization must take measures to reduce the risk, e.g. the probability component of the risk index or the severity component of the risk index. After the risk reduction, the respective safety risk has to be reassessed to prove that it falls into a lower region. Otherwise, the part of operation associated with the risk must be cancelled.
- If the safety risk falls into the tolerable region, the risk has to be mitigated, using adequate mitigation measures.
- If the safety risk falls into the acceptable region, it can be accepted.

The inverted pyramid in Table 2-4 reflects the continuing effort to bring the risk index down in the pyramid to the lowest reasonable risk level [2]

Table 2-5 ICAO alternate safety risk tolerability matrix [2]

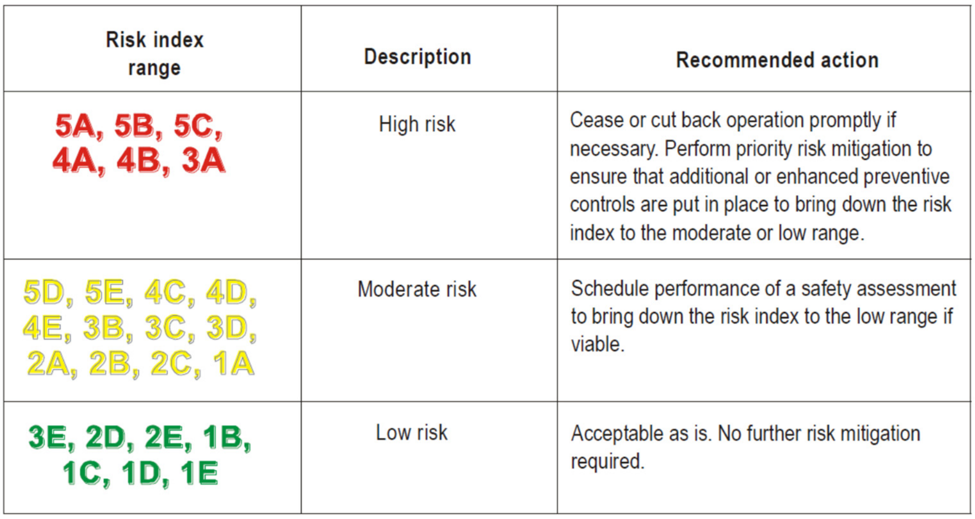

Risk index range	Description	Recommended action
5A, 5B, 5C, 4A, 4B, 3A	High risk	Cease or cut back operation promptly if necessary. Perform priority risk mitigation to ensure that additional or enhanced preventive controls are put in place to bring down the risk index to the moderate or low range.
5D, 5E, 4C, 4D, 4E, 3B, 3C, 3D, 2A, 2B, 2C, 1A	Moderate risk	Schedule performance of a safety assessment to bring down the risk index to the low range if viable.
3E, 2D, 2E, 1B, 1C, 1D, 1E	Low risk	Acceptable as is. No further risk mitigation required.

The safety risk matrix of ICAO can be treated as an example only and is not necessarily suited to the requirements of the assessment of all risks. The ARMS working group introduced the term ***event risk***, which focuses on a certain safety event only, without taking into consideration all similar events, which are the result of the same hazard [16,17]. A safety event is an undesired occurrence or state with the potential of a loss, e.g. an incident or a significant deviation from a limit (i.e. "near miss") [7].

2.6 Event Risk Classification (ERC)

The safety risk assessment as shown in the previous section comes to a limit when dealing with the risk of historical events. The main objective of an Event Risk Classification (ERC) is to allow initial risk classification of any incoming safety event on a standardized basis. Individual safety events may contain a high level of risk, and therefore immediate action is required [16]. The aggregation of individual event risks is an adequate means for safety performance monitoring.

Since risk is a state of uncertainty about the possibility of a loss or damage, risk should technically relate to something in the future where the outcome is uncertain [16]. Most of the considered safety events contain no risk at the moment, in which they are assessed, since they have already occurred. However, at the moment they occurred, they did carry risk. Hence, the event risk can be described as the risk, which was there when the event happened.

The ERC does not replace a risk assessment according to the previous section, because it does not consider the number of events as well as the number of flights without events. The ERC is based on the concept of "event-based risk level", which represents an assessment of the risk level of this one event and not of the risk associated with all similar events, i.e. all events which result from the same hazard [17]. The difference lies in the probability part of the respective risk. While the probability of the risk of all similar events is the overall probability of a certain consequence, caused by a hazard, the probability of an event risk is the conditional probability of the consequence, caused by the specific event. In other words, the event risk is a sub-group of the overall risk, which was contributed by the specific event.

This principle can be seen in Figure 2-9. For a certain hazard, the overall risk is defined by the severity of the consequence as well as the *overall probability of consequence*, as indicated at the bottom of the graph. This overall probability is equal to the product of the *average event probability* and the *average conditional probability*, which is the probability of the consequence, once the event has occurred. The *average event probability* is defined by the number of events in relation to the number of conducted flights or flight hours.

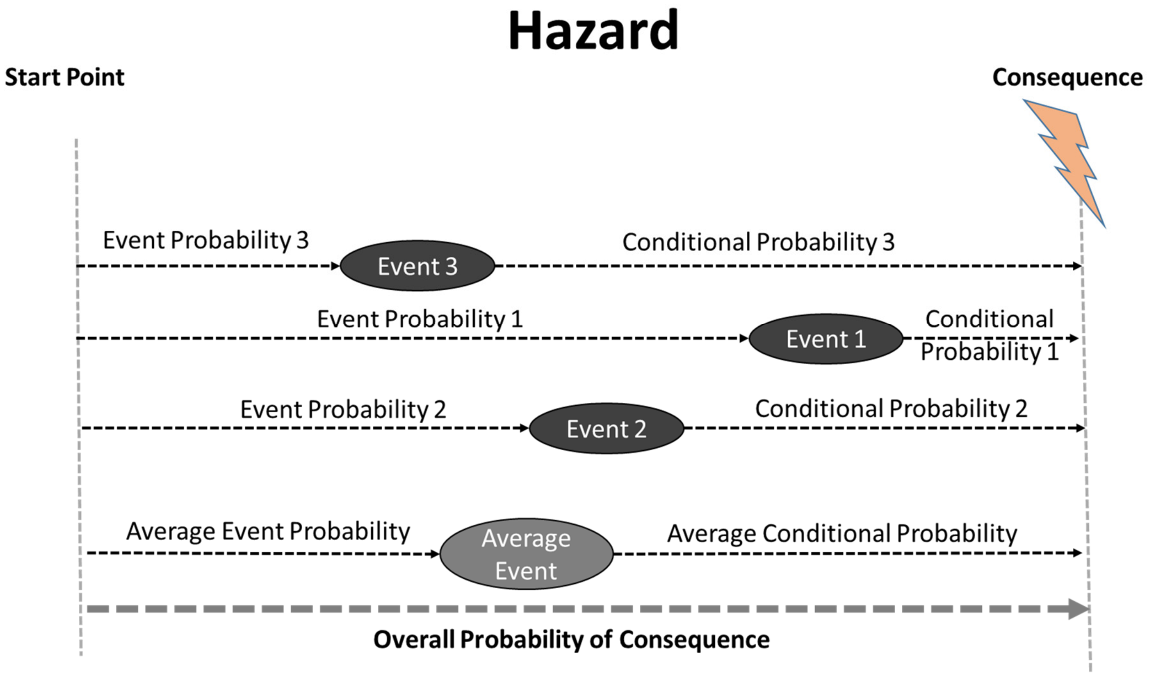
Hazard
Start Point
Consequence
Event Probability 3
Event 3
Conditional Probability 3
Event Probability 1
Event 1
Conditional Probability 1
Event Probability 2
Event 2
Conditional Probability 2
Average Event Probability
Average Event
Average Conditional Probability
Overall Probability of Consequence

Figure 2-9 Relationship between overall risk and event risk. A shorter arrow length indicates a higher conditional probability. Source: own research

If focusing on individual events, which is conducted in ERC, each event might be either closer or more distant to the considered consequence, i.e. accident scenario, regarding probability. In above graph, Event 1 is drawn closer to the consequence, thus, the conditional probability of Event 1 is higher than for the other events. Since all events refer to the same consequence, the risk level of an event is higher, if the respective conditional probability is higher. Hence, Event 1 has the highest event risk level in this example.

2.6.1 The Methodology of ERC

The ARMS working group recommends that the ERC should preferably be carried out within one or two days of the occurrence of the the safety event and should be conducted by a person with operational experience trained in risk assessment (Safety Analyst) [16].

A key priority of the ARMS methodology is the utmost reduction of subjectivity of the Safety Analyst. Instead of assessing the risk of a similar event taking place in the future, the analyst should focus on the remaining safety barriers, which avoided the event resulting in the considered consequence. The ARMS method therefore considers only the likelihood of the remaining barriers failing, not the probability of the event itself or the overall probability of the worst foreseeable outcome happening. Even though the consideration of these safety barriers is still subjective to a certain extent, this subjectivity can be reduced by a good understanding of the barriers present in typical scenarios. The sum of all event risks indicates the "historic" amount of risk which was taken.

The event risk classification is conducted by use of an ERC matrix. The ARMS working group proposes a 4 x 4 matrix, as shown in Figure 2-10. The event risk classification result is based on two questions [16]:

- *If this event had escalated into an accident, what would have been the most credible accident outcome?*
- *What was the effectiveness of the remaining barriers between this event and the most credible accident outcome?*

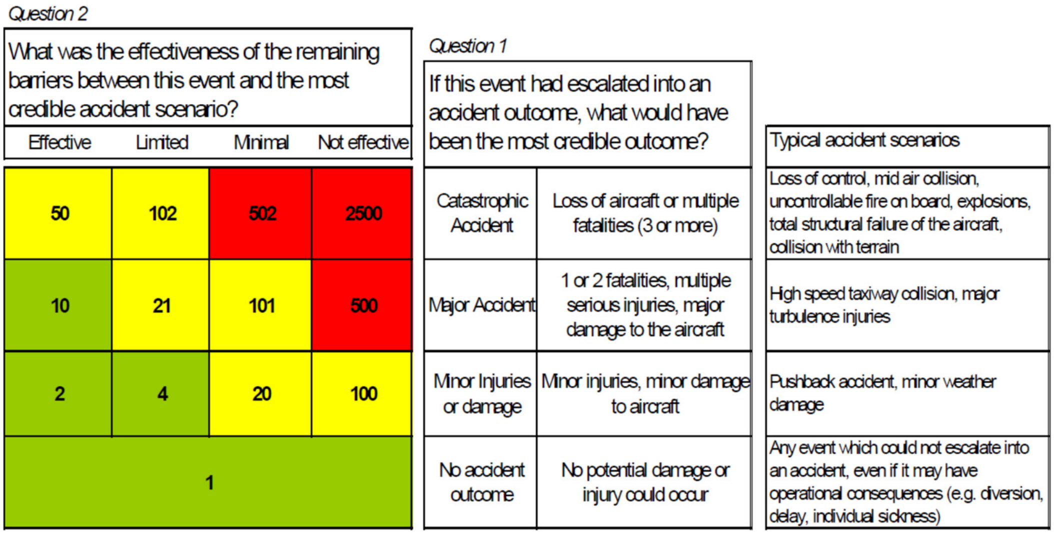

Question 2

What was the effectiveness of the remaining barriers between this event and the most credible accident scenario?

Question 1

If this event had escalated into an accident outcome, what would have been the most credible outcome?

Effective	Limited	Minimal	Not effective			Typical accident scenarios
50	102	502	2500	Catastrophic Accident	Loss of aircraft or multiple fatalities (3 or more)	Loss of control, mid air collision, uncontrollable fire on board, explosions, total structural failure of the aircraft, collision with terrain
10	21	101	500	Major Accident	1 or 2 fatalities, multiple serious injuries, major damage to the aircraft	High speed taxiway collision, major turbulence injuries
2	4	20	100	Minor Injuries or damage	Minor injuries, minor damage to aircraft	Pushback accident, minor weather damage
1				No accident outcome	No potential damage or injury could occur	Any event which could not escalate into an accident, even if it may have operational consequences (e.g. diversion, delay, individual sickness)

Figure 2-10 Event risk classification matrix, as proposed by ARMS working group [16]

According to ARMS, the purpose of the first question is to evaluate the accident outcome that is of most concern when the event occurs [16]. The question, what kind of accident should be tried to avoid by the reported kind of event, is not asking for the most probable outcome. The most probable outcome is usually "nothing", and therefore ignores any risk that the event has carried. However, considering the worst possible outcome as the worst-case scenario may not be the most obvious accident to expect from the reported event. If it is virtually impossible that the event could have escalated into an accident, the bottom line in the ERC risk matrix should be selected ("*no accident outcome*"). Otherwise, if in doubt about the possible accident scenario, the table on the right-hand side of Figure 2-10 can be used, which indicates *typical accident scenarios*.

A certain amount of subjectivity between different analysts can be expected in the answer to the first question. This depends on the background knowledge or experience of the analysts regarding the causes of the event. The overall results of the ERC in terms of risk level is nevertheless expected to be similar, since the event risk level depends also on the answer to the second question. The second question considers the remaining safety barriers, and hence the probability of the accident scenario. Since the probability depends on the considered accident scenario, this probability will vary accordingly to fit this accident scenario.

The second question only considers the remaining safety barriers. The purpose is to estimate the probability of further escalation into the most credible accident outcome (of Question 1). Only those safety barriers, which eventually stopped the event from escalating, are considered, since they were still in place. The already failed barriers, however, are not considered for the answer of question 2.

For the determination of the correct answer to the second question, the ARMS working group provides the following definitions regarding the effectiveness of the remaining barriers [16]:

- ***Not effective:*** *The accident could only be prevented by either pure luck or exceptional skills, which is neither trained nor required.*
- ***Minimal:*** *Some safety barriers were still in place, but their total effectiveness was minimal, e.g. a Ground Proximity warning (GPWS) just before an imminent Controlled Flight into Terrain (CFIT).*
- ***Limited:*** *The effectiveness of the remaining safety barriers was limited. This is usually an abnormal situation, which is more demanding to manage, but with still a considerable remaining safety margin, e.g. a moderate error in load sheet or loading with the effect of slight rotation problems at takeoff.*
- ***Effective:*** *The safety margin was effective, typically consisting of several good safety barriers, e.g. a passenger smoking in the lavatory versus in-flight fire accident.*

Since still a certain subjectivity in the answer to the second question can be expected, a data-driven approach, as presented in this dissertation thesis, can significantly reduce this subjectivity. In this case, instead of focusing on the remaining safety barriers, which was used as a work-around to reduce subjectivity in the estimation, the conditional probability can be evaluated directly from operational (flight) data. The conditional probability is the probability that the considered accident scenario evolves, under the condition that the event takes place [17].

However, an evaluation of remaining barriers by means of flight data analysis is not exactly possible. Instead, the approach of risk assessment in this dissertation deviates to a certain extent from the ARMS method.

If a safety event that occurred in the past is to be assessed, this event has usually not resulted in an accident. However, if the same event would reoccur in the future, it can be expected that the environmental conditions might slightly differ and thus, a certain probability of an accident will exist.

As an example, a runway overrun scenario can be considered. A certain landing scenario is assumed to be repeated several times with exactly the same conditions regarding aircraft state, i.e. the energy status of the aircraft and the remaining runway distance, as observed in the considered event. However, the environmental conditions, i.e. the runway friction values, are varied. The influence of the different environmental conditions on the aircraft state finally results in a certain probability of an overrun. This variation of runway friction values seems to be reasonable, since in the real environment this kind of uncertainty is actually observable. The risk of the considered safety event is therefore evaluated under the assumption, that the pilot would behave exactly in the same way as observed in the event, but with slightly different environmental conditions. The latter might lead eventually to an accident and therefore defines the probability part of the event risk.

2.6.2 Risk Tolerability

The ERC has two outputs. The first output is the color of the matrix element, which indicates what should be done about the event. The results should be interpreted as follows, see also Figure 2-11 [16]:

- *Red:* The event can be considered to be a safety issue. An immediate in-depth investigation is due
- *Yellow:* The event should be investigated and/or risk assessed in more depth
- *Green:* Use for continuous improvement, flows into the safety database

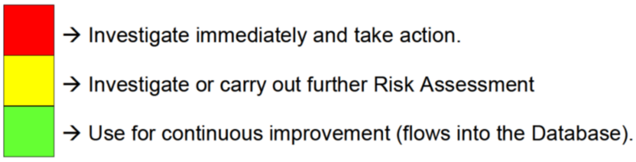
🟥 → Investigate immediately and take action.
🟨 → Investigate or carry out further Risk Assessment
🟩 → Use for continuous improvement (flows into the Database).

Figure 2-11 Recommended actions on the ERC results [16]

The second output is the ERC risk index, which provides a quantitative relative risk value. This risk index enables the aggregation of safety or risk data for the compilation of statistics [16], see chapter 2.6.4. The risk index can be derived from the ERC risk matrix directly (see Figure 2-10) and ranges from 1 (lowest risk index) up to a value of 2,500 (highest risk index). If several accident scenarios are evaluated for the same event, which lead to different risk indices, the highest risk index shall be used.

Several considerations on the risk index have been made by the ARMS working group. Agreement existed about an exponential scale in both dimensions to reflect the difference in risk between the matrix elements. Since the differences in risk contained in actually reported events are indeed significant, the group decided on the difference between highest and lowest risk index at a factor of 2,500. The relationship between the different severities of the accident scenarios in adjacent ERC matrix rows were evaluated at a value of 5 each. For the probabilities, a factor of 2 was used for the lower probabilities, i.e. the difference between effective and limited barriers, and a factor of 5 was used between the higher probabilities. The bottom row, however, is a single block due to the fact, that this row corresponds to the case "no potential damage or injury could occur" and thus, it makes no sense to estimate the respective effectiveness of the remaining safety barriers. To clearly assign every matrix element one defined risk index value, risk indices of the same magnitude have been adjusted by adding a small increment of 2 for the top-row values and 1 for the second-row values. The impact caused by those increments on the ERC index values are negligible.

2.6.3 Customized Risk Matrix

According to the ARMS working group, the proposed methodology including the ERC matrix might not fit the needs of all organizations [16]. Daily practical use of the methodology has shown that especially the resolution of the matrix may not be accurate enough to classify safety events accurately enough. E.g. for the needs of FDA events, where a more precise differentiation of the probability levels might be possible due to data-driven methods, the resolution of the matrix is not adequate.

Mickel therefore proposes a 7 x 13 matrix, containing 7 different accident scenarios and 13 conditional probabilities [17], as shown in Figure 2-12. Since this extended matrix, also referred to as *Event Severity Classification* (ESC) matrix, is more adequate for practical safety work, this customized matrix is meanwhile widely used by several airlines within Europe. EASA is currently in a development process of a similar approach, using a 5 x 10 matrix, called *European Risk Classification Scheme* (ERCS) [41]. Instead of risk indices ranging from 1 to 2,500, which are used in the ARMS ERC matrix, Mickel uses Risk Units (RUs), ranging from 0.000001 to 100. In this risk metric, a serious incident is represented by one Risk Unit. For simplification purpose, besides the logarithmic scale of the Risk Units, a linear scale is additionally used, containing values from *h* to *a*. Mickel uses the term *Event Severity Index* for this linear scale. After the initial development, the matrix contained less elements. However, during daily practical safety work, the requirement for a more precise differentiation lead to the deployment of intermediate matrix elements on the probability scale, since some conditional probabilities did not adequately fit the scenario. Thus, the number of matrix elements in the probability scale was doubled. The same applied to the severity scale.

Due to its high level of practical use, the event severity classification matrix of Mickel is used as a basis for risk classification within the scope of this thesis. However, since the classification in this thesis is data-driven and does not rely on a safety expert estimation, a discrete matrix is not necessary. Thus, only the scale of the ESC matrix is used, not the matrix itself. The resulting Risk Units can therefore fall between the discrete event severity indices.

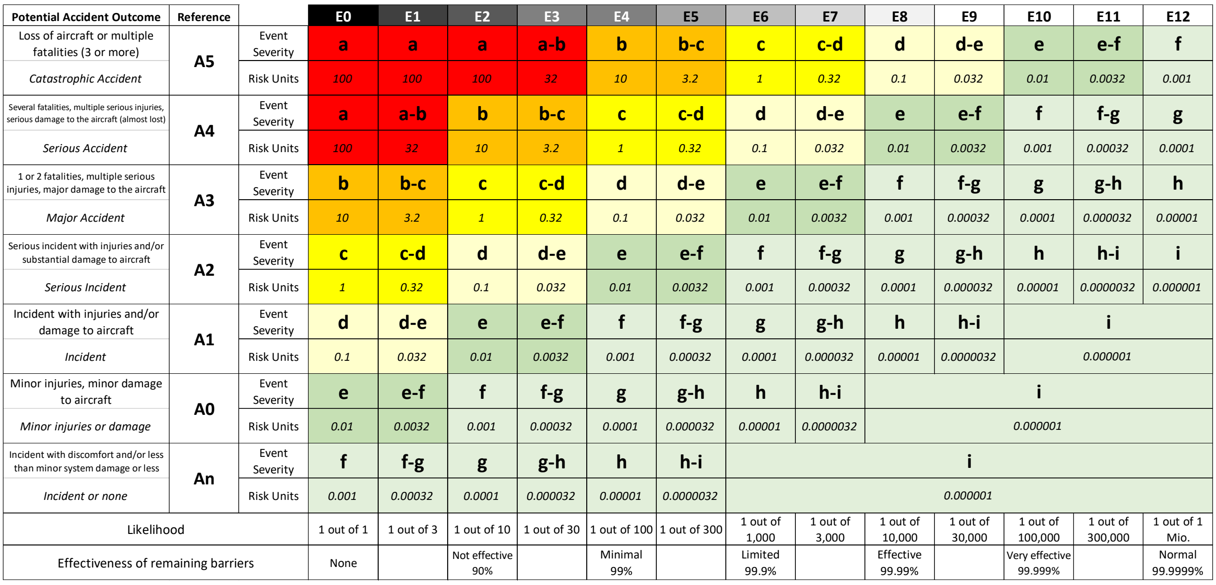

Potential Accident Outcome	Reference		E0	E1	E2	E3	E4	E5	E6	E7	E8	E9	E10	E11	E12
Loss of aircraft or multiple fatalities (3 or more)	A5	Event Severity	a	a	a	a-b	b	b-c	c	c-d	d	d-e	e	e-f	f
Catastrophic Accident		Risk Units	*100*	*100*	*100*	*32*	*10*	*3.2*	*1*	*0.32*	*0.1*	*0.032*	*0.01*	*0.0032*	*0.001*
Several fatalities, multiple serious injuries, serious damage to the aircraft (almost lost)	A4	Event Severity	a	a-b	b	b-c	c	c-d	d	d-e	e	e-f	f	f-g	g
Serious Accident		Risk Units	*100*	*32*	*10*	*3.2*	*1*	*0.32*	*0.1*	*0.032*	*0.01*	*0.0032*	*0.001*	*0.00032*	*0.0001*
1 or 2 fatalities, multiple serious injuries, major damage to the aircraft	A3	Event Severity	b	b-c	c	c-d	d	d-e	e	e-f	f	f-g	g	g-h	h
Major Accident		Risk Units	*10*	*3.2*	*1*	*0.32*	*0.1*	*0.032*	*0.01*	*0.0032*	*0.001*	*0.00032*	*0.0001*	*0.000032*	*0.00001*
Serious incident with injuries and/or substantial damage to aircraft	A2	Event Severity	c	c-d	d	d-e	e	e-f	f	f-g	g	g-h	h	h-i	i
Serious Incident		Risk Units	*1*	*0.32*	*0.1*	*0.032*	*0.01*	*0.0032*	*0.001*	*0.00032*	*0.0001*	*0.000032*	*0.00001*	*0.0000032*	*0.000001*
Incident with injuries and/or damage to aircraft	A1	Event Severity	d	d-e	e	e-f	f	f-g	g	g-h	h	h-i	i		
Incident		Risk Units	*0.1*	*0.032*	*0.01*	*0.0032*	*0.001*	*0.00032*	*0.0001*	*0.000032*	*0.00001*	*0.0000032*	*0.000001*		
Minor injuries, minor damage to aircraft	A0	Event Severity	e	e-f	f	f-g	g	g-h	h	h-i	i				
Minor injuries or damage		Risk Units	*0.01*	*0.0032*	*0.001*	*0.00032*	*0.0001*	*0.000032*	*0.00001*	*0.0000032*	*0.000001*				
Incident with discomfort and/or less than minor system damage or less	An	Event Severity	f	f-g	g	g-h	h	h-i	i						
Incident or none		Risk Units	*0.001*	*0.00032*	*0.0001*	*0.000032*	*0.00001*	*0.0000032*	*0.000001*						
Likelihood			1 out of 1	1 out of 3	1 out of 10	1 out of 30	1 out of 100	1 out of 300	1 out of 1,000	1 out of 3,000	1 out of 10,000	1 out of 30,000	1 out of 100,000	1 out of 300,000	1 out of 1 Mio.
Effectiveness of remaining barriers			None		Not effective 90%		Minimal 99%		Limited 99.9%		Effective 99.99%		Very effective 99.999%		Normal 99.9999%

Figure 2-12 Event risk classification matrix, as proposed by Mickel [17]

Mickel adapted the risk tolerability scheme of ARMS, as shown in Figure 2-12, to fit the Event Severities of the customized ESC matrix. Moreover, he added recommended actions for every involved stakeholders within the safety structure of the organization, aiming especially for airlines [17], see Table 2-6.

Table 2-6 Recommended action [17]

Event Severity	ASR/CSR (Accident/Incident Investigation Team)	FDA Team	Safety Assurance Team	Safety Promotion Team
a, a-b	Investigate immediately and take action if required	Check ASR/CSR or request trusted pilot, consider event for quarterly report (especially if ORG error)	Update or add hazard in hazard registry, update bow tie, consider or update operational risk assessment, presentation in Safety Review Board (SRB)	Publication in Safety Bulletin is recommended, presentation for seminars and pilot meetings is recommended
b, b-c	Investigation candidate			
c, c-d	Potential investigation candidate, use for continuous improvement	Optionally check ASR/CSR or request trusted pilot, may be mentioned in report	May be used for Safety Performance Indicators (SPIs)	Use is optional (typically if HUM error is involved)
d, d-e	Flows into the database	May be used for safety campaigns	Monitor	Optional
e, f	No action required			

Sometimes the safety analysts may have difficulties in estimating the remaining barriers in terms of quantification. To facilitate the classification, Mickel introduced additional guidance by fuzzy event severity categories providing a verbal description of the five main ESC outcomes, which can be seen in the following table [17]:

Table 2-7 Verbal description of the five main ESC outcomes [17]

Event Severity	Verbal description
a	close call or major damage, accident
b	heavy stuff
c	take seriously
d	interesting
e	nice to know
f - i	no significant additional risk, single event not safety relevant

A conversion between Risk Units and ERC indices and vice versa is easily possible using Table 2-8. Note that there is no fixed equation for the conversion, since the scale of the ERC indices is skewed from a certain point.

Table 2-8 Conversion between ERC risk indices and Risk Units [17]

Event Risk	Risk Units	ERC index	ARMS Recommendation
a	100	2,500	Investigate immediately and take action
a-b	32	1000*	
b	10	500	
b-c	3.2	200*	
c	1	100	Investigate or carry out further risk assessment
c-d	0.32	40*	
d	0.1	20	
d-e	0.032	6*	
e	0.01	2	Use for continuous improvement (flows into database)
f-i	≤ 0.001	1	

*interpolated

2.6.4 Safety Data Analysis

With safety data analysis, i.e. the aggregation of the gathered safety data, a trend analysis can be compiled, if the data is displayed in chronological order. Also, clusters of related events can be identified, if the data is broken down for certain aspects, e.g. location or flight phase of the events [16]. With this method, safety issues affecting the current operation can be identified. In general, safety data analysis can provide a picture of the current safety performance of the organization.

Aggregated safety data can be presented as "number of events", which is a value without the context of reference values. Usually, the "rate of events" is more meaningful, since the number of reference values is taken into consideration. E.g. the number of unstable approaches might be the highest at the home base airport. Since the number of flights is much higher at this airport, the rate of unstable approaches to this airport might be even the lowest of all airports. However, both methods might not reflect the actual risk, which is contained in the data. Coming back to the example, the risk, which evolves from the unstable approaches, e.g. the risk of a runway overrun following an unstable approach, also depends on e.g. the respective runway length and runway condition [14].

The ARMS methodology enables a risk-based data analysis, because the risk index of each event reflects the contained risk and thus, a sort of "weight" regarding safety. Since each event is independent from the others, provided only one event per flight or hazard is taken into consideration, the amount of the resulting risk indices can be summed up to obtain the cumulative risk of a batch of events [16].

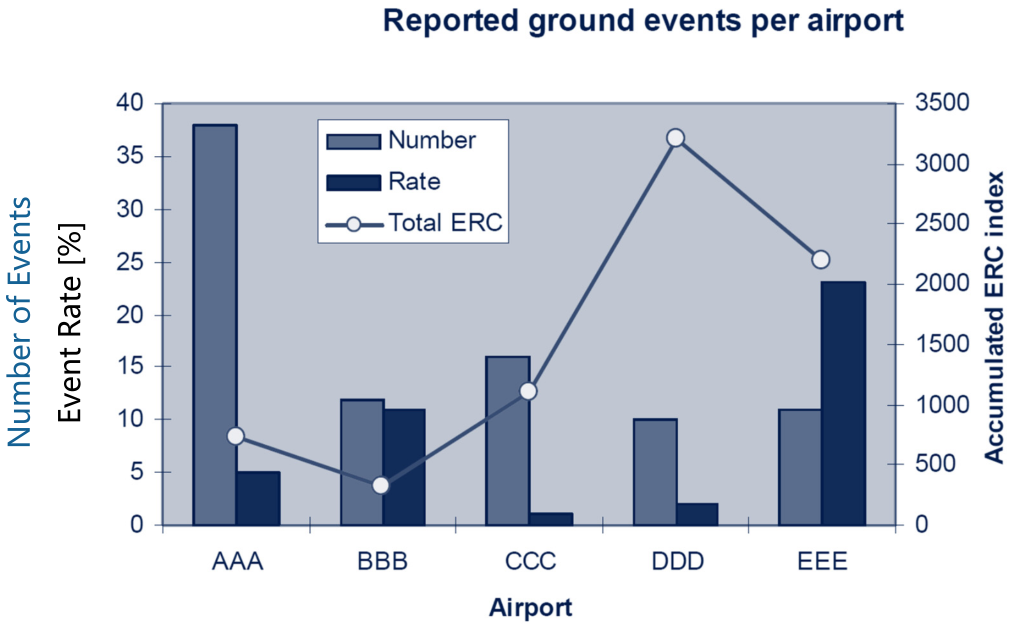

Figure 2-13 A fictitious example of cumulative ERC risk index use, adapted from [16]

Figure 2-13 shows a fictitious example of a data analysis of ground events, broken down by airports. In this diagram, the respective number of events, rate of events as well as the cumulated ERC risk index are displayed. The highest number of events could be observed at airport *AAA*, however, the rate of events is relatively low. The highest rate of events could be observed at airport *EEE*, even though the absolute number of events is at an average level. But neither of both airports contain the highest risk. According the ERC risk index, airport *DDD* could be identified as the airport with the highest risk of all airports, even though both the number of events as well as the rate of events is relatively low. As a result, the ground events at airport *DDD* could typically become a safety issue. This example shows that focusing on risk instead of a pure "counting" of events is an added value from the perspective of safety management.

It is worth noting that the risk level also depends on the number of flights. If e.g. the number of flights of an airline would increase, the absolute number of events would be expected to increase proportionally. However, provided the probabilities of the different events are constant, the event rate would stay constant even with the increase in the number of flights. The ERC risk index would increase, since the risk exposure would increase due to the higher number of flights.

On the other hand, if the portion of unreported events is high, the risk will be underestimated, since not all events are considered in the cumulated ERC risk index. Sometimes the proportion of unreported events is unknown, which is even more concerning. This typically applies in the context of safety reports.

In contrast to safety reports, with Flight Data Analysis the number of undetected events can be estimated without much effort, which results in a more reliable cumulative risk level. The data acquisition rate r_{Ev} is defined as the number of flights available in the FDA system in relation to the number of conducted flights [7]. If the considered event type is equally distributed over all flights, the cumulated risk index can be corrected by dividing the cumulated ERC risk index by the data acquisition rate r_{Ev} [7].

Another problem with the aggregation of risk indices is redundancy of events. The risk contributions of different event types within the same flight, which are related to the same occurrence category, cannot be simply added, since a certain correlation of the results is contained in the risk indices. This can typically be observed in FDA, where a lot of redundant, slightly different event types exist to cover the same occurrence category. An example is the occurrence category *runway excursion*, which might be covered by the event types "*landing on critical runway*", "*long flare*", "*tailwind limit exceedance on landing*" and "*high speed when approaching runway end*".

The event "*landing on critical runway*" describes a landing, where the required landing distance under the observed environmental factors is critical in relation to the available runway length. The event "*long Flare*" describes a situation where the air segment of the landing is longer than expected and thus, results in a shorter remaining distance to stop the aircraft. "*Tailwind limit exceedance on landing*" is an event where the maximum allowable tailwind component is exceeded during landing, which increases the ground speed and thus, the energy of the aircraft. "*High speed when approaching runway end*" is a scenario, where the speed of the aircraft is still relatively high at a close distance of the aircraft to the runway end. All four events therefore describe a scenario with an increased probability of a runway overrun. However, in a situation where all four events are triggered and thus, have to be assessed, it might be difficult to separate the risk contributions of the individual events to the runway overrun scenario, since in this example the event "*high speed when approaching runway end*" may be the result of one or more of the first three event types.

Two possibilities exist to circumnavigate this problem. If the risk index is assessed by a safety analyst, only the event with the strongest relation to the consequential hazard can be considered; the rest may be ignored or downgraded. The other possibility is the implementation of a single event covering the scope of all other events. In the example of the runway overrun given above, in chapter 5 such a single event will be presented, covering the scope of all four mentioned events.

Finally, events which cannot be measured, are not considered for the overall risk within an occurrence category. An example is the event "*bird strike*", which does not exist in FDA, since no sensor or parameter exist to measure this scenario.

3 The Concept of a Safety Management System

A safety management system can generally be defined as "*a planned, documented and verifiable method of managing hazards and associated risks*" [42]. ICAO defines an SMS more specifically as "*a systematic approach to managing safety, including the necessary organizational structures, accountabilities, policies and procedures*" [2].

The concept of a Safety Management System shifts responsibility towards the organizations by managing their risks on their own, instead of the solely regulatory approach. This concept was originally implemented in the occupational health and safety from the mid-1970s following catastrophic events, e.g. the Seveso disaster in the chemical industry in 1976, with the intention to protect individual employees from harm [43].

The concept is based on a transition from the traditional compliance-based prescriptive scheme towards a performance-based approach, where safety responsibilities are partly transferred from the authorities towards the service providers. These organizations must find a way to achieve the required safety performance standards without detailed requirements on how to achieve this [10]. The organizations which have to implement the SMS have the deepest insight into their internal managerial structures and procedures, and thus, are able to identify hazards in their operation more efficiently than the respective authority.

The difference between the traditional regulatory scheme and the performance-based approach with regard to safety is depicted in Figure 3-1.

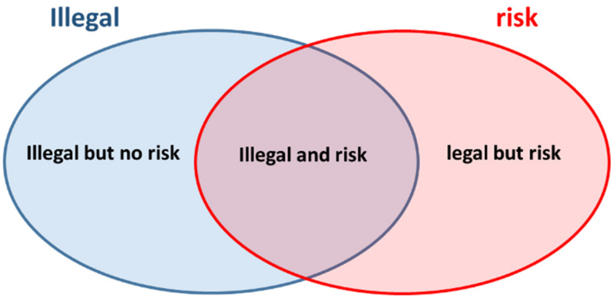

Figure 3-1 Difference between compliance and safety based on [44]

In this graph, the compliance-based scheme is displayed as a blue ellipsoid, while the performance-based scheme is symbolized as a red ellipsoid. Not all of the rules and requirements of the compliance-based scheme are related to the management of risk. The major part of the blue ellipsoid is regulated, even though there is a lack of risk, which can be considered as a poor use of resources ("*Illegal but no risk*") [44]. Only the overlapping part of the ellipsoids symbolizes an efficient safety regulation in this prescriptive regulatory approach ("*illegal and risk*"). On the other hand, not all areas of risk can be covered by regulations ("*legal but risk*"). A more efficient way to manage the risks is the shift of responsibility towards the service provider, which is able to manage with the focus on risk. An efficient functioning SMS is capable to shift the focus towards the right-hand side of the graph, i.e. focused on risk. The regulatory part of the authority is reduced to verify that the requirements of the implementation of the SMS are met, and the respective safety performance is achieved.

Safety management is considered by ICAO as a management process with responsibilities at two levels: the state level and the level of the individual service provider [28]. The states are responsible for the establishment of a safety program, which consists of an integrated set of regulations and activities aiming for the improvement of safety. As part of such program the service providers must establish a Safety Management System, which has to be accepted by the state. According ICAO, the minimum requirements of an SMS are [2]:

- *Identification of safety hazards,*
- *To ensure the implementation of remedial action, which is necessary to maintain an agreed level of safety*
- *Monitoring and assessment of safety performance and*
- *A continuous improvement of the overall performance of the SMS.*

Many elements of a safety management system have evolved from an industry best practice towards a regulatory requirement. The basic concept was developed in the mid-2000s by ICAO in cooperation with the Industry Safety Strategy Group (ISSG)[7] through a Global Aviation Safety Roadmap, which aimed for the reduction of accident risks for commercial aviation by a more proactive approach [8]. Based on that concept, ICAO developed an integrated approach to safety initiatives and provided a global framework for the coordination of safety policies and initiatives. This proactive approach to safety required the involvement of all concerned stakeholders.

ICAO published the first edition of the Safety Management Manual (SMM)[8] in 2006, which served as a guideline for the implementation of a Safety Management System in aviation. The SMM was the successor of the Accident Prevention Manual (ICAO Doc 9422), which had been

[7] Members of the ISSG are Airbus, Boeing, Airports Council International (ACI), Civil Air Navigation Services Organization (CANSO), International Air Transport Association (IATA), International Federation of Air Line Pilots' Associations (IFALPA) and Flight Safety Foundation (FSF) [8]

[8] Also called ICAO Doc 9859

published in 1984 for the first time, and formed the basis of the Accident Prevention Program, a previous concept to proactively prevent aviation accidents. The SMM was revised two times until 2012, when the safety regulations, which had been widely distributed over six different ICAO Annexes, were consolidated into a new Annex in 2013. This novel ICAO Annex 19 was the first new release of an ICAO Annex for the last 30 years, which emphasizes the importance of SMS from the perspective of ICAO [19].

ICAO Annex 19 refers to both ICAO member states and to service providers[9]. Service providers must implement a safety management system. However, the implementation is enforced on a national level, e.g. for Germany, commercial airlines had to implement an SMS by 2009.

From 2012, when the European Commission released the Commission Regulation (EC) No 965/2012, the corresponding regulation, called *Implementing Rules – Operations (IR-OPS)*, is "*binding in its entirety and directly applicable in all Member States*" [9]. Within the scope of EASA, a Safety Management System is mandatory for all commercial airlines since October 28th 2012 [9]. EASA provides additional information about how to comply with the requirement of a safety management system in the Acceptable Means of Compliance (AMC) and the Guidance Material (GM), which are both non-binding documents.

[9] including airlines, airports, air navigation service providers etc.

3.1 Structure of a Safety Management System (SMS)

The structure of a Safety Management System consists of four components, as depicted in Table 3-1. Each component consists of several elements. The four components are described in more detail in the following subchapters.

Table 3-1 Components and elements of a Safety Management System [2]

SMS framework components	SMS framework elements
1. Safety policy and objectives	1.1 Management commitment and responsibility 1.2 Safety accountabilities 1.3 Appointment of key safety personnel 1.4 Coordination of emergency response planning 1.5 SMS documentation
2. Safety risk management (SRM)	2.1 Hazard identification 2.2 Risk assessment and mitigation
3. Safety assurance	3.1 Safety performance monitoring and measurement 3.2 The management of change 3.3 Continuous improvement of the SMS
4. Safety promotion	4.1 Training and education 4.2 Safety communication

3.1.1 Safety Policy and Objectives

The safety policy and objectives form the regulatory framework of a Safety Management System. This component shall in general be defined by top management, which commits itself to safety by defining safety objectives [2,19]. The safety objectives are the basis of the Safety Management System. Since an SMS shall be a top-down approach, the involvement of top management at this point is of great importance. The safety commitment and responsibility shall be documented in the safety policy in accordance with international and national requirements. The safety policy is signed by the accountable executive and shall be accessible by all employees throughout the organization.

Besides the identification of the accountable executive who has the ultimate responsibility and accountability on behalf of the organization, also the accountabilities of all members of management as well as of employees with regard to safety have to be defined [2]. This includes the appointment of a safety manager, who is responsible for the implementation and maintenance of the SMS.

In general, the top management is responsible for provision and allocation of resources, which are necessary to achieve the safety objectives. The available resources have to be allocated efficiently to navigate through the safety space, which can be imagined as an optimum balance between the contradictory factors of production and protection, as depicted in Figure 3-2.

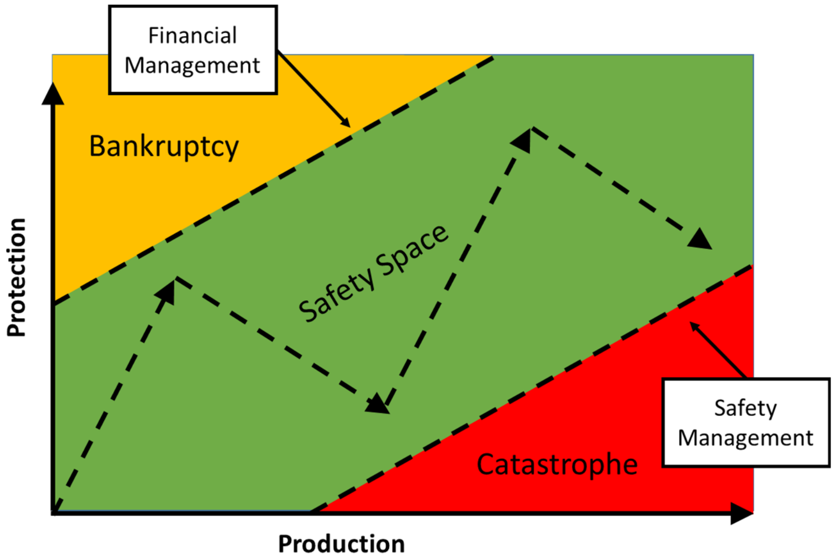

Figure 3-2 Safety space based on [2]

If the organization primarily focuses on production, the probability of a catastrophic outcome by means of an accident rises. On the other hand, if the organization focuses primarily on protection, it is likely that the organization will end up in bankruptcy due to the high costs of safety. A functioning and effective SMS will help the organization to smoothen the zig-zagged pathway through the safety space, making it more transparent where the organization is currently located with regard to the borderlines between catastrophe and bankruptcy.

Another important element is the SMS documentation. In addition to the safety policy, the ICAO lists the following items that an SMS documentation must contain [2]:

- *SMS requirements*
- *SMS processes and procedures*
- *Accountabilities, responsibilities and authorities for SMS processes and procedures*
- *SMS outputs*

As part of the documentation, an SMS manual shall be developed and maintained.

3.1.2 Safety Risk Management

The Safety Risk Management component is one of the core operational activities within the SMS. The process is activated whenever a new hazard has been identified, as described in chapter 2.4. The identification of a new hazard can occur during routine operation, e.g. by an Air Safety Report due to an operational incident, or proactively during a planned change within the operation (e.g. a new destination). In the latter case, the identification usually occurs during the operational risk assessment, which is required for every planned change which might affect the safety [2,45].

If a new hazard has been identified, the underlying risk has to be assessed in terms of severity and probability, which has been described in chapter 2.5. Once the assessment of the risk has been conducted and the risk level has been identified, the risk tolerability has to be evaluated. If the risk level falls into an acceptable region, the operation can be continued without further action. However, if the risk is not acceptable, it has to be checked whether the risk can be eliminated or mitigated. Only if the risk level is acceptable after mitigation, the operation can be continued. Otherwise, the operation has to be cancelled.

The Safety Risk Management process can be seen in Figure 3-3.

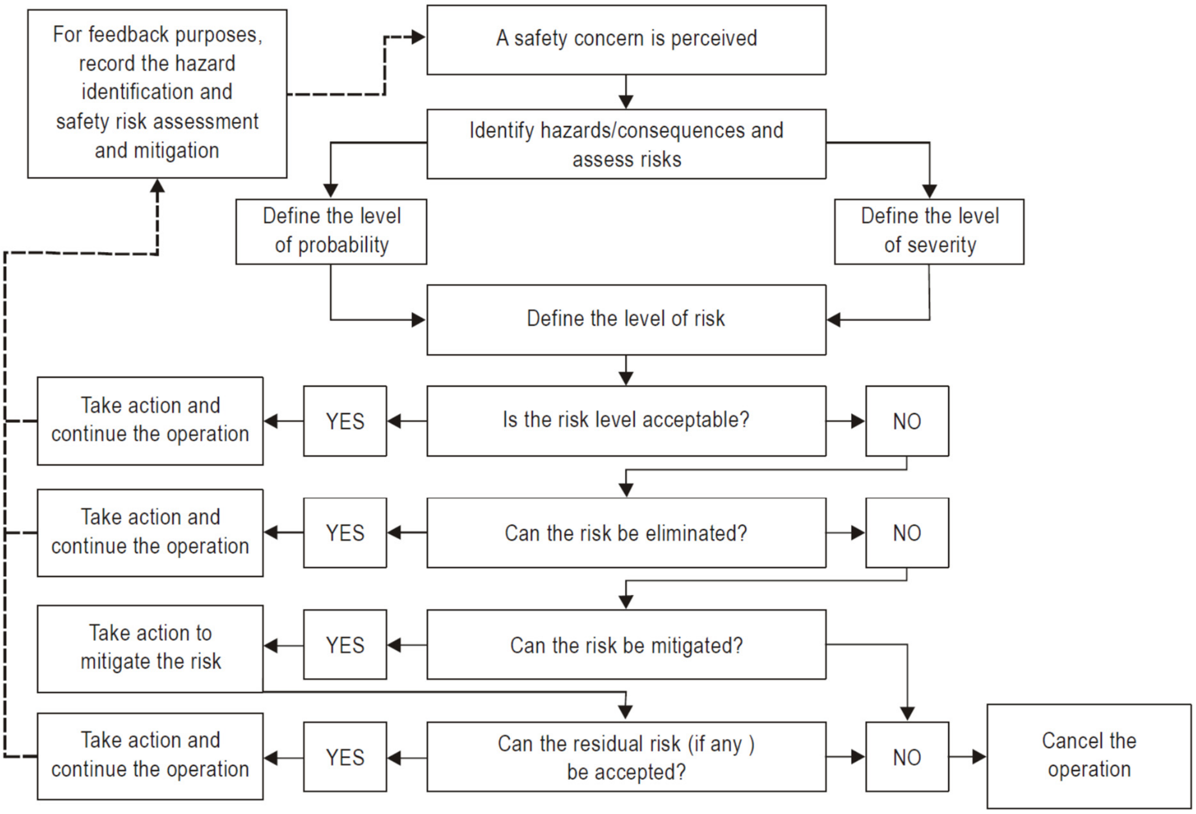
For feedback purposes, record the hazard identification and safety risk assessment and mitigation
A safety concern is perceived
Identify hazards/consequences and assess risks
Define the level of probability
Define the level of severity
Define the level of risk
Take action and continue the operation
YES
Is the risk level acceptable?
NO
Take action and continue the operation
YES
Can the risk be eliminated?
NO
Take action to mitigate the risk
YES
Can the risk be mitigated?
Take action and continue the operation
YES
Can the residual risk (if any) be accepted?
NO
Cancel the operation

Figure 3-3 Safety Risk Management process according ICAO [2]

3.1.3 Safety Assurance

The component of Safety Risk Management is only one part of the overall safety management cycle. To complete this cycle, feedback on the safety performance is necessary [3]. A good understanding of operational processes and the environment enables safety management to develop and implement appropriate safety risk controls where deficiencies have been identified. Continuous monitoring and feedback after the implementation assure that all risk controls work as intended. A well performing safety assurance can detect safety risks emerging from internal or external changes, or any deviation from the desired baseline (practical drift, see 2.2) [19]. This requires an adequate measurement of the actual safety performance in the organization. The safety assurance process provides the required confidence about an acceptable level of safety and the effectiveness of existing safety risk controls in an organization [3].

The safety assurance process and the traditional process of quality assurance complement each other. Both of them have requirements for analysis, auditing, management reviews and documentation to verify that certain performance criteria are met [2]. However, the focus of quality assurance is on compliance with regulatory requirements, while safety assurance monitors the effectiveness of safety risk controls.

The close relationship between certain supporting processes of both safety assurance and quality assurance enables an integration of those processes in order to achieve synergies in monitoring the objectives of the organization’s safety and quality.

Figure 3-4 shows the relationship between the safety risk management process and the safety assurance process. While the safety risk management process is applied during the initial design of an organization, the safety assurance process is a continuous process throughout time to monitor the effectiveness of safety risk controls and that the SMS is operating according to expectations and requirements. However, as soon as any deviation in safety performance is detected, the safety risk management process is initiated to identify the involved hazards and, as a consequence, to control the risk. This results in a continuous loop and interaction between both processes. Also, in the case of any planned change in the organization, which might affect the safety of the system, the associated risks have to be managed before the implementation of the change. This process is called *management of change*.

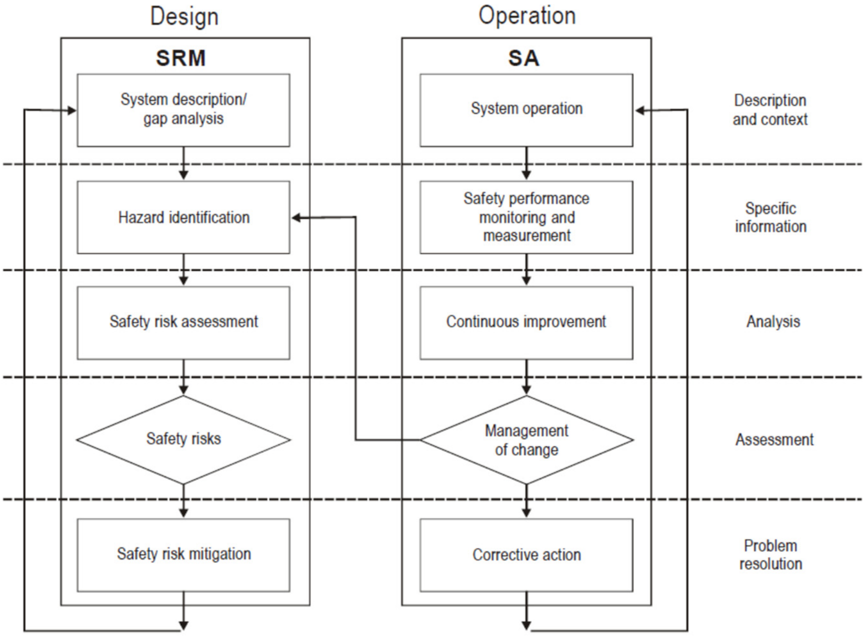

Figure 3-4 Safety Risk Management and Safety Assurance [3]

3.1.3.1 Safety Performance Indicators (SPIs)

To monitor the safety performance on a continuous basis, the safety assurance process requires the definition of adequate metrics, which are called *safety performance indicators* (SPIs). The safety performance indicators should be objective, i.e. quantified indicators, such as occurrence outcomes, deviations or any other events that reflect the safety level [2,3,19]. It is important to focus on occurrence rates rather than absolute numbers, to compensate for changes in the size of operations.

A distinction between leading and lagging indicators is often made. Lagging indicators are related to high-consequence events like accidents or serious incidents, thus, associated with reactive processes. In an ultra-safe system like aviation they are not meaningful, since a continuous monitoring makes no sense with a very low, sometimes even absent accident rate [2,46]. In contrast, leading indicators are associated with proactive or predictive processes and are generally related to low-consequence events, which are measured before any event in the actual operation needs to take place. Therefore, they can valuably contribute to the safety improvement of the aviation system, which is the primary goal of a good safety management. While lagging indicators have been widely used in the past, leading indicators are relatively new. Since the relationship between the indicator and the contained accident risk has yet to be evaluated, research is required [46]. ICAO suggests that service providers should initially focus on the development of high-consequence SPIs. Once the implementation phase has matured, low-consequence events can be used [2].

According to Verstraeten et al., aviation safety performance indicators should *provide an indication of accident probability*. Thus, the SPIs should be quantifiable with a relation to accident probability [46]. For the selection of adequate safety performance indicators, the following characteristics should be existing [10,46]:

- **Quantifiable:** Can be counted or measured unambiguously
- **Representative:** Since the indicator should be a metric for safety, an association with risk should be existent
- **Minimum variability when measuring the same conditions:** Any measuring device should produce the same results under equal conditions
- **Sensitive to environmental changes:** This assures a possible detection of environmental and behavioral conditions
- **Cost-efficient:** The costs for obtaining and using the indicator should be acceptably low
- **Comprehensive:** To make sure all parts of the risks in the system are covered

- **Manageable set of indicators:** The set of indicators should not exceed an amount which makes the management impracticable

Besides the safety performance indicator (SPI), corresponding alert and target values have to be defined, which define the framework in which the safety performance indicators are managed [2]. Both the target levels as well as alert levels should be derived from previous safety performance. The alert level is required to identify unacceptable performance regions and may be based on the average value and the standard deviation of the historical performance of the respective safety performance indicator. Target levels should be established at a lower level than the average value of the past, since a Safety Management System aims for a continuous improvement of safety, e.g. 5 percent lower than the average indicator's value of last year.

The safety performance should be regularly updated and monitored, e.g. the safety performance indicators can be compiled or aggregated for a specific monitoring period [2]

Both the safety performance indicators as well as the associated targets should be accepted by the respective authority during certification. SPIs are supplementary to legal or regulatory requirements [2].

An example from ICAO is given in Figure 3-5, where the monthly reportable incident rate is displayed for the current and previous year [2]. Besides the event rate, for the current year an alert level is indicated, which is based on the performance of the previous year. In this example, three different alert levels are indicated, which result from the average value of the previous year plus one, two, and three standard deviations (SD). According to ICAO, the alert could be triggered, if any single point exceeds the three SD level, alternatively two consecutive values exceed the two SD level or three consecutive values exceed the one SD level. An alert indicated a potential high-risk situation, and appropriate follow-up action is necessary to investigate and manage the root causes of the abnormal event rate.

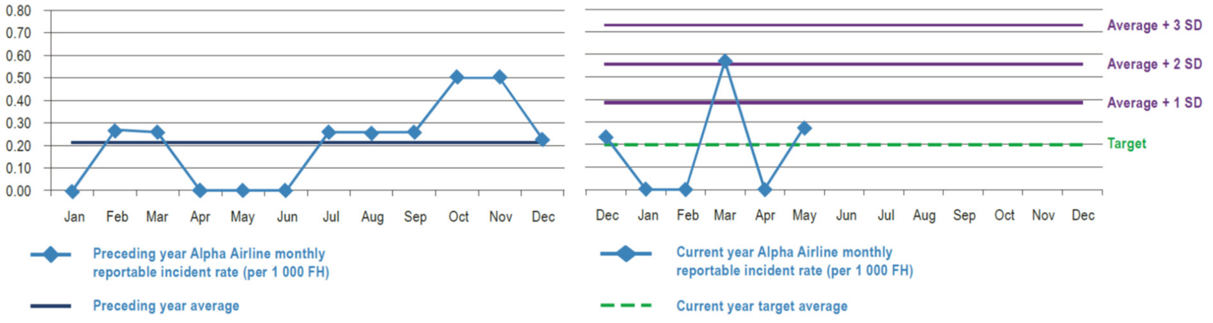

Figure 3-5 Example of a safety performance indicator (SPI) with target and alert level, example from [2]

Furthermore, a target level is defined for the current year that can be less structured than the alert level definition. Since the goal of a Safety Management System is to continuously improve the safety, the target level should aim for an improvement of the previous year's average, in the above example the target level is defined to be 5 percent below the average value of the previous year. If the target level can be reached by the end of the current year, the target level of the next year can be adapted to an even lower value accordingly.

Note that in the example of ICAO in the data of the previous year a rate of zero events is indicted for the months between April and June, which suggests a zero risk according to this indicator. However, the trend increases significantly in the following months, which shows that even though the indicator looked well for three months, the system was not safe. Also, the large fluctuations of the indicator in the current year between January and April raises doubts about the significance of the indicator in this period. Also, since only the number of events is taken into account, without considering the content of the reports, the relation to risk is not clearly reflected by this indicator, even though a correlation with risk might exist.

3.1.3.2 Management of Change

Once the organizational system of a service provider has been established, this system will continuously be subject to operational and organizational changes, which might affect the safety of the system. Therefore, new risks may enter the system, which have to be assessed and managed before the change is conducted [2]. The aviation system is a complex and highly dynamic system, including many different stakeholders, interactions between them, dependencies and parameters which influence the final outcome [47]. Therefore, the aviation system cannot be treated as a static system, once the initial system has been assessed in terms of risk. Instead, the management of change process assures that also the dynamic components of the system are under managerial control.

According to ICAO, those changes include the following factors [2]:

- *Organizational expansion or extraction*
- *Changes to internal systems, processes or procedures*
- *Changes to the environment of the organization*

The management of change is conducted by the safety risk management process. New hazards might be introduced into the existing system by the planned or already occurring changes, which have to be assessed. Once the risk associated with those hazards are not acceptable, adequate risk control measures have to be defined and implemented to assure that the risk is as low as reasonably practicable. The effectiveness of those mitigations has to be monitored thereafter by the safety assurance process, which may be ensured by definition of adequate safety performance indicators.

An example is a planned flight to a new destination, which is likely to influence the safety of the operation. The first step of the associated risk assessment is the identification of possible hazards. If the destination is an airport surrounded by complex geography, the hazard might be identified as a controlled flight towards terrain (CFTT) due to inaccuracies in navigation performance. In this example, possible risk controls might be the use of aircraft with specific navigational equipment (TEC) or specific training of flight crews (HUM). The effectiveness of the implemented risk controls can be monitored by use of e.g. Flight Data Analysis.

3.1.3.3 Continuous Improvement of the SMS

According ICAO, "*the service provider shall monitor and assess the effectiveness of its SMS processes to enable continuous improvement of the overall performance of the SMS*" [2]. The continuous improvement can be verified through the measurement of the safety performance indicators in relation to the safety targets, which aim for an improvement of the safety performance. The improvement in safety is related to the maturity and effectiveness of an SMS [2]. A continuous process of verification as well as required actions in the aftermath are necessary to achieve such improvements. Several means are available to support such a process:

- **Internal evaluations** carried out by persons or organizations that are functionally independent of the processes to be evaluated. Evaluations include *safety management functions, policymaking, safety risk management, safety assurance and safety promotion* [2]
- **Internal audits** are a systematic and scheduled assessment of the activities of an organization, conducted by functionally independent persons or departments within the organization
- **External audits** by the relevant authorities responsible for the acceptance of the SMS or by *industry associations or other third parties selected by the service provider.*

3.1.4 Safety Promotion

The Safety Promotion component consist of a safety training program that ensures that all employees are trained and competent to perform their SMS duties [2]. It is important that the *scope of the training program is appropriate to each individual's involvement in the SMS.*

Moreover, the Safety Promotion shall include a safety communication, which formally distributes the outcome of the SMS including background information on safety actions, which have been taken, and why safety procedures have been introduced or changed [2].

3.2 State Safety Program (SSP)

ICAO requires the states to establish a State Safety Program (SSP), which is the complement to the safety management systems (SMS) of a service provider. The purpose of the SSP is to achieve an acceptable level of safety (ALoS) in civil aviation within the respective state [2].

Figure 3-6 shows the relationship between an SSP and an SMS. While states are responsible for developing and establishing the SSP, the service providers are responsible for developing and establishing their SMS. However, the acceptance and oversight of development, implementation and operational performance of the service provider's SMS is part of the activities of the state's SSP.

In Figure 3-6, which is incorporates both dimensions from Figure 3-2, protection and production, the SSP is located on the protection side only, since the solely goal of the SSP is to ensure public safety at the state level. The oversight by the state through the SSP is twofold: The initial acceptance of the service provider's SMS is conducted by verification that all components and elements of the service provider's SMS comply with existing regulation. This mainly prescriptive process is the traditional way of administrative oversight in terms of regulatory compliance [3].

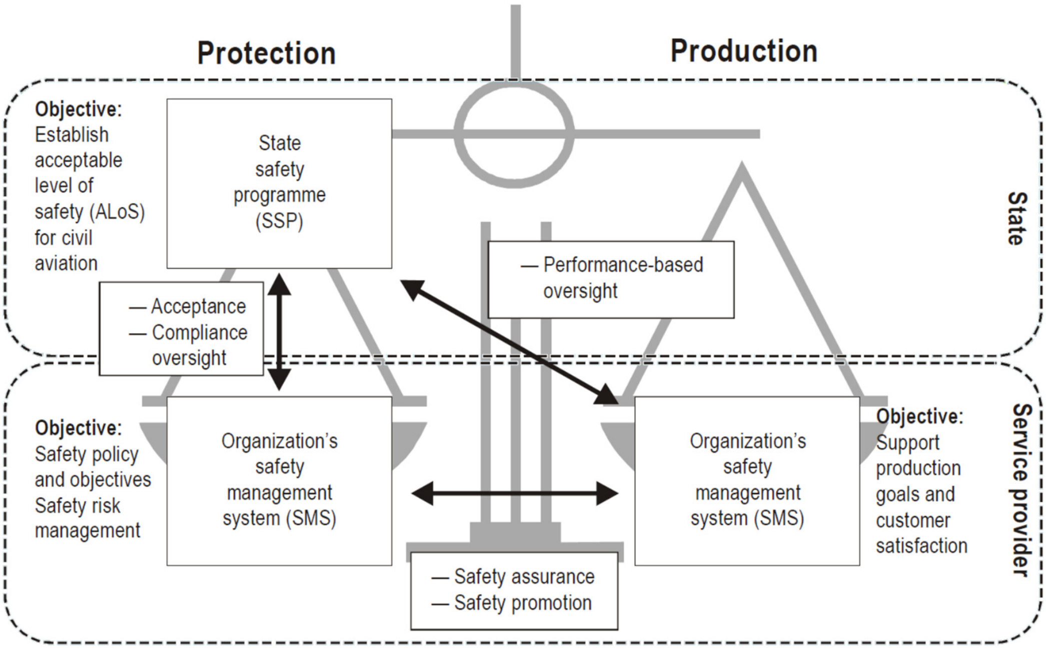
Protection
Production
Objective:
Establish acceptable level of safety (ALoS) for civil aviation
State safety programme (SSP)
State
— Performance-based oversight
— Acceptance
— Compliance oversight
Objective:
Safety policy and objectives
Safety risk management
Organization's safety management system (SMS)
Organization's safety management system (SMS)
Objective:
Support production goals and customer satisfaction
Service provider
— Safety assurance
— Safety promotion

Figure 3-6 The relationship between an SSP and an SMS [3]

However, ensuring regulatory compliance does not guarantee adequate SMS performance, once the SMS is running. The second part of oversight refers to the achieved performance on a regular basis, which is drawn on the production side in Figure 3-6. The service provider has to achieve commercial goals and deliver customer satisfaction, which is the primary purpose of the service provider. During the production, the service provider has to manage the associated risks by using the structure of its SMS. To proof compliance on the agreed target level of safety, the service provider has to measure its safety performance by means of safety performance indicators on a regular basis and report it towards the state authority. The state authority verifies through the SSP that the defined ALoS is achieved [3].

Hence, in the new structure of SSP and SMS, the traditional prescriptive-based approach of acceptance and compliance oversight is extended to a performance-based oversight of safety performance indicators and targets [3].

4 Flight Data Analysis (FDA)

The British Civil Aviation Authority (CAA) defines Flight Data Analysis (FDA)[10] as "*the systematic, pro-active use of digital flight data from routine operations to improve aviation safety*" [13]. A transition from a purely reactive mode to a more proactive mode, i.e. the early identification of hazards and a timely implementation of mitigation measured, becomes possible with FDA [48].

A huge amount of objective data, representing the routine flight operations, enables the identification of deviations from standards and limits. Thus, a proactive identification and assessment as well as elimination of hazards and their associated risks becomes possible on a broad basis [7].

Individual safety events can be analyzed within a general context. This context contains either the whole flight operation of an airline, or at least the relevant parts of this operation, which are related to the considered event. During the investigation of accidents or incidents, contributing factors can be identified with FDA, which supports the understanding of the root causes and facilitates the analysis of the systemic aspects of the investigation [49]. FDA allows airlines to compare their Standard Operating Procedures (SOPs) with the performance that is actually achieved in the flight operation on a routine basis [13].

Flight Data Analysis constitutes an important data source for proactively identifying hazards, controlling and mitigating the associated safety risks and thus, is an effective tool for the safety assurance component of a Safety Management System [49]. FDA aims for the continuous improvement of safety of an airline. It supports the safety management by a wide range of applications, e.g. [49]:

- Identify safety trends
- Monitor the effectiveness of corrective actions taken
- Optimize training procedures

However, an FDA system does not aim for any disciplinary actions on human errors, which are often the result of deviations from rules and regulations [7].

[10] Also referred to as Flight Data Analysis Program (FDAP), Flight Data Monitoring (FDM), Flight Data Monitoring Program (FDMP), Flight Operations Quality Assurance (FOQA) and Flight Operations Data Analysis (FODA) [13,48,49]

4.1 Regulations

Even though flight data analysis has been conducted for decades in association with aviation accidents [49], the systematic and proactive analysis of flight data from routine operations is a relatively new technology. One of the reasons is the requirement to handle a large amount of data, which requires adequate computer technology.

Flight Data Analysis became an ICAO standard for all Air Transport operations of aircraft over 27 tons with effect 1st January 2005, which is documented in ICAO Annex 6, Part I [13]. Further guidance is provided in a separate document, the ICAO Flight Data Analysis Programme Manual (Doc 10000), which highlights the importance of an FDA program from the perspective of ICAO [49]. ICAO emphasizes that an FDA program shall be non-punitive, i.e. no disciplinary action shall be taken against flight crews, and the program shall contain adequate safeguards to protect the data sources [49].

Nowadays, within the scope of EASA, Flight Data Analysis is a requirement under European legislation [13]. The paragraph ORO.AOC.130 of the Commission Regulation (EU) 965/2012, Annexes III (Part ORO), applicable since 29 October 2014. The acceptable means of compliance of this paragraph are contained in AMC1 ORO.AOC.130 of EASA Executive Director (ED) Decision 2012/017/R [48].

4.2 Technical Background

The FDA program generally consists of components for flight data acquisition, flight data transformation into an appropriate format for analysis, and a software to analyze the data [49].

A mandatory means to record flight data is the Flight Data Recorder (FDR). The requirements on Flight Data Recorders are specified in EU-OPS 1.715 to 1.727 [50]. The main purpose of an FDR is the analysis of the flight data following an aircraft crash. Thus, the housing of the FDR is required to be crash-protected. Since the end of the 1980s, FDRs are required to record the flight data in a binary format [51]. Depending on the recording media, the FDR is either referred to as Digital Flight Data Recorder (DFDR, tape based) or Solid State Flight Data Recorder (SSFDR, solid state memory) [13].

Depending on the date of certification, the maximum certified takeoff weight, and the maximum number of seats, the required parameters, which have to be recorded on the FDR for each aircraft, have been specified by ICAO and adopted by EASA and the FAA. Depending on the above, between 18 and 88 different flight parameters have to be recorded. Also, for each parameter the required range, accuracy of the sensor input, sampling rate, and resolution are specified. Even though modern FDRs are capable of recording significantly more flight parameters than required[11] [52], the use of an FDR as a recording tool for FDA is limited. The main restriction is the limited recording time of 25 to 50 flight hours, combined with the time-consuming and expensive access to the data of an FDR on a regular basis [13].

Thus, other types of recording tools have to be used for the Flight Data Analysis program. Quick Access Recorders (QARs), especially designed for the use with FDA, provide a large memory, combined with an easy access of the data rather than crash-protection. Different types of QARs exist:

- QARs with changeable recording media, such as Optical disc QARs (OQARs) or flash memory like Personal Computer Memory Card International Association (PCMCIA) memory QARs (PQAR). These recording media are based on standard PC technology and provide high capacities combined with high transfer rates [13,19].
- Small solid state recorders, which can be plugged directly into the data bus of the aircraft and thus, can be changed as a whole instead of just a change of the recording media. An example is the Mini QAR (MQAR) [13].
- Wireless QARs (WQARs), which collect the flight data into a buffer memory during the flight. Once the aircraft is on ground, a certain trigger logic (e.g. engine shutdown) starts the data transmit process, where the buffered data of the whole previous flight is sent via either mobile phone technology or short-range transmission to an airport based local area network. The flight data is then forwarded to the FDA data server at the respective airline. During such transmission processes the data has to be encrypted accordingly [13].

Even though the capacities of the data storage media significantly exceed the required time between the download intervals, a tradeoff between maintenance costs for replacement of the recording media, and the urgency to act on high risk events should be carefully taken into consideration. Some events need immediate action with regard to safety [13]. The use of wireless transmission of the data reduces such logistic problems associated with the change of recording media.

The increasing amount of data to be recorded on board of an aircraft requires a coordinated process to prepare all incoming information for recording on the FDR [19]. This is achieved by means of a Flight Data Acquisition Device (FDAU)[12]. The FDAU converts and multiplexes analog sensor signals into a binary data stream, which can be directly recorded onto both, the FDR and

[11] FDRs of modern aircraft, e.g. Airbus A380, are capable of recording far more than 1000 flight parameters [52]

[12] Also referred to as Digital Flight Data Acquisition Unit (DFDAU), Flight Data Information Management (FDIMU), and Flight Data Interface Unit (FDIU) [13,19,48]

QAR. Thus, the FDR and the QAR use the same data source. However, since requirements on the FDR reliability is higher, the communication between the FDAU and the FDR is bidirectional for verification and synchronization purposes. This reduces the probability of recording errors. On the other hand, the communication between the FDAU and the QAR occurs only in one direction, thus, synchronization errors will occur more frequently on QARs [19].

The format of the data stream generated by the FDAU is based on e.g. the ARINC[13] 717 specification, which currently represents the standard that is most commonly used[14] [19]. The ARINC 717 standard is based on frames, subframes and words. Each subframe contains one second of flight data. Four subframes form one frame, which therefore equals four seconds of data. Each word contains 12 bits. The data rate of the recorder corresponds to the number of words, which are contained in one subframe, i.e. words per second (*wps*). The data rate is limited by both, the speed of the data bus and the speed of the recording device [19]. For the ARINC 717 specification, data rates between 64 *wps* up to 1024 *wps* are specified.

Most of the words within a subframe contain data. Additionally, for each subframe a sync word exists, which indicates whether the subframe might contain a synchronization error. In this case, the content of the data word might contain corrupt data and should be treated with caution. A special recorded data value is the frame counter, which usually uses one word and thus, ranges from 0 to 4,095. With each frame, the frame counter is increased by a value of one. If this counter reaches the maximum value, it is reset to a value of zero at the next frame. The frame counter indicates possible interruptions of the data recording [53].

Depending on the resolution of the recorded flight parameters, each word may contain more than one parameter, or a parameter can be split up and distributed over different words. In the example of Figure 4-1, three parameters share one word. While in this example parameter 1 uses 7 bits, parameter 2 uses 4 bits, and parameter 3 uses the remaining bit. If the resolution of a parameter requires a capacity of more than 12 bits, the information can also be distributed over more than one word. E.g. the air/ground switch, which indicates whether the aircraft is on ground or not, is a discrete value and thus, requires only one bit. On the other hand, the latitude of the aircraft position usually requires more than 12 bits, since this parameter ranges from -90° to +90° and thus, using 12 bits would result in a resolution of 180/4,096 = 0.04° of latitude, which corresponds with 2.64 Nautical Miles. An additional word can be used to enhance the precision of the recorded parameter. If 10 additional bits of this additional word would be used, the resolution would result in 0.00004° of latitude, which corresponds to 4.8 meters. In this case,

[13] Aeronautical Radio Incorporated

[14] E.g. the standard of the Airbus A320 family and Boeing 777

the parameter with the highest resolution is called "coarse" part and the other is called "fine" part [48].

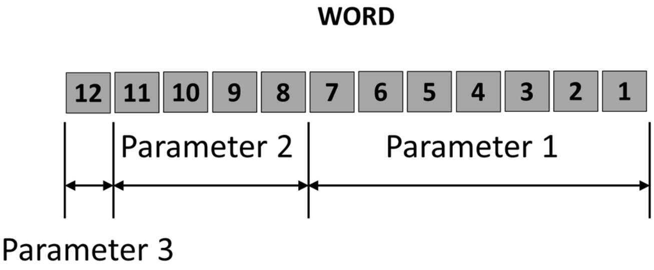

Figure 4-1 Example of three parameters sharing one word based on [48]

The different words are recorded sequentially according to their position in the subframe. Thus, the first word of a subframe is recorded nearly one second before the last word of the same subframe. Each parameter is buffered in a temporary memory, called the parameter pool. The parameter pool is asynchronously updated, depending on the frequency of the respective parameter on the data bus [19]. Consequently, the recorded flight data does not necessarily belong to the same point in time, even though the data is recorded within the same subframe.

Some parameters represent signals of higher bandwidth. If these parameters have to be recorded more than once per second, i.e. the required recording frequency is higher than one Hertz, the parameter should be equally distributed over time within the subframe. E.g. a parameter recorded with 4 Hertz in a 128 *wps* subframe should be placed 128/4 = 32 words apart from each other. If the first recorded value is stored in e.g. word number 10, the other values should be ideally stored in word numbers 42, 74, and 106 to result in a timely equally distributed coverage of this parameter. An example can be seen in Figure 4-2.

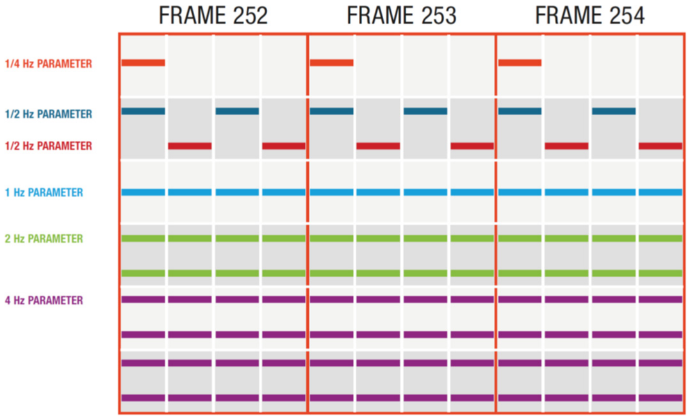

Figure 4-2 Example of parameter locations within a frame and subframe, depending on different frequencies [48]

Some parameters are subject to very small changes over time, e.g. the aircraft mass. Such parameters are not required to be recorded in each subframe. Instead, parameters with lower frequencies than 1 Hertz can be recorded only once or twice per frame, as indicated in Figure 4-2. Using this mechanism, a certain word position can be shared between different parameters within a frame. Following this mechanism, the lowest frequency for recording is one value each 4 seconds.

To enable recording frequencies, which are even lower, a so called superframe has been incorporated. A superframe consists of a sequence of 16 frames. The advantage of the superframe principle is to enable the recording of more parameters, which are not subject to rapid changes, e.g. the date of the flight or the flight number, by sharing recording space.

A certain word is reserved for this purpose within each frame or subframe. A superframe counter indicates the frame number within the superframe cycle. This counter ranges from 0 to 15 and thus, requires four bits per frame. The remaining bits of the reserved word can be used for the data of the superframe parameters. Depending on the actual superframe number, the recorded superframe parameter will differ. The lowest possible recording frequency is therefore reduced to a value of 1/64 Hertz.

Figure 4-3 shows an example of a superframe word, reserved in word number 50 of the first subframe of each frame. In this example, the superframe word is shared by the parameters flight number, month of the date, year of the date, aircraft identification, and the time [48].

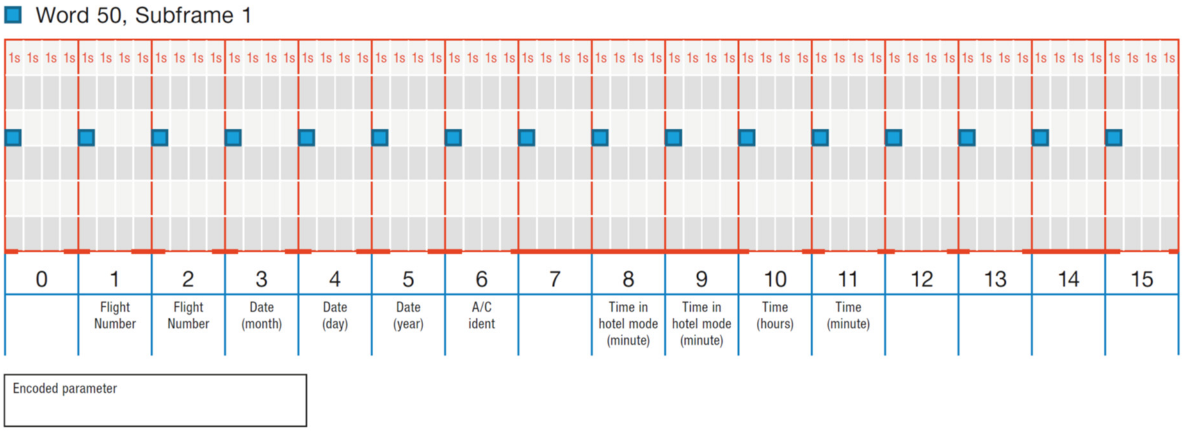

Figure 4-3 Example of a superframe word, reserved in word number 50 of the first subframe of each frame [48]

Based on the described frame layout, the *Dataframe Layout (DFL)* indicates the position of the parameters within the recorded binary data stream. The DFL is the guidance how to decode the binary data stream. Besides the location of the parameters within a frame, subframe or superframe, the DFL provides further information about each parameter, such as the number of bits used, the type and method of encoding (discrete, linear etc.), and functions for determining the actual engineering values [19]. Thus, the DFL is a vital link between the recorded binary data stream and the engineered flight data, which can be used for the safety analysis. The DFL can be customized to meet the needs of the airline.

Different FDA software[15] and FDA service providers are commercially available, which support airlines in handling and analyzing the data. This includes the generation of time series flight data from the recorded raw data by means of the DFL. An adequate preprocessing of the data is required, e.g. the separation of the continuous data stream into individual flights, the determination of the takeoff and landing locations, the generation of trajectories, or the gathering and assignment of meteorological data concerning the takeoff and landing [7,13]. The data has to be securely stored to protect this sensitive information [49]. The analysis of the data is conducted in an anonymous way in many airlines due to internal or legal regulations with the purpose of data protection. This strengthens the level of confidence between management and pilots, which is necessary for a well-developed safety culture [7].

The FDA software usually consists of three basic elements [7]:

- A software for data collection and data storage, which includes an automatic pre-procession of the data in terms of the separation of the continuous data stream into individual flights, determination of departure and destination airport, trajectory calculation, assignment of weather data etc.
- A data mining software capable of both, detecting deviations from safety standards and calculating performance indicators, by means of adequate algorithms. The results are stored in a results database.
- An analysis software which is capable of filtering the results database and displaying the results.

While the flight data itself might be deleted after a predefined period of time for security reasons, the results in the database usually remain available even beyond this period. This enables the generation of long-term trends [7].

A visualization software is an optional software tool, which enables the visualization of the flight by displaying the cockpit instruments, flight control inputs and cockpit view, based on the recorded flight data [19]. This tool assists safety personnel in analyzing even highly dynamic situations, where multiple parameters fluctuate within a short timeframe. It also assists flight crews in recapping the original perspective, which has been experienced during the analyzed event.

4.3 Flight Data Analysis

The analysis of the flight data is the high-level safety work and thus, the core process of the FDA program. Once the preprocessing is completed, and the flight data is available in the storage of

[15] Within the scope of this thesis, the Event Measurement System (EMS) of GE Aviation was used

the FDA system, the FDA software supports the safety analysts in doing their work. There are two basic approaches to analyze the flight data, threshold analysis and statistical analysis.

4.3.1 FDA Events

Exceedance detection by means of FDA events is the traditional approach to FDA. This includes non-compliance with flight manual limits and deviations from Standard Operating Procedures (SOPs) or good airmanship [13].

The easiest definitions of exceedance thresholds are red-line values. More complex definitions are based on a combination of multiple parameters, defining certain flight modes or configurations, which indicate an increased risk status during the event [49]. Once the defined threshold value is exceeded, an FDA event will be assigned by the software [7]. More than one event of the same type can be generated per flight, if the respective threshold is exceeded multiple times.

Depending on the magnitude or severity of the deviation, different levels of exceedance can be defined. According to the level of exceedance, the event can be classified e.g. as "Low", "Medium", "High" or even "Extreme" [7,19]. This classification can be defined e.g. by safety surveys conducted with a group of training captains [7]. However, such classification depends primarily on the individual preferences of the flight safety department of the respective airline.

Sometimes the event trigger algorithms generate an event even though in reality nothing happened. This is called a *false positive event* [7,19]. False positive events are often triggered by erroneous flight parameters (see also Figure 7-5 on page 199). Erroneous or corrupt flight data often leads to significant deviations from standard and thus, the classification of the respective event results in higher severities, which therefore are more affected by false positive events than lower severities. For the purpose of quality assurance, FDA events have to be reviewed by safety experts whether they are valid or not. This systematic process is called the *event review process*. Due to limited resources, the event review process has to be restricted to events with higher severities, e.g. severity "High" or "Extreme". Thus, the number of false positive events for lower severity classifications is usually unknown [7]. During the event review process, the safety expert may additionally assess the associated event risk, based on expert estimation. The severity "Extreme" is usually the result of such an expert assessment and should not be generated automatically by the software [7].

According to Mickel, the event algorithms should be fine-tuned to result in an amount of approximately 1000 "High" or "Extreme" events for a major airline per year, which is a good balance between workload for the required event review and the expected results. A false positive rate of about 50 percent indicates a good relationship between sensitivity and robustness of the underlying FDA event algorithm [7].

The opposite of a *false positive event* is the so-called *false negative event*, which has not been generated in the FDA system even though the event has happened in reality. The reason is the lack of implementation of the respective filtering algorithm in the software as a result of either insufficient coverage of filter algorithms or even the lack of knowledge about the associated hazard at all. The latter may be the result of an insufficient hazard identification process. If the respective event cannot be detected by other means, e.g. crew report, the event is not visible to the safety department [19]. Hence, FDA cannot replace the hazard identification process [7].

A typical FDA software contains up to 200 pre-defined FDA events, also called FDA event algorithms, which cover a broad range of possible deviations and hazards. Depending on actual safety issues as well as special company needs (e.g. special procedures), the set of FDA events can be modified and/or extended by the user. Also, the implementation of new events is possible. In order to support cross-company cooperation between different airlines to enhance the flight safety, some FDA software systems support the exchange of FDA event algorithms by the means of standard FDA event libraries [7].

The aggregation of individual exceedances to a general event type is desirable to cover the risk of certain aspects or phases of the flight, e.g. a high sink rate during approach is an element of an unstable approach. If the aggregated event is generated by several exceedances, the assessment of the associated risk should lead to higher severities, since multiple barriers might have failed on the pathway towards a potential accident [7].

A statistical summary of the events can be aggregated in a statistical report, which can be distributed to management and/or staff on a regular basis. The storage of the events in a database provides the ability to monitor event trends over time [48,49].

This thesis focuses on the assessment of the risk of such FDA events on a quantitative way, which is beyond state-of-the-art.

4.3.2 Statistical Analysis

A statistical analysis of the flight data provides a more comprehensive picture of the overall safety, since the whole operation is incorporated in the analysis. A statistical analysis incorporates all flight data instead of focusing on only those flights which have triggered FDA events. With a statistical analysis, certain aspects of flight operation can be investigated, using e.g. statistical mean values or standard deviations [19].

Instead of using events, statistical analyses usually use so called measurements. While an event does not necessarily occur during each flight but might also occur more than once within a single flight, a measurement exists exactly once per flight. An example for an FDA event is a TCAS RA, which occurs only on very few flights. However, within a single flight, more than one TCAS RA might occur. On the other hand, an example of a measurement is the height above touchdown when the landing gear is lowered. This happens on each flight, but at different heights. The statistical analysis could e.g. analyze the distribution of these heights of all flights (or a subgroup, e.g. a particular fleet or destination) by means of mean value and standard deviation. For more advanced analyses, which might be beyond the capabilities of the FDA software, the measurements can be exported into a tabular file, which can be used as an import of any statistics software, e.g. MATLAB.

4.4 Safety Performance Measurement in FDA

In the early 2000s, when Flight Data Analysis started to evolve, the focus was on event rates rather than safety trends. Safety analysts have been highly satisfied by the fact that they could monitor operational flight data for the first time, and campaigns aimed to lower the event rates had been very efficient [54]. There has not been a very deep knowledge about how to implement events tailored to own needs at this time, and thus, predefined event algorithms provided by the FDA software manufacturers have been applied, even though the trigger thresholds of these events might not have been in accordance with the procedures or limits of the respective operator. These event definitions have often been more related to compliance than risk. Even though non-compliance events contain a certain amount of risk, it is difficult to quantify this risk portion. Also, there is no method how to compare different event types with each other, since the relation between the risk levels of the different event types are not precisely known. This finally results in a risk picture full of uncertainties, which is difficult to quantify in terms of risk.

With the requirements of a Safety Management System to monitor the safety performance, the focus had to be turned from event rates towards risk trends. Event rates without assessing the contained risk are not precisely associated with an accident probability. Thus, event rates without considering the risk level are less meaningful in terms of safety performance.

This dissertation thesis presents a new data-driven methodology to evaluate the risk level of an FDA event. This enables the measurement of the risk contribution of a single flight. Since every flight can be assessed individually, a continuous trend monitoring is possible on a daily basis by compiling the individual event risks to determine a trend. This trend can be used to immediately identify outliers in terms of risk. This is in accordance with the common practice in FDA, where outliers are continuously searched for in terms of risk. Since high risk events are often related to extreme values, which might be based on corrupt data, the event review process assures a high level of data quality, which reduces the probability of false risk classifications due to data errors.

The event risk classification in this thesis is based on the ARMS method with the modified ESC matrix from Mickel, which was described in sections 2.6.1 and 2.6.3. This common risk metric is used for all presented categories and event types described in the following sections. Hence, the new method is an essential and useful extension of existing methods.

5 The Risk Level of a Runway Overrun

This chapter is based on a paper, presented at the 27th edition of the European Safety and Reliability Conference ESREL, which is an international conference under the auspices of the European Safety and Reliability Association (ESRA), held in Portorož, Slovenia, 18-22 June 2017 [55].

In this chapter, the risk of a runway overrun is evaluated. According to [56] runway overruns during landing are one element of runway safety related events, which are one of the three high-risk accident occurrence categories besides loss of control in-flight and controlled flight into terrain. Runway overruns during landing account for nearly 40 percent of all runway excursions besides veer offs and excursions during takeoff. Runway excursions have been the accident category with the highest frequency in recent years [24]. Even though the probability to survive a runway excursion is relatively high (see Figure 5-1), there have also been several fatal accidents within this category.

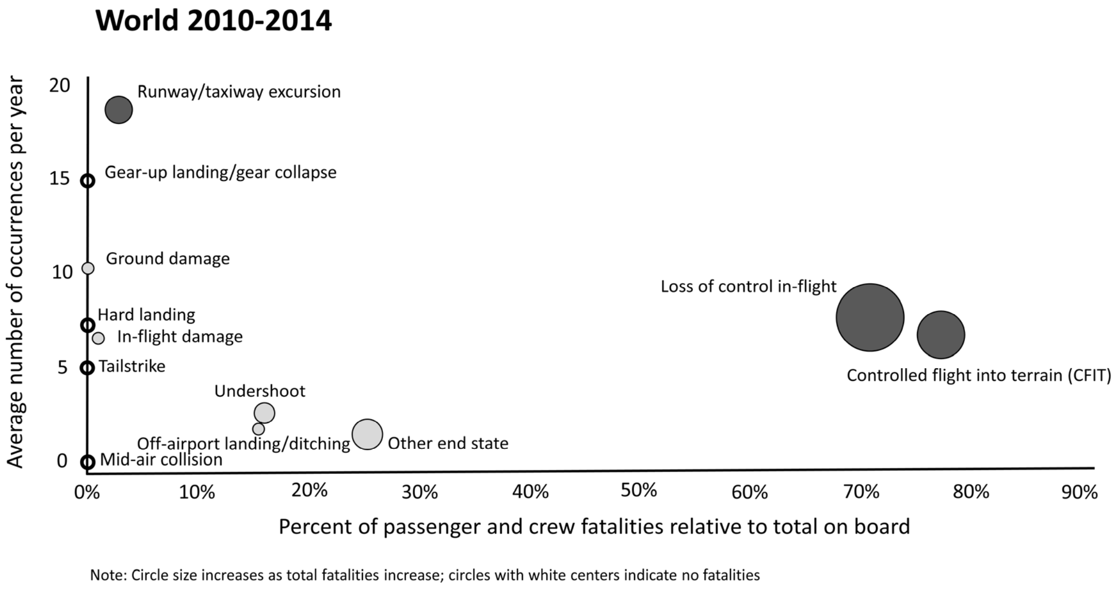

Figure 5-1 Comparison of occurrence rate versus fatality of different accident categories [24]

Excursions are estimated to cost between USD 500 million [57] and USD 900 million [58] in total a year. Airbus estimates that the cumulative costs for runway excursions from 1985 to 2010 have been USD 6.8 billion, and will increase to USD 9.2 billion until the year 2020 [59]. A recent study by van Eekeren et. al. estimates the total cost of runway events at an average of USD 500 million per month, about 18 percent of which is caused by runway overruns [60]. According to this study, within the recent past (January 2015 until May 2018) there is no indication of a weakening trend. Therefore, runway excursions must be considered as a major threat to aviation safety.

The new methodology as presented in this dissertation is based on the interaction between the aircraft state and the environmental conditions. For each risk category, appropriate means must be used to model the environmental conditions. In the following example, the evaluation of the environmental conditions is based on a **physical model**, since the environmental conditions can be completely derived from the flight data of a set of previous flight.

Chapter 5.1 starts with the description of the severity of a runway overrun, which is one component of the associated risk.

The other component of risk is the corresponding probability, which is far more difficult to determine. The new method refers to this component and is presented in chapters 5.2 and 5.3. In chapter 5.2, the aircraft state is developed. A flight dynamics model of the aircraft is established to determine the minimum runway friction, which is sufficient to stop the aircraft right at the end of the runway. This required runway friction is based on the flight data of the considered landing, in particular the velocity and remaining runway length at the most critical point. Hence, the aircraft state corresponds to the energy level of the aircraft in relation to the remaining runway distance.

In chapter 5.3, the environmental conditions are modeled in terms of probability of the available runway friction. It is evaluated by means of an analysis of a large number of previous flights. From this analysis the distribution of the available friction coefficients is determined, also using a flight dynamics model. This also includes the determination of the missing aerodynamical coefficients during rollout, which are not available in any documentation. The risk level can finally be determined by the probability that the available friction is less than required.

However, the available friction coefficients can only be derived from those parts of the flight data, where full brake demand has been applied. Thus, adequate means had been developed to identify these portions of flights: First, the correlation between a certain amount of brake pedal deflection and the respective maximum available friction. Second, landings with the use of autobrake, where the target deceleration could not be achieved.

For the verification of the model, a large number of simulations with randomly distributed environmental conditions has been performed in chapter 5.4. Finally, in chapter 5.5 a method of how to aggregate the event risks of the individual flights to generate a trend is provided.

5.1 Severity of a Runway Overrun

The expected severity level as one component of the risk has to be evaluated first. Two possibilities can be considered for a runway overrun:

First, for the evaluation of the corresponding probability, the physical model is designed to provide not only the probability of an overrun, but also probabilities of different runway exit speeds during the overrun, which might influence the severity level. Kirkland has analyzed the level of aircraft damage incurred by passenger aircraft during runway overruns, based on overruns in the U.S., Canada, U.K. and Australia from 1980 to 1998 [61]. With a probability of 48 percent none or minor damage was produced, however, in 33 percent substantial damage was observed and in 8 percent the aircraft was destroyed. Analyzing 52 runway overruns, Kirkland comes to the conclusion that there is no observable correlation between runway exit speed and damage to the aircraft, suggesting that other factors like obstacles beyond the runway end, may also contribute to the level of damage.

Because of the erratic distribution of outcome scenarios, another approach of how to evaluate the severity level, is used within the context of this thesis: The physical model is designed to evaluate only the probability of an overrun without distinguishing between different runway exit speeds. Instead, an average severity is used to describe the risk, irrespective of the runway exit speed, as it is not known which specific damage will be produced in advance of the potential accident.

Mickel evaluated an average severity level of a runway overrun during landing for his model [7]. He uses a scale ranging from S0 (no damage) to S5 (hull loss) for severity classification. The lowest two severity classes S0 and S1 are not used, because even if the aircraft has experienced no damage, the cost of recovery of the wreck is assumed to be at least in the area of S2. On the other hand, only few runway overruns are fatal accidents (see also Figure 5-1), only 3 percent result in a hull loss (S5). According to his calculations, the expected damage is 3.4 million Euro per overrun and therefore slightly above the typical value of severity S4 (3 million Euro). In order to not underestimate the risk, the average expected severity within the context of this thesis is defined as one category below the highest severity according chapter 2.6.3, which is classified as a *serious accident* (accident scenario *A4*).

5.2 Definition of the Aircraft State

Due to the high number of accidents over the last decades, a large variety of contributing factors leading to an overrun have been identified. The various contributing factors are visualized in Figure 5-2, where also the frequency of the different factors is specified [62].

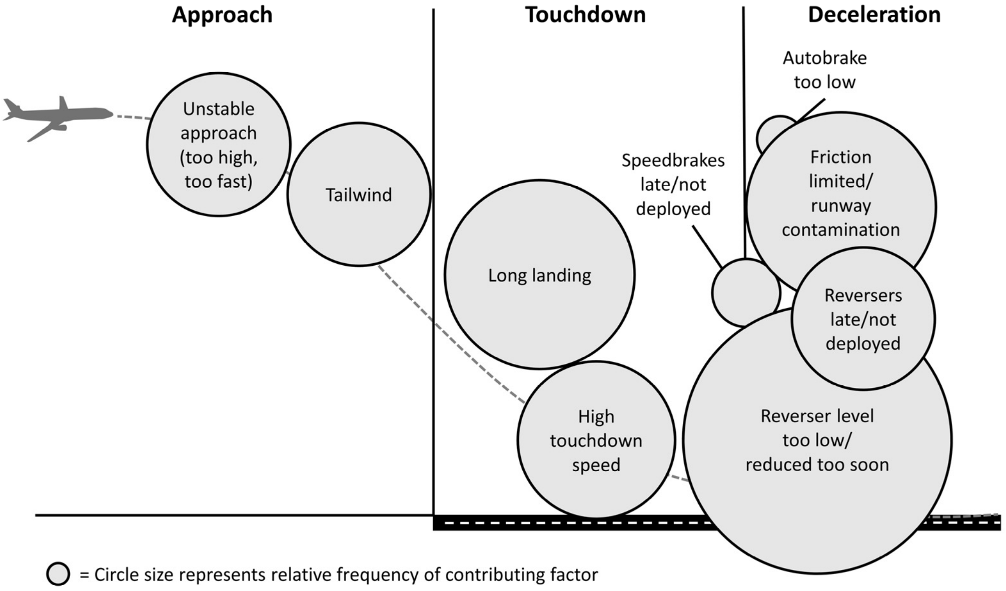
Approach
Touchdown
Deceleration
Unstable approach (too high, too fast)
Tailwind
Long landing
High touchdown speed
Speedbrakes late/not deployed
Autobrake too low
Friction limited/ runway contamination
Reversers late/not deployed
Reverser level too low/ reduced too soon
○ = Circle size represents relative frequency of contributing factor

Figure 5-2 Contributing factors of runway overruns based on [62]

Van Es analyzed the main contributing factors of worldwide landing overruns. The percentage of runway overruns, where the respective contributing factors could be observed, can be seen in Table 1 [58]. More than one factor can contribute to an accident.

Table 5-1 Contributing factors of a runway overrun and their associated frequencies [58]

Contributing factor	percentage
Wet or contaminated runways	66.7%
Long landing	44.5%
Speed too high	22.1%
Incorrect decision to land	16.8%
Aquaplaning	16.2%
Tailwind	15.9%
Late and/or incorrect use of brakes	10.3%
Late and/or incorrect use of reverse thrust	10.0%
Too high on approach	7.2%

Other contributing factors are visual or non-precision approaches, which could finally have an adverse effect on several factors listed in Table 5-1, e.g. speed too high or too high on approach [18], and also technical malfunctions of brake devices [18].

For the visualization of the risk model a bow tie model is used according Figure 5-3.

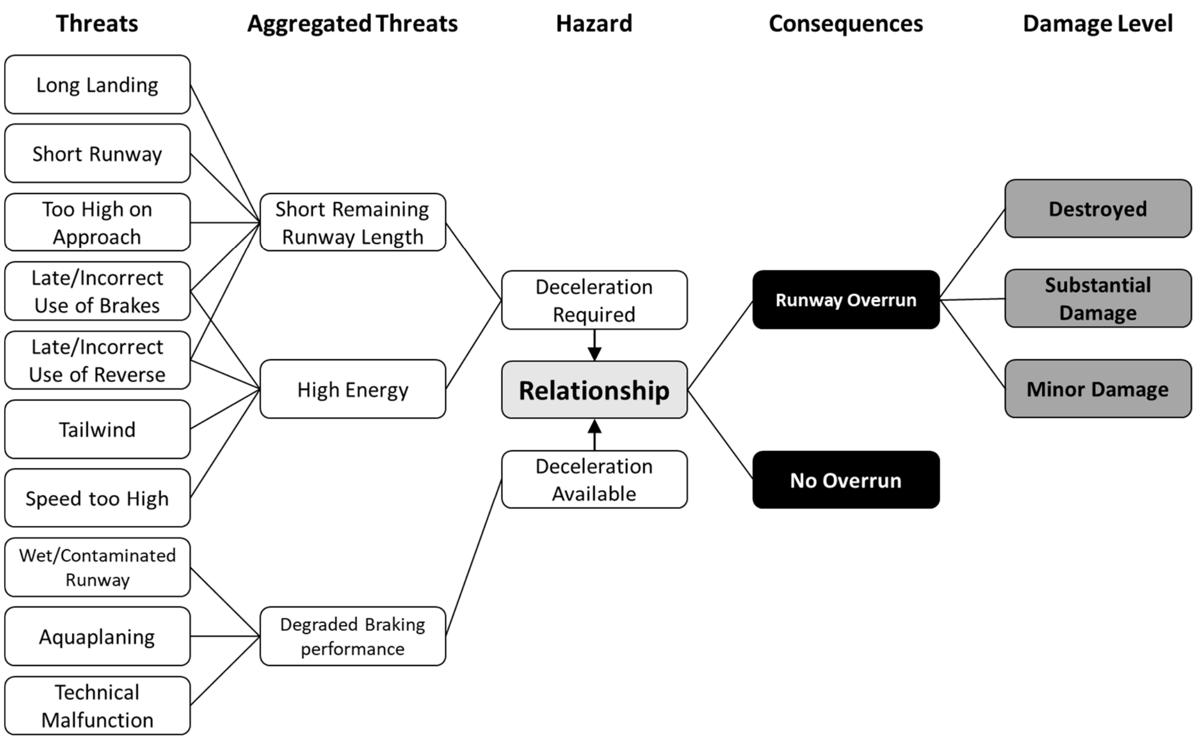

Figure 5-3 Bow tie model of a runway overrun, source: own research

The fault tree part of the bow tie model consists of the contributing factors, also called threats, which can be clustered into three different aggregated threats: The first two are short remaining runway length, represented by the remaining runway distance R, and high kinetic energy, represented by the actual ground speed of the aircraft V_G. For each point in time during landing, an equivalent constant deceleration d_r can be calculated, which would be required to stop the aircraft before the runway end:

$$d_r = \frac{{V_G}^2}{2 \cdot R}. \qquad \textbf{Eq. 5-1}$$

While ground speed can be taken from flight data directly, R can be derived by integration of the ground speed, starting from runway threshold overflight, where the landing phase begins (see Figure 5-4). The equivalent constant deceleration d_r represents the aircraft state in the risk model.

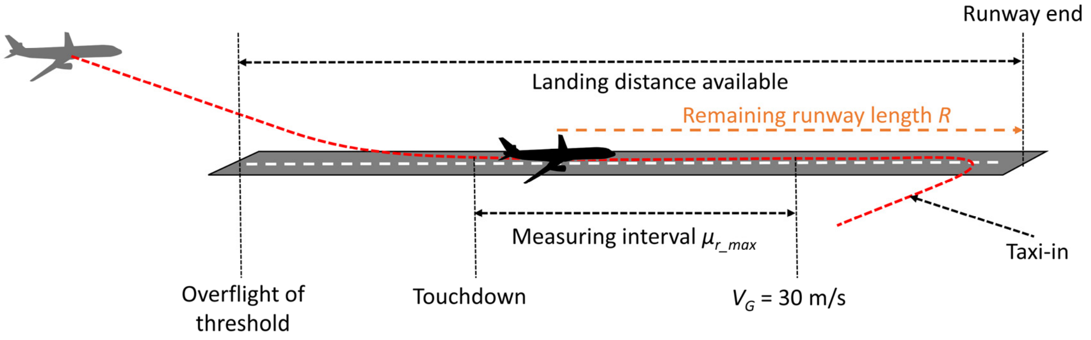
Runway end
Landing distance available
Remaining runway length R
Measuring interval μ_{r_max}
Taxi-in
Overflight of threshold
Touchdown
V_G = 30 m/s

Figure 5-4 Landing phase

The third aggregated threat is a degraded braking performance, which influences the available deceleration for the particular landing. The available deceleration represents the environmental conditions in the risk model. To describe this available deceleration d_a, a physical consideration of the deceleration during landing is necessary. Deceleration of the aircraft during landing can be described by the equation of motion in the longitudinal direction [63]:

$$d_a = \frac{1}{m} \cdot [D + X + mg \cdot \sin\gamma + \mu_a \cdot (mg \cdot \cos\gamma - L)] \,. \qquad \textbf{Eq. 5-2}$$

Besides the aircraft mass m, the available deceleration d_a is a function of four different terms: Aerodynamic drag D, reverse engine thrust X, the contribution of the runway slope γ, with the constant of gravity g, and the brake force, which depends on the available friction coefficient μ_a, the vertical component of aircraft weight and aerodynamic lift L.

The aerodynamic drag D is defined as

$$D = \frac{\rho}{2} \cdot {V_A}^2 \cdot S \cdot C_D \,, \qquad \textbf{Eq. 5-3}$$

and the aerodynamic lift L is defined as

$$L = \frac{\rho}{2} \cdot {V_A}^2 \cdot S \cdot C_L \,, \qquad \textbf{Eq. 5-4}$$

with the air density ρ, the airspeed V_A, the reference wing area S, and the drag and lift coefficients C_D and C_L, respectively. The airspeed V_A can be taken from flight data directly, and the longitudinal wind component during landing V_W can be calculated from the difference between the airspeed V_A and the ground speed V_G

$$V_W = V_A - V_G \,, \qquad \textbf{Eq. 5-5}$$

where positive values of V_W indicate a headwind component.

A runway overrun, which is the only outcome considered in the risk model, occurs when the available deceleration is less than the required deceleration:

$$\frac{d_a}{d_r} < 1 \,. \qquad \textbf{Eq. 5-6}$$

Hence, the ratio of the two decelerations d_a and d_r in Inequality 5-6 influences the probability of a runway overrun. The value of this ratio is the hazard in the risk model as depicted in Figure 5-3, which correlates with the probability and therefore with the risk. If the value of this quotient becomes smaller, the risk increases. It is important to know that both deceleration values d_a and d_r are subject to changes during the landing phase.

The application of the described method starts with the touchdown of the aircraft, where d_r is defined by the ground speed and the available landing distance from the touchdown point. Immediately after touchdown, the value of d_r will first increase, as the remaining runway length

R will decrease without a significant reduction of ground speed V_G, while d_a stays approximately constant. As soon as braking begins, both values of d_r and d_a start to decrease. As the decrease of d_r is proportionally higher than the decrease of d_a, the quotient starts to rise and an overrun becomes more unlikely. In order to avoid d_r from becoming zero, the measuring interval has to be limited to a certain amount of remaining ground speed which is considered to be safe with regard to the risk of an overrun, but with the aircraft still on the runway.

This requirement is also in line with the fact that in daily flight operation an aircraft would normally not decelerate towards a complete stop on the runway. Instead, the aircraft usually leaves the runway via an exit with a certain amount of ground speed, as the runway occupation time has to be limited as much as possible for an efficient operation from the perspective of the aerodrome operator. Also, a continuous transition from the landing towards the taxi-in phase reduces block time and therefore is in favor of passenger convenience.

A value of $V_G = 30\,m/s$ (appr. 60 knots) can be determined empirically by Flight Data Analysis where the aircraft still remains on the runway centerline[16] in more than 99.7 percent of all landings.

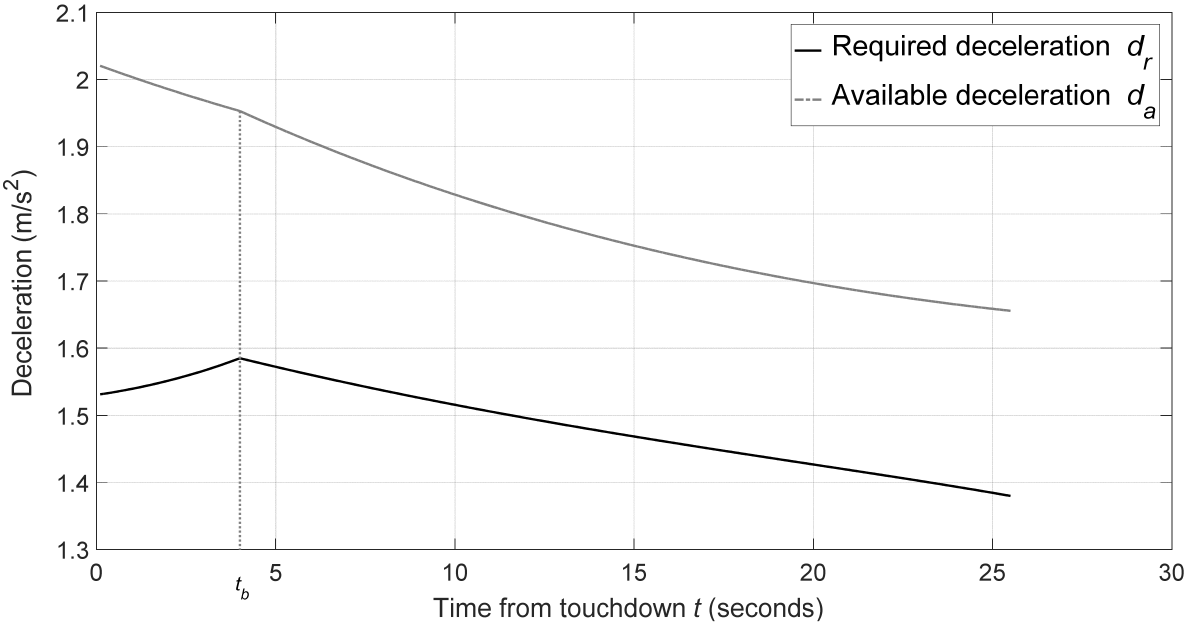

Figure 5-5 Behavior of required deceleration d_r and available deceleration d_a, assuming an available friction coefficient of $\mu_a = 0.15$, touchdown at 400 m beyond runway threshold on a 2000 m runway, aircraft type A320 with typical landing weight, idle reverse thrust and no wind. Braking starts 4 seconds after touchdown at t_b, source: own research

Figure 5-5 shows the typical behavior of d_r and d_a. In this example, the aircraft touches down with ground speed $V_G = 70\,m/s$, 400 meters beyond the runway threshold of a 2000 meters-

[16] This condition is defined by a difference between the aircraft heading and the runway heading of less than 10 degrees.

runway, so remaining runway distance R is 1600 meters at this point. As just after touchdown only aerodynamic drag and rolling friction influences the speed, resulting in only slight deceleration, d_r initially increases. Four seconds later, at point t_b, braking begins with a braking friction of 0.15, which is sufficient to decelerate the aircraft in time. The graph ends at a groundspeed of $V_G = 30\,m/s$. In this example, the available friction coefficient μ_a is 0.17 and hence, close to the braking friction. With decreasing airspeed, the available deceleration d_a also decreases, as both the aerodynamic drag as well as the effect of idle reverse thrust decrease and hence, d_a converges towards a fixed value, predominately depending on μ_a and idle reverse thrust. However, as both graphs d_r and d_a do not intersect each other, the aircraft can stop in time without ending in a runway overrun.

Some of the influencing factors of d_a are considered to be fixed in the model, e.g. the aerodynamic coefficients C_D and C_L, the runway slope γ and also reverse thrust. The latter is considered to be always idle in the model.

While some of the influencing factors of d_r are manageable by the flight crew during landing, e.g. overspeed or long landing, which both result in higher values of d_r, the available friction coefficient μ_a is associated with some degree of uncertainty. Especially under changing environmental conditions the friction values on the runway might not be at a constant level. According to Table 5-1, the runway condition is the most contributing factor. Accident investigations revealed that actual friction sometimes might be considerably lower than anticipated by the flight crew [64].

Hence, the friction coefficient, which is available for a certain landing, is dominating the uncertainty and therefore the probability part of the risk the flight crew has to deal with during landing. Uncertainty is a typical characteristic of risk.

5.3 Definition of the Environmental Conditions

Taking this perception into the risk model, Inequality 5-6 can be solved for μ_a, combining Eq. 5-1 with Eq. 5-2. A runway overrun occurs, if

$$\mu_a < \frac{m \cdot d_r - D - X - m \cdot g \cdot \sin\gamma}{m \cdot g \cdot \cos\gamma - L}. \qquad \textbf{Eq. 5-7}$$

The term on the right-hand side of this inequality represents the required friction coefficient μ_r, which leads to an overrun, once it is higher than the available friction coefficient μ_a.

While an overrun occurs in any case once μ_r exceeds μ_a, it can also occur at a lower value due to the non-linear behavior of μ_r. With decreasing airspeed, μ_r becomes higher, as both aerodynamic drag and reverse thrust decrease. To evaluate the correct value of μ_r at each sampling point during landing, a simulation, using the right-hand term of Inequality 5-7, with all possible magnitudes of the friction coefficient is necessary. The value of the sought-for μ_r at this sampling point is derived from the simulation, where V_G reaches zero exactly at the runway end.

In general, considering each sampling point during an individual landing, the risk during this landing is at the highest level where μ_r reaches its maximum value μ_{r_max}. Since the risk evaluation within this dissertation is based on an FDA event, the point of the highest risk during landing defines this FDA event.

To reduce processing power, an effective approximation of μ_{r_max} is the calculation of μ_r only at the maximum value of d_r during landing (d_{r_max}), which is easy to determine using Eq. 5-1. The simulation must then only be conducted at this timepoint rather than for all sampling points during landing. An empirical comparison of 4,198 flights between the standard determination and the simplified method has shown that for more than 50 percent of all flights the results for μ_r are identical and the resulting difference between μ_r at d_{r_max} and μ_{r_max} is less than $1.5 \cdot 10^{-3}$ in 95 percent of all landings, with a maximum error of $3.5 \cdot 10^{-3}$. This error is well below the average rolling resistance and is therefore considered to be acceptable.

During an average landing the value of μ_{r_max} normally stays significantly below μ_a. Hence, a conditional probability of an overrun following a runway condition with friction coefficient μ_{r_max} has to be found in order to evaluate the respective risk level. This is possible by using a probability distribution of μ_a. The conditional probability can then be described as

$$P(overrun) = F\left(\mu_a = \mu_{r\_max}\right), \qquad \textbf{Eq. 5-8}$$

where $F\left(\mu_a = \mu_{r\_max}\right)$ is the cumulative probability distribution function (CDF) of the available friction coefficients μ_a at the value of $\mu_a = \mu_{r\_max}$.

The evaluation of this CDF is therefore essential to get the conditional probability and finally the risk level of a runway overrun.

5.3.1 Evaluation of the Runway Condition

Runway friction coefficients highly correlate with the runway condition, which is predominately influenced by airport weather, especially present or past precipitation and temperature [65]. Hence, it is desirable to distinguish between different runway conditions.

Weather information is available through METAR[17] data, which is provided by the Flight Data Analysis software [14]. The runway condition is estimated by analyzing METAR data. Usually the runway condition is clustered into four different conditions: dry, damp, wet and contaminated

[17] **MET**eorological **A**erodrome **R**eport, a format for reporting aerodrome weather information, updated every 30 minutes. Used as weather information to flight crew.

[66]. In general, if no precipitation is recorded, the runway condition is considered to be dry. Light or moderate precipitation at all temperatures as well as freezing precipitation or snow above 0 °C is considered to result in wet runways. Heavy precipitation at all temperatures as well as freezing precipitation or snow at or below 0 °C is considered to result in contaminated runways. Table 5-2 provides an example, how the runway condition may be classified based on METAR data. This classification is used in the presented risk model. Note that other classifications may be possible. As the classification relies on the presence or absence of precipitation only, damp runways cannot be classified by this method and hence, are not considered separately. If available, MOTNE[18] data is preferably used as distinct information about the runway condition is provided. In this case, precipitation and temperature values from METAR data are ignored.

Table 5-2 Different runway condition classification and their associated precipitation types and/or temperatures, source: own research

Runway condition classification	**Contamination type***	**Precipitation type****	**Temperature****
Dry	Dry	None	All temperatures
Wet	Damp, wet	Showers or thunderstorm in the vicinity, drizzle, showers of rain, light or moderate rain, snow grains, light or moderate thunderstorm	All temperatures
		light or moderate freezing drizzle, light freezing rain, drifting snow, light showers of snow, blowing snow, light snow, light snow grains, light thunderstorm rain	above 0°C
Contaminated	frost, dry snow, wet snow, slush, ice, compacted snow, frozen ruts	heavy freezing drizzle, heavy rain, moderate or heavy freezing rain, heavy showers of snow, moderate or heavy snow, heavy snow grains, hail, heavy thunderstorm rain, heavy thunderstorm snow	All temperatures
		light or moderate freezing drizzle, light freezing rain, drifting snow, light or moderate showers of snow, blowing snow, light snow, light snow grains, light thunderstorm rain	At or below 0°C

* if MOTNE exists, in this case ignore precipitation

** according METAR which is chronologically closest to the point in time of landing

5.3.2 Evaluation of Missing Coefficients and Aircraft Parameters

Not all of the required parameters, which are necessary to solve Inequality 5-7, can be derived from flight data directly, as they are neither measured nor recorded. In particular, these parameters are:

[18] **M**eteorological **O**perational **T**elecommunications **N**etwork **E**urope, a coded information regarding runway condition, runway contamination and braking action/friction values.

- The rolling-resistance μ_{roll}, if no aircraft braking is applied,
- The amount of reverse thrust,
- Aerodynamic coefficients.

Other means have to be used for the evaluation of these parameters. While the first two parameters can be derived from tables or graphs, either specific or generic, the aerodynamic coefficients can be derived from flight data in a statistical approach.

The following analysis is based on operational flight data of aircraft types A319-112, A320-214 and A321-231, gathered by the flight data of a major European airline.

5.3.2.1 Rolling Resistance

For the purpose of the parameter estimation, only landing segments are used, where no aircraft brakes are applied, as the influence of the brake pressure on the deceleration force is not yet known. In this particular case, the friction coefficient μ from Eq. 5-2 is a pure rolling-resistance coefficient μ_{roll}.

However, this rolling-resistance coefficient depends on various influencing factors. First of all, the rolling-resistance coefficient is influenced by the runway surface texture. This influence cannot be evaluated for each considered runway and is treated to be unknown. The same applies to other influencing factors like tyre type and tyre wear condition. Hence, a mean rolling-resistance coefficient is used. According to the following graphs from Leland and Taylor [67], the magnitude of the rolling-resistance correlates especially with the tire inflation pressure, the forward velocity and the runway condition.

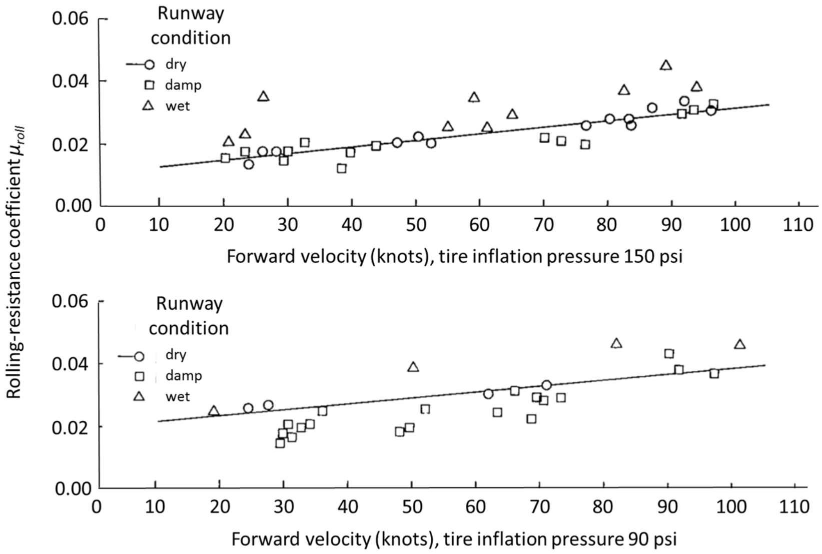

Figure 5-6 Effect of runway condition on the rolling resistance coefficient of an un-braked tire, tire inflation 150 psi versus 90 psi based on [67]

Higher tire-inflation pressure results in lower friction coefficients on dry and damp runway conditions [67]. Figure 5-6 shows tire-inflation pressures of 90 psi and 150 psi. The aircraft types of the Airbus A320-family use even higher pressures between 180 psi (A319) and up to 230 psi (A321). So, according to above graphs, the rolling-resistance coefficients are expected to be even lower than shown in the graphs [68].

The rolling-resistance coefficient increases with higher ground speeds V_G, as indicated by the rising solid line in the graphs in Figure 5-6. It is also shifted to higher values, if the runway is wet due to fluid drag on the tire, while it is shifted towards lower values on a damp surface due to lubrication by the water film [67]. However, a wet surface in the above graphs is defined as a water depth of between 0.1 to 0.3 inches. This corresponds to the definition of a contaminated runway according ICAO [69]. Hence, the effect of higher rolling-resistance coefficients on wet runway surfaces is not considered in the risk model.

Within the scope of this thesis, the mean rolling-resistance coefficient μ_{roll} consists of a fixed part, which is lower than in Figure 5-6 due to the higher tire pressure, combined with a speed dependent part, which corresponds with the solid line in Figure 5-6. The rolling-resistance coefficient μ_{roll} is estimated to be

$$\mu_{roll} = 0.005 + 3 \cdot 10^{-4} \cdot V_G \, . \qquad \textbf{Eq. 5-9}$$

This is also in accordance with Currey, who specifies the coefficients of rolling friction in a range between 0.008 and 0.02 on a normal runway [70], which would be reached at ground speeds between 10 meters per second (appr. 20 knots) and 50 meters per second (appr. 100 knots) with above equation.

For the last step of parameter evaluation, the estimation of the aerodynamic coefficients, only landings on dry and wet runways are used. Landings on contaminated runways are not considered, as the rolling-resistance cannot be estimated precisely and the variance is estimated to be larger than on dry or wet runways.

5.3.2.2 Reverse Thrust

Reverse thrust normally accounts only for a small proportion of the overall deceleration force. However, if the runway surface is wet or slippery, the amount of reverse thrust force can easily dominate the overall deceleration force and become the main stopping force.

In modern high bypass engines, only the fan thrust is reversed, while the core engine thrust is still producing forward thrust. As the fan thrust is only reversed to a certain angle against forward direction, the overall amount of reverse thrust is significantly lower than the equivalent thrust which would be produced in the direction of aircraft movement. The graphics in Figure 5-7 shows this behavior. The net reverse thrust in this graphic, which is the reverse thrust in longitudinal direction, would be equal to $cos\theta \cdot F_2 - F_1$.

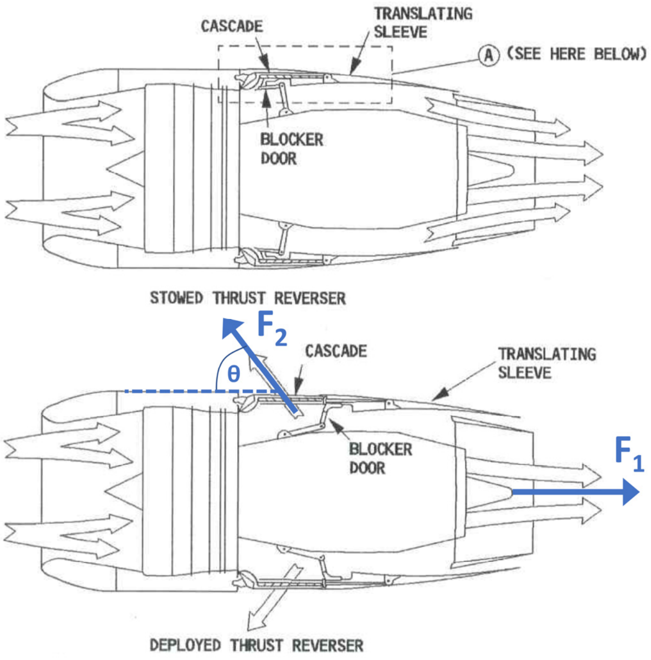

Figure 5-7 Schematic of thrust reverse forces based on [68]

The amount of reverse thrust for a certain engine type can be derived from graphs provided by the aircraft manufacturer. Figure 5-8 shows the net reverse thrust of a CFM56-5B4 and -5B6 engine with a maximum thrust of 27,000 lbs (120.1 kN) and 23,500 lbs (104.5 kN), respectively, which are used on the considered aircraft types A320-214 and A319-112. Figure 5-9 shows the net reverse thrust of an IAE V2533-A5 engine with a maximum thrust of 32,000 lbs (142.3 kN) [71], which is used on the considered aircraft type A321-231.

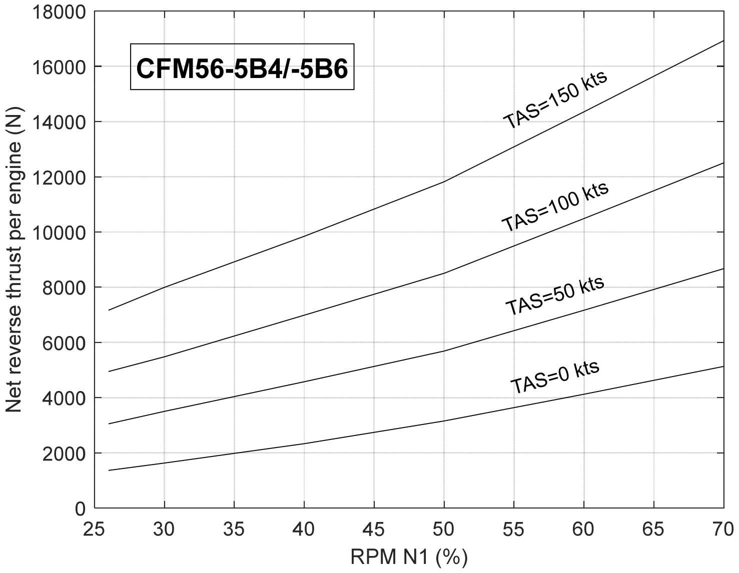

Figure 5-8 Net reverse thrust of a CFM56-5B4 and -5B6 engine on a standard day at sea level for different RPMs and true airspeeds based on [71]

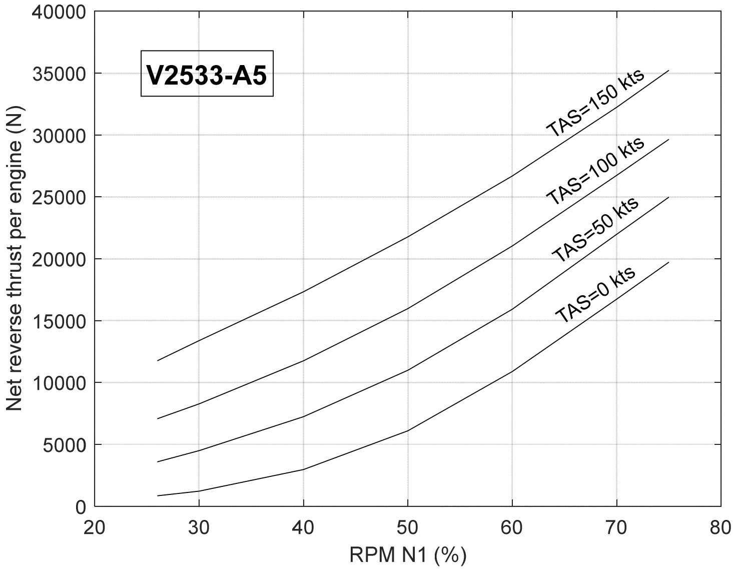

Figure 5-9 Net reverse thrust of an IAE V2533-A5 engine on a standard day at sea level for different RPMs and true airspeeds based on [71]

The amount of net reverse thrust mainly depends on the N1 RPM and the true airspeed for a particular engine type. Even though both engine types show a similar behaviour, the gradient of the thrust curves and also the maximum amount of reverse thrust relative to the maximum thrust of the engine, is different. The reason among others is a different bypass ratio (CFM: 5.7, IAE: 4.5) and a different reverser construction (CFM: Pivoting doors, IAE: Cascade reverser).

The above charts show that the net reverse thrust produced by the V2500-type engines is significantly higher than that of the CFM56-type engines. The exact amount of reverse thrust can be evaluated by using the above graphs with linear interpolation.

Even though operating procedures from aircraft manufacturers recommend full reverse thrust [68], many airports request flight crews to use idle reverse thrust for noise abatement reasons in normal operations, e.g. Frankfurt/Main airport:

"Reverse thrust not AVBL [available] on any RWY. Exception: Idle thrust or safety reasons." [72]

According flight data analysis, the use of reverse thrust which is higher than idle can be observed in less than five percent of all landings at any destination. Therefore, within the risk model of this thesis, in order to evaluate the most critical point in time of an individual landing according chapter 5.3, it is assumed that the flight crew uses idle reverse thrust only.

This assumption is also convenient, as especially for a combination of low friction values with crosswind, full reverse thrust cannot be used due to a wind vane effect. If the runway friction is low, the crab angle of the aircraft, which was maintained during the approach, has to be maintained during rollout for directional control. The sideward component of the reverse thrust then pulls the aircraft towards the lee side, which leads to an unstable situation with the increased risk of a lateral runway excursion, see Figure 5-10 [73].

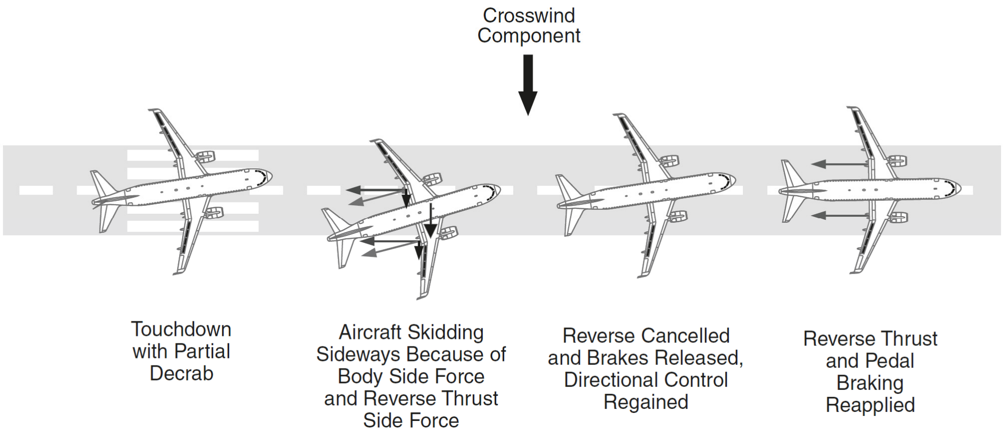
Crosswind Component
Touchdown with Partial Decrab
Aircraft Skidding Sideways Because of Body Side Force and Reverse Thrust Side Force
Reverse Cancelled and Brakes Released, Directional Control Regained
Reverse Thrust and Pedal Braking Reapplied

Figure 5-10 Wind vane effect due to reverse thrust in combination with crosswind [73]

When selecting reverse thrust by using the idle reverse thrust lever position, the engine normally increases N1 RPM to a higher value than idle reverse (CFM56: 43 percent, IAE V2500: 39 percent), and thereafter approaches idle values of 27 percent within a certain timespan (CFM56: 6 seconds, IAE V2500: 9 seconds), see also Figure 5-11. This behavior can be derived by flight data, when comparing the thrust lever position with the Reverse N1.

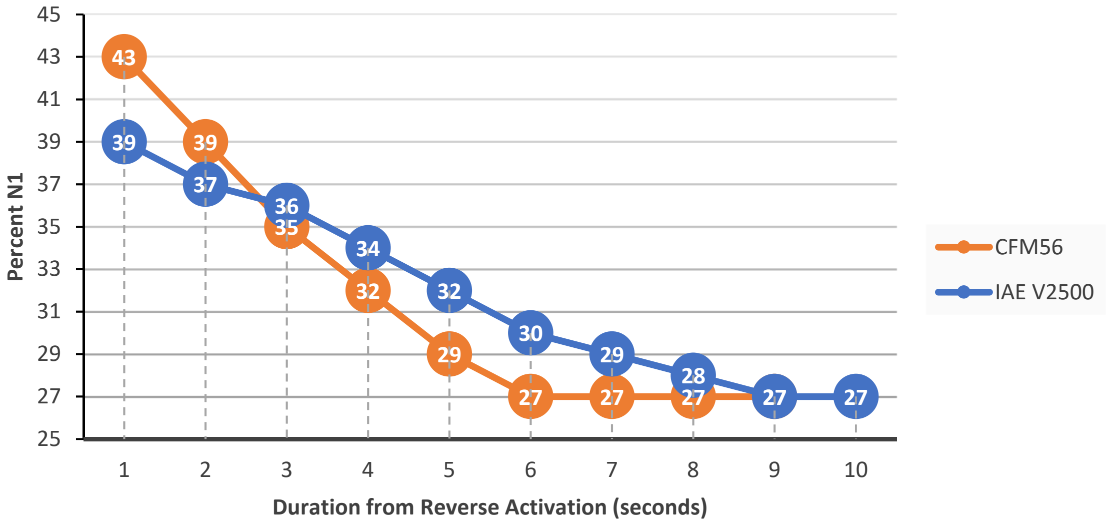

Figure 5-11 Behavior of reverse N1 after selection of idle reverse thrust. For both engine types, idle reverse N1 is approximately 27 percent, source: FDA

As the reverse thrust is slightly higher during this time period, this effect will be incorporated in the risk model, depending on the position in time of the most critical point of μ_{r_max}. If at this point in time no reverse was selected yet, it is assumed, that idle reverse will be selected immediately, following the graphs in Figure 5-11. If idle reverse N1 is selected already at 27 percent, it is assumed that it stays at this level. On the other hand, if reverse N1 is higher than 27 percent at the most critical point, it is assumed, that it is reduced to idle reverse thrust immediately, but still following graph of Figure 5-11.

Only for the validation of the overall risk of the underlying risk model, which is described in chapter 5.4, the amount of full reverse thrust is required for the purpose of a back-test of the estimated accident rate, as a certain proportion of landings is performed with full reverse thrust.

5.3.2.3 Evaluation of Aerodynamic Coefficients

For the estimation of drag and lift coefficients in landing configuration, the BADA database[19] can be used. The BADA database provides aircraft performance models of the most common aircraft types for the purpose of trajectory simulation and prediction [74]. BADA contains, among other parameters, drag coefficients for different A320 family types for different configurations. Other sources use this report exactly for this purpose, e.g. [75]. However, the objective of the BADA database is to provide information about inflight performance for air traffic management, while the influence of ground spoilers and ground effect during landing roll is not considered at all. Hence, other means to evaluate the aerodynamic coefficients have to be used within the scope of this thesis. Nevertheless, for an approximation of the scale as well as the relationship of the aerodynamic coefficients between the different aircraft types, the data of the report can be used for validation.

According to a "Pilot Guide to Takeoff Safety", provided by the FAA, for a typical mid-size two-engine airplane, the lift is reduced by a proportion of 102 percent, i.e. the lift is slightly negative [76]. For simplification purpose, it will be assumed that the lift is zero in this case, so Eq. 5-2 can be simplified in the following way:

$$d_a = \frac{1}{m} \cdot [D + X + mg \cdot \sin\gamma + \mu_a \cdot mg \cdot \cos\gamma]\,. \qquad \textbf{Eq. 5-10}$$

The only missing aerodynamic coefficient is the drag coefficient C_D then. As this is only a single value, it can easily be derived from flight data by minimizing the absolute value of the difference $n_{x,diff}$ between the measured longitudinal load factor $n_{x,data}$ at a certain point in time from flight data and a calculated value $n_{x,calc}$. The latter value is based on the calculation of the deceleration at the considered point in time, using recorded gross weight of the aircraft, measured air density, the average slope of the considered runway and the estimated parameters rolling-resistance and reverse thrust from chapters 5.3.2.1 and 5.3.2.2 in combination with the actual measured airspeed, ground speed and reverse thrust N1:

[19] Base of aircraft data from Eurocontrol (European Organization for the Safety of Air Navigation), a database in which aircraft performance data is provided mainly for air traffic control purposes, see [125,126]

$$n_{x,diff} = n_{x,data} - n_{x,calc} \,. \qquad \textbf{Eq. 5-11}$$

A set of 164,658 landings of aircraft types A319, A320 and A321 have been analyzed for this reason. To focus on the measurement of aerodynamic coefficients, only samples with no brake application are used, as the influence of aircraft braking on the deceleration is not known. Landings with no braking, i.e. no brake pressure, is quite common on runways which are long enough and the flight crew aims to leave at the runway end to save taxi time, so a large set of data is available. The requirements for a sample to be used for evaluation of the drag coefficient is:

- all wheels on ground,
- no brake pressure applied (free rolling),
- ground spoilers extended,
- reverse thrust activated.

In this case, a comparable scenario during rollout can be assured. Within the time series of flight data during rollout, all relevant flight data samples have been exported, where ground speed of the aircraft went through values of 72 meters per second (140 knots) to 15.4 meters per second (30 knots) in steps of 5.1 meters per second (10 knots) each, and additionally from 66.9 meters per second (130 knots) to 41.2 meters per second (80 knots) in steps of 1 meter per second (2 knots) each, so overall up to 32 values per landing have been considered in this analysis.

The measured longitudinal load factor $n_{x,data}$ is plotted versus the calculated value $n_{x,calc}$ in Figure 5-13 to Figure 5-17, one graph for each aircraft type and valid landing configuration. Different colors are used for different amounts of reverse thrust.

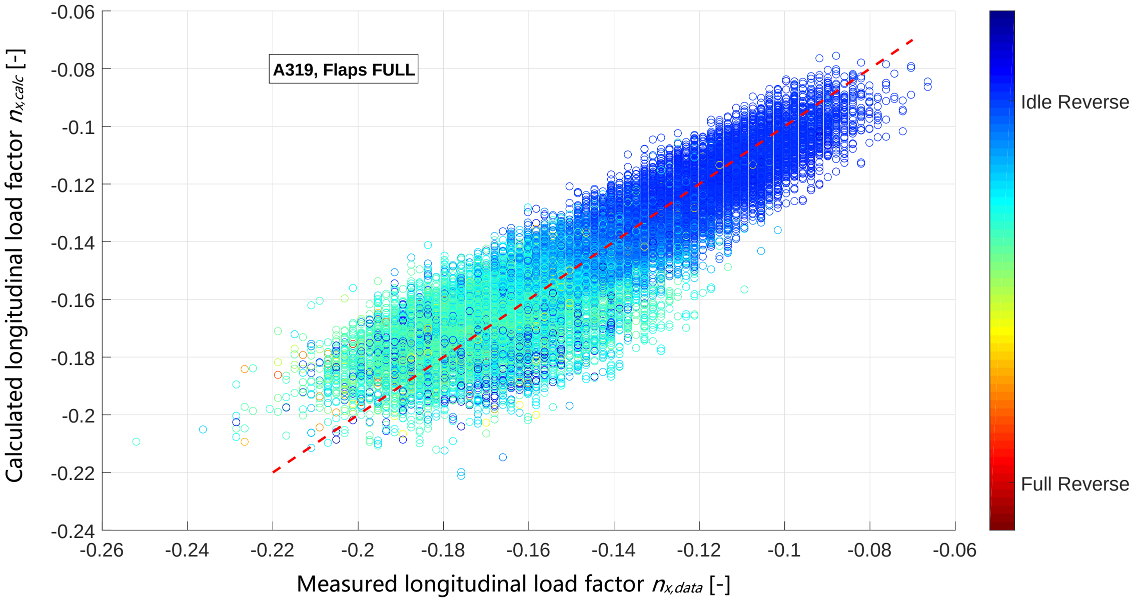

Figure 5-12 Calculated versus measured longitudinal load factor, A319 with flaps full,

source: own research

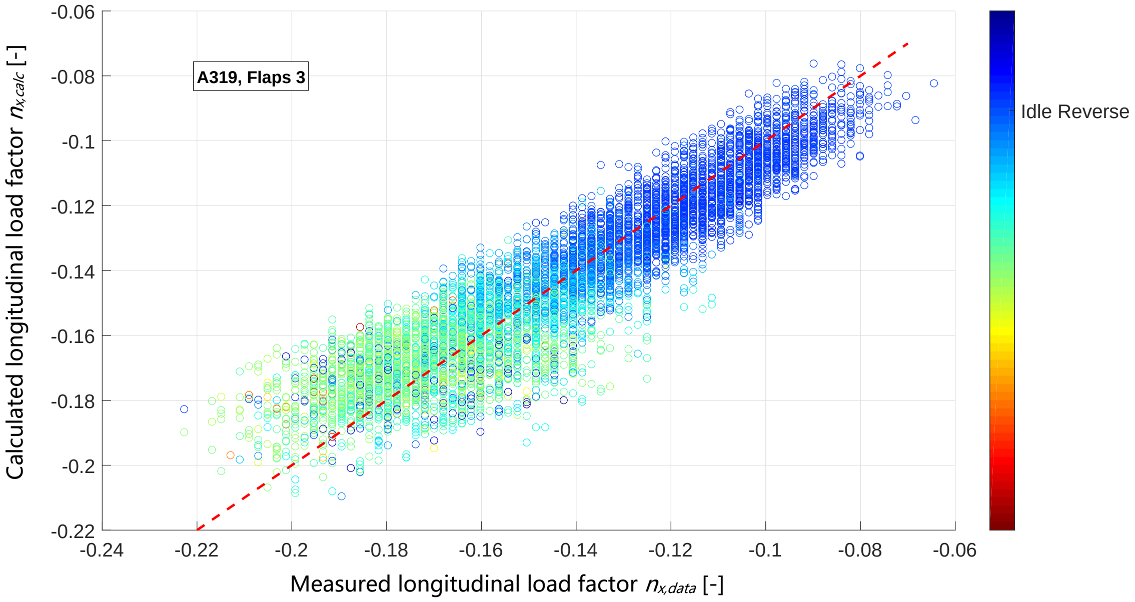

Figure 5-13 Calculated versus measured longitudinal load factor, A319 with flaps 3,

source: own research

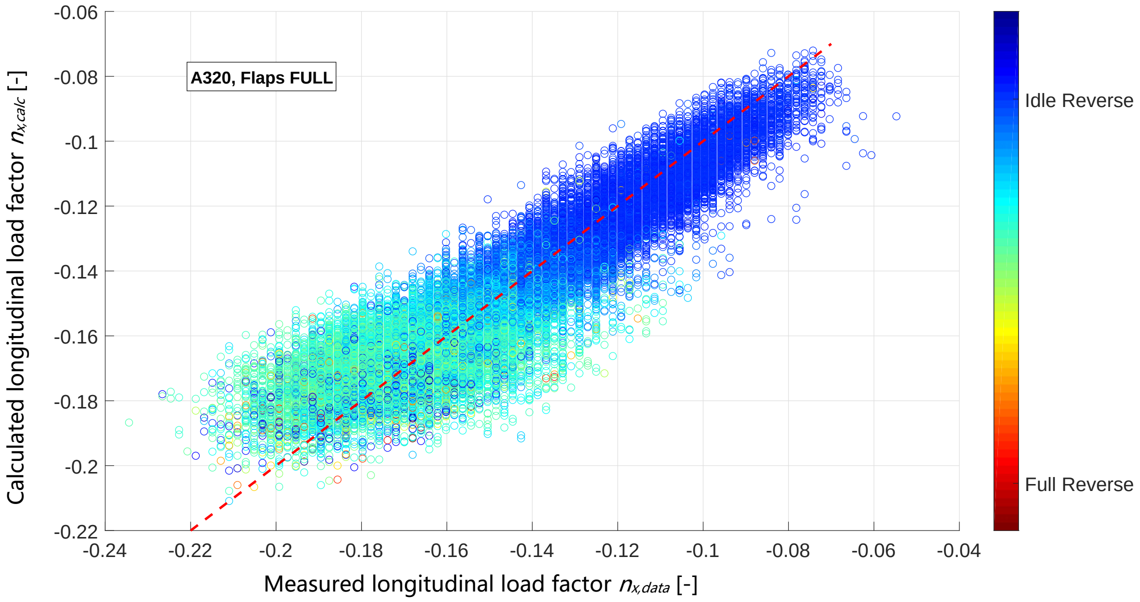

Figure 5-14 Calculated versus measured longitudinal load factor, A320 with flaps full, source: own research

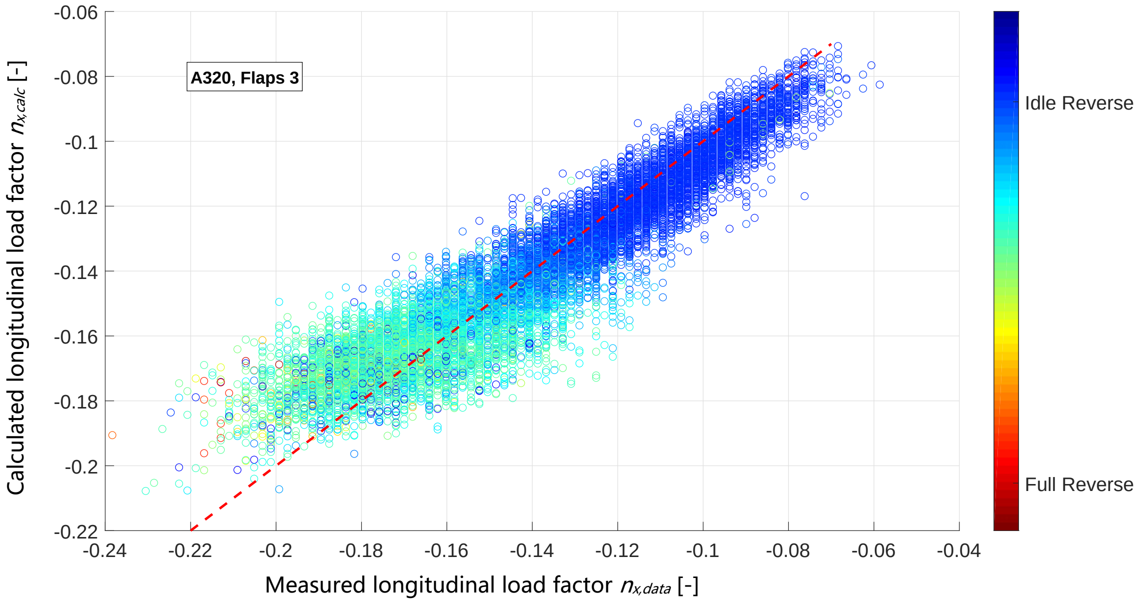

Figure 5-15 Calculated versus measured longitudinal load factor, A320 with flaps 3, source: own research

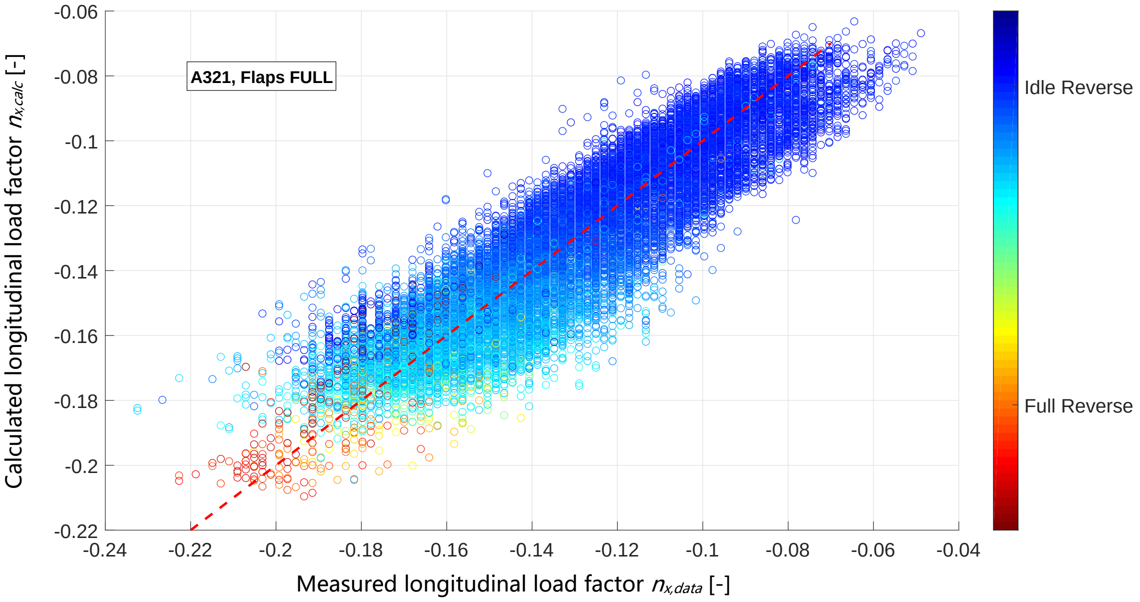

Figure 5-16 Calculated versus measured longitudinal load factor, A321 with flaps full, source: own research

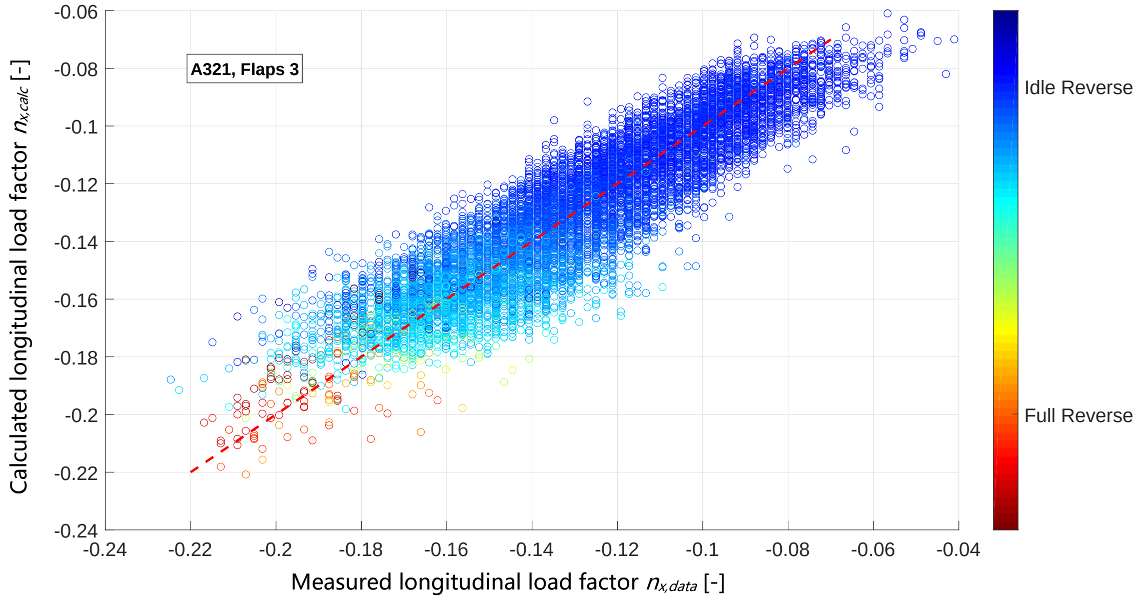

Figure 5-17 Calculated versus measured longitudinal load factor, A321 with flaps 3, source: own research

Out of the 164,658 flights, in total 133,103 samples of different speeds and different reverse thrust settings have been used to evaluate the drag coefficient C_D. The results can be seen in Table 5-3. Mean value of the difference $n_{x,diff}$, $\mu_{nx,diff}$, is near zero for all aircraft types and configurations, as this value was minimized to provide a symmetrical distribution of all values of $n_{x,diff}$. The standard deviation $\sigma_{nx,diff}$ ranges between 0.01068 and 0.01178, 95 percent of all absolute values of $n_{x,diff}$ are within 0.022 in average. Since the standard deviation of the differences is lower than the rolling resistance, the error is considered to be low enough to evaluate the available friction coefficient μ_a with a reasonable precision.

Table 5-3 Overview of the resulting aircraft parameters, source: own research

Aircraft Type	Configuration	No of samples	Drag coefficient C_D	Mean value $\mu_{nx,diff}$	Standard deviation $\sigma_{nx,diff}$	95% absolute values $n_{x,diff95}$
A319	Flaps Full	29,709	**0.269**	-0.00012	0.01157	0.02323
A319	Flaps 3	7,193	**0.220**	-0.00009	0.01147	0.02256
A320	Flaps Full	46,008	**0.247**	-0.00009	0.01068	0.02164
A320	Flaps 3	14,441	**0.211**	0.00022	0.01103	0.02234
A321	Flaps Full	24,769	**0.210**	0.0	0.01169	0.02304
A321	Flaps 3	10,983	**0.191**	-0.00021	0.01178	0.02328

The BADA database provides only values for configuration "FULL" for the different types of the A320 family during approach, i.e. without ground spoilers and ground effect, and also, as lift is assumed to be zero, without induced drag. According to BADA, the drag coefficient is the highest for A319 and the lowest for A321, which corresponds with the results in Table 5-3. Even though all aircraft types have the same wing span with the same wing surface area of 122.6 square meters, the flap system is different. The maximum flap deflection is the highest on A319 with a value of 40 degrees and the lowest on A321 with only 25 degrees [68]. The wing of the A321 has to produce much more lift during approach due to the higher aircraft weights, and this is not possible with the normal flap construction as used on A319 and A320. Instead, the 321 is equipped with a much more complex double slatted flap system, which is capable of producing much more lift with a better lift to drag ratio, which results in an overall level of lower drag [68].

Inaccuracies in the calculated longitudinal load factor $n_{x,calc}$ may be caused by different effects:

The effect of the runway slope γ from Eq. 5-2 is based on an average runway slope from the Navigation database. In most cases, this approach is accurate enough, however, on some runways the average slope differs significantly from certain sections of the runway, which might exclusively be used by the landing aircraft. E.g. on Runway 01 in Moscow Vnukovo, in average there is no runway slope (Figure 5-18), but the touchdown zone has an average uphill slope of 1.0 percent.

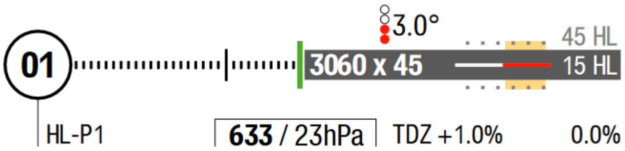

Figure 5-18 Schematic of the landing runway 01 at Moscow Vnukovo with indication of the average runway slope in the lower right, which is used by the flight data analysis software, and the indication of the slope of the touchdown zone (TDZ) [77]

When looking at Figure 5-19, a more detailed schematic of the runway profile is provided. As the landing normally takes place in the first half of the runway only, the slope differs by 1.0 percent [77]. If looking at the pitch value of the aircraft during landing roll, even values of 1.4 degrees (more than 3 percent) can be measured temporarily, which indicates, that even the runway profile description from Figure 5-19 is only an average value in the first part of the runway. This difference between actual slope and assumed slope would already account for 0.025 g.

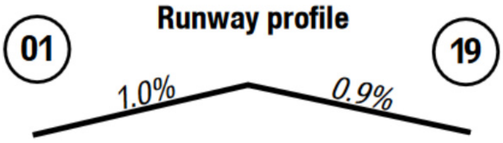

Figure 5-19 More detailed schematic of the runway profile of runway 01 in Moscow Vnukovo [77]

The amount of reverse thrust according to Figure 5-8 and Figure 5-9 is based on a standard air density and temperature. Variations of these atmospheric conditions can influence the amount of reverse thrust significantly, which is not taken into consideration in the risk model.

The rolling resistance coefficient μ_{roll} is only an average value, which might vary with different environmental conditions, as mentioned in chapter 5.3.2.1.

Also, both the frequency and also the resolution of the recorded aircraft parameters lead to inaccuracies of the input values, which finally influence the accuracy of the calculated longitudinal load factor $n_{x,calc}$.

5.3.3 Determination of the Available Friction Coefficient

In the next step, statistics about the available friction coefficients μ_a for each runway condition have to be evaluated from past flight data to enable a risk forecast for an individual landing. It is assumed that the resulting distribution of friction coefficients can be expected also for future landings for all aircraft types. The risk of a runway overrun correlates with the probability of a lower available friction than required, depending on the influencing factors of the individual landing, expressed by the required friction μ_r.

For the evaluation of these distributions for each runway condition, a large set of past flights has to be analyzed. By use of Eq. 5-2, solved for the available friction coefficient μ_a, an average μ_a can be derived from the flight data for each analyzed flight.

As the sought-for distribution consists of the available friction coefficients μ_a, only flight data can be used, where the maximum deceleration demand was higher than the friction was providing. Most of the analyzed landings have deceleration demands which are significantly lower than friction available, so suitable landings have to be identified to enable an evaluation of the available friction.

The maximum available friction coefficient μ_a of an individual landing depends, besides the influence factors described above, also on the ground speed of the aircraft during landing. This effect is much higher on non-grooved wet runways than on dry runways or grooved wet runways, as depicted in Figure 5-20. This effect is nearly negligible for dry runways and grooved wet runways, however, for un-grooved wet runways it is significant. The reason is mainly the hydroplaning of the aircraft tyres on un-grooved wet runways when the rolling or sliding tire is lifted off the pavement surface by the water pressures built up under the tire [69].

As the goal of the risk model in this thesis is to provide a single distribution of the available friction, depending on the runway condition without further differentiation of runway surfaces, the model contains a simplification of the speed effect on the friction coefficient. This is also necessary, as calculation of a required friction would be too complex if the distribution of the available friction changes with aircraft speed.

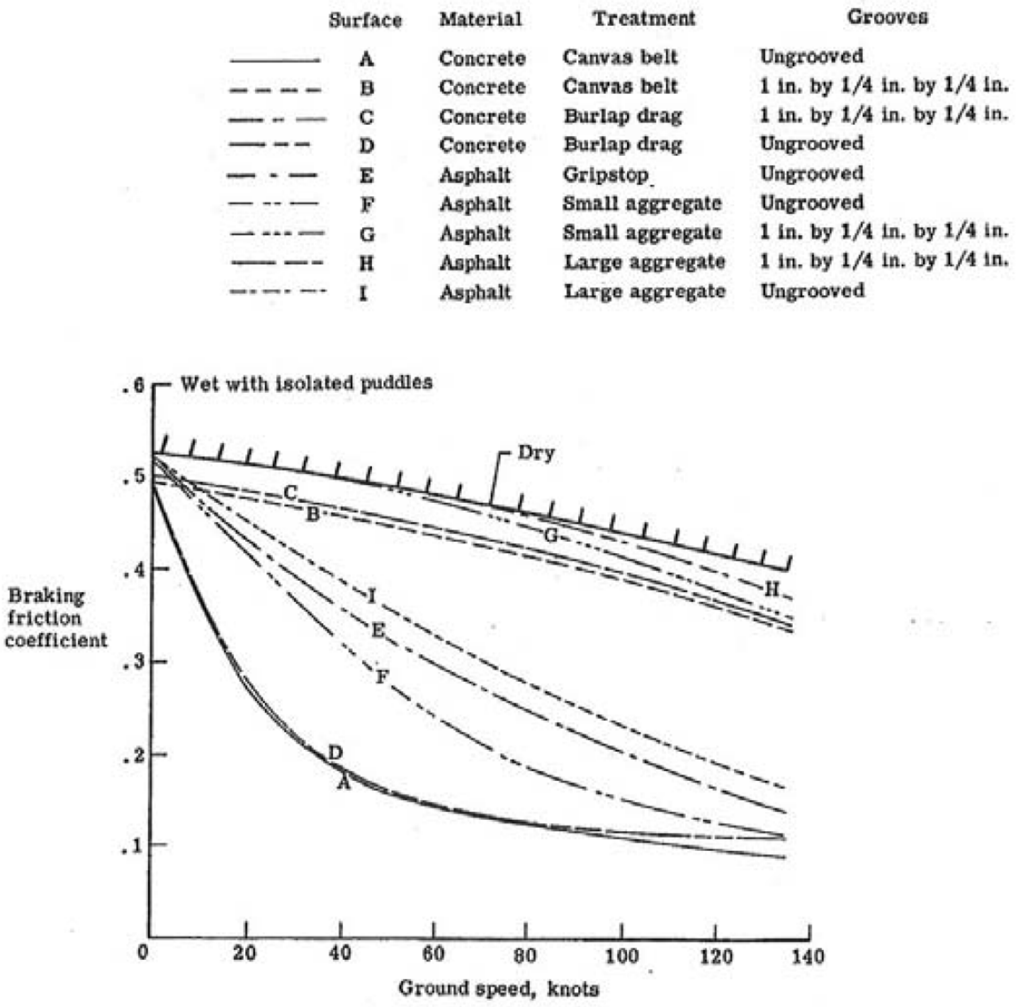

Surface	Material	Treatment	Grooves
A	Concrete	Canvas belt	Ungrooved
B	Concrete	Canvas belt	1 in. by 1/4 in. by 1/4 in.
C	Concrete	Burlap drag	1 in. by 1/4 in. by 1/4 in.
D	Concrete	Burlap drag	Ungrooved
E	Asphalt	Gripstop	Ungrooved
F	Asphalt	Small aggregate	Ungrooved
G	Asphalt	Small aggregate	1 in. by 1/4 in. by 1/4 in.
H	Asphalt	Large aggregate	1 in. by 1/4 in. by 1/4 in.
I	Asphalt	Large aggregate	Ungrooved

Figure 5-20 Friction coefficient versus velocity and runway surface [78]

Taking Figure 5-20 as a reference, a speed interval should be used for evaluation of the available friction coefficient μ_a, where this coefficient reaches values, which are representative for the whole speed range during landing roll. For a typical landing, the speeds of the aircraft are within the depicted range in Figure 5-20.

For higher speeds, the friction is less relevant for stopping as the aerodynamic braking and reverse thrust result in higher decelerations and hence dominate the overall braking force in case of poor friction (see also Figure 5-13 to Figure 5-17). Hence, the effect of high ground speeds on the friction coefficient is not as relevant as at lower speeds.

An interval between 46.3 meters per second (90 knots) and 15.4 meters per second (30 knots) ground speed is assumed to adequately represent the average friction coefficient of an individual landing without the risk of over- or underestimating the friction.

Figure 5-21 and Figure 5-22 depict the speed correlation of the available friction coefficient, measured by use of flight data with the autobrake method, as described in chapter 5.3.3.2. The graphs show a box plot of the available friction coefficients depending on different ground speed regimes, discretized in steps of 5.1 meters per second (10 knots) each. In each box, the central mark indicates the median, and the bottom and top edges of the box indicate the 25th and 75th percentiles, respectively. The whiskers contain all values within +/- 2.7 times the standard deviation.

Both graphs confirm the analysis of Yager et al [79]. For wet runways (Figure 5-21), the average friction coefficient increases with lower speeds and the standard deviation decreases. Also, at ground speeds of 36 meters per second (70 knots) and below the outliers to the low side disappear, so friction is at a homogenous level, towards a relatively high level.

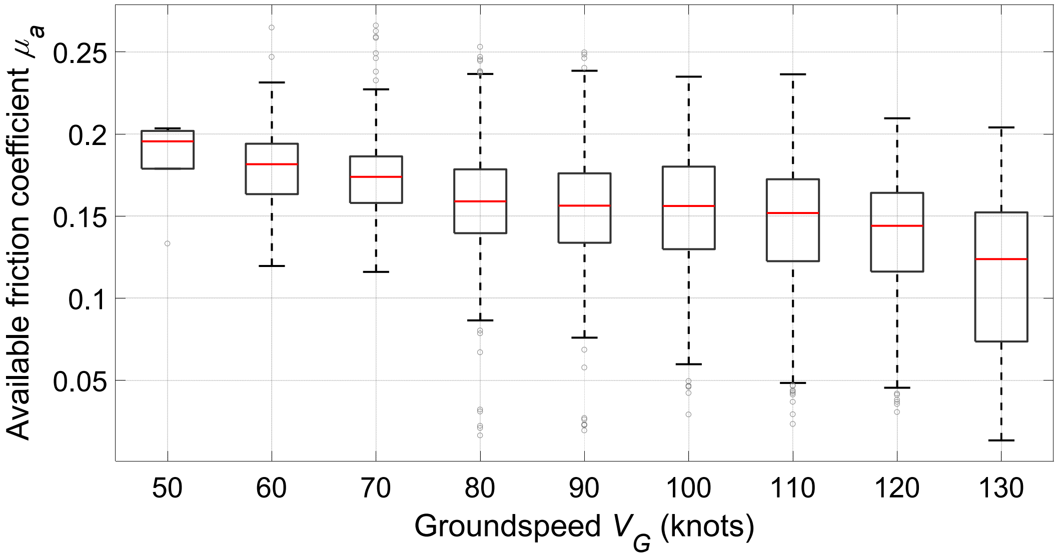

Figure 5-21 Wet runway, source: own research

For contaminated runways, as depicted in Figure 5-22, the friction coefficients also increase to higher levels at lower speeds. However, the standard deviation stays at relatively high levels with still a certain amount of measurements ranging into low areas of friction. As the speed is low, this effect may not be caused by hydroplaning due to water on the runway as seen on wet runways at higher speeds. Instead, this effect could be caused by contaminants like snow or ice on the runway.

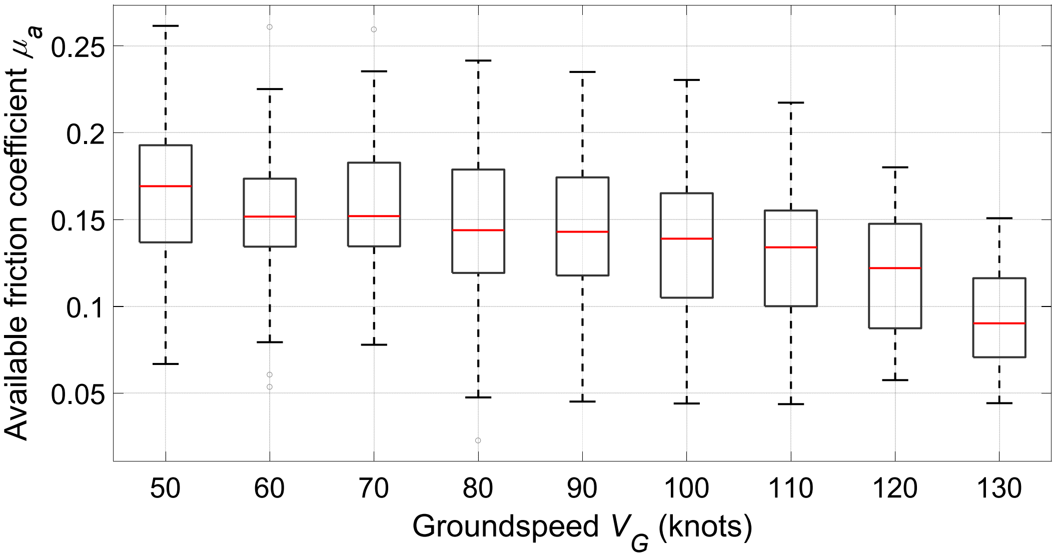

Figure 5-22 Contaminated runway, source: own research

In general, during braking antiskid aims to take the most advantage of the runway friction by controlling the brake pressure to enable a critical slip of the tire. Therefore, the optimum friction can be achieved by the system depending on the runway condition.

The relationship between friction coefficient and braking pressure is a linear function as depicted by the dashed line in Figure 5-23, as long as the demanded friction is lower than the available friction.

If the demanded friction becomes higher than the available friction, the pressure is limited by antiskid, so that the achieved friction equals the maximum available friction μ_a [80]. There is no parameter which indicates whether the maximum value was reached. Hence, to evaluate μ_a, the demand must be higher than the maximum friction which is available.

Two different methods are used to find such landings: The first one identifies brake pedal applications during manual braking, where the braking demand was higher than the friction of the runway supported (brake pedal deflection, BPD method).

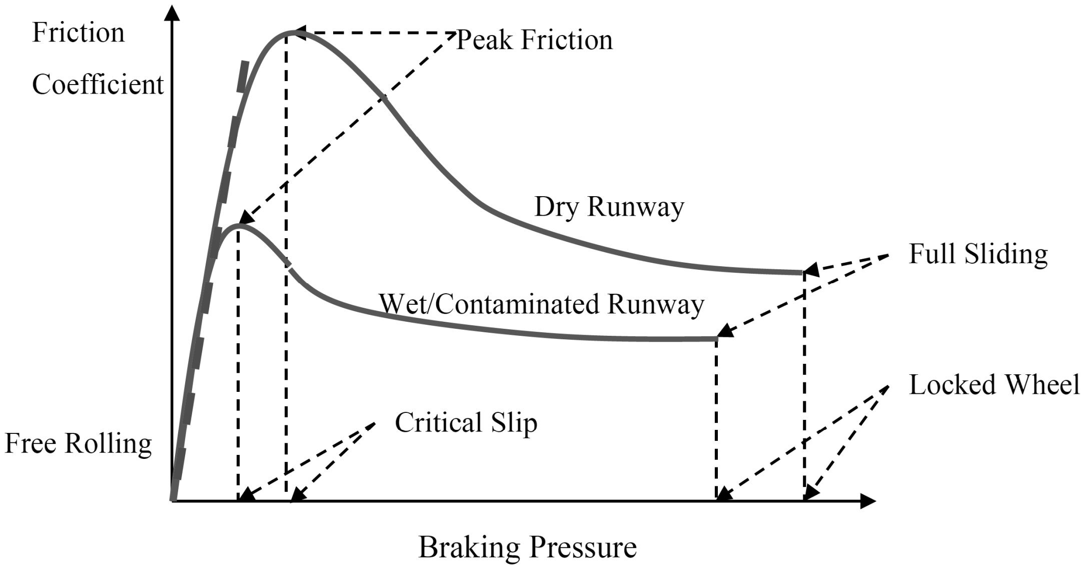

Figure 5-23 Functional principle of the antiskid system of modern aircraft, brake pressure application depending on the friction [80]

The second method identifies landings with autobrake selection, where the target deceleration rate was not reached (autobrake, AB method).

For the development of the two methods, flight data of 164,658 landings have been analyzed, conducted by aircraft types Airbus A319, A320 and A321.

5.3.3.1 Brake Pedals (BPD Method)

At first glance, if looking for high brake demands at the maximum available friction, landings with manual brake application near the maximum possible brake pedal deflection seems to lead to suitable results. However, this assumption is not correct.

Figure 5-24 shows a box plot of the brake pressures, which were measured in the flight data depending on different brake pedal deflections (BPDs), discretized in steps of five degrees of BPD each.

In each box, the central mark indicates the median, and the bottom and top edges of the box indicate the 25th and 75th percentiles, respectively. The whiskers contain all values within +/- 2.7 times the standard deviation.

Approximately 2.3 million samples with manual brake application were analyzed to create this graph. Up to 55 degrees BPD, a clear correlation between deflection angle and mean brake pressure can be observed with small variations. However, above 60 degrees BPD, the average brake pressure starts to drop significantly. At 80 degrees BPD, the mean brake pressure is near zero, which indicates a high brake demand without any effect. The combination of high BPD and low brake pressure indicates a high brake demand with low friction. This shows that even it seems to be favorable to consider only landings with high BPDs for evaluating the available friction due to the high braking demand, the resulting values do not represent the distribution of available friction, even though demand is higher than friction available. The graph suggests that high BPDs are used only if the available braking is less than demanded. Using the underlying distribution of a very high BPD would therefore underestimate the friction.

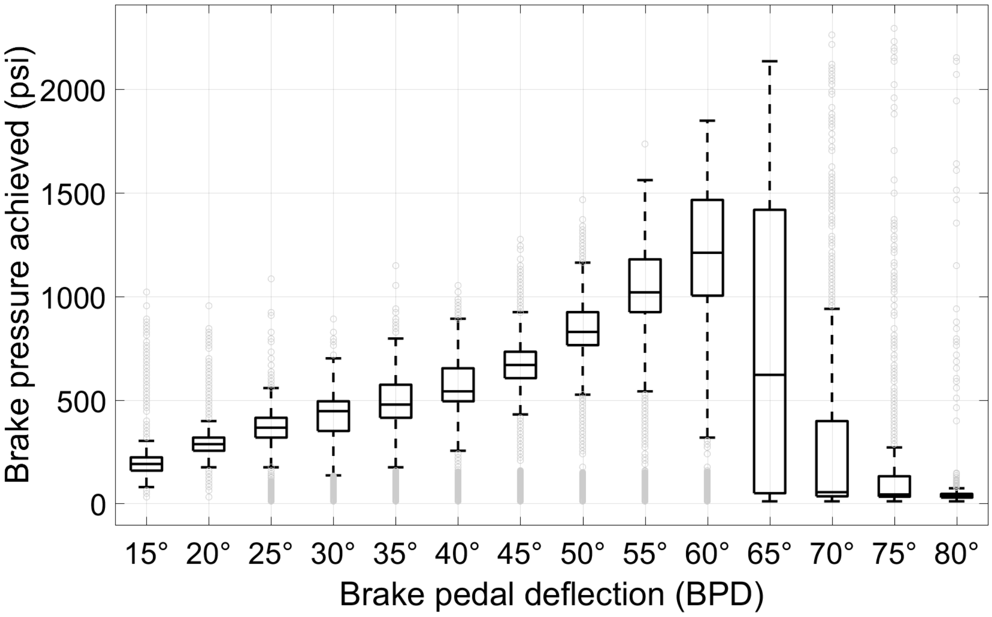

Figure 5-24 Brake pressure achieved versus different brake pedal deflection intervals. Each BPD value contains is the indicated value +/- 2.5 degrees, source: own research

On the other hand, at low BPD values of e.g. 40 degrees or lower the demand is usually less than friction available. This also leads to an underestimation of the friction. This applies to most of landings, as the required deceleration is usually very low and it is avoided to decelerate more strongly than necessary.

A BPD of around 55 to 60 degrees seems to represent the distribution of μ_a best, as both high and low values of μ_a are contained. A slight underestimation of friction is expected in the area around the median of the respective values, as some of the demands are still lower than the available friction. The diagram in Figure 5-24 illustrates that the brake pressure is not suitable for determining landings with maximum brake demand.

In the next step, depending on the BPD, the friction coefficient μ according Eq. 5-2 can be calculated for each sample in relation to the corresponding BPD, which does not necessarily represent the maximum available friction coefficient μ_a for the considered sample, as the brake demand might not be at the maximum friction level. However, for some of the samples the maximum level will be reached. For the evaluation of the maximum friction coefficient μ_a only landings or at least parts of a landing, where the μ of the brake demand was at or above the maximum friction μ_a, can be used. However, there is no indication in the flight data whether or not this condition was fulfilled for a particular sample.

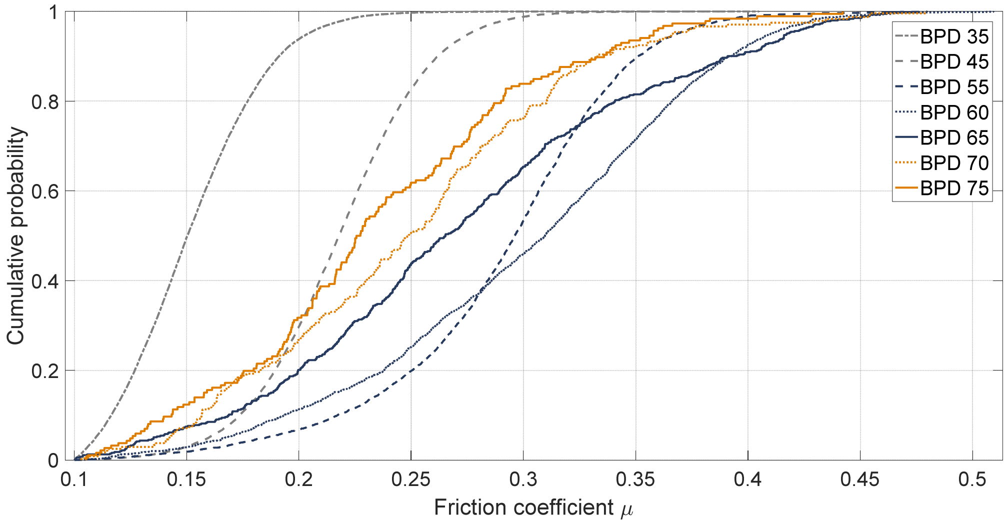

Figure 5-25 Cumulative probability distributions of μ for wet runway, source: own research

In Figure 5-25 the cumulative probabilities of different BPDs for wet runways are displayed, i.e. a value of e.g. $\mu = 0.3$ at a probability level of 0.6 indicates that 60 percent of all measured values μ are lower than or equal to 0.3.

A BPD of 35° seems to provide the worst friction in the graph, as the distribution is reaching higher probability levels at lower friction coefficients. The slope of this CDF is very steep, and 90 percent of all values are within a narrow band of friction coefficients between 0.11 and 0.20, with a probability of 50 percent at a friction coefficient of 0.15. However, in most cases of this BPD the demand can be assumed as being lower than friction available, so the maximum available friction cannot be derived by this CDF. A BPD of 35° corresponds to a braking with a median friction coefficient of 0.15, even though the available friction might be much higher, since brake demand is at relatively low levels.

At a BPD of 45°, the achieved median friction coefficient is shifted to a higher value of 0.22, and this shift is parallel to the distribution of BPD at 35°.

The shape of the CDF changes, especially in the lower part, at a BPD of 55°, which indicates, that there is a higher probability for the available friction to be less than the demanded brake force. Especially this range of lower friction contains the phenomenon that must be considered to determine the distribution of the maximum available friction coefficients. The median friction coefficient is at 0.29 in this case, but the variation is much higher than at lower BPDs, as also depicted in Figure 5-25: 90 percent of all friction coefficients are between 0.18 and 0.37.

With higher than 55° of BPD, the trend reverses, and the CDFs are shifted back again to worse friction values, at least for the lower parts of friction coefficients, which is an indicator for the use of higher BPDs as soon as the brake demand is higher than friction available.

Hence, it can be assumed that the distribution of available friction coefficients is described by the envelope curve of all CDFs in above graph on the far-right side, as along this envelope curve the highest achievable friction is represented, which the pilot has demanded.

The envelope curve for wet runways follows the CDF of BPD 55° up to a threshold value of 0.28, from where it is superseded by the CDF of BPD 60°. This is reasonable, as higher BPDs are necessary if higher friction is available and also demanded by the pilot. At a threshold value of 0.39, the envelope curve follows the CDF of BPD 65°.

This envelope curve can be approximated by an artificial distribution, derived from the distributions of the different relevant BPDs. The only problem with this approach is the fact that every BPD interval contains a different number of measurements. A normalization of these different numbers can be achieved by using the BPD interval with the lowest number of measurements as a reference. This is usually the interval containing the highest BPD values, since higher brake pedal deflections are used less frequently.

Therefore, all measurements of the BPD interval with the lowest number of measurements, which are within the associated boundaries, are considered for the sought-for envelope distribution in a first step. Thereafter, all other relevant BPD intervals are considered within their respective boundaries, but the number of considered measurements has to be reduced proportionally to the reference number of the BPD interval with the lowest number of measurements. This can be achieved by randomly selecting a certain number of measurements.

E.g. for wet runways in Figure 5-25, the BPD interval around 55° contains $N_{55} = 4.331$ measurements, and the BPD interval around 65° contains $N_{65} = 553$ measurements. Hence, in the relevant interval of BPD 55° from friction coefficient 0 up to 0.28, only $N_{65}/N_{55} = 0.127$, i.e. 12.7 percent of all available measurements, will be selected randomly for the determination of the distribution, which defines the envelope curve. The results for wet runways can be seen in Figure 5-26, where the envelope curve is colored red. This approximated distribution of the maximum friction coefficients μ_a can then be parametrized using a Generalized Extreme Value distribution type. Within the BPD method, there is a lack of data below friction coefficients of 0.15, so another method has to be used to evaluate the distribution below $\mu_a = 0.15$, which will be described in chapter 5.3.3.2.

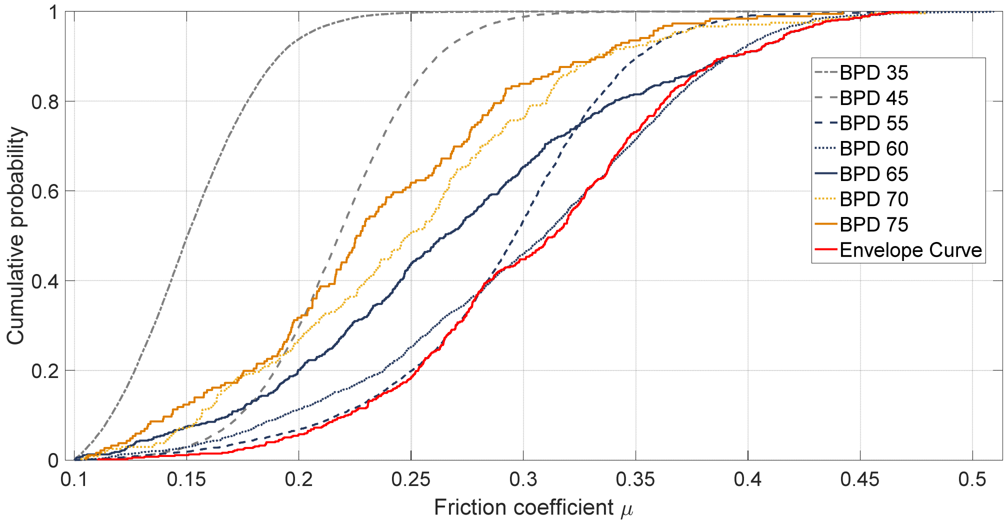

Figure 5-26 Cumulative probability distributions of μ for wet runways with envelope curve, source: own research

The same can be done for runway conditions dry and contaminated. Figure 5-27 shows the cumulative probability distributions for dry runways, where the available friction coefficients as expected are shifted towards higher values.

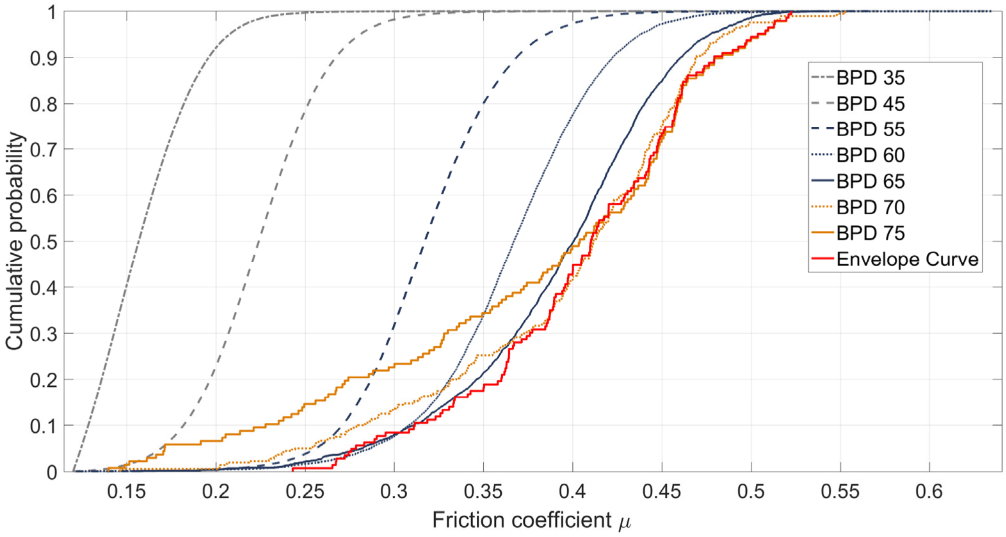

Figure 5-27 Cumulative probability distributions of μ for dry runways with envelope curve, source: own research

For contaminated runways, as shown in Figure 5-28, these friction coefficients are shifted towards lower values. As this runway condition is experienced more rarely than the others, the curves are less smooth, especially at higher BPDs, which are observed less frequently.

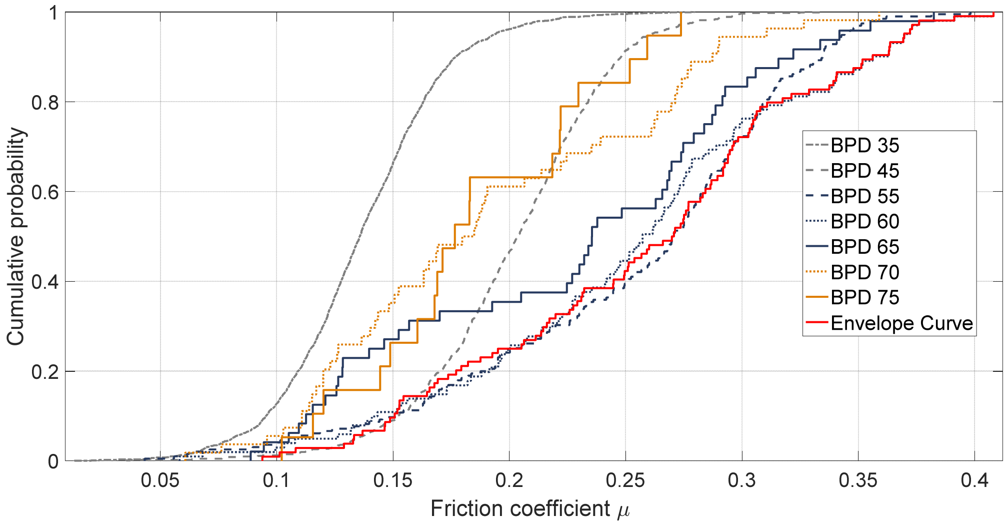

Figure 5-28 Cumulative probability distributions of μ for contaminated runways with envelope curve, source: own research

Parametrization of these envelope curves is conducted with a Generalized Extreme Value distribution of type III (Weibull type), where the shape parameter k is negative. The negative value of this parameter is due to the physical limit of friction. The Kolmogorov-Smirnov hypothesis test is an adequate tool to validate the fit of the parametrized data [81]. This test results in p-values of between $p = 0.33$ for wet runways and $p = 0.85$ for dry runways, which is clearly above the significance level of 0.05 and thus, confirms that this distribution type is adequate to fit the data.

The probability density function of the Generalized Extreme Value distribution (GEV) with location parameter μ, scale parameter σ, and shape parameter k is [82]

$$p(\mu_a) = \left(\frac{1}{\sigma}\right) \cdot exp\left(-\left(1 + k\frac{(\mu_a - \mu)}{\sigma}\right)^{-\frac{1}{k}}\right) \cdot \left(1 + k\frac{(\mu_a - \mu)}{\sigma}\right)^{-1-\frac{1}{k}}. \qquad \textbf{Eq. 5-12}$$

The BPDs used for parametrization and the derived parameters of the GEV including the 95% confidence values for all different runway conditions are presented in Table 5-4.

Table 5-4 Parameters of the general extreme value distribution for μ_a from BPD method, source: own research

Runway condition	**Considered BPDs**	**Shape parameter *k***			**Scale parameter σ**			**Location parameter μ**		
		Mean	*95% lower*	*95% upper*	*mean*	*95% lower*	*95% upper*	*mean*	*95% lower*	*95% upper*
Dry	55° - 75°	-0.455	-0.551	-0.358	0.069	0.061	0.079	0.384	0.372	0.396
Wet	55° - 65°	-0.338	-0.387	-0.288	0.071	0.069	0.076	0.284	0.277	0.291
Contaminated	45° - 60°	-0.375	-0.508	-0.242	0.084	0.072	0.098	0.214	0.197	0.231

Above distributions together with the underlying measurements of the envelope data are combined in Figure 5-29.

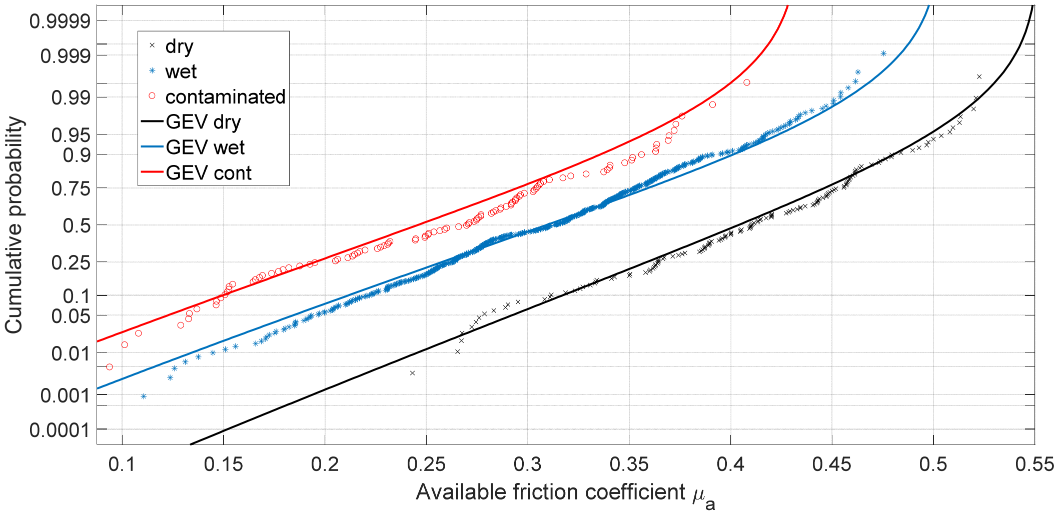

Figure 5-29 Available friction coefficients μ_a depending on runway condition, BPD method, source: own calculations

Only a few values of μ_a are available below $\mu_a = 0.15$. Therefore the autobrake method (AB method) will be used to model the probabilities at the lower end of the distribution with higher accuracy, since more data within this lower region of values is available using this method. For dry runways, there is a lack of data even below friction coefficients of 0.25, so it is expected that in the region between 0.25 down to 0.15, where the AB method starts, the prediction of probability of friction coefficients is of low confidence. However, as discussed in chapter 5.4, the importance of low friction on dry runways is much lower than on wet or contaminated runways, since only few accidents have been observed on dry runways when compared to the other runway conditions.

As lower friction coefficients contribute more often to overruns than higher ones (see Table 5-1), the lower part of the distribution is the more interesting part for evaluation of the risk level of an overrun.

5.3.3.2 Autobrake (AB Method)

The second method to analyse flights with maximum brake demand is the analysis of landings, where autobrake was used and the target deceleration was not reached. It is quite common to use autobrake setting "medium" during landing on Airbus A319, A320 and A321, which is the mode with the highest autobrake deceleration of $3\ m/s^2$ during landing.

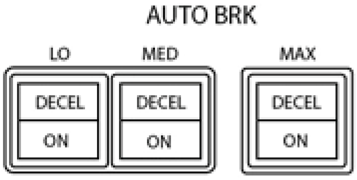

Figure 5-30 Possible autobrake settings on the Airbus A320 [68]

This mode is used in nearly 44 percent of all landings, so it is expected to be equally distributed over all runway conditions.

Figure 5-31 depicts the typical deceleration forces during landing roll if using an autobrake system.

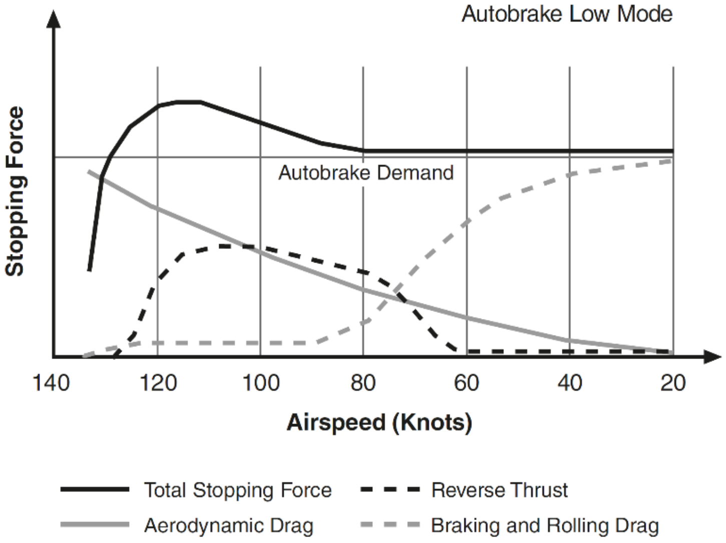

Figure 5-31 Typical deceleration forces during landing roll if using an autobrake system [66]

The brake pressure is controlled by the autobrake system to reach the target deceleration, which depends on the autobrake setting. Only if the target deceleration cannot be reached by other elements from Eq. 5-2, brake pressure is applied by the autobrake system.

On the other hand, if the target deceleration cannot be reached, it can be assumed that the friction coefficient for the respective runway is too low to enable a sufficient deceleration. To avoid inaccuracies of measurements, the presented method uses only deceleration values, which are at or below 80 percent of the target deceleration at ground speeds of 46.3 meters per second (90 knots) or lower. Within the time series of flight data during rollout all relevant flight data samples have been exported, where ground speed of the aircraft went through values of 46.3 meters per second (90 knots) to 15.4 meters per second (30 knots) in steps of 5.1 meters per second (10 knots) each, and additionally from 46.3 meters per second (90 knots) to 41.2 meters per second (80 knots) in steps of 1 meter per second (2 knots) each, so overall up to 11 values per landing have been taken into account for this analysis.

For all values, which comply with above criteria, the available friction coefficient μ_a is determined.

However, not all of the resulting friction values are used for evaluation of the distribution. Since only the extreme lower part of the distribution is of interest, for each runway condition a threshold value μ_{thr} is defined. Only the values of the friction coefficients μ_a below this threshold are used for parametrization. This is called the peak over threshold method (POT), a commonly used method in extreme value statistics [83]. The resulting conditional probability distributions are also GEVs of the Weibull type, where shape parameter k is also negative:

$$p(\mu_a|\mu_a \leq \mu_{thr}) = \left(\frac{1}{\sigma}\right) \cdot \exp\left(-\left(1 + k\frac{(\mu_a - \mu)}{\sigma}\right)^{-\frac{1}{k}}\right) \cdot \left(1 + k\frac{(\mu_a - \mu)}{\sigma}\right)^{-1-\frac{1}{k}}. \qquad \textbf{Eq. 5-13}$$

The respective parameters can be looked up in Table 5-5. Like before, the Kolmogorov-Smirnov hypothesis test results in p-values above the significance level of 0.05 and confirms that this distribution type is adequate to fit the data (range between $p = 0.284$ for wet runways and $p = 0.923$ for contaminated runways).

Table 5-5 Parameters of the general extreme value distribution for μ_a from AB method,
source: own research

Runway condition	**Shape parameter *k***			**Scale parameter *σ***			**Location parameter *μ***		
	mean	*95% lower*	*95% upper*	*mean*	*95% lower*	*95% upper*	*mean*	*95% lower*	*95% upper*
Dry	-0.821	-1.029	-0.612	0.023	0.017	0.030	0.121	0.115	0.128
Wet	-0.840	-0.918	-0.762	0.017	0.016	0.019	0.129	0.128	0.131
Contaminated	-0.712	-0.806	-0.617	0.021	0.019	0.024	0.120	0.117	0.123

Finally, to evaluate the probability of friction coefficients μ_a below the threshold value μ_{thr}, the CDF has to be multiplied with the probability p_{thr} from Table 5-6, which is the quotient of the number of friction coefficient values μ_a used for the evaluation, which are below μ_{thr}, and the number of reference values, where autobrake was used, irrespective of the available friction values. The 95 percent confidence bounds of p_{thr} is also provided in Table Table 5-6, based on the number of reference and used values.

Table 5-6 Parameters of the general extreme value distribution for μ_a from AB method,
source: own research

Runway condition	***μ***	**Values used**	**Reference values**	**Probability below μ_{thr}, p_{thr}**		
				mean	*95% lower*	*95% upper*
Dry	0.15	51	86,206	$5.9 \cdot 10^{-4}$	$4.4 \cdot 10^{-4}$	$7.8 \cdot 10^{-4}$
Wet	0.15	341	18,428	$1.9 \cdot 10^{-2}$	$1.7 \cdot 10^{-2}$	$2.1 \cdot 10^{-2}$
Contaminated	0.15	212	2,546	$8.3 \cdot 10^{-2}$	$7.3 \cdot 10^{-2}$	$9.5 \cdot 10^{-2}$

The resulting graphs are displayed in Figure 5-32 for all runway conditions.

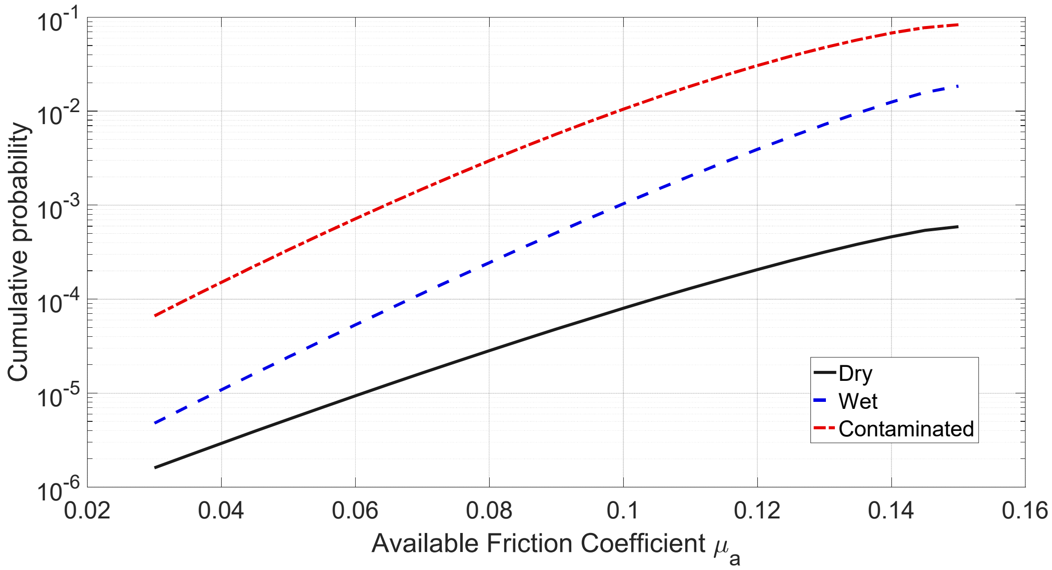

Figure 5-32 Available friction coefficients depending on runway condition, derived from AB method, source: own research

5.3.3.3 Combining both Methods

In order to get the complete distribution of the available friction coefficients for all runway conditions, the graphs resulting from both, BPD method and AB method, have to be combined. As the probability values at μ_{thr} derived from the AB method are more accurate than the lower part of the BPD method because of the lack of measurements in this area with the latter method, the distribution parameters of the BPD method are adjusted within their 95 percent-confidence bounds in order to match a probability of p_{thr} at $\mu_a = \mu_{thr}$. For this, the parameters of the GEV distributions from Table 5-4 are varied randomly, until the probability at μ_{thr} fits the value of p_{thr} within certain limits, with simultaneously maximizing the p-value of the Kolmogorov-Smirnov hypothesis test. This enables a shift of the fitting curve especially in the region with only few underlying measurements of the BPD method towards the probability value derived by the AB method, which is very accurate at the border between both methods.

The results can be seen in Table 5-7 and Figure 5-33. Since the method does not aim for probability, but for the risk of a runway overrun, the probability has to be converted into risk units. This conversion can be conducted by taking into consideration the respective accident scenario as described in chapter 5.1. According the risk matrix in chapter 2.6, the risk level for an accident scenario "*Serious Accident*" is one risk unit, if the conditional probability is 0.01. The resulting risk units can be seen on the right axis of the graph in Figure 5-33.

Table 5-7 Adapted Parameters of the general extreme value distribution for μ_a from BPD method, *see also Table 5-4*

Runway condition	Shape parameter k	Scale parameter σ	Location parameter μ	p-value
Dry	-0.5551	0.0661	0.3911	0.720
Wet	-0.364	0.0724	0.2803	0.108
Contaminated	-0.4103	0.0775	0.2320	0.667

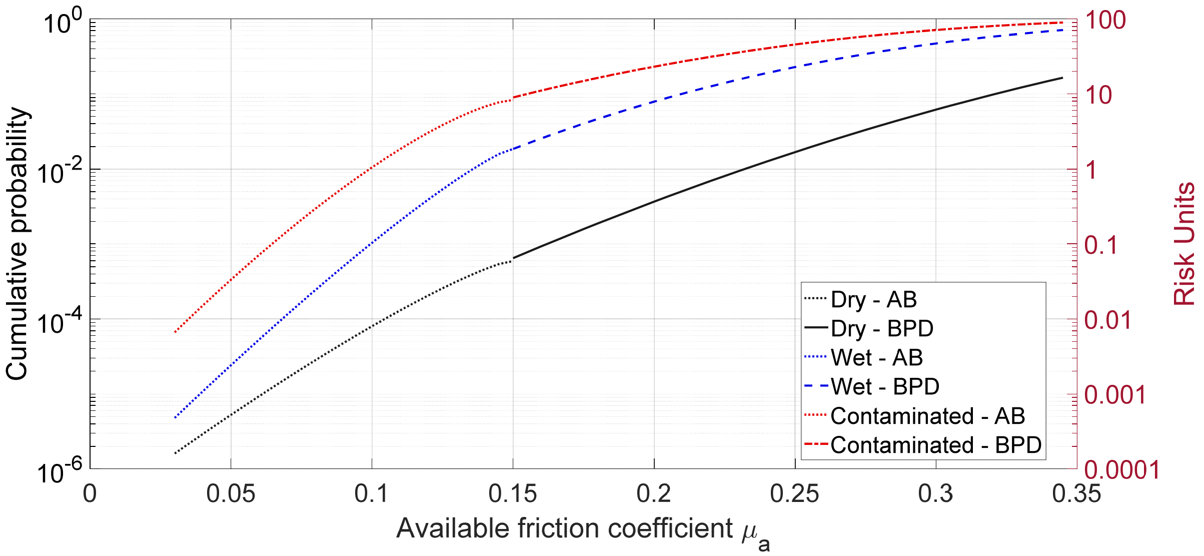

Figure 5-33 Available friction coefficients μ_a and corresponding risk units depending on runway condition, combined graph, source: own research

Since the results of the method is data driven, a discretization by means of a risk matrix is not necessary in order to evaluate the associated risk level. Discretization by means of a risk matrix is only a tool used by the expert to determine the risk level on the basis of the discretely determined values for severity and probability.

Nevertheless, Table 5-8 provides an overview of the resulting risk levels depending on the required friction coefficient μ_{r_max}, which was measured for an individual landing for the different runway conditions.

Table 5-8 Discretization of the results, leading to different discrete risk levels, source: own research

probability risk level runway condition classification	$3.3 \cdot 10^{-5}$ e-f	10^{-4} e	$3.3 \cdot 10^{-4}$ d-e	10^{-3} d	$3.3 \cdot 10^{-3}$ c-d	10^{-2} c	$3.3 \cdot 10^{-2}$ b-c	10^{-1} b
Dry	0.08	0.105	0.13	0.165	0.20	0.23	0.275	0.32
Wet	0.055	0.07	0.08	0.10	0.12	0.13	0.17	0.215
Contaminated	< 0.035	0.035	0.05	0.065	0.08	0.10	0.12	0.155

5.4 Verification of the Results

To verify the new method, the risk model has to be compared with observed accident rates of worldwide air traffic. The IATA accident reports of 2015 and 2016 contain 27 runway excursions, which equals a rate of 0.35 per million flights [23,25]. A more in-depth analysis of these excursions shows that 13 of these accidents are runway overruns during landing. This results in a rate of 0.17 runway overruns per million flights. All overruns occurred on wet or even contaminated runways, thus a higher overrun probability is expected under these runway conditions.

IATA considers only hull losses and substantial damages in their accident reports. Accidents with lower damage are often not documented at all or not sufficiently documented. For the risk model, however, the total rate of landing overruns must be estimated as a reference, including none or minor damages. According to Kirkland, 43 percent of all landing overruns result in a damage level which is lower than substantial [61]. Taking these aspects into consideration, a total of 22.8 landing overruns can be assumed for the mentioned years, which equals a landing overrun rate of 0.29 per million flights with a 95-percent confidence between 0.19 and 0.43 accidents per million flights.

For the comparison, a Monte Carlo method is used. The environmental conditions, i.e. the resulting probability of the available friction from Figure 5-33, are combined with the aircraft states, i.e. the distribution of the observed maximum required friction μ_{r_max} from actual flight data. The latter distribution has yet to be determined and parametrized for the application of the Monte Carlo method.

The required friction, i.e. the aircraft state within the risk model, is the result of different influencing factors like runway length, flare distance, ground speed etc. These factors can be influenced by the flight crew in certain limits, e.g. a short runway can be rejected by the flight crew in case of adverse runway conditions by either choosing a longer runway, if available at the destination, or even diverting to another airport. Flare distance and ground speed can be reduced by more accurate flying without accepting large fluctuations of the desired path and/or speed. Hence, the distribution of the maximum required friction μ_{r_max} will be different for different airlines.

As the behavior of the flight crew varies with these influencing factors [22], especially if the runway condition is other than dry, the corresponding distributions of the required friction will also vary, depending on the runway condition. Hence, for each runway condition a separate distribution has to be evaluated from flight data.

For this purpose, the maximum required friction coefficient μ_{r_max} is derived for each landing as described in chapter 5.2. It is important to know, that the value of μ_{r_max} can theoretically be zero or even less, as sometimes the available runway length is very large when compared to the required distance, which is necessary to stop the aircraft exactly at the runway end. A negative value of the such calculated friction coefficient indicates, that the aircraft is capable to stop within the remaining runway by use of aerodynamic drag, idle reverse thrust and/or gravity only, and no friction is necessary at all.

On wet runways for example, only 69.7 percent of the landings require a friction coefficient of more than zero. Furthermore, only 25.5 percent of all landings on wet runways require a friction which is beyond the mean rolling resistance of 0.017. Only these landings require active braking in order to stop the aircraft just before the runway end.

In chapter 5.2 only idle reverse thrust was assumed in the risk model to cover the worst-case scenario. However, for the verification of the risk model, the use of maximum reverse thrust should be considered with the same likelihood as observed in real flight data to obtain realistic results. Maximum reverse thrust is the last recovery measure to prevent an overrun whenever the available friction is less than the required one.

The bow tie model of Figure 5-3 can be modified as depicted in Figure 5-34, incorporating this additional recovery measure. As a reminder, within the risk model described so far, only idle reverse thrust was taken into consideration in order not to underestimate the risk of an individual landing.

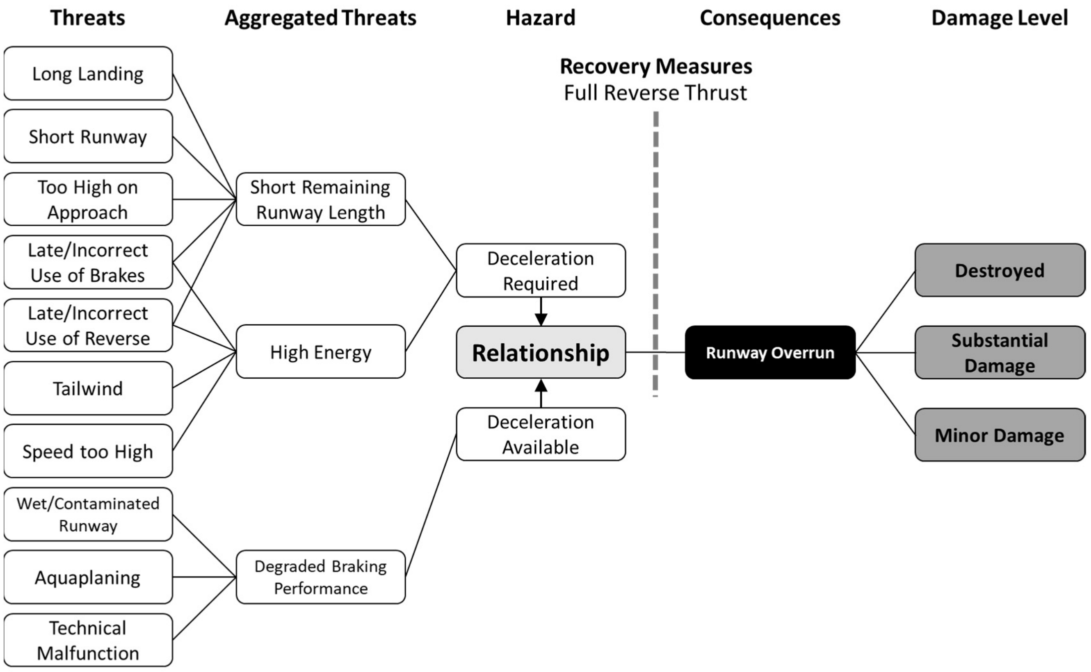

Figure 5-34 Adapted bow tie model [from Figure 5-3], including the recovery measure "full reverse thrust", source: own research

In the flight data, a clear correlation between the use of full reverse thrust and the maximum required deceleration d_{r_max} can be identified. Instead of the required friction, the required deceleration is used for this correlation, since the evaluation of this value is less complex and fits the point of the highest required friction coefficient for the majority of the considered landings[20]. The relationship between use of full reverse thrust and maximum required deceleration can be seen in Figure 5-35.

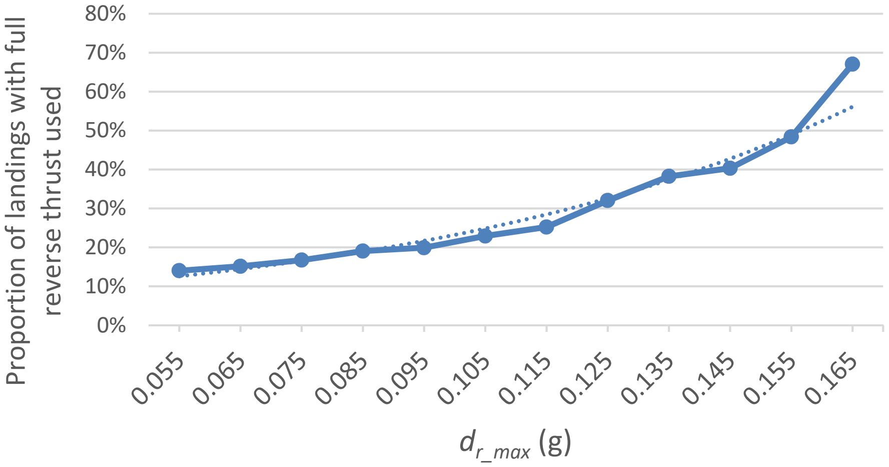

Figure 5-35 Proportion of landings which used full reverse thrust depending on maximum required deceleration in *g*, source: own research

[20] see page 75 for detailed explanation of the simplified calculation

The determined correlation can be parametrized by an exponential approximation of the measured relationship (see dotted line in Figure 5-35):

$$P(full\ reverse) = 0.11 \cdot e^{1.38 \cdot (d_{r\_max} - 0.44)}\ . \qquad \textbf{Eq. 5-14}$$

For every considered landing, an equally distributed random number is generated. In case this random number is equal or less than Eq. 5-14, maximum reverse thrust is assumed in the evaluation of the corresponding required friction coefficient μ_{r_max} for the respective landing.

The resulting distribution of the required friction coefficients e.g. for wet runways, can be seen in Figure 5-36. This distribution refers only to those values, which are greater than zero. The resulting data can be parametrized using a Generalized Extreme Value distribution (GEV) with location parameter μ, scale parameter σ, and shape parameter k as follows [82]:

$$p\left(\mu_{r\_max} \middle| \mu, \sigma, k\right) = \left(\frac{1}{\sigma}\right) \cdot exp\left(-\left(1 + k\frac{(\mu_{r\_max} - \mu)}{\sigma}\right)^{-\frac{1}{k}}\right) \cdot \left(1 + k\frac{(\mu_{r\_max} - \mu)}{\sigma}\right)^{-1-\frac{1}{k}}, \qquad \textbf{Eq. 5-15}$$

with the shape parameter $k = -0.019$, the scale parameter $\sigma = 0.008$, and the location parameter $\mu = 0.011$. This parametrization can be confirmed by the Kolmogorov-Smirnov hypothesis test, which results in a p-value of 0.51, which is well above the significance level of $\alpha = 0.05$. For the other runway conditions, the respective values can be seen in Table 5-9.

Table 5-9 Parameters of the distribution fitting of required friction coefficients μ_{r_max}, source: own research

Runway condition	**Shape parameter *k***			**Scale parameter *σ***			**Location parameter *μ***		
	mean	*95% lower*	*95% upper*	*mean*	*95% lower*	*95% upper*	*mean*	*95% lower*	*95% upper*
Dry	0.033	-0.024	0.091	0.008	0.007	0.008	0.011	0.010	0.011
Wet	-0.019	-0.111	0.073	0.008	0.007	0.008	0.011	0.010	0.012
Contaminated	0.075	-0.020	0.171	0.007	0.006	0.008	0.010	0.009	0.011

Table 5-10 Values used for the determination of the distribution of required friction coefficients μ_{r_max}, including the quality of fitting, source: own research

Runway condition	**Values used *N_R***	**Values above 0 *N_{R0}***	***p*-value**
Dry	1268	904	0.274
Wet	416	290	0.510
Contaminated	390	273	0.870

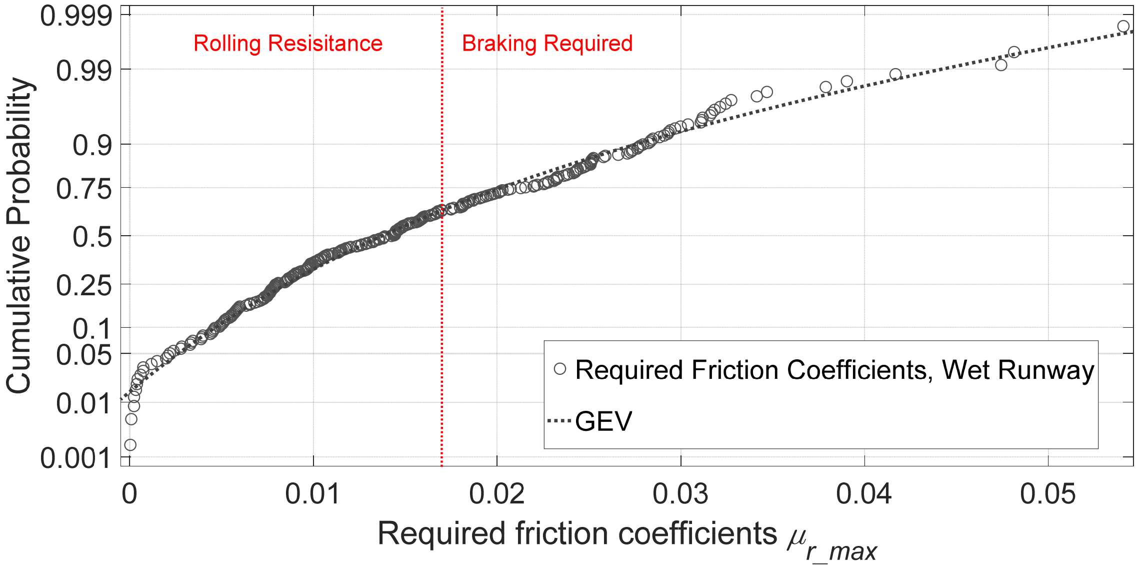

Figure 5-36 Maximum required friction coefficients $\mu_{r\_max} \geq 0$ for wet runway conditions, source: own research

Once the distributions have been evaluated, the Monte Carlo method can be conducted in the following way:

The first step is to determine the proportion of landings on the different runway conditions. According to the considered flight data, 13.8 percent of all landings occurred on wet runways, and 0.9 percent on contaminated runways. All other landings took place on dry runways.

First an equally distributed random variable is generated for each simulated landing, defining the runway condition C_R in the same proportion as described above. A flowchart of this approach is provided in Figure 5-37. Then the maximum required friction coefficient μ_{r_max} can be generated for the simulation of the respective landing, using the results from Table 5-9. For this reason, another equally distributed random number is generated, which determines whether μ_{r_max} shall be above zero, based on the relationship of N_{R0} and N_R from Table 5-9. In this case, μ_{r_max} is generated by a random number following the respective GEV distribution from Table 5-9. Otherwise, it is defined to be zero.

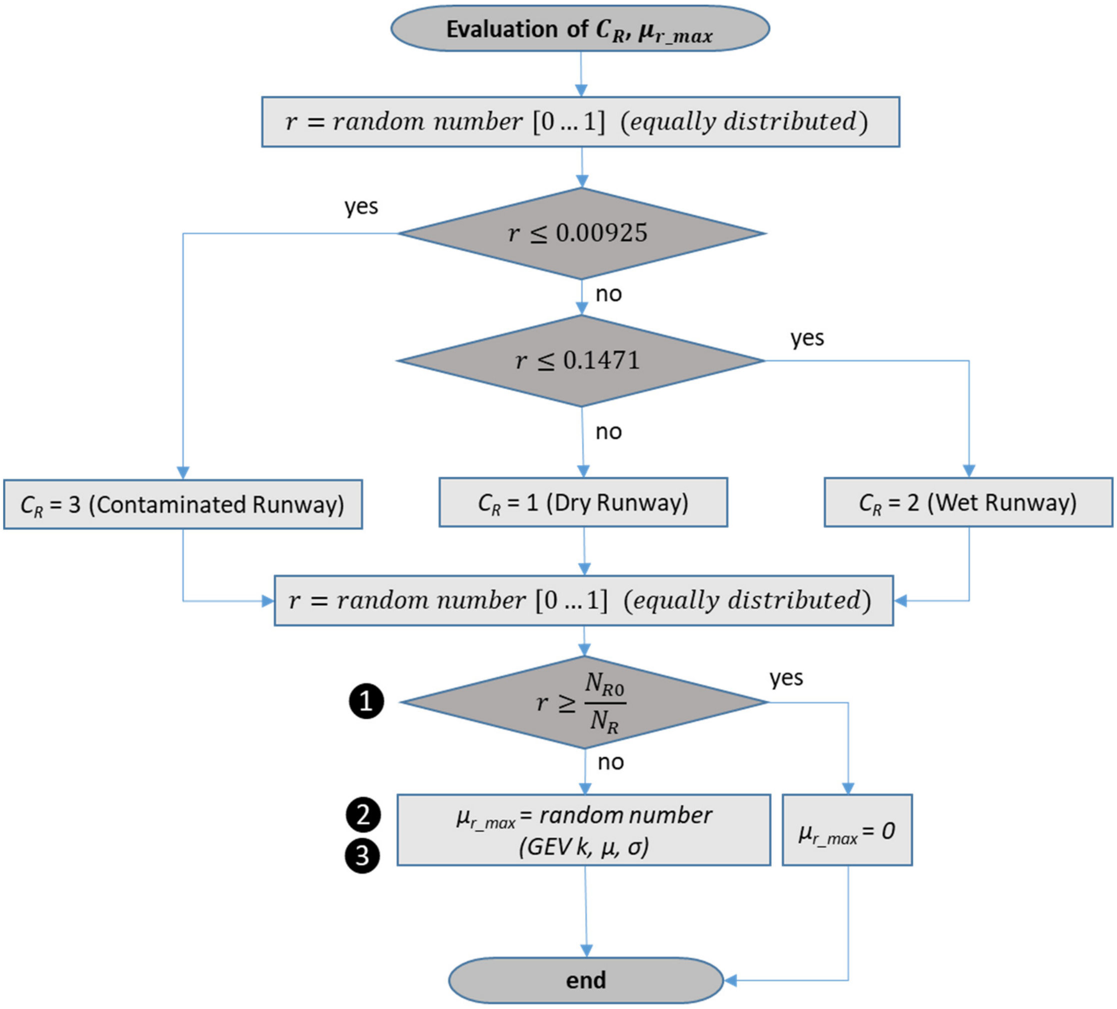
Evaluation of C_R, μ_{r_max}
r = random number [0 ... 1] (equally distributed)
yes
$r \leq 0.00925$
no
$r \leq 0.1471$
yes
no
C_R = 3 (Contaminated Runway)
C_R = 1 (Dry Runway)
C_R = 2 (Wet Runway)
r = random number [0 ... 1] (equally distributed)
1
$r \geq \frac{N_{R0}}{N_R}$
yes
no
2
3
μ_{r_max} = random number (GEV k, μ, σ)
μ_{r_max} = 0
end

❶ N_{RO} and N_R according Table 5-10, depending on runway condition C_R

❷ k, σ and μ according Table 5-9, depending on runway condition C_R

❸ *random Number (GEV k, μ, σ)* is a random value following a General Extreme Value-distribution with shape parameter k, location parameter μ, and scale parameter σ

Figure 5-37 Flowchart of the evaluation of the simulated runway condition C_R and the maximum required friction coefficient μ_{r_max}

The available friction μ_a can be evaluated as shown in the flowchart in Figure 5-38. An equally distributed random number determines whether the lower part of the distribution of Figure 5-33 shall be used, which was derived from the AB method. This is the case, if the random number is at or below the threshold probability between both distributions as shown in Table 5-6. Depending on the used part of the distribution and the simulated runway condition C_R from above, μ_a is determined by a random number, following the respective GEV distribution either from Table 5-5 and Table 5-6 or from Table 5-7. Only in case the resulting μ_a is above the threshold value μ_{thr} for the lower part (AB method) or below μ_{thr} for the upper part (BPD method) of the distribution, the generation of this random μ_a is repeated, as the decision, whether μ_a is above or below μ_{thr} was already determined by the first random number in this flowchart.

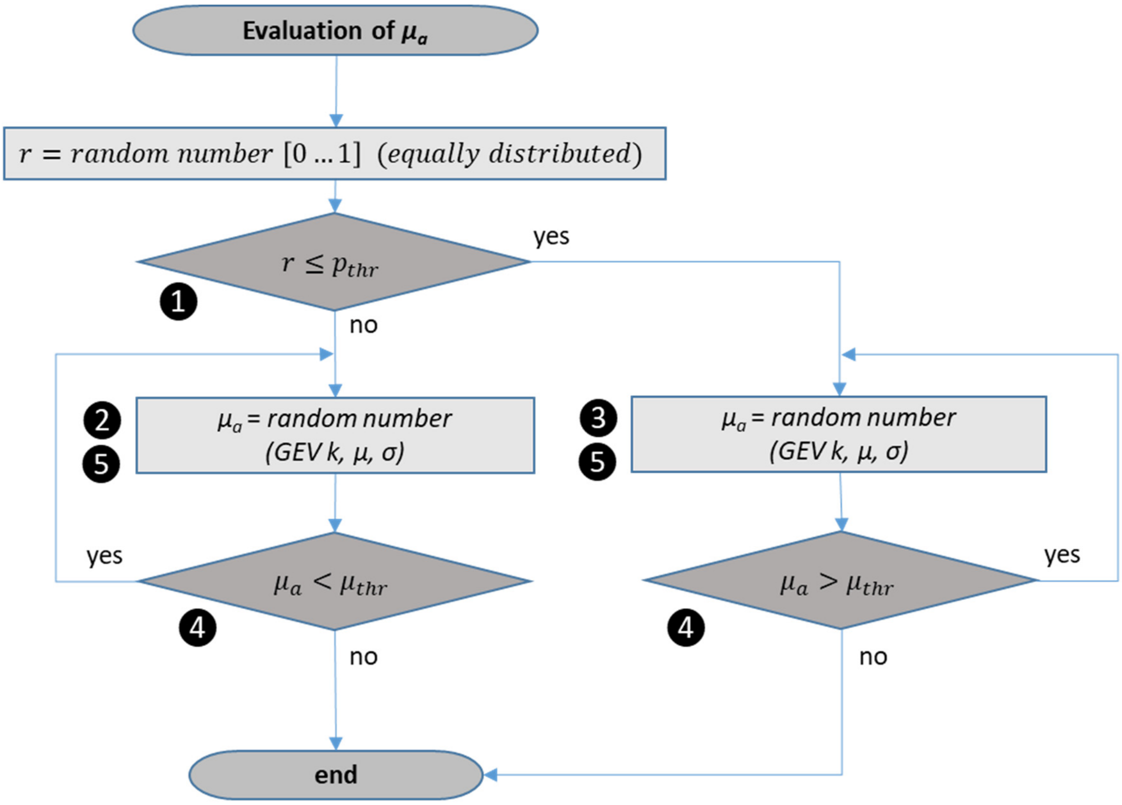
Evaluation of μ_a
$r = random\ number\ [0 \dots 1]\ \ (equally\ distributed)$
$r \le p_{thr}$
1
yes
no
2
5
μ_a = random number (GEV k, μ, σ)
3
5
μ_a = random number (GEV k, μ, σ)
yes
$\mu_a < \mu_{thr}$
4
no
$\mu_a > \mu_{thr}$
4
yes
no
end

❶ p_{thr} according Table 5-6, depending on runway condition C_R

❷ k, μ and σ according Table 5-7, depending on runway condition C_R

❸ k, μ and σ according Table 5-5, depending on runway condition C_R

❹ μ_{thr} according Table 5-6, depending on runway condition C_R

❺ *random Number (GEV k, μ, σ)* is a random value following a General Extreme Value-distribution with shape parameter k, location parameter μ, and scale parameter σ

Figure 5-38 Evaluation of available friction μ_a

Both routines, the evaluation of the runway condition C_R and the maximum required friction μ_{r_max} as well as the evaluation of the available friction μ_a will then be conducted 25 million times by means of a Monte Carlo method. Each iteration simulates a single landing with the distributions of the runway condition C_R, the maximum required friction μ_{r_max} as well as the available friction μ_a as observed in real flight data. As it is assumed that at least the average rolling-resistance friction is available, the lower bound for μ_a is defined to be 0.017, which is the average rolling-resistance friction of a landing, ranging between speeds of 66.9 and zero meters per second (130 and zero knots). The flowchart can be seen in Figure 5-39.

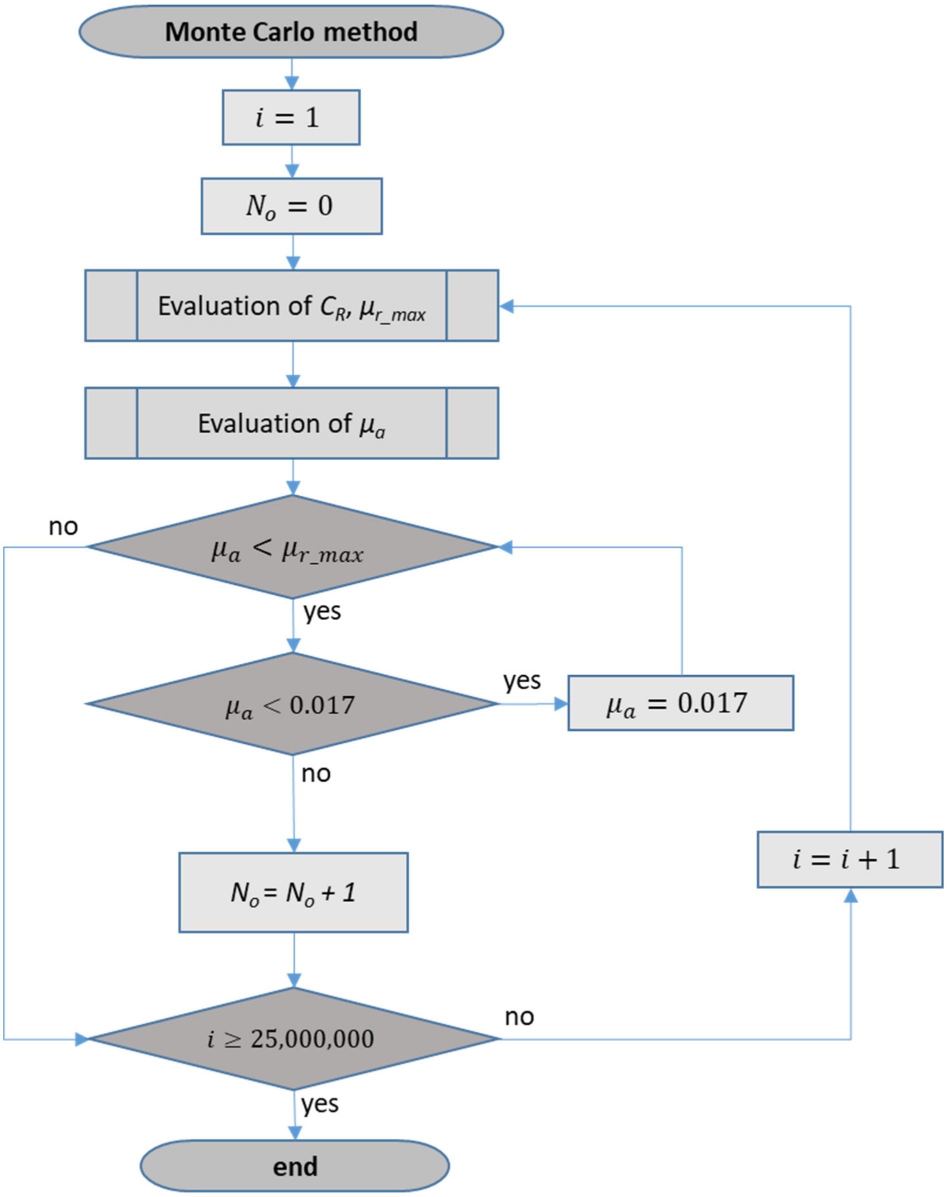

Figure 5-39 Flowchart of the Monte Carlo method

The simulation results in 13 runway overruns, which equals an overrun rate of 0.52 per million flights. The 95-percent confidence interval ranges between 0.29 and 0.86 landing overruns per million flights and hence, overlaps the confidence bounds of the observed landing overruns by IATA. Six simulated overruns occurred on contaminated runways, 3 on wet runways, and 4 on dry runways. Due to the low reference number of contaminated runways, the evaluated probability of a landing overrun on contaminated runways is $6.5 \cdot 10^{-5}$. For wet runways, the evaluated probability results in $2.2 \cdot 10^{-6}$, and for dry runways it results in $4.7 \cdot 10^{-7}$.

All simulated runway overruns occurred with available friction coefficients below 0.15, which emphasizes the importance of the lower part of the distribution of the available friction, resulting from the AB method. The simulated accident rate is at a comparable level with the observed accident rate. This confirms the prognosis quality of the presented method. The slight overestimation of the average probability tends towards the safe side, which is desirable in safety management.

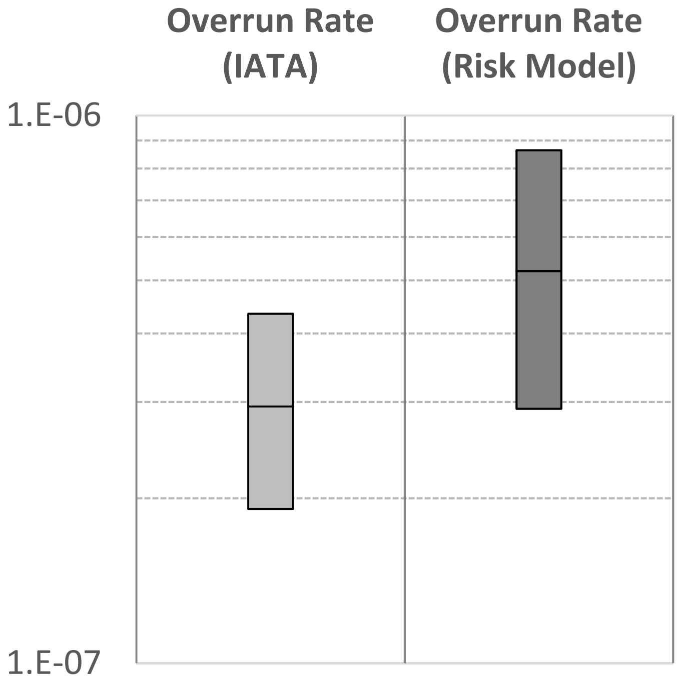

Figure 5-40 95%-confidence bounds of observed runway overruns by IATA versus simulated overruns (risk model), source: own research

As mentioned in chapter 5.3.3, the use of a mean friction coefficient over the whole speed interval during landing might contribute to this overestimation. Especially for wet or contaminated runways, which account for most of the simulated runway overruns, the outliers of very low friction disappear with ground speeds below 41.2 meters per second (80 knots) completely, and the average available friction tends to higher values towards levels, which can also be observed on dry runways, as depicted in Figure 5-21, see also Figure 5-20. Especially at higher speeds, the aerodynamic and reverse braking effect is more dominant than during lower speeds. Since at lower speeds the available friction increases, the overall effect leads to improved stopping force and hence, to a lower risk of runway overrun.

For dry runways, it should be considered that the determination of the runway condition in the presented risk model is based on precipitation rather than runway contamination due to a lack of information about the latter. This results in a higher uncertainty of the runway condition for dry runways than for wet runways, as the absence of precipitation does not necessarily mean that the runway is free of contamination, e.g. from previous precipitation (e.g. snow on the runway or runway still wet without further precipitation).

Flight crews usually have more information about possible contamination and can adapt their behavior and their decisions to these conditions. Hence, for these landings the distribution of μ_{r_max} will tend towards more conservative, i.e. lower values, which has to be considered during a simulation. As such information is not available, the Monte Carlo method for dry runways might result in higher than expected overrun rates.

5.5 Aggregation of Data

As an example, the presented method is applied to operational data of a major European airline, using 40,340 landings of aircraft types Airbus A319, A320 and A321 within a time period of 12 months.

For each landing, the required friction coefficient μ_r, calculated at the time of maximum required deceleration, as well as the maximum available friction coefficient μ_a, depending on the runway condition classification, as shown in Table 5-2, is evaluated. Depending on the respective conditional probability shown in Figure 5-33, combined with the common accident scenario, evaluated in chapter 5.1, the risk units for each landing are evaluated, as shown in Figure 5-33. The results are then cumulated for each month, in order to obtain a risk trend over time, indicated in Figure 5-41. Note that this calculated risk is higher than the risk determined during the verification (see chapter 5.4) due to the maximum reverse thrust not included in the calculation, which is in accordance with the underlying risk model.

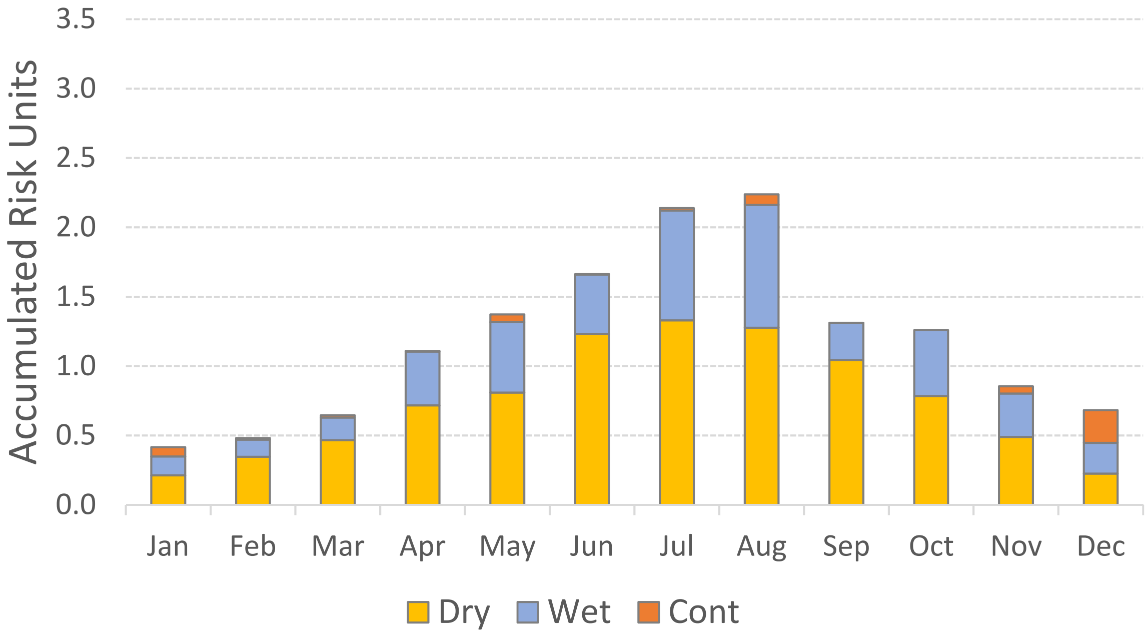

Figure 5-41 12-month risk trend for runway overrun, source: own research

The data of this risk trend indicate the following characteristics:

- The risk trend shows a seasonal pattern. In summer months, the risk is usually higher than in winter months. Further analysis shows, that this behaviour is mainly caused by an increase of critical values of d_r (Eq. 5-1) rather than critical runway conditions in the summer months, i.e. the increase of risk is generally not induced by environmental factors. An increase in number of flights during the summer months also slightly contributes to the increased risk.

- The portion of landings on contaminated runways increases in the meteorological winter months (December to February), as expected. A further analysis of data reveals the following behaviour: While in winter months generally the contaminated runway conditions are caused by light or moderate precipitation at low temperatures, in summer months the contaminated runway conditions are mainly caused by heavy precipitation at higher temperatures.

In comparison to the presented method, a risk classification by safety experts is only possible for those FDA events, which contain a higher risk. The reason is the limitation in human resources. However, the new method as described above can be applied to all landings, independent of the expected risk level. Review of FDA events containing higher risk levels by safety experts is still necessary for the new method, since events, where the risk level is supposed to be high, are often caused by flight data errors. However, the rate of false positive events at low risk levels is lower, and inadvertent use of those events does not influence the aggregated risk level significantly.

Mickel recommends to validate events with a risk level of at least 0.032 risk units [17]. Since only those events are classified by a safety expert accordingly, only a part of the overall risk is evaluated by expert estimation.

With expert estimation alone, the evaluation of the proportion of the unclassified risk part in comparison to the overall risk level is not possible, the presented method in this thesis enables such evaluation. For this purpose, the cumulated number of risk units of events with a risk level of at least 0.032 risk units is compared to the aggregated risk level of all events.

In total, 14.2 risk units have been cumulated during the 12-month analysis period. From those 14.2 risk units, 2.9 risk units exceeded the threshold of 0.032 risk units per landing, i.e. only 20.7 percent of the overall risk would be covered by expert estimation, the rest would be ignored.

Possible countermeasures to reduce the risk from the perspective of the safety management is the reduction of the required friction coefficient μ_r for each landing, by the use of

- **Technical measures:** E.g. a runway overrun protection system (ROPS), Head-up display for more accurate flying, etc.
- **Human Factors:** Training of flight crews to conduct a go around in case of un-stabilized approach or long flare, adequate braking during landing
- **Organizational measures:** Procedures for stabilized approaches, avoiding long flares, adequate braking etc.

6 The Risk Level of a TCAS Induced Midair Collision

In this chapter, the risk of a midair collision, which has been induced by the Traffic Collision Avoidance System (TCAS), is evaluated. The risk of midair collision is an integral part of the European Aviation Safety Plan (EASp) 2012-2015 [12]. TCAS provides Resolution Advisories (RAs) to the flight crew if a collision is imminent. Since the reaction to this system is based on the interaction with the pilot, a wrong input is possible and thus, an *induced collision* might occur.

Due to the different nature of the associated risk in this category, a physical model is not suitable. The environmental conditions of a TCAS induced collision mainly depend on two aspects: First, the relative vertical positions and the vertical rate of both involved aircraft at the begin of the TCAS encounter, and second, the reaction of the pilots of both aircraft. An inadequate combination of both aspects can finally lead to a midair collision.

While both, the vertical rate as well as the reaction of the pilot of the own aircraft is known by means of flight data, these same elements of the other aircraft are usually unknown and thus, have to be modelled. In other words, the vertical rate as well as the subsequent reaction of the pilot of the own aircraft can be considered as the aircraft state, while for the intruder aircraft these two elements represent the environmental conditions.

For the evaluation of possible initial conditions with regard to the intruder's relative vertical position and vertical rate, a set of random initial conditions is generated. A *system model* of the Traffic Collision Avoidance System is then used to verify whether a TCAS RA of the same type as observed in flight data would have been triggered in the own aircraft. In case this verification is positive, the initial conditions are treated as valid, and the development of the vertical distance between both aircraft through the whole encounter is evaluated by means of a *pilot model*, which models the reaction of the pilot of the intruder aircraft. A combination of valid initial conditions and the modelling of the development of the encounter represents one simulation of the Monte Carlo method, which finally evaluates the collision probability.

Chapter 6.1 describes the mechanism of a TCAS induced collision. In chapter 6.2, a general overview of the TCAS functions is provided. Thereafter, the system model of the Collision Avoidance System (CAS), which is the core part of TCAS, is developed from the TCAS requirements specification (chapter 6.3). The pilot model, which describes a typical pilot response, is derived from external studies (chapter 6.4).

In chapter 6.5, a large number of simulations is performed, starting from the initial conditions as defined above. During the simulated encounter potential RA modifications are considered, depending on the reaction of both pilots. The risk of collision is determined from the frequency of simulated collisions.

Finally, the method is applied to real TCAS events (chapter 6.6) and the results are compared with the probability of TCAS induced collisions based on an external study, using radar data (chapter 6.7).

6.1 The Risk Associated with a TCAS RA

The Traffic Collision Avoidance System is a system designed to be a last-resort safety net to prevent a midair collision between two or more aircraft. Due to the fast-growing air traffic in combination with the call for continuously improved safety standards, TCAS nowadays has become a vital element in aviation safety. The equipage with TCAS was mandated for the first time in the United States from 1993 on for civil fixed-wing turbine-engine aircraft capable of carrying more than 30 passengers, and from 2000 on also in Europe [84]. Since then, the mandate has become more restrictive, including smaller aircraft and revised versions of TCAS in the mandate[21] [84]. This makes TCAS to a widely-deployed and technically matured system; meanwhile, TCAS is installed on more than 25,000 aircraft worldwide.

A midair collision can be considered as the most significant aviation safety-relevant event due to its huge social impact [85]. In a midair collision, at least two aircraft are involved with a catastrophic outcome with nearly no chance to survive. Even though the number of midair collisions at least in the commercial airline industry sector has been zero for the past years [24], see also Figure 5-1, near midair collisions still occur frequently, and the organizations have to

[21] In the United States, TCAS has been mandated on 30 December 1993 for all civil fixed-wing turbine-engined aircraft capable of carrying more than 30 passengers.

Europe followed this mandate from 1 January 2000 including civil fixed-wing turbine-engined aircraft with a maximum take-off mass of more than 15,000 kg or capable of carrying more than 30 passengers, which became more restrictive (maximum take-off mass exceeding 5,700 kg or a maximum approved passenger seating configuration of more than 19) from 1 January 2005.

Since 1 December 2015, the latest TCAS version 7.1 is mandatory within European airspace.

Furthermore, ICAO proposed a worldwide mandate for TCAS equipage.

After a midair collision between two military aircraft off the Namibian coast in 1997, many military aircraft have been equipped with TCAS, and e.g. in German airspace, a carriage and operation of TCAS is mandatory for all military transport aircraft since 2003 [84].

deal with them. Also, the number of TCAS events is relatively high. After all, a TCAS RA is a state of increased collision risk in combination with a significant interruption to normal flight operation [86]. For this reason, organizations have to invest valuable resources for possible mitigation measures to reduce the number of RAs, e.g. by enhancement of technical equipment and continuous training of flight crews.

TCAS is only one component of the multi-layered protection against midair collisions. Besides strategic layers consisting of the airspace structure and operational procedures, the tactical layers are the organization of the traffic flows by air traffic controllers (ATC), giving commands to the flight crews to provide sufficient separation in distance and altitude between aircraft. Only if both defense layers fail, besides the still important "see and avoid" by the pilots, TCAS serves as a last line of defense, providing last-minute avoidance advisories based on a collision avoidance algorithm [86], see Figure 6-1.

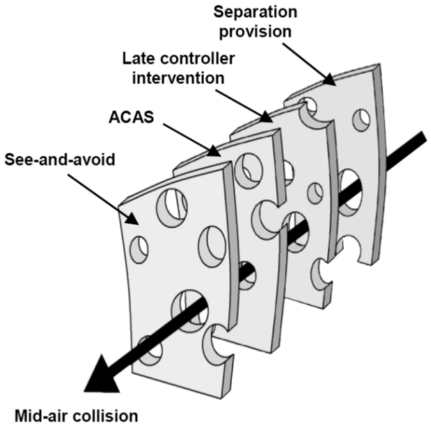

Figure 6-1 Multi-layered protection against midair collisions based on [87]

TCAS uses information received from transponders in other aircraft in order to calculate the relative motion of the aircraft. Two layers of protection are in place. When the trajectories of two aircraft converge, in a first step a Traffic Advisory (TA) is issued, which acts as a warning to the crew with information where the intruder might be [88]. The second step is a Resolution Advisory (RA) with an aural advisory combined with a notification on the primary flight display, giving guidance of the calculated avoidance maneuver, which are strictly limited to the vertical plane. Due to the lack in horizontal accuracy, course-altering maneuvers are not considered by TCAS [89].

The underlying collision avoidance algorithm, also called the threat logic, originally developed by the research institute MITRE[22] on behalf of the FAA, is able to solve nearly all possible conflict geometries between two or even more aircraft. Only very few, very rare occurring geometries have been identified in simulations, where the algorithm was not able to prevent a midair

[22] MITRE is a U.S. non-profit company, emerged from the Massachusetts Institute of Technology (MIT)

collision. Due to a continuous development process, the algorithm has been increasingly improved and the number of false alarms could be reduced over time. This contributes to the pilot's trust into the system [86].

However, the concept of TCAS does not rely solely on the threat logic. Instead, the model on which the algorithm is based on, incorporates a standard pilot reaction on the advisory given by the system. In the concept of TCAS, the system is not capable to solve the traffic conflict on its own. Instead, due to the constructed interaction between system and human being, i.e. the pilot, this interaction is a key component in the overall safety which the system is able to provide.

On the night of 1 July 2002, this interaction between system and flight crew manifested in a dramatic way. A Boeing B-757 operated by DHL collided with a Russian Tupolev Tu-154 near the small city of Überlingen, Germany. Both aircraft were destroyed, nobody survived the accident. The accident investigators were especially concerned about the fact that both aircraft had been equipped with the latest TCAS version.

The collision evolved due to some organizational problems within the Swiss air traffic control center at Zürich, combined with an error made by the responsible air traffic controller, which led to less separation than usual, with both aircraft on a collision course at 36,000 feet. Because of this conflict, the controller advised the Russian aircraft to descend 43 seconds before the collision. During this instruction of the controller by voice, the onboard TCAS advised the crew to climb. A coordinated descent advisory was issued to the DHL crew at the same time. While the DHL crew followed their RA correctly, the Russian crew followed the ATC instruction and hence, also started a descent. Shortly thereafter, the RAs on each aircraft were strengthened to "increase climb" on the Russian aircraft and "increase descent" on the DHL aircraft. Approximately 35 seconds after the TCAS RAs had been issued, the collision between both aircraft occurred.

The German accident report came to the conclusion, that one of the immediate causes of the accident was the fact that the Russian flight crew followed the ATC instruction to descend instead of following the TCAS RA to climb [90]. However, rather than pointing the finger towards the Russian flight crew, making them solely responsible for the collision, the report aimed for investigating the root causes for the motivation of the Russian crew not to follow the TCAS advisory.

The report revealed contradictory regulations and advises in the relevant procedural information of different organizations which was available at this time. While Eurocontrol literature advised pilots to always follow an RA, even when in conflict with an ATC advice, the Tupolev 154M Operations Manual stated that *"the main means to prevent in-flight collision are visual control of the situation by the crew, and following ATC-instructions."* Furthermore it stated that *"TCAS is an additional means that enables identification of conflicting traffic,* *classification of the hazard, and, if necessary, following a command through initiation of a vertical manoeuvre"* [89].

As flight crew training is based on the underlying regulations and procedures, the actions of the flight crew are driven not solely by the behavior of an individual human being. Instead, these actions are driven also by organizational factors, which eventually influence the behavior of the individuals dealing with the system, and therefore the system as a whole.

The fact, that both aircraft have been equipped with TCAS, played an important role in the development of the collision. Without TCAS, the accident would most likely not have happened, as the ATC controller noticed his error in time and advised the Russian aircraft to descend to a lower level, which would have produced enough vertical separation between both aircraft to prevent the collision. On the other hand, if both crews would have followed their RAs correctly, the collision could have also been avoided. But having TCAS installed, and one crew which did not follow their RA correctly, finally led to the accident, which emphasizes the importance of the interaction between the technical system and the flight crew. Hence, the accident of Überlingen can be classified as a *TCAS induced collision*.

Each technical system aiming for enhancing the safety can bring other risks into play. In the same manner as TCAS can resolve midair collisions, it can also induce such collisions that would not have occurred had TCAS not been deployed. As long as the number of midair collisions, that TCAS avoids, outweighs the number of midair collisions that TCAS induces, the overall safety is still enhanced by the system [87]. As the exact collision geometry between two aircraft is rather difficult to determine, a 'Near Midair Collision' (NMAC) is commonly used instead. An NMAC is defined as an encounter where *the horizontal separation of two aircraft is less than 500 feet and the vertical separation of the aircraft is less than 100 feet* at the same time [87]. The barriers between an NMAC towards a midair collision are very small, maybe even fortuitous. It can be seen more as a coincidence, if it does not come to a collision in this situation. Several studies estimate this conditional collision probability at a value of 0.1 [87,91].

To evaluate the safety enhancement by TCAS, a common measure is the risk ratio R_{TCAS}, which can be calculated by comparing the number of expected midair collisions, which would occur without a TCAS system, N_0, with the number of midair collisions, which are expected to be induced by TCAS, N_i, and the number of midair collisions which TCAS is not able to resolve, N_u [87]:

$$R_{TCAS} = \frac{N_u + N_i}{N_0}. \qquad \textbf{Eq. 6-1}$$

There is no specific safety target defined, which TCAS has to achieve. Hence, a risk ratio, which is at a value below one, is sufficient, which indicates a reduction of the midair collision probability at all.

The risk ratio highly depends on the considered airspace. In general, in the upper airspace the risk ratio is lower, i.e. the system works more efficiently. On the one hand, the proportion of TCAS equipped aircraft is higher due to higher requirements, which leads to a higher probability of coordinated RAs, where both involved aircraft are guided through the encounter. On the other hand, both the alert time and the velocity of the involved aircraft is higher, which makes a visual acquisition by the pilots more difficult, and therefore pilots deviate from TCAS RAs less frequently [87].

In lower airspace, a lot of unequipped traffic is involved, flying under visual flight rules (VFR), where the barrier of "see and avoid" has priority, which leads to a higher probability of abrupt trajectory changes in order to avoid a collision. This makes it difficult for the TCAS collision avoidance logic to solve the conflict. Also, pilots tend to assess the risk of collision based on their own perception instead of adhering to the procedures, if they have visual contact to the intruder. Hence, the probability of false reaction rises [92].

The risk ratio in the upper airspace in Europe is estimated to be at 0.017, which is a safety enhancement of a factor of approximately 60. In the lower airspace, the risk ratio is estimated to be ten times higher [87].

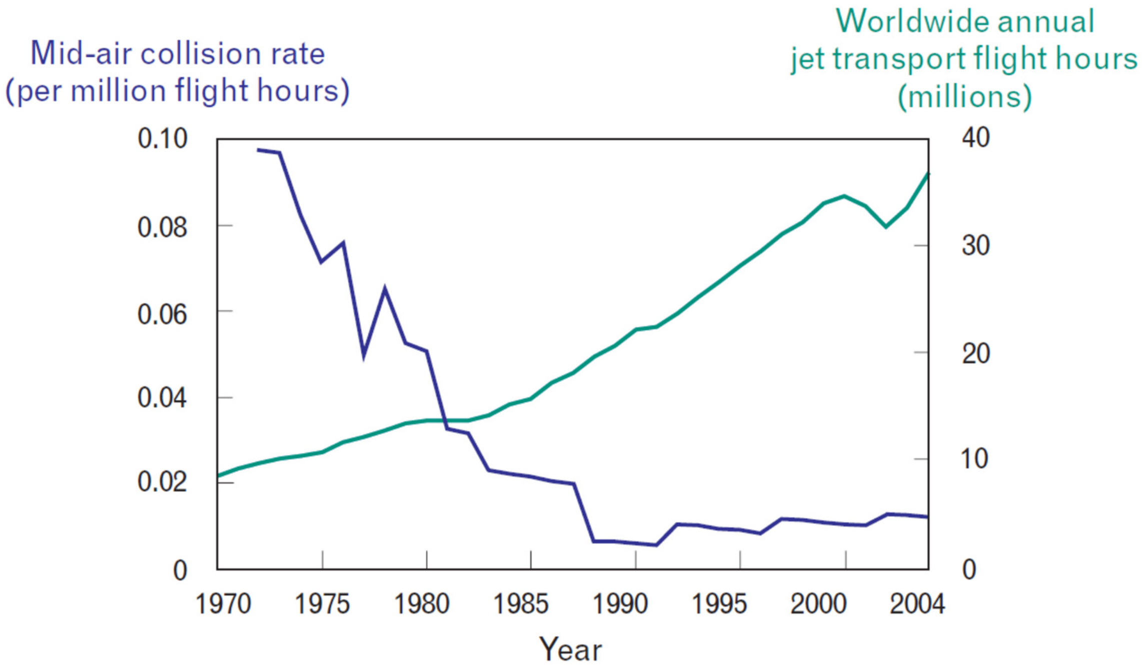

Figure 6-2 Midair collision rate versus flight hours [86]

This results in a very low, meanwhile nearly constant rate of midair collisions despite a continuous growth in worldwide air traffic, as shown in Figure 6-2.

The evaluation of the safety performance of midair collision of a certain airline is difficult. State-of-the-art is the use of the TCAS RA rate [2,11] without a distinction between the various event risk levels of the concerned TCAS events. The results of the presented method can easily range within three orders of magnitude in the risk level between the different events. One high risk level TCAS event can outweigh more than 1,000 low risk TCAS events.

While the consideration of the TCAS RA rate alone allows only the focus on lowering the number of TCAS RAs, consideration of the risk levels of the TCAS events can lower the overall risk level more efficiently. Investigation of high risk events can reveal root causes, and appropriate measures can be implemented by the management to reduce the event risk levels in future and therefore reduce the overall risk level in this accident category. Thus, an effective evaluation of the safety performance is only possible by considering the associated risk level of the events.

6.2 The Concept of TCAS

In general, TCAS uses information received from transponders of other aircraft to estimate the relative motion of the involved aircraft [88]. Most of the time, TCAS works as a surveillance system, monitoring and displaying the proximate traffic using relative range, bearing and altitude of this traffic. By extrapolating the trajectories of the monitored traffic in combination with the estimated trajectory of the own aircraft, a continuous process of potential threat detection is conducted. If the trajectory of an aircraft converges towards the trajectory of the own aircraft, then, in a first step, a Traffic Advisory (TA) is generated, which should enhance the situational awareness and alert the crew to prepare for a possible collision avoidance maneuver. If the trajectories continue to converge, the intruder aircraft is declared to be a threat, and the resolution of the conflict is handed over to the threat resolution logic of TCAS. This principle is shown in Figure 6-3.

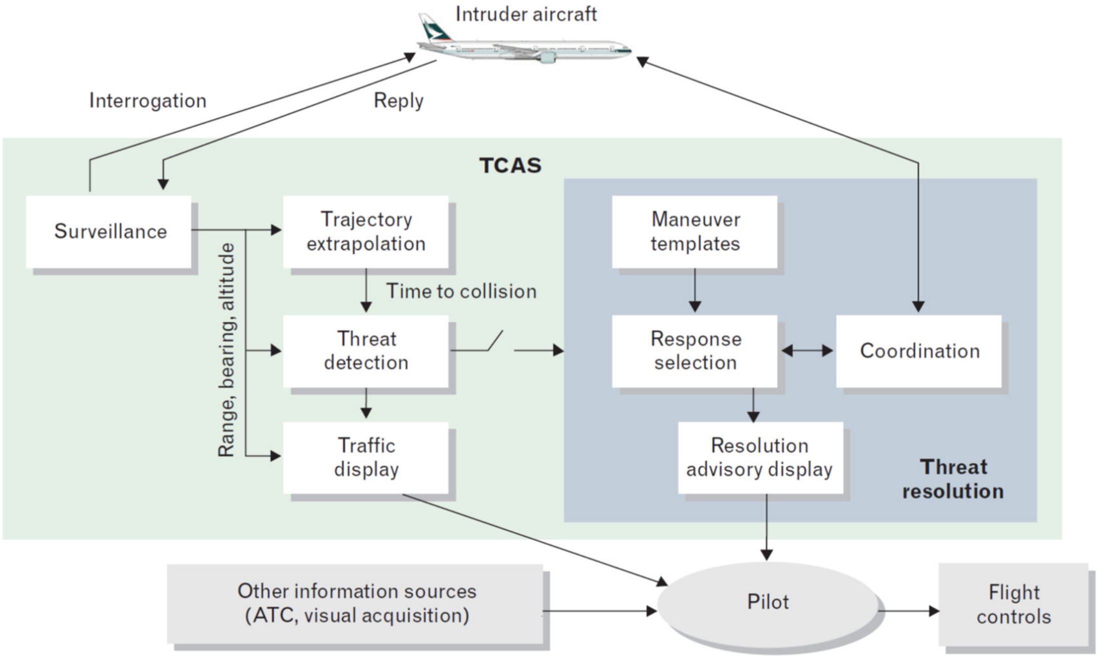

Figure 6-3 Principle of TCAS [86]

The result of the threat resolution is coordinated with the TCAS of the intruder aircraft, if the intruder is TCAS equipped, and is then visually displayed to the pilot on the resolution advisory display in combination with an aural instruction. Both, the visual display as well as the aural annunciation, represent the interface between the pilot and the TCAS system. In Figure 6-3 it is clearly visible that the pilot is part of the overall system, as he has to transfer the displayed resolution advisory to the flight controls in order to follow the advised trajectory. TCAS is an advisory system only. It tells the pilot how he can avoid a collision, but does not take control of the aircraft itself [86].

The resolution advisory is generated solely in vertical direction, as the bearing is not sufficiently accurate to support the initiation of horizontal maneuvers [84] and also, horizontal maneuvers cannot be conducted quickly enough to provide sufficient separation. However, the pilot is still influenced by other information sources. These sources include visual acquisition of the intruder, leading to possible maneuvers based on the pilot's own assessment of the situation. Also, the flight crew might receive contrary advises from air traffic control. These additional information sources might eventually lead to the pilot's deviation from the resolution advisory.

6.2.1 System Components

Figure 6-4 depicts the system components of TCAS and their interactions [84].

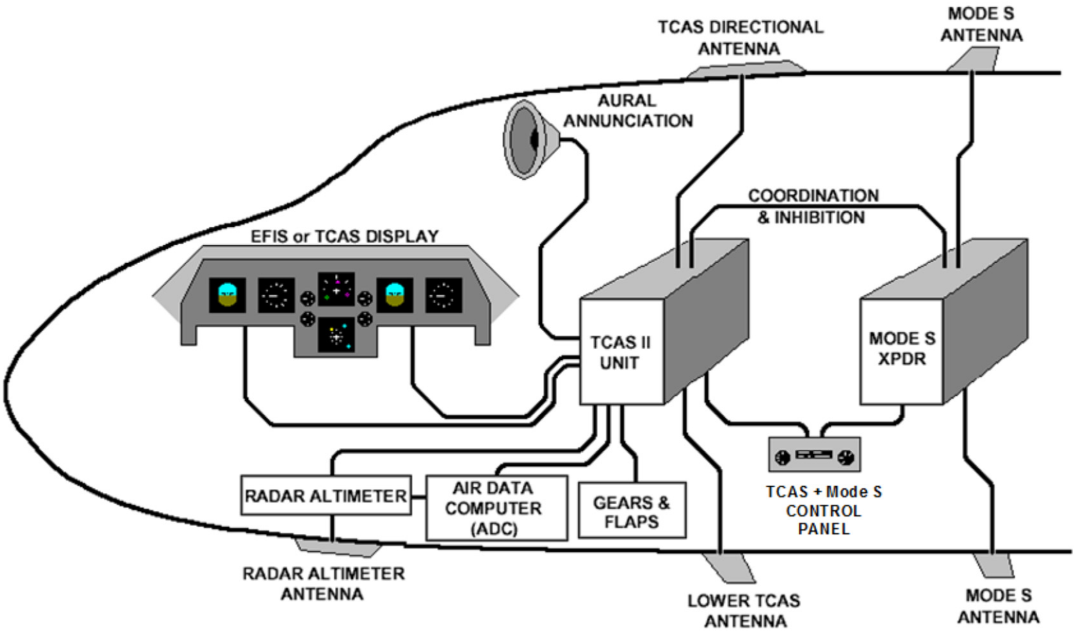

Figure 6-4 Schematic of the TCAS system [84]

The TCAS computer performs the surveillance and threat detection and, if necessary, calculates avoidance maneuvers and generates required advisories. The TCAS system can be controlled by the pilot via an integrated TCAS/transponder control panel (an example can be seen in Figure 6-5).

In the stand-by-mode (STBY), the TCAS system is off, i.e. no interrogation will be issued, and the Mode S transponder will only reply to discrete interrogations. In the transponder-mode (XPNDR), the Mode S transponder is fully operational and will reply to all interrogations from ground stations and other TCAS systems, however, TCAS remains in stand-by. TA-only-mode (TA ONLY) enables full operation of Mode S transponder, and TCAS is limited to issue TAs only while RAs are inhibited. The automatic mode (TA/RA) provides normal TCAS- and Mode S transponder operation [84].

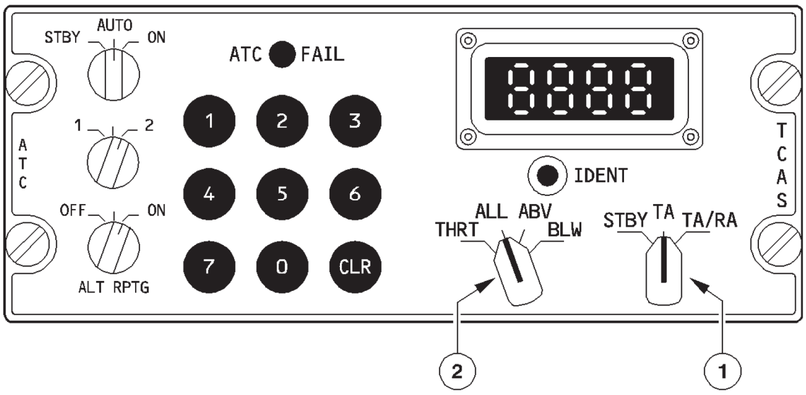

Figure 6-5 Example of an integrated TCAS/transponder control panel. The TCAS is controlled via the two rotary switches on the right-hand side (1 and 2) [68]

Traffic surveillance and intruder tracking is conducted by interrogations via two TCAS antennas, one at the top and one at the bottom of the aircraft. These antennas are capable of both, sending interrogations at 1030 MHz and receiving transponder replies at 1090 MHz. In addition, two antennas for the Mode S transponder are required. Because both, the TCAS unit as well as the transponder, generate transmission signals at the receiver frequency of the other system, both systems are connected to an aircraft suppression bus, which disables the receiving system when the other system is transmitting.

A connection between the TCAS system and the transponder is required to coordinate RAs between two or more TCAS-equipped aircraft and issue complementary RAs.

The air data computer (ADC) provides the current own aircraft altitude, typically in 1-foot-increments. The radio altimeter inhibits RAs if the aircraft is close to the ground and also determines whether a possible intruder is on the ground.

Some other data relating to the aircraft performance is also considered, e.g. landing gear, flaps and the operational performance ceiling, which can influence the type of the generated RA.

TCAS is designed to work autonomously. It is independent of the onboard auto flight system and the ground systems used to provide air traffic control services. Hence, information about the selected altitude and therefore a possible intention to level off instead of crossing the intruder altitude is not taken into consideration by TCAS. Instead, a simple extrapolation of the current flight trajectory is used for the calculation of possible threats.

Finally, a traffic display provides information about proximate traffic identified by the surveillance system and displays generated RAs to the pilot. This deals as the interface between man and machine. Installed loudspeakers are used to additionally provide aural annunciations in case of an RA.

6.2.2 Surveillance

The surveillance part of TCAS provides a picture of the surrounding traffic to the flight crew and enables the calculation of possible conflict geometries between two or more aircraft by measuring the relative range, bearing and altitude of the aircraft in which transponders are installed. This finally enables the generation of a resolution advisory when required to prevent a midair collision.

For the purpose of adequate collision avoidance protection, TCAS requires a minimum surveillance range by simultaneously reducing the transmitting power as much as possible to prevent transponder overload of the surrounding aircraft [86]. The surveillance is based on interrogations by TCAS once per second using a common frequency of 1030 MHz. Transponders of nearby aircraft receive these interrogations and reply on 1090 MHz [86]. Both Mode S and Mode A/C equipped aircraft can be processed. TCAS is capable to track up to 30 aircraft simultaneously, within a nominal range of 14 nautical miles for Mode A/C targets and 30 nautical miles for Mode S targets. Mode S transponders are equipped with a unique 24-bit Mode S address, which can be interrogated selectively. This reduces both the likelihood of garbled or overlapping replies as well as frequency congestion [86].

Only targets which are within 10,000 feet of the own altitude are taken into consideration for tracking [84]. Within dense traffic areas both the interrogation rate can be reduced up to once per 5 seconds for non-threatening aircraft and the surveillance range might be reduced down to 5 nautical miles in order to avoid transponder overload [84].

The own aircraft uses the altitude from the air data computer (ADC), typically in 1-foot increments for the calculation of the own trajectory. For Mode S intruders, typically a 25-foot increment is used, while for Mode A/C intruders, a 100-foot increment is used [84]. Due to altimetry error in real aircraft systems, the estimation of vertical separation of two aircraft is accompanied by a certain amount of inaccuracy, which might increase the risk, if the projected separation is lower than calculated [87]. Also, the vertical speed of the intruder, which is derived by a differentiation of altitude in the calculation of TCAS, can deviate from the actual vertical speed due to the relatively low resolution, especially if the intruder changes its trajectory quickly and the altitude of the intruder is provided in 100-foot increments only. This altimetry error is not taken into consideration within the scope of this thesis. Instead, in the following model a perfect altitude surveillance is assumed, see also [93].

Some transponders do not provide altitude information. In this case, the respective aircraft is tracked as a non-altitude reporting target using range and bearing information only. The non-altitude reporting traffic is only shown on the TCAS traffic display, if the own aircraft is below FL155. While TAs will be generated against those targets once the range test for TA generation is satisfied, no RA will be generated.

6.2.3 Traffic and RA Display

The nearby traffic, delivered by the surveillance component, is displayed on the traffic display to support the flight crew in the visual acquisition of transponder equipped aircraft. The bearing and altitude of the traffic is displayed relative to the own aircraft.

In modern glass cockpits, which are equipped with an Electronic Flight Instrument System (EFIS), the traffic display is usually integrated in the Navigation Display (ND), and the RA display is usually integrated in the Primary Flight Display (PFD). In most implementations, the pilot is able to select different ranges for the traffic display and to select different altitude layers to enhance situational awareness by focusing on relevant parts of the overall traffic situation.

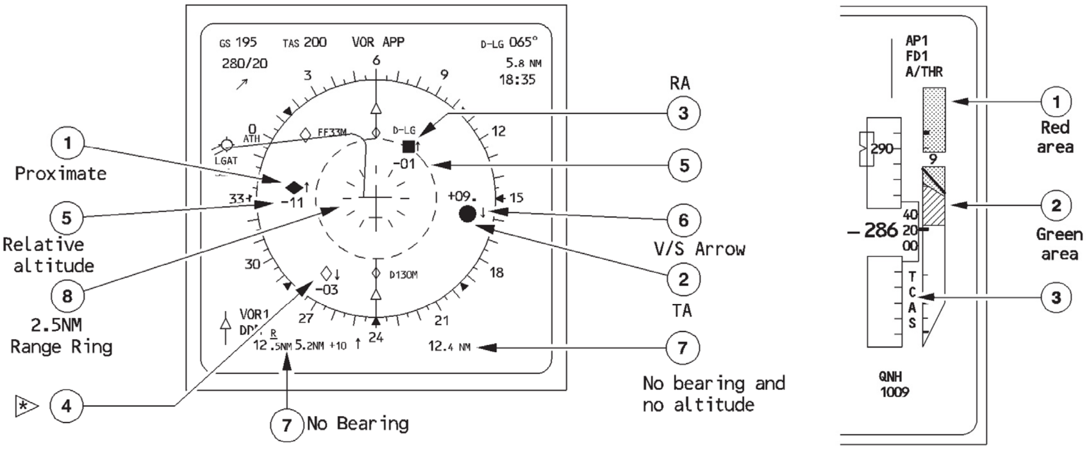

Figure 6-6 Traffic display and RA display, integrated in the Navigation Display and Primary Flight Display (Airbus A320) [68]

On the left-hand side of Figure 6-6, a typical traffic display is shown, which is integrated in the ND. The background color of the traffic display is dark. Non-intruding traffic within 6 NM horizontally and 1200 feet vertically of the own aircraft is called proximate traffic and is displayed as a solid white diamond (1). Intruder aircraft, which trigger a TA, are displayed as solid yellow circles (2). As soon as intruders become a threat and generate an RA, the symbol changes to a solid red square (3). Other traffic is displayed as a hollow white diamond (4).

Vertical separation, displayed as relative altitudes from the own aircraft in 100 feet steps, is shown above or below the respective symbol (5). If the traffic is in a climb or descent of at least 500 feet per minute, an up or down arrow is additionally displayed next to the respective symbol (6).

The display accuracy depends on the selected range. At a scale of 10 NM, the range accuracy is approximately ±1 NM, and the bearing accuracy around ±10 degrees [84]. Not all transponder equipped aircraft may be displayed at once in high density traffic areas, as most of the displays are limited, e.g. on Airbus A320, only the 8 most threatening intruders are displayed [68].

For the RA display, two different implementations can be used. The most common method is the integration of different colored arcs or band in the vertical speed indicator (VSI). A red arc (or band) indicates the range of vertical speeds which have to be avoided (no-fly zone). When appropriate, a green arc (or band) indicates vertical speeds, which the pilot has to aim for. An example of this kind of display can be seen in Figure 6-6 on the right-hand side. Another possibility of an RA display is the pitch-cue display, which is only possible on EFIS aircraft, integrated in the PFD. In this case, a red or orange trapezoid is displayed on the artificial horizon of the PFD, indicating the pilot the area of pitch, which has to be avoided. In this case, no green fly-to-area is provided to the pilot [84].

Additionally, loudspeakers in the cockpit provide an aural annunciation of the RA, which is inhibited below 500 feet above ground level or in case of active higher priority warnings like wind shear of the ground proximity warning system (GPWS) [84].

6.3 System Model of the Collision Avoidance System

In this chapter, the system model of the Traffic Collision Avoidance System (TCAS) will be developed. This system model represents one of the two elements to determine the environmental conditions.

The collision avoidance algorithm, also called threat logic, is the core part of TCAS. Originally developed by the MITRE Corporation on behalf of the FAA, starting from the 1970s, it was for the first time deployed as TCAS Version 6.04A in the early 1990s. In this early version, some elements were still missing, e.g. the reversal logic, which enables TCAS to reverse an already issued RA, if the geometry of the encounter changes during the RA and as a consequence, the projected separation provides no sufficient separation anymore. This enhancement was introduced in Version 7.0 in 2000 for the first time. Following the accidents of Yaizu [94] and Überlingen [90], the reversal logic was further enhanced in Version 7.1, which has been deployed from 2008 [86].

The following model of the logic is based on TCAS II version 7.1, which is mandated by ICAO since 1 January 2014 for new installations and since 1 January 2017 for all other TCAS units. Within the European Union airspace, TCAS II version 7.1 is mandatory since 1 December 2015 for all aircraft above 5700 kg or authorized to carry more than 19 passengers [84]. The description of the logic can be found in the TCAS Requirements Specification [95].

Several models of the Collision Avoidance Logic are existing [96–98]; however, they are not precise enough for the simulation of the risk model. Hence, an adequate model is developed, which is directly derived from the TCAS requirements specification, a document consisting of more than 650 pages of state-chart diagrams, functions and macros [95], which are converted from a functional description into a mathematical model. The boundary conditions and assumptions of the encounter scenarios are summarized at the end of each section.

6.3.1 Trajectory Extrapolation and Threat Detection

The treat detection component of TCAS identifies potential collision threats. A threat leads to a resolution advisory. For this reason, the logic tracks the positions and relative movements, i.e. rates, of each intruder altitude-reporting aircraft within the surveillance range [93,97], nominally at one-second intervals [99]. The resulting picture of the surrounding traffic situation must be divided into a horizontal and a vertical plane.

While it is assumed that the horizontal criterion is always fulfilled in the presented model, for the vertical plane a variation of all theoretically possible geometries leading to the analyzed RA type will be evaluated to estimate the risk. The reason is, that the risk of induced collisions mainly relies on the reaction of the involved flight crews, which takes place solely in the vertical plane. Nevertheless, for the evaluation of the accident probability, it is necessary to also understand the mechanism of the horizontal plane; therefore, it will be described below.

6.3.1.1 Threat Detection in the Horizontal Plane

In the horizontal plane, TCAS computes both, the relative slant distance, which is approximately the horizontal distance, and the respective closure rate for each intruder aircraft. The basic concept for the logic is to use time-to-go rather than distance-to-go for the estimation of the closest point of approach (CPA), expressed by the value tau [99], which is the projected amount in time, where the shortest horizontal distance between both aircraft can be expected. This projection is based on the assumption that the closure rate is constant for the remainder of the encounter [93].

Let $x_{h,t}^{ik}$ be the horizontal distance between the own aircraft i and the intruder aircraft k at time t, and similarly, $v_{h,t}^{ik}$ the relative velocity between both aircraft at time t, with a positive value of the relative velocity indicating converging aircraft, i.e., a reducing value of the horizontal distance between both aircraft. The time $\tau_{h,t}^{ik}$ to CPA, also called *tau*, can then be estimated by the quotient of the horizontal distance between both aircraft and the relative velocity for $v_{h,t}^{ik} \neq 0$ [84], i.e.,

$$\tau_{h,t}^{ik} = \frac{x_{h,t}^{ik}}{v_{h,t}^{ik}}. \qquad \textbf{Eq. 6-2}$$

Both, the horizontal distance and the relative velocity of all intruder aircraft are updated periodically by the surveillance component of the TCAS system. As the aircraft trajectories are multidimensional, the calculated time *tau* and the actual time to CPA coincide only if the corresponding aircraft are on a perfect collision course and not accelerating [99].

An example can be seen in Figure 6-7, where the development of *tau* during an encounter with two aircraft is shown as a blue solid line. The aircraft are flying one after the other on parallel courses with a horizontal miss distance of one nautical mile at CPA. In this case, tau is only an approximation of the time to CPA.

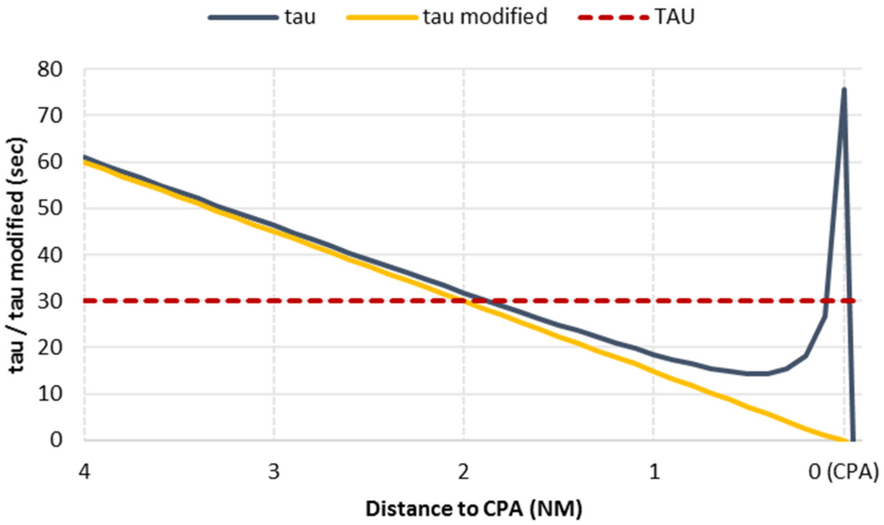

Figure 6-7 Development of tau (τ) during an encounter with two aircraft, which are flying one after the other on parallel courses with a horizontal miss distance of 1 nautical mile at CPA, source: own research

The value of *tau* first decreases constantly down to the alarm threshold for an RA, in this example 30 seconds, indicated by the dashed red line. It then continues to decrease towards a minimum value shortly before actual CPA, and thereafter sharply increases and becomes unreasonably large until the CPA, where *tau* is undefined. Especially if close to the CPA, the value of *tau* therefore gives a false estimate of the remaining time until CPA [93]. After passing the CPA, the value of *tau* becomes negative, as the aircraft diverge and hence, the horizontal distance starts to increase.

The definition of *tau* might be inefficient when the closure rate between two aircraft is very slow, leading to higher than intended values of *tau* and hence, might not generate a resolution advisory even if the intruder is very close to the own aircraft. For this reason, a horizontal distance threshold was introduced, called distance modification (DMOD), which is acting like a safety buffer around the own aircraft. The definition of *tau* is modified accordingly to a value called *modified tau*, which is approximately the amount of time the intruder requires to penetrate the safety buffer of DMOD. *Modified tau* is always less than *tau* [99]:

$$\tau_{h\_mod,t}^{ik} = \frac{{x_{h,t}^{ik}}^2 - DMOD^2}{x_{h,t}^{ik} \cdot v_{h,t}^{ik}}. \qquad \textbf{Eq. 6-3}$$

The interval between *modified tau* and *tau* is also called the critical interval, in which it is assumed that horizontal separation between both aircraft is lost.

Another reason for the use of the definition of *modified tau* instead of *tau* is that the *modified tau* enables sufficient reaction time if an intruder accelerates towards the own-ship in the future. If the distance between the aircraft is large, the *modified tau* is nearly identical to the true value of *tau*, but becomes smaller and hence, more conservative, if the distance and/or closure rate is smaller. Closure rates at a value of zero are not considered. Whenever the distance between both aircraft falls below DMOD, a resolution advisory is immediately generated. The respective development of *modified tau can* be seen in Figure 6-7 as a yellow line.

Yet another problem could arise with the definition of *modified tau*. If the closure rate between the own ship and the intruder is high, but no real collision threat exists due to a projected large Horizontal Miss Distance (HMD) at CPA, a nuisance alert would be triggered. To reduce the number of those nuisance RAs, TCAS Version 7.0 and higher uses a horizontal Miss Distance Filter (MDF). The MDF employs different noise filters and continuous maneuver checks, which eventually suppresses RAs for horizontal miss distances at CPA, which are approximately equal to or greater than DMOD [99]. These values are shown as HMD values in Table 6-1. They are the same values as the respective DMOD values, even though they are expressed in different units.

In general, a resolution advisory is issued when both horizontal and vertical criteria are fulfilled. In the horizontal plane, this corresponds to either a slant distance which is below the distance threshold DMOD, or the time to CPA is lower than a time threshold $\tau_{h,RA}$, which is generally equal to TAU according Table 6-1. In the latter case, only those encounters are not considered, where the projected horizontal miss distance is above DMOD or HMD.

A balance between necessary protection and unnecessary advisories is required for an effective collision avoidance system. This can partly be managed by a Sensitivity Level (SL), which varies with the altitude of the own-ship and controls the time thresholds and the dimensions of the protected airspace around each TCAS-equipped aircraft. Higher altitudes correspond to higher Sensitivity Levels and hence, higher threshold values, as speeds and separations between aircraft are generally larger at higher altitudes. The different sensitivity levels and the respective alarm threshold values for resolution advisories can be seen in Table 6-1.

Table 6-1 TCAS sensitivity levels definitions and alarm thresholds for resolution advisories [84]

Own altitude	**Sensitivity level (SL)**	**TAU** *sec*	**TVTHR** *sec*	**DMOD** *NM*	**ZTHR** *feet*	**ALIM** *feet*	**HMD** *feet*
0 – 1000 ft AGL	2	no RA	no RA	no RA	no RA	no RA	no RA
1000 – 2350 ft AGL	3	15	15	0.20	600	300	1215
2350 ft AGL – FL50	4	20	18	0.35	600	300	2126
FL50 – FL100	5	25	20	0.55	600	350	3342
FL100 – FL200	6	30	22	0.80	600	400	4861
FL200 – FL420	7	35	25	1.10	700	600	6683
Above FL420	7	35	25	1.10	800	700	6683

If the trajectories of both aircraft are currently diverging horizontally, or the MDF suppresses a threat due to a large projected HMD, but the relative trajectories of the aircraft change in a way that the geometry suddenly becomes a threat horizontally, the time to CPA when the RA is generated could become even lower than the threshold value $\tau_{h,RA}$.

For simplification purposes, in the presented model the time to CPA is assumed to be perfectly known and is defined to be always $\tau_{h,t}^{ik}$, regardless of the actual horizontal encounter geometry. Encounters with slow closure rates (DMOD) are not considered.

In summary, the following assumptions are made for the horizontal plane:

- **The horizontal criteria for issuing a TCAS RA are always fulfilled, with**
- **Horizontal trajectories converging in range, and**
- **The TCAS RA was not issued due to a slowly converging geometry (DMOD)**
- **The time to CPA is assumed to be perfectly known and defined to be $\boldsymbol{\tau_{h,t}^{ik}}$**

6.3.1.2 Threat Detection in the Vertical Plane

In the vertical plane, the general filter to declare an intruder as a threat and therefore initiate a TCAS RA, is called the *altitude test* [95].

Let $x_{z,t}^{ik} = x_{z,t}^{i} - x_{z,t}^{k}$ be the vertical distance separation and $v_{z,t}^{ik} = v_{z,t}^{i} - v_{z,t}^{k}$ be the vertical closure rate between both own aircraft i and the intruder aircraft k at time t, with $x_{z,t}^{i}$ being the altitude of aircraft i at time t and $v_{z,t}^{i}$ being the vertical rate, and similarly for aircraft k (see Figure 6-8).

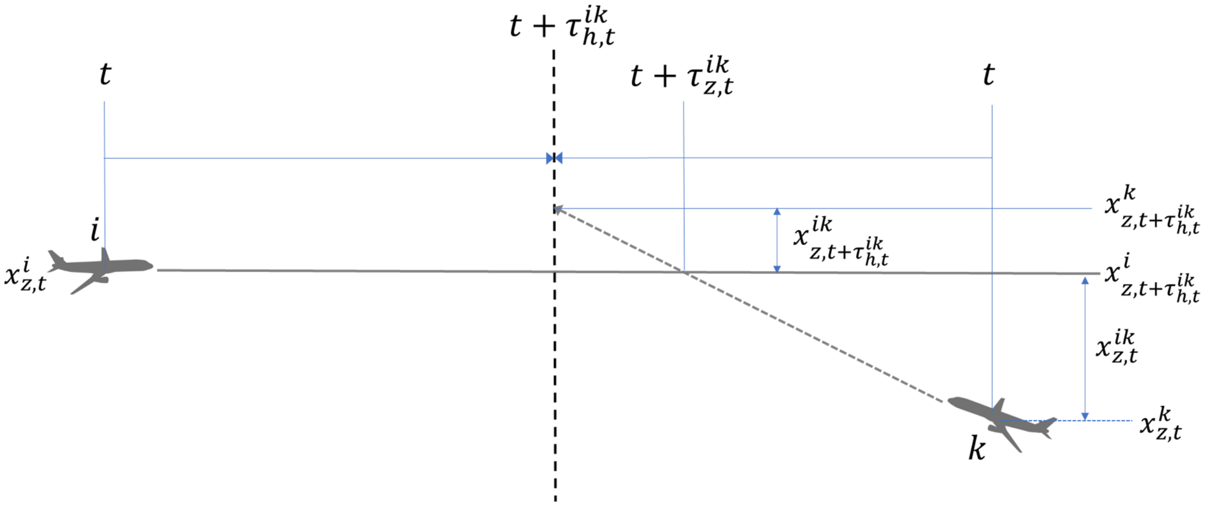

Figure 6-8 Principle of trajectory extrapolation based on [97]

The projected vertical miss distance at CPA $x^{ik}_{z,t+\tau^{ik}_{h,t}}$ without change of the vertical trajectories is then [95]:

$$x^{ik}_{z,t+\tau^{ik}_{h,t}} = x^{ik}_{z,t} + v^{ik}_{z,t} \cdot \tau^{ik}_{h,t}\,. \qquad \textbf{Eq. 6-4}$$

Similar to the horizontal plane, in the vertical plane the potential threat is considered by means of time to closest approach vertically and a vertical distance threshold.

The vertical tau $\tau^{ik}_{z,t}$ is the time to co-altitude, where both aircraft are at the same altitude. It is defined as [95]:

$$\tau^{ik}_{z,t} = \begin{cases} 0, & if\ v^{ik}_{z,t} = 0 \\ \dfrac{-x^{ik}_{z,t}}{v^{ik}_{z,t}}, & else. \end{cases} \qquad \textbf{Eq. 6-5}$$

The vertical tau is only of interest if greater or equal than 0, otherwise the aircraft are diverging vertically, and no threat exists. The time threshold for the vertical plane $\tau_{z,RA}$ is variable and can be lowered to a smaller value $TVTHR$ according Table 6-1 for an aircraft which is near level flight, i.e. vertical rate less than 600 feet per minute, or the vertical rate has the same direction but smaller magnitude than that of the intruder [95]. The reason for this reduced time threshold is twofold. First, it delays the generation of an RA for the level aircraft to detect a possible level off manoeuvre of the intruder and thus, can prevent a nuisance RA. And second, an RA is generated for the climbing/descending aircraft rather than for the level flying aircraft, which produces less impact on the air traffic system as a whole, as the level flying aircraft is not disturbed in its trajectory. The time threshold in the vertical plane $\tau^{i}_{z,RA}$ for airplane i is therefore [95]:

$$\tau^{i}_{z,RA} = \begin{cases} TVTHR, & if\ \left(\left|v^{i}_{z,t}\right| \leq 600\ ft/min\right) \vee \left[\left(v^{t}_{z,t} \cdot v^{k}_{z,t} \geq 0\right) \wedge \left(\left|v^{i}_{z,t}\right| < \left|v^{k}_{z,t}\right|\right)\right] \\ TAU, & else. \end{cases} \qquad \textbf{Eq. 6-6}$$

The same applies to aircraft k for the respective time threshold $\tau^{k}_{z,RA}$.

The vertical distance threshold $ZTHR$, as indicated in Table 6-1, is the corresponding vertical complement to the horizontal distance threshold DMOD.

In general, the *altitude test* determines whether the involved aircraft are currently close in altitude, i.e. below the vertical threshold $ZTHR$, and whether this will also apply at CPA, or projected to be at the same altitude within a given time threshold [95].

In particular, the *altitude test* is passed if

- The current vertical rate of the intruder is equal to or less than 10,000 feet per minute, i.e.

$$\left(|v_{z,t}^{k}| \leq 10{,}000\frac{ft}{min}\right), \tag{Eq. 6-7}$$

- and either
    - both the current altitude separation and the projected altitude separation at CPA are below the vertical threshold $ZTHR$, i.e.

$$\left(|x_{z,t}^{ik}| < ZTHR\right) \wedge \left(\left|x_{z,t+\tau_{h,t}^{ik}}^{ik}\right| < ZTHR\right), \tag{Eq. 6-8}$$

    - or the current altitude separation is $ZTHR$ or above and both aircraft are converging in altitude and the vertical closure rate is greater than 60 feet per minute, the time to co-altitude is less than the vertical threshold $\tau_{z,RA}^{i}$, and either the projected vertical distance at CPA is less than $ZTHR$or the co-altitude is predicted to occur before CPA, i.e.

$$\left(|x_{z,t}^{ik}| \geq ZTHR\right) \wedge \left(v_{z,t}^{ik} \cdot \operatorname{sgn}\left(x_{z,t}^{ik}\right) < -1\frac{ft}{s}\right) \wedge \left(\tau_{z,t}^{ik} < \tau_{z,RA}^{i}\right) \wedge \left[\left(\left|x_{z,t+\tau_{h,t}^{ik}}^{ik}\right| < ZTHR\right) \vee \left(\tau_{z,t}^{ik} < \tau_{h,t}^{ik}\right)\right]. \tag{Eq. 6-9}$$

Even though the sense selection will be subject of the next section, in certain situations the sense of the intruder aircraft, if TCAS equipped, can influence the threat detection significantly, and therefore the coordination process must be discussed at this point.

An aircraft equipped with TCAS will send an intent message u through the Modes S datalink in form of a coordination interrogation to prevent from both aircraft select the same vertical sense as soon as an RA was issued. This intent message contains the Vertical Resolution Complement (VRC), which is the information for the other aircraft, which sense should not be selected. The receiving aircraft uses the complementary sense, $s_t^i = -s_t^k = -u_t^k$, the VRC [95]. Within the scope of this thesis, the climb sense is defined as $s = 1$, and a descent sense is defined as $s = -1$.

The *altitude test* must be passed to declare an intruder as a threat and therefore issue a TCAS RA, except for one special case: If the intruder is TCAS equipped and has issued an RA already, and both the received sense of the intruder s^k as well as the altitude difference between the own aircraft and the intruder aircraft indicate, that an altitude crossing will occur, a TCAS RA will immediately be issued without any further tests, including the *altitude test* [95]. The intended altitude crossing is detected, if [95]:

$$\left[(s^k = +1) \wedge \left(x_{z,t}^{ik} \geq 100ft\right)\right] \vee \left[(s^k = -1) \wedge \left(x_{z,t}^{ik} \leq -100ft\right)\right]. \qquad \textbf{Eq. 6-10}$$

Above definition contains a 100 feet-threshold, which is the necessary vertical separation for the crossing definition. If both aircraft are within 100 feet in altitude, they are declared to be in co-altitude.

In all other cases, the *altitude test* has to be passed. If an intent message u^k from the intruder aircraft k has been received already, and the encounter is non-altitude-crossing according Eq. 6-10, the *altitude test* will be sufficient to issue the RA.

Otherwise, an additional test will be conducted, called the *altitude separation test*. In the presented model, this test will only be applied towards unequipped intruders, because in the other case it is assumed that an intent message has already been received by the own aircraft, as normally the intruder issues its RA first, and therefore sends an intent message well before the issuance of an own RA.

Prediction of vertical rates by the use of broadcasted altitude of the intruder is extremely difficult. Both, the update frequency as well as the resolution of the intruder altitude are relatively low, which leads to a weak prediction quality of the vertical rate, especially during accelerated vertical movements [100]. There is evidence that a climbing or descending threat which is projected to merely pass the own aircraft is more likely to level-off instead of maintaining the current vertical rate. It is therefore desirable to bias the selection of an RAs towards a possible level-off-maneuver of the intruder during the encounter.

Especially if an intruder is projected to cross the own altitude, the selection of both sense and strength of an RA is extremely difficult, as the intruder might or might not level-off during the encounter. If the own aircraft has to cross through the level of the intruder, it might be considered counter-intuitive by flight crews, as an initial maneuver towards the intruder aircraft is required during those encounters. It is not possible to avoid such maneuvers entirely, but at least the number of those RAs should be reduced as much as possible.

The *altitude separation test* reduces the probability of an induced close encounter due to a threat levelling off or reducing its vertical rate during the encounter. If the intruder is equipped with TCAS and issues an RA, it is most probably that the intruder might have received a level-off-type RA. By delaying the issuance of own RA due to the *altitude separation test*, the intruder is given the chance to reduce its vertical rate, and a non-crossing encounter becomes more likely.

The *altitude separation test* is conducted under certain circumstances only. It prevents the threat to be declared, if the threat is a new threat and the sense s^i that would be selected against this threat would be altitude crossing, i.e.:

$$\left[(s^i = +1) \wedge \left(x^{ik}_{z,t} \leq -100ft\right)\right] \vee \left[(s^i = -1) \wedge \left(x^{ik}_{z,t} \geq 100ft\right)\right]. \qquad \textbf{Eq. 6-11}$$

The criteria for the selection of the sense s^i are described in the following section, called *initial sense selection*.

Additionally, the current altitude separation x^{ik}_t needs to exceed a certain value A_c, which is smaller than the standard vertical separation between aircraft flying under Instrument Flight Rules (IFR), i.e. 1000 feet, to cover altimeter error and possible slight altitude excursions. In this case, the altitude separation is passed, and the RA will not be triggered:

$$\left|x^{ik}_{z,t}\right| > A_c\,. \qquad \textbf{Eq. 6-12}$$

The required altitude separation A_c depends on the vertical rates of both involved aircraft. It is smaller, if either aircraft is close to level flight, i.e. the absolute vertical rate is less or equal than 600 feet per minute, or the vertical rates of both aircraft are in the same direction [95], i.e.:

$$A_c = \begin{cases} 850\,m, & if\,\left(\left|v^i_{z,t}\right| > 600\,ft/min\right) \wedge \left(\left|v^k_{z,t}\right| > 600\,ft/min\right) \wedge \left(sgn\left(v^t_{z,t}\right) \neq sgn\left(v^k_{z,t}\right)\right) \\ 600\,m, & else. \end{cases} \qquad \textbf{Eq. 6-13}$$

If both Eq. 6-11 and Eq. 6-12 are fulfilled, the *altitude separation test* will be passed and therefore prevent the RA.

In a scenario as depicted in Figure 6-9, there is a high probability that the intruder aircraft k would level off below own aircraft i, irrespective whether the intruder is TCAS equipped or not. This is a typical scenario in high density airspaces with over-powered jet aircraft, which can achieve high vertical rates in combination with a relatively small standard vertical IFR-separation of 1000 feet. If TCAS equipped, the intruder k would receive a level-off-RA, which would be generated 30 seconds before CPA, assuming a Sensitivity Level of 6 (FL100 to FL200). Table 6-2 shows the development of the vertical rate of the intruder and both actual altitude separation and projected vertical separation at CPA, assuming that the intruder would follow the RA, and level-off. Additionally, the time to co-altitude is provided for each step. These values would still apply, if the intruder would not be TCAS equipped, but intending to level off at an altitude which is 1000 feet below the level of the own aircraft, following its ATC clearance.

Due to the reduced time threshold for a level flying aircraft according Eq. 6-6, the threshold for threat declaration would be delayed to $TVTHR$, i.e. 22 seconds from CPA for Sensitivity Level 6. At that time, the projected altitude separation at CPA would be 499 feet, which is below the vertical separation threshold $ZTHR$. However, the time to co-altitude never falls below the reduced time threshold $TVTHR$, so no RA would be generated for the level aircraft.

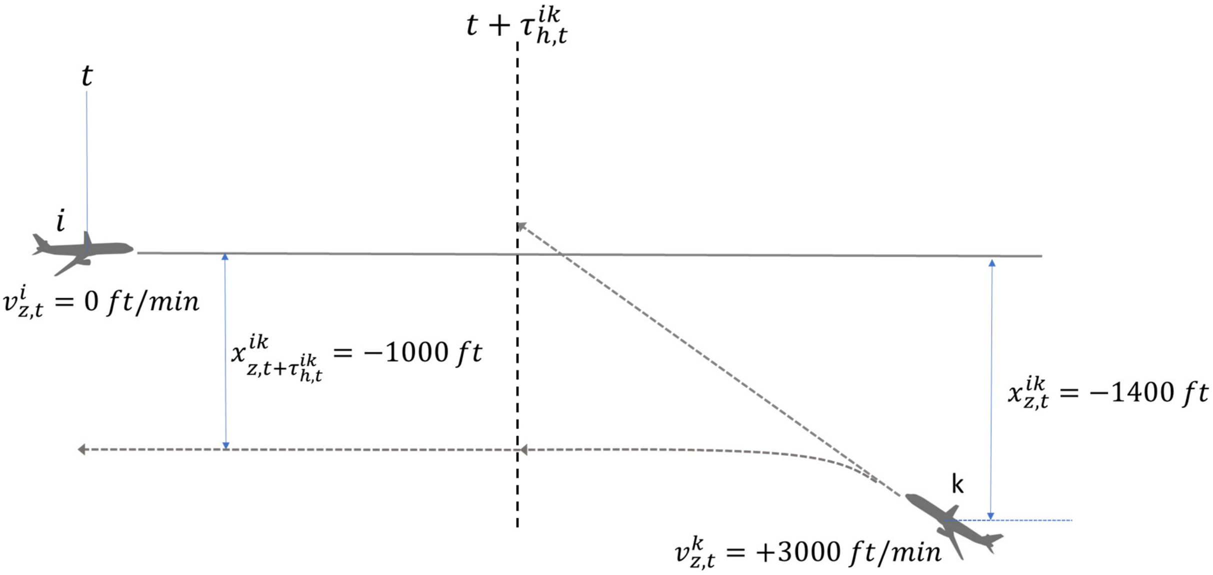

Figure 6-9 Encounter example with 1000 feet separation at high vertical rate

Also, the *altitude separation test* would prevent this RA, as the vertical separation during the whole encounter never falls below the threshold value A_c.

In fact, during level off/level coordinated encounters, where both aircraft are TCAS equipped, only 3 percent of the level-flying aircraft issue an RA [101].

Table 6-2 Example with intruder levelling off 1000 feet below own aircraft

Time to CPA	30	28	26	24	22	20	18	16
Vertical rate of intruder (ft/min)	3000	3000	3000	2500	1500	500	0	0
Intruders relative altitude (ft/min)	-1400	-1300	-1200	-1108	-1049	-1022	-1000	-1000
Projected relative altitude at CPA (ft)	100	100	100	-108	-499	-855	-1000	-1000
Time to co-altitude (s)	28	26	24	26.6	42	123	n.d.	n.d.

If, in contrast, the intruder aircraft would continue its vertical rate without levelling off timely, the relative altitude between both aircraft would further decrease, and at the time threshold $TVTHR$ the intruder would normally be declared a threat. In the described model, this would only apply if the intruder would be TCAS equipped and the own aircraft would have received an intent message. However, if the intruder would not be equipped, the altitude separation test would delay the issuance of an RA until the intruder's altitude would be at or below A_c, i.e. 600 feet, still letting the intruder aircraft time to level off.

However, 14 seconds before CPA, the current altitude separation falls below 600 feet, and hence, the RA will be issued. As the projected up-sense separation at CPA, a^i, would be only 86 feet, which is below $ALIM$ (see next section, *Initial sense selection*), a crossing descent RA would be issued, leading own aircraft through the altitude of the intruder.

Table 6-3 Example with intruder not levelling off

Time to CPA	30	26	22	18	14	10	6	0
Vertical rate of intruder (ft/min)	3000	3000	3000	3000	3000	3000	3000	3000
Intruders relative altitude (ft/min)	-1400	-1200	-1000	-800	-600	-400	-200	+100
Projected relative altitude at CPA (ft)	100	100	100	100	100	100	100	100
Time to co-altitude (s)	28	24	20	16	12	8	4	-2

Due to the combination of high vertical rates and very late RA generation, there is a certain probability, that an encounter cannot be solved in time [100]. This is the tradeoff which has to be accepted in order to reduce unnecessary TCAS RAs produced by this kind of encounter geometries.

6.3.2 Threat Resolution

Once an intruder is declared to be a threat, the threat resolution component becomes active. This is conducted solely in the vertical plane and consists of several steps.

The first step is the sense selection, thereafter a strength selection is conducted. The logic determines the required vertical rate and evaluates whether the RA is preventive or corrective. Thereafter, the logic defines the type of RA, depending on the combination of the above.

After issuance of the RA, TCAS continuously monitors the projected trajectories of both aircraft and modifies the RA, if necessary, to meet the minimum separation requirements of TCAS. This can lead either to a weakening, a strengthening RA or even a reversal RA. If the conflict has been solved, a "Clear of Conflict" will be announced, and the RA terminates.

6.3.2.1 Initial Sense Selection

As mentioned in the previous section, the own sense selection is superseded by the Vertical Resolution Complement (VRC) if an intent message u was received. In this case, the own sense s_t^i will be selected in the complementary sense as the intruder's sense s_t^k, i.e.

$$s_t^i = -s_t^k = -u_t^k \, . \qquad \textbf{Eq. 6-14}$$

Only if the two aircraft would simultaneously select the same sense, the slave aircraft, i.e. the aircraft with the higher Mode S address, would detect the incompatibility and would reverse the sense of its RA to the complementary sense of the other aircraft's RA. This reversal is called a coordination or tiebreak reversal [84], and will not be considered within the context of this thesis. Instead, if an RA will be issued for both aircraft at the same time, the master aircraft, i.e. the aircraft with the lower Mode S address, will always select it's sense first, and will then coordinate this sense with the other aircraft.

Otherwise, the sense will be selected by each aircraft independently. The sense selection is based on a comparison between a projected upwards correction and downwards correction of the own aircraft, assuming that the trajectory of the intruder does not change during the whole encounter, irrespectively whether the intruder is TCAS equipped or not.

The own trajectory projection is calculated as follows [93]. Target rate $\mathit{\Delta}_t^i(up)$ for the upwards sense is 1500 feet per minute, if actual vertical speed is of smaller magnitude than this value. If the current vertical speed is higher than 1500 feet per minute, the actual rate is used, up to a maximum of 4400 feet per minute

$$\Delta_t^i(up) = \max\left[1500\, ft/min, min\left(v_{z,t}^i, 4400\, ft/min\right)\right]. \qquad \textbf{Eq. 6-15}$$

For the downwards sense, the respective value is:

$$\Delta_t^i(down) \\ = \min\left[-1500\, ft/min, max\left(v_{z,t}^i, -4400\, ft/min\right)\right]. \qquad \textbf{Eq. 6-16}$$

The maneuver is assumed to be initiated after a delay time t_d of 5 seconds with a change in vertical speed $\dot{v}^i$ of 8 feet per second squared. The duration of the change in vertical speed t_c to reach the target value Δ_t^i can therefore be evaluated as follows:

$$t_c = \frac{\left|\Delta_t^i - v_t^i\right|}{\dot{v}^i}. \qquad \textbf{Eq. 6-17}$$

After reaching the target rate, it is assumed that the own aircraft is climbing or descending, respectively, for the remainder of the RA with the advised rate Δ_t^i. The duration of this constant rate segment t_s is therefore

$$t_s = \max\left(\tau_{h,t}^{ik} - t_d - t_c, 0\right). \qquad \textbf{Eq. 6-18}$$

Figure 6-10 shows the principle of the sense selection in a graphical way.

The projected own altitude at CPA in case of trajectory change $x_{z,t+\tau_{h,t}^{ik}}^i(up)$ or $x_{z,t+\tau_{h,t}^{ik}}^i(down)$ can be calculated in the following way:

$$x_{z,t+\tau_{h,t}^{ik}}^i(up, down) = x_{z,t}^i + t_d \cdot v_{z,t}^i + t_s \cdot \Delta_t^i + \frac{1}{2} \cdot t_{_C} \cdot \left(\Delta_t^i + v_{z,t}^i\right). \qquad \textbf{Eq. 6-19}$$

The projected altitude at CPA in case of no reaction, $x_{t+\tau_{RA}}^i(current)$, would be:

$$x_{z,t+\tau_{h,t}^{ik}}^i(\text{current}) = x_{z,t}^i + \tau_{h,t}^{ik} \cdot v_{z,t}^i. \qquad \textbf{Eq. 6-20}$$

The projected altitude $x_{z,t+\tau_{h,t}^{ik}}^k(up, down, current)$ at CPA for the intruder aircraft k can be calculated respectively.

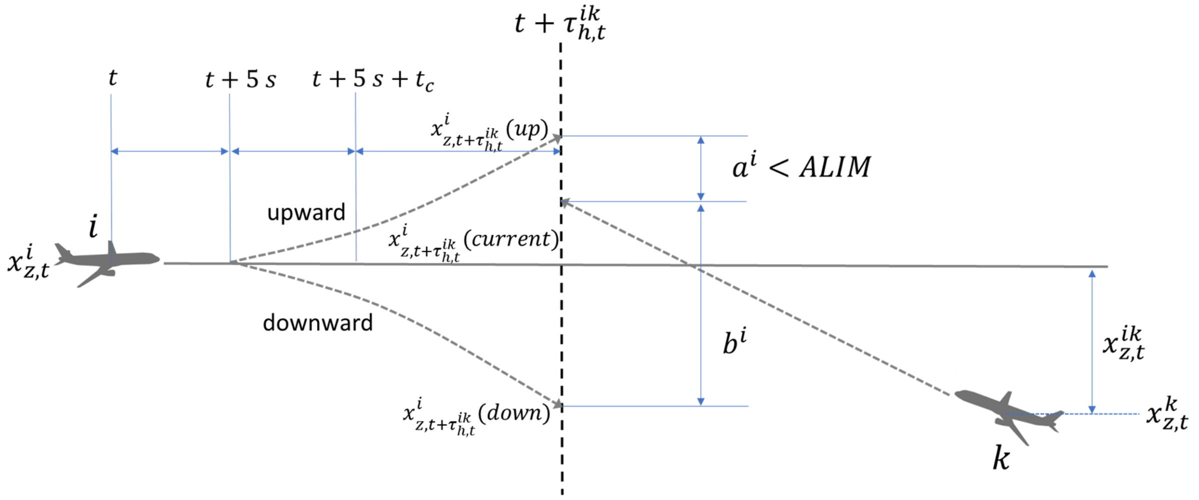

Figure 6-10 TCAS RA sense selection (illustrative example) based on [98]

The projected vertical miss distances at CPA, a_t^i and b_t^i, for trajectory changes in both directions according Figure 6-10 are then

$$a_t^i = x^i_{z,t+\tau^{ik}_{h,t}}(up) - x^k_{z,t+\tau^{ik}_{h,t}}(current)\,, \qquad \textbf{Eq. 6-21}$$

$$b_t^i = x^k_{z,t+\tau^{ik}_{h,t}}(current) - x^i_{z,t+\tau^{ik}_{h,t}}(down)\,. \qquad \textbf{Eq. 6-22}$$

In general, the sense, which provides the larger projected vertical separation between both aircraft, will be selected. However, TCAS is biased to avoid altitude crossing advisories, i.e. advisories, where both aircraft are crossing their altitudes during the encounter. Hence, the non-crossing sense will be selected, even if the gained separation is smaller than would be achieved by the crossing advisory, if at least the vertical separation threshold $ALIM$ can be reached at CPA.

The geometry, whether an RA would result in a crossing situation, must therefore be considered. For the evaluation of this geometry, it must also be verified, that the aircraft's trajectories are not crossing each other during the avoidance manoeuvre, i.e. if the own aircraft is climbing but advised to descent, it will initially climb further during the delay and manoeuvre phase, and could therefore cross the intruder's altitude, even though the direction will be reversed during the manoeuvre. For that reason, the altitude of both aircraft has to be evaluated, which will be reached during this manoeuvre. For the own aircraft, which is assumed to correct the vertical rate, this altitude $x^i_{z,t+LO}$ would be calculated as follows [95], with the standard delay $t_d = 5\,s$:

$$x^i_{z,t+LO} = x^i_{z,t} + v^i_{z,t} \cdot t_d + 0.5 \cdot v^i_{z,t} \cdot \frac{|v^i_{z,t}|}{t_c \cdot \frac{8ft}{s^2}}\,. \qquad \textbf{Eq. 6-23}$$

The altitude $x^k_{z,t+LO}$ of the intruder, at which the own aircraft just reached level flight, is calculated with the assumption of a simple extrapolation of its trajectory, without any corrections on the vertical rate:

$$x^{k}_{z,t+LO} = x^{k}_{z,t} + \left(t_d + \frac{|v^{i}_{z,t}|}{8ft/s^2}\right) \cdot v^{k}_{z,t}\,. \qquad \textbf{Eq. 6-24}$$

The sense s^i_t will be selected according to the following logic [95]. An up-sense will be selected in any case, if the up-separation a^i is greater than the down-separation b^i, and either the generated RA would be non-crossing (see line 1 of Eq. 6-25) or the down-separation would not provide enough separation, i.e. less than $ALIM$, irrespective of whether the RA would be crossing or not (see line 2 of Eq. 6-25). If the up-separation would be equal or less than the down-separation, but would provide enough separation, the up-sense would be selected, if the down-sense would result in a crossing RA (see line 3 of Eq. 6-25). For the crossing geometries, a 100 feet threshold is included, as aircraft are considered to be at co-altitude, if they are within a 100 feet altitude difference. Hence, the up-sense $s^i_t = 1$ would be selected under the following conditions [95]:

$$\begin{aligned}
&\{a^i > b^i \wedge [x^{ik}_{z,t} > 100\,ft \vee (v^i_{z,t} > 0 \wedge x^i_{z,t+LO} > x^k_{z,t+LO} - 100\,ft)]\} \vee \\
&(a^i > b^i \wedge b^i < ALIM) \vee \qquad \textbf{Eq. 6-25} \\
&\{a^i \leq b^i \wedge a \geq ALIM \wedge [x^{ik}_{z,t} \geq 100\,ft \wedge (v^i_{z,t} \geq 0 \vee x^i_{z,t+LO} \geq x^k_{z,t+LO} + 100\,ft)]\}\,.
\end{aligned}$$

In contrast, a down-sense will be selected in any case, if the down-separation b^i is equal or greater than the up-separation a^i, and either the generated RA would be non-crossing (see line 1 of Eq. 6-26) or the up-separation would not provide enough separation, i.e. less than $ALIM$, irrespective of whether the RA would be crossing or not (see line 2 of Eq. 6-26). If the down-separation would be less than the up-separation, but would provide enough separation, the down-sense would be selected, if the up-sense would result in a crossing RA (see line 3 of Eq. 6-26). Hence, the down-sense $s^i_t = -1$ would be selected under the following conditions [95]:

$$\begin{aligned}
&\{a^i \leq b^i \wedge [x^{ik}_{z,t} < 100\,ft \vee (v^i_{z,t} < 0 \wedge x^i_{z,t+LO} < x^k_{z,t+LO} + 100\,ft)]\} \vee \\
&(a^i \leq b^i \wedge a^i < ALIM) \vee \qquad \textbf{Eq. 6-26} \\
&\{a^i > b^i \wedge b^i \geq ALIM \wedge [x^{ik}_{z,t} \leq 100\,ft \wedge (v^i_{z,t} \leq 0 \vee x^i_{z,t+LO} \leq x^k_{z,t+LO} - 100\,ft)]\}\,.
\end{aligned}$$

The RA is considered to be crossing, i.e. $c^i_t = 1$, if the altitude difference $x^{ik}_{z,t}$ is equal or greater than 100 feet for down-sense RAs, or equal or less than -100 feet for up-sense RAs, respectively:

$$c^i_t = \begin{cases} 1, & if - x^{ik}_{z,t} \cdot s^i_t \geq 100\,ft \\ 0, & else. \end{cases} \qquad \textbf{Eq. 6-27}$$

6.3.2.2 Initial Strength Selection

After the sense has been selected, the initial strength can be evaluated. In general, for the strength two aspects are important. First, the vertical separation between both aircraft at CPA should be at least the minimum separation $ALIM$ from Table 6-1, which TCAS aims for during an encounter resolution. If the projected separation is below this threshold, a corrective RA will be issued, and the aircraft has to adapt its vertical trajectory accordingly. Second, a target vertical rate will be selected, which is least disruptive to the current vertical trajectory in order to minimize any departure from an ATC clearance [100] and therefore, aims to avoid further conflicts with other traffic. If $ALIM$ can be achieved at CPA without change of the current vertical trajectory, a preventive RA will be issued [99].

In case a preventive RA was issued, no pilot's input is needed. TCAS only has to assure continuously during the encounter, that the projected vertical separation at CPA stays above the required minimum separation. If this cannot be assured from a certain point during the encounter, the RA has to be modified immediately into a corrective RA (see section *Modification of the RA* below).

The least disruptive RA type is a Vertical Speed Limit (VSL). However, a Vertical Speed Limit may only be used under certain conditions, which are limited to less severe encounter geometries. For this reason, a consideration about sufficient separation structures regarding both the current altitude separation as well as the projected altitude separation at CPA has to be made first.

The current separation at CPA is considered to be sufficient, if the current absolute altitude difference is greater than $ALIM$, and the currently selected sense leads the own aircraft away from the intruder vertically [95]. This is indicated by the flag $q_{z,t}^{ik}$, which is zero, if above conditions are fulfilled:

$$q_{z,t}^{ik} = \begin{cases} 1, & if \ \left[s_t^i = 1 \wedge x_{z,t}^{ik} < ALIM\right] \vee \left[s_t^i = -1 \wedge x_{z,t}^{ik} > -ALIM\right] \\ 0, & else. \end{cases} \qquad \textbf{Eq. 6-28}$$

The same applies to the projected separation at CPA $x_{z,t+\tau_{h,t}^{ik}}^{ik}$, which is considered to be sufficient, i.e. $q_{z,t+\tau_{h,t}^{ik}}^{ik} = 0$, if the projected absolute altitude difference at CPA is greater than $ALIM$, and the currently selected sense leads away the own aircraft from the intruder at CPA vertically, with $x_{z,t+\tau_{h,t}^{ik}}^{ik}$ being the projected altitude difference at CPA using the current vertical rates according Eq. 6-20 [95]:

$$q_{z,t+\tau_{h,t}^{ik}}^{ik} = \begin{cases} 1, & if \ \left[s_t^i = 1 \wedge x_{z,t+\tau_{h,t}^{ik}}^{ik} < ALIM\right] \vee \left[s_t^i = -1 \wedge x_{z,t+\tau_{h,t}^{ik}}^{ik} > -ALIM\right] \\ 0, & else. \end{cases} \qquad \textbf{Eq. 6-29}$$

In general, a Vertical Speed Limit will only be considered, if either the intruder does not have a substantial vertical rate and either current altitude separation is considered sufficient, or current altitude separation is considered not sufficient, but projected altitude separation at CPA is considered sufficient, or the current altitude separation is considered not sufficient, but the own absolute vertical rate is greater than 600 feet per minute. A Vertical Speed Limit will also be considered, if the intruder has a substantial rate, and either the projected altitude separation at CPA is considered sufficient or the own absolute vertical rate is greater than 600 feet per minute. Hence, a Vertical Speed Limit will be considered, if

$$\left\{ \left|v^k_{z,t}\right| < 1000ft/min \wedge \left[\begin{matrix} q^{ik}_{z,t} = 0 \vee \left(q^{ik}_{z,t} = 1 \wedge q^{ik}_{z,t+\tau^{ik}_{h,t}} = 0\right) \vee \\ \left(q^{ik}_{z,t} = 0 \wedge \left|v^i_{z,t}\right| > 600ft/min\right) \end{matrix}\right]\right\} \vee$$

$$\left\{ \left|v^k_t\right| \geq 1000ft/min \wedge \left[q^{ik}_{z,t+\tau^{ik}_{h,t}} = 0 \vee \left|v^i_{z,t}\right| > 600ft/min \right]\right\}.$$

Eq. 6-30

In order to use the least disruptive change of the vertical trajectory, all four possible VSL are tested first, starting with the highest Vertical Speed Limit, $VSL = 2000$. If not sufficient, the test will be repeated according Eq. 6-32 to Eq. 6-35 for the other VSLs.

The decision, whether the projected separation at CPA is sufficient to use the respective VSL, is based on whether the current vertical rate is in the target area already, i.e. a preventive RA will be issued ("Monitor Vertical Speed"), or the current vertical rate is outside this area, in this case, a corrective RA will be issued ("Level Off"). In case, the current vertical rate is already in the target area, i.e.

$$v^i_{z,t} \cdot s^i_t < VSL\,.$$

Eq. 6-31

the projected altitude separation at CPA would be [95]:

$$x^{ik}_{z,t+\tau^{ik}_{h,t}} = x^{ik}_{z,t} + \left(-s^i_t \cdot VSL - v^k_{z,t}\right) \cdot \tau^{ik}_{h,t}\,.$$

Eq. 6-32

Otherwise, if the current vertical rate is outside of the target area, a delay and correction have to be considered in the vertical projection of the own altitude. In this case, the own projected altitude at CPA would be

$$x^i_{z,t+\tau^{ik}_{h,t}} = x^i_{z,t} + 5 \cdot v^i_{z,t} + t_s \cdot \Delta^i_t + \frac{1}{2} \cdot t_C \cdot \left(\Delta^i_t + v^i_{z,t}\right),$$

Eq. 6-33

with the target rate $\Delta^i_t = -s^i_t \cdot VSL$ and t_C from Eq. 6-16 using a rate change $\dot{v}^i = 8ft/s^2$, and the time of constant target rate t_s according Eq. 6-17.

The projected altitude separation at CPA in this case would be [95]:

$$x^{ik}_{z,t+\tau^{ik}_{h,t}} = \left(x^i_{z,t+\tau^{ik}_{h,t}} - x^k_{z,t}\right) - v^k_{z,t} \cdot \tau^{ik}_{h,t}\,.$$

Eq. 6-34

The VSL would be accepted, if [95]

$$\left[s^i_t = 1 \wedge x^{ik}_{z,t+\tau^{ik}_{h,t}} < ALIM + A_{mod}\right] \vee \left[s^i_t = -1 \wedge x^{ik}_{z,t+\tau^{ik}_{h,t}} > -ALIM - A_{mod}\right],$$

Eq. 6-35

with $A_{mod} = 75\,feet$, if the VSL is higher than 0, and $A_{mod} = 0\,feet$, if the VSL is 0. This modification enables a higher buffer whenever a Vertical Speed Limit higher than 0 is used, i.e. the use of higher VSLs is more restrictive.

If the condition of Eq. 6-35 fails for all VSLs, a VSL 0 can still be used, if the intruder is TCAS equipped, and the following conditions are fulfilled: The own absolute vertical rate is greater than 1000 feet per minute, the intruder's absolute vertical rate is less than 1000 feet per minute, the vertical rate of the own aircraft is opposite to the intruder's vertical rate. Furthermore, the sense of the RA is not in crossing direction and the vertical separation, which would be achieved, if both aircraft would level off, is greater than 800 feet. This condition is called *TCAS_TCAS_Level-Off* [95] and biases the TCAS RA towards a Level Off-RA, if the own aircraft climbs or descends towards a (near) level-flying intruder with high vertical rate:

$$\begin{gathered}\left(\left|v_{z,t}^{i}\right| > 1000\,ft/min\right) \wedge \left(\left|v_{z,t}^{k}\right| < 1000\,ft/min\right) \wedge \\ \left[\operatorname{sgn}\left(v_{z,t}^{i}\right) \neq \operatorname{sgn}\left(x_{z,t}^{ik}\right)\right] \wedge \\ \left[\left(s_t^i = 1 \wedge x_{z,t}^{i} \leq -100\,ft\right) \vee \left(s_t^i = -1 \wedge x_{z,t}^{i} \geq 100\,ft\right)\right] \wedge \\ \left(\left|x_{z,t+LO}^{i} - x_{z,t+LO}^{k}\right| > 800\,ft\right), \end{gathered} \qquad \textbf{Eq. 6-36}$$

with $x_{z,t+LO}^{i}$ according Eq. 6-23 and $x_{z,t+LO}^{k}$ according Eq. 6-23, if the intruder is approaching the own altitude, i.e. $\operatorname{sgn}(v_{z,t}^{k}) = \operatorname{sgn}(x_{z,t}^{ik})$. Otherwise, the current altitude of the intruder is used for $x_{z,t+LO}^{k}$, i.e. $x_{z,t+LO}^{k} = x_{z,t}^{k}$.

In general, VLS RAs are also called Negative RAs. Even though they are sometimes corrective, it still means a correction of the vertical trajectory toward a weaker vertical rate, whereas Positive RAs are in most cases a correction towards higher vertical rates, either upwards or downwards.

For each sense, 4 different VSLs are available. The available VSLs are 2000, 1000, 500 and 0. For sense $s_t^i = -1$, VSL means a climb limit to either maximum 2000 feet per minute, 1000 feet per minute, 500 feet per minute or 0 feet per minute (i.e. level flight). For sense $s_t^i = 1$, a descent limit is generated to either -2000 feet per minute, -1000 feet per minute, -500 feet per minute or 0 feet per minute (i.e. level flight), respectively.

While in TCAS Version 7.0 all 4 VSLs could also be corrective ("Adjust Vertical Speed"), in Version 7.1 only the VSL 0 is used in case a corrective RA is required ("Level Off"), all other VSLs are only possible for preventive RAs. Even though, the vertical rate reduction to 0 feet per minute is sometimes stronger than required, this change was implemented due to misinterpretation of "Adjust Vertical Speed" in the past [102], with "Level Off" being a more intuitive advisory for the pilot [84]. Hence, if the current vertical rate is not within the target rate, i.e. Eq. 6-32 is not fulfilled, the VSL is defined to be VSL 0, as long as either Equation 6-35 or 6-36 are fulfilled for VSL 0.

To enable a numerical processing of the RA type T^i within the presented model in chapter 6.5, the different RA types have been coded according Table 6-4. Down-sense RAs are coded negative, while up-sense RAs are positive numbers. Some of the numbers are also acting as a flag, i.e. "Maintain Vertical Speed" is a 3-digit number, a crossing RA is indicated by a 5-digit number, and a reversal RA is indicated by a 4-digit number.

Table 6-4 Different TCAS RA types for Climb- and Descent-Sense, respectively, and their associated vertical rates and values for T, source: own research

TCAS RA type (Up-sense)	**RA type T^i**	**TCAS RA type (Down-sense)**	**RA type T^i**		
No RA	0	No RA	0		
Monitor V/S max. -2000 feet/min	+4	Monitor V/S max. 2000 feet/min	-4	**Negative (VSL)**	**Preventive (VSL)**
Monitor V/S max. -1000 feet/min	+3	Monitor V/S max. 1000 feet/min	-3		
Monitor V/S max. -500 feet/min	+2	Monitor V/S max. 500 feet/min	-2		
Monitor V/S max. 0 feet/min	+1	Monitor V/S max. 0 feet/min	-1		
Level Off max. 0 feet/min	+11	Level Off max. 0 feet/min	-11		**Corrective**
Climb 1500 feet/min	+20	Descent -1500 feet/min	-20	**Positive**	
Maintain V/S 1500 to 4400 feet/min	+120	Maintain V/S -1500 to -4400 feet/min	-120		
Crossing Climb 1500 feet/min	+10020	Crossing Climb -1500 feet/min	-10020		
Crossing Maintain 1500 to 4400 feet/min	+10120	Crossing Maintain -1500 to -4400 feet/min	-10120		
Climb Now 1500 feet/min	+1020	Descent Now -1500 feet/min	-1020		
Increase Climb 2500 feet/min	+30	Increase Descent -2500 feet/min	-30		

For some calculations in chapter 6.5, the flags of T^i have to be eliminated, leading to the modified RA type $T^i_{m,t}$:

$$T^i_{m,t} = T^i_t \bmod 100\,. \qquad \textbf{Eq. 6-37}$$

In general, if $|T| \geq 20$, the RA is positive, and if $|T| < 20$, the RA is negative. Moreover, if $|T| < 10$, the RA is preventive.

For preventive RAs, the area of vertical rates beyond the limit rate is displayed as a red area in the VSI display. The red area is an avoidance zone, and sometimes in theory, the aircraft could deviate from the current vertical trajectory towards the intruder without penetrating this area. The aural warning is for all preventive RAs "Monitor Vertical Speed", irrespective of the displayed vertical rate limit.

Figure 6-11 shows an example. It is assumed, that the own aircraft is flying level at an altitude of 4000 feet, and the intruder aircraft is crossing 500 feet above, also flying level. The resulted Sensitivity Level is therefore SL 4 (compare Table 6-1). Both the actual altitude difference as well as the projected altitude difference are below the vertical threshold value $ZTHR$ of 600 feet, so according Eq. 6-7 and Eq. 6-8, an RA will be triggered.

The down-sense is determined for the RA, i.e. $s_t^i = -1$ according Eq. 6-26. According to Eq. 6-28 to Eq. 6-30, a Vertical Speed Limit can be considered. The projected altitudes for the different VSLs at CPA can be seen in Figure 6-11 and Table 6-5.

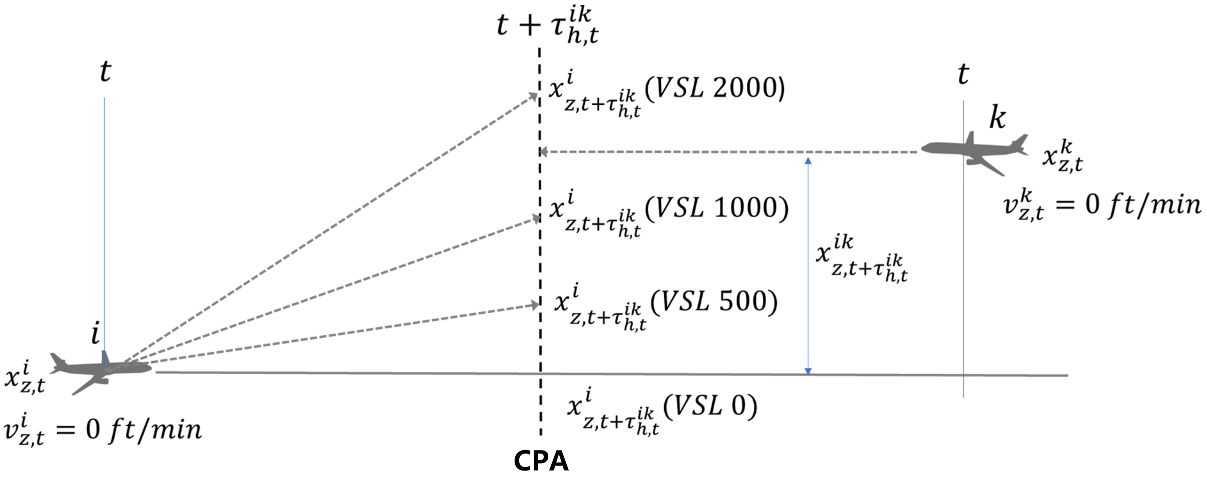
$t + \tau_{h,t}^{ik}$
t
$x_{z,t+\tau_{h,t}^{ik}}^{i}$ $(VSL\ 2000)$
t
k
$x_{z,t}^{k}$
$v_{z,t}^{k} = 0\ ft/min$
$x_{z,t+\tau_{h,t}^{ik}}^{i}$ $(VSL\ 1000)$
$x_{z,t+\tau_{h,t}^{ik}}^{ik}$
$x_{z,t+\tau_{h,t}^{ik}}^{i}$ $(VSL\ 500)$
i
$x_{z,t}^{i}$
$v_{z,t}^{i} = 0\ ft/min$
$x_{z,t+\tau_{h,t}^{ik}}^{i}$ $(VSL\ 0)$
CPA

Figure 6-11 Example of the selection of a Vertical Speed Limit (VSL)

The evaluation of the vertical rate limit starts with the least restrictive value, i.e. the highest VSL 2000. Equations 6-32 to 6-35 are used for all VSLs, but both VSLs 2000 and 1000 would not provide enough separation at CPA, so the test is negative. The VSL 2000 could even lead to a crossing encounter in the worst case. A VSL of 1000 would not lead to a crossing, however, the projected altitude of the own aircraft at CPA would be just 167 feet below the intruder's altitude, i.e. the target separation at CPA $ALIM$ would not be reached. The first vertical speed limit that would lead to a vertical separation at CPA which is at least $ALIM$, is a limit of 500 feet per minute. However, as described before, an additional safety margin in vertical separation at CPA of 75 feet is implemented, whenever the VSL is above 0, therefore this limit would not be used for the advisory. Instead, the VSL 0 is the first VSL, which meets all requirements of Equations 6-32 to 6-35 (see Table 6-5). Hence, the type of RA $T^i = -1$ according Table 6-4.

Table 6-5 Example of the selection of a Vertical Speed Limit (VSL)

Vertical Rate Limit	**0 ft/min**	**500 ft/min**	**1000 ft/min**	**2000 ft/min**
Projected altitude of own aircraft i	4000 feet	4167 feet	4333 feet	4667 feet
Projected altitude of intruder aircraft k	4500 feet	4500 feet	4500 feet	4500 feet
Projected vertical separation at CPA	**500 feet**	**333 feet**	**167 feet**	**-167 feet**

If a VSL is not sufficient for the RA, a Positive RA has to be issued. This is also called *Nominal 1500 feet per minute*-RA [95]. It could be either a "Climb"-, "Descent"- or "Maintain Vertical Speed"-RA, depending on the sense and the current vertical rate. The target rate Δ_t^i is evaluated by using Eq. 6-15 for up-sense RAs, and Eq. 6-16 for down-sense RAs, respectively. If Δ_t^i is higher than 1500 feet per minute for up-sense RAs or lower than -1500 feet per minute for down-sense RAs, respectively, the target rate Δ_t^i will be rounded to the nearest 100-feet-per-minute-value.

Hence, in this case the advised rate is approximately the current own vertical rate. However, the maximum absolute value of the advised rate is 4400 feet per minute in each direction, even if the absolute current rate of the own aircraft is higher. This is the design limit of the logic for Positive RAs. On the VSI display, a red area for all vertical speeds below the advised rate will be displayed for the climb sense, or above the advised rate for the descent sense, respectively. The corresponding aural warning is "Maintain Vertical Speed, Maintain", if the altitudes of the own aircraft and the intruder are non-crossing during the encounter ($c^i = 0$), and "Maintain Vertical Speed, Crossing Maintain" else.

If the current vertical rate of the own aircraft is not within the target area yet and the trajectories of the own aircraft and the intruder are non-crossing ($c^i = 0$), the aural warning will be "Climb, climb" or "Descent, descent" for the up-sense or down-sense, respectively. If the current vertical rate of the own aircraft is not within the target area yet and the trajectories of the own aircraft and the intruder are crossing ($c^i = 1$), the aural warning will be "Climb, crossing climb" or "Descent, crossing descent".

In summary, the following assumptions are made for the vertical plane:

- **Both, the current altitude and vertical rate of the intruder are perfectly known and tracked. Hence, no altimetry error is assumed.**
- **If both aircraft are TCAS equipped and select their sense at the same time, it is assumed that the slave aircraft has already received the intent message from the master aircraft, i.e. no tie-break reversal is considered.**
- **Multi-aircraft encounters are not considered.**

6.3.2.3 Modification of the RA

Both TCAS Versions 7.0 and 7.1 have the capability to reverse a TCAS RA in case the projected separation at CPA is not sufficient to prevent a collision.

During an encounter, the projections of the involved aircraft are continuously recalculated on each cycle, and if necessary, the RA will be modified.

The modification can be either strengthening or weakening, depending on the progress of the conflict geometry. Weakening of any RA is handled more restrictive by the logic to achieve sufficient separation at CPA. On the other hand, it is necessary to prevent trajectory changes which could lead to other conflicts. Weakening RAs are not considered within the scope of this thesis.

A reversal RA is the first choice for any modification. However, there is a time threshold to allow the crew to react on the RA, before a Reversal RA can be initiated. During this delay, still other modifications are possible, as described in the following section.

In TCAS Version 7.1, the reversal logic was extended as a result of the midair collision near Ueberlingen in 2002 (see chapter 6.1). This extension is called CP112 Reversal Geometry. For simplification purpose the reversal conditions in the presented model are based on TCAS Version 7.0 only. Especially the CP112 Reversal Geometry is a rather complex algorithm, which consists of 12 pages of code in the TCAS Requirements [95].

Conditions for a Reversal RA

In general, a reversal RA can be issued against both equipped ($m^k > 0$) or non-equipped ($m^k = 0$) intruders. If the intruder is TCAS equipped and has the lower Mode S address, i.e. intruder is master ($m^k = 2$), the RA can only be reversed by the own aircraft, if an intent message u^k with a reversed sense has been received from the intruder aircraft. In this case, the intruder is responsible for a test of the reversal conditions, and the own aircraft will reverse the RA immediately without any further tests.

On the other hand, if the own aircraft has the lower Mode S address, i.e. the own aircraft is master ($m^k = 2$), the reversal logic checks for a certain reversal geometry of the encounter. This reversal geometry has to be observed not only on the current cycle, but also on one of the last two cycles; otherwise, no reversal will be issued.

Against non-equipped intruders, it is sufficient if the reversal geometry is observed on the current cycle only [95].

The reversal geometry condition is fulfilled, if the altitude separation at CPA, which could be achieved with the current RA, falls below the separation minimum $ALIM$, but the separation, which could be achieved with a reversed sense, must be greater than 0 feet. However, several other conditions have to be fulfilled, depending on different parameters, which will be discussed below.

If the RA is positive, i.e. $|T^i| \geq 20$, the altitude separation at CPA, which could be achieved with the current RA is the *Nominal Separation*, which is the difference between a projected trajectory of the own aircraft and the projected intruder altitude at CPA. For the projected intruder altitude $x^k_{t+\tau_{RA}}$, an extrapolation of the current vertical rate v^k_t is used, i.e.

$$x^k_{z,t+\tau^{ik}_{h,t}} = x^k_{z,t} + \tau^{ik}_{h,t} \cdot v^k_{z,t}\,. \qquad \textbf{Eq. 6-38}$$

For the projected altitude of the own aircraft at CPA $x^i_{t+\tau^{ik}_{h,t}}$, three different calculation methods are used, based on the duration the positive RA has been issued already, and the progression of the trajectory of the own aircraft until the current time t.

If the duration of the positive RA is less than 9 seconds and the current trajectory is at or below the nominal trajectory for this RA type (based on the 5 seconds delay and the vertical rate change of 8 feet per seconds squared from the start of the positive RA, followed by a climb with 1500 feet per minute for up-sense or descent with -1500 feet per minute for down-sense, respectively, see grey dotted line in Figure 6-12), the nominal trajectory will be used.

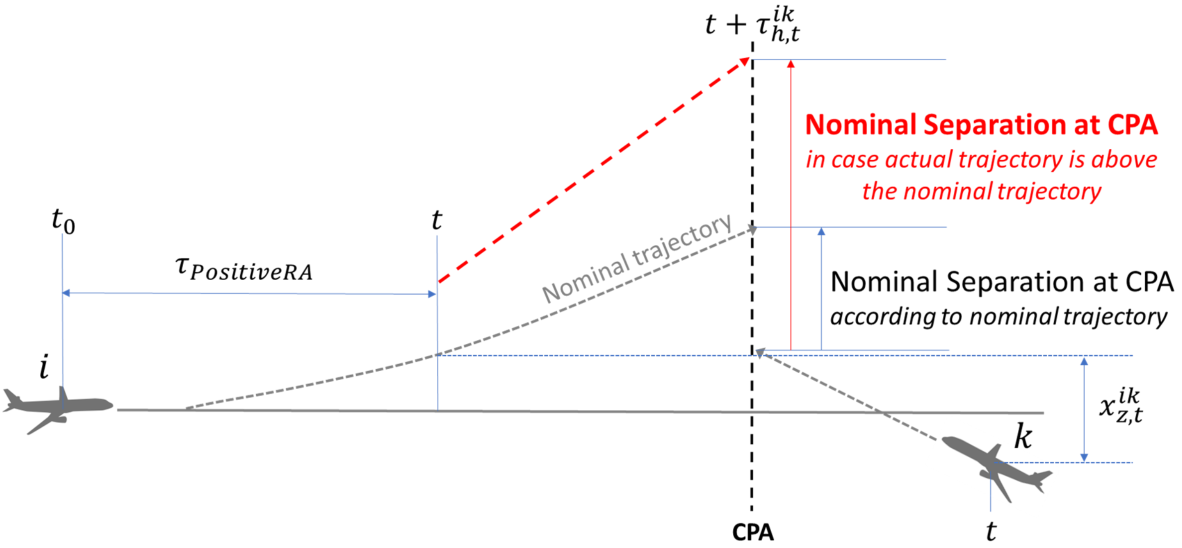
$t + \tau^{ik}_{h,t}$
Nominal Separation at CPA
in case actual trajectory is above the nominal trajectory
t_0
t
$\tau_{PositiveRA}$
Nominal trajectory
Nominal Separation at CPA
according to nominal trajectory
i
k
$x^{ik}_{z,t}$
CPA
t

Figure 6-12 Nominal Separation for compliant response

Otherwise, if the current altitude of the own aircraft is of higher magnitude than the nominal trajectory, this altitude will be used as the starting point for projection with a vertical rate, which is the current vertical rate $v_{z,t}^{i}$, if greater than +1500 feet per minute, but limited to a maximum value of +4400 feet per minute, otherwise a vertical rate of +1500 feet per minute is used according Eq. 6-15 for up-sense RAs. For down-sense RAs, the vertical rate used for the projection is as defined by Eq. 6-16 (see red dotted line in Figure 6-12). In case of a duration of the current positive RA $\tau_{PositiveRA}$ of less than 5 seconds and the vertical rate below the rate used for projection, for the remaining delay time $t_d = \max(5 - \tau_{PositiveRA}, 0)$ the current vertical rate will be used, followed by the duration of rate change according Eq. 6-17 with the average vertical rate during this change.

If the current altitude of the own aircraft is of lower magnitude than the nominal trajectory, this altitude will be used as the starting point for extrapolation with the current vertical rate $v_{z,t}^{i}$, projected to the CPA according Eq. 6-20 (see red dotted line in Figure 6-13).

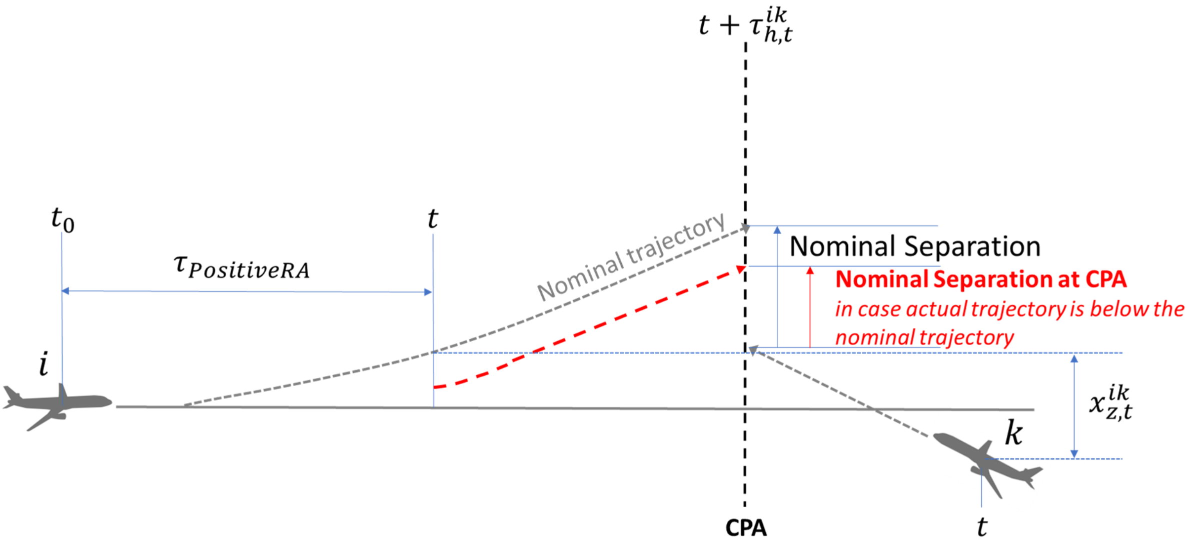

Figure 6-13 Nominal Separation for non-compliant response

The *Nominal Separation* is then calculated according to Eq. 6-21 for "Climb"-RAs, according to Eq. 6-22 for "Descent"-RAs and is considered to be 0 feet for Negative RAs, i.e. $|T^i| < 20$. Only if the *Nominal Separation* is less than $ALIM$, a reversal will be considered [95].

The separation, which could be achieved with a reversed sense being greater than 0 feet, is the second condition which is required for the reversal geometry. The achieved separation is a^i according to Eq. 6-19 for reversals from down-sense RAs, and b^i according to Eq. 6-20 for reversals from up-sense RAs, respectively, with a maximum delay of $t_d = 2.5\ s$ and a vertical rate change $\dot{v}^i = 11.2\ ft/s^2$. The starting point in altitude $x_{z,t}^{i}$ and vertical rate $v_{z,t}^{i}$ for the projection is evaluated in the same way as for the *Nominal Separation*. If the duration of the positive RA is less than 9 seconds and the current trajectory is at or below the nominal trajectory for this RA type, the altitude and vertical rate, which would have been reached during the duration of the RA, when following the nominal trajectory, is used. Otherwise, the current altitude and vertical rate will be used as the starting point.

As mentioned before, additional conditions need to be fulfilled for the reversal geometry, depending on whether or not the RA is in a crossing state. The RA is considered to be in the non-crossing state $c_t^i = 0$, if

$$\left[(T^i > 0) \wedge \left(x_{z,t}^{ik} \geq 100\,ft\right)\right] \vee \left[(T^i < 0) \wedge \left(x_{z,t}^{ik} \leq -100\,ft\right)\right] \vee \left[\tau_{h,t}^{ik} < 4\,s\right]. \tag*{Eq. 6-39}$$

In case the RA is in the non-crossing state, either the aircraft are vertically converging, but are still more than 100 feet separated in altitude, and the remaining time to CPA is less than 4 seconds, i.e.:

$$\left[(T^i > 0) \wedge \left(x_{z,t}^{ik} < -100\,ft\right)\right] \vee \left[(T^i < 0) \wedge \left(x_{z,t}^{ik} > 100\,ft\right)\right] \wedge \left[\tau_{h,t}^{ik} < 4\,s\right], \tag*{Eq. 6-40}$$

or the intruder is not TCAS equipped, and the own aircraft is climbing or descending, but currently in the opposite direction of the advised rate Δ_t^i, the vertical separation, which would be achieved, if the own aircraft would immediately level off (according to Eq. 6-23 and Eq. 6-24 with a delay of $t_d = 0\,s$) would be not positive, and the RA was already in the same sense one cycle before, i.e.:

$$\begin{gathered}\left(\left|v_{z,t}^i\right| > 600\,ft/min\right) \wedge \left(\Delta_t^i \cdot v_{z,t}^i < 0\right) \wedge \\ \left[\left(x_{z,t+LO}^i - x_{z,t+LO}^k\right) \cdot s^i \leq 0\right] \wedge \left(s_t^i = s_{t-1}^i\right),\end{gathered} \tag*{Eq. 6-41}$$

or the intruder is not TCAS equipped, both aircraft are climbing or descending in the same direction with a high vertical rate, the own RA is positive and the vertical rate is in the same direction as the advised rate of the RA, the current vertical separation is more than 100 feet, but not more than 600 feet, and the estimated vertical separation at CPA, assuming that the current vertical rates of both aircraft would not change, is predicted to be less than 100 feet:

$$\begin{gathered}\left(\left|v_{z,t}^i\right| > 1000\,ft/min\right) \wedge \left(\Delta_t^i \cdot v_{z,t}^i > 0\right) \wedge \\ \left(\left|v_{z,t}^k\right| > 1000\,ft/min\right) \wedge \left(v_{z,t}^i \cdot v_{z,t}^k > 0\right) \wedge \\ \left(\left|x_{z,t}^i - x_{z,t}^k\right| > 100\,ft\right) \wedge \left(\left|x_{z,t}^i - x_{z,t}^k\right| \leq 600\,ft\right) \wedge \left(\left|T^i\right| \geq 20\right) \wedge \\ \left[(T^i > 0) \wedge \left(x_{z,t}^{ik} + v_{z,t}^{ik} \cdot \tau_{h,t}^{ik} < 100\,ft\right)\right] \vee \left[(T^i < 0) \wedge \left(x_{z,t}^{ik} + v_{z,t}^{ik} \cdot \tau_{h,t}^{ik} > -100\,ft\right)\right].\end{gathered} \tag*{Eq. 6-42}$$

In case the RA is in the crossing state, the reversal geometry is only fulfilled, if more than 4 seconds remain to CPA and a *crossing reversal geometry* is observed.

For the *crossing reversal geometry*, it is important to distinguish between a crossing situation, where the own aircraft is considered responsible for crossing the intruder's altitude (*own cross*,

$c_t^i = 1$), and a crossing situation, where the intruder is considered responsible for crossing the altitude of the own aircraft (*int cross*, $c_t^i = 2$).

For both crossing situations, the remaining time to CPA must be at least 4 seconds, and the sense of own TCAS RA must point towards the intruder's altitude, but the current vertical separation must be at least 100 feet [95]:

$$\left[(T^i > 0) \wedge \left(x_{z,t}^{ik} \leq -100\,ft\right)\right] \vee \left[(T^i < 0) \wedge \left(x_{z,t}^{ik} \geq 100\,ft\right)\right] \wedge \left[\tau_{h,t}^{ik} \geq 4\,s\right]. \qquad \textbf{Eq. 6-43}$$

Additionally, for the *int cross* situation $c_t^i = 2$, the RA must either be a Negative, or a Positive RA with the intruder not in level flight, and either a "Climb"-RA with the own altitude above the projected intruder's altitude, or a "Descent"-RA with the own altitude below the projected intruder's altitude:

$$\left(|T^i| < 20\right) \vee \left\{\left(|v_{z,t}^k| \geq 600\,ft/min\right) \wedge \begin{bmatrix} T^i = 20 \wedge \left(x_{z,t}^i > x_{z,t}^k + v_{z,t}^k \cdot \tau_{h,t}^{ik}\right) \vee \\ \\ T^i = -20 \wedge \left(x_{z,t}^i < x_{z,t}^k + v_{z,t}^k \cdot \tau_{h,t}^{ik}\right) \end{bmatrix}\right\}. \qquad \textbf{Eq. 6-44}$$

For the own cross situation $c_t^i = 1$, the RA has to be Positive, and either the intruder has to be level, or the RA is not a "Climb"-RA and the own altitude is equal to or above the intruder's projected altitude, or the RA is not a "Descent"-RA and the own altitude is equal to or below the intruder's projected altitude [95]:

$$\left(|T^i| \geq 20\right) \wedge \left\{\left(|v_{z,t}^k| < 600\,ft/min\right) \vee \begin{bmatrix} T^i \neq 20 \wedge \left(x_{z,t}^i \geq x_{z,t}^k + v_{z,t}^k \cdot \tau_{h,t}^{ik}\right) \vee \\ \\ T^i \neq -20 \wedge \left(x_{z,t}^i \leq x_{z,t}^k + v_{z,t}^k \cdot \tau_{h,t}^{ik}\right) \end{bmatrix}\right\}. \qquad \textbf{Eq. 6-45}$$

Once, the *own cross* state is established, the transition to the *int cross* state, i.e. $\left(c_{t-1}^i = 1\right) \wedge \left(c_t^i = 2\right)$, in general requires the same conditions as described above. However, there is a certain hysteresis implemented for both the vertical separation and the time threshold, where the transition might occur latest before CPA, so Eq. 6-43 is modified in this situation as follows [95]:

$$\left[(T^i > 0) \wedge \left(x_{z,t}^{ik} \leq -200\,ft\right)\right] \vee \left[(T^i < 0) \wedge \left(x_{z,t}^{ik} \geq 200\,ft\right)\right] \wedge \left[\tau_{h,t}^{ik} \geq 10\,s\right]. \qquad \textbf{Eq. 6-46}$$

The *crossing reversal geometry* is fulfilled, if the sense of the own RA points towards the intruder's altitude, still separated by a certain crossing threshold c_{thr}, which is greater for encounter situations closer to CPA. The threshold values are [95]:

$$c_{thr} = \begin{cases} 200\,ft, & if\ \tau_{h,t}^{ik} \leq 10\,s \\ \\ 100\,ft, & else. \end{cases} \qquad \textbf{Eq. 6-47}$$

For *int cross* situations, additionally the own altitude must be below the projected altitude of the intruder at CPA for up-sense RAs, and above the projected altitude of the intruder at CPA for down-sense RAs, respectively, i.e.

$$\left(c_t^i = 2\right) \wedge \begin{bmatrix} (T^i > 0) \wedge \left(x_{z,t}^i \le x_{z,t}^k - c_{thr}\right) \wedge \left(x_{z,t}^i < x_{z,t}^k + v_{z,t}^k \cdot \tau_{h,t}^{ik}\right) \vee \\ (T^i < 0) \wedge \left(x_{z,t}^i \ge x_{z,t}^k + c_{thr}\right) \wedge \left(x_{z,t}^i > x_{z,t}^k + v_{z,t}^k \cdot \tau_{h,t}^{ik}\right) \end{bmatrix}. \qquad \textbf{Eq. 6-48}$$

Finally, for *own cross* situations, if the current RA is up-sense, a down maneuver shall provide a vertical separation at CPA, which is by 100 feet greater than for the up maneuver. If the current RA is a down-sense advisory, an up maneuver shall provide a vertical separation at CPA, which is greater by 100 feet than for the down maneuver.

For the evaluation of the vertical separation at CPA for the respective maneuvers, Eq. 6-19 is used with the same parameters as for the evaluation of the initial sense (a delay $t_d = 5\,s$, followed by a vertical rate change $\dot{v}^i = 8\,ft/s^2$, thereafter maintaining the target rate according to Eq. 6-15 or Eq. 6-16, respectively, for the remainder of the encounter). The vertical separation at CPA is then calculated according to Eq. 6-21 for the up maneuver and according to Eq. 6-22 for the down maneuver, respectively. For *own cross* situations, instead of Eq. 6-48, the following condition is used [95]:

$$\left(c_t^i = 1\right) \wedge \begin{bmatrix} (T^i > 0) \wedge \left(x_{z,t}^i \le x_{z,t}^k - c_{thr}\right) \wedge \left(b_t^i > a_t^i + 100\,ft\right) \vee \\ (T^i < 0) \wedge \left(x_{z,t}^i \ge x_{z,t}^k + c_{thr}\right) \wedge \left(a_t^i > b_t^i + 100\,ft\right) \end{bmatrix}. \qquad \textbf{Eq. 6-49}$$

Conditions for an Increase Modification

A modification of the current RA to an Increase RA is only considered for Positive RAs. Reversal of RAs has always priority over any strengthening of RAs, however, sometimes the conditions for reversal RAs are not met, while the conditions for an increase of the current RA are.

An increase of an already issued Positive RA against a TCAS equipped intruder can be initiated after a delay only, depending on the Sensitivity Level, to allow the pilot to follow the advisory first. This delay ranges between 2 and 9 seconds. However, sometimes a Positive RA with an advised rate of 1500 feet per minute is not capable of solving a conflict geometry, and Increase RAs are not available during the initial strength selection. An Increase RA can only be issued, if the RA in the previous cycle was also a Positive RA with the same sense, and the current vertical rate as well as the advised rate is not exceeding the Increase rate [95]:

$$\left(\operatorname{sgn}\left(T_t^i\right) = \operatorname{sgn}\left(T_{t-1}^i\right)\right) \wedge \left(\left|T_t^i\right| \ge 20\right) \wedge$$

$$\begin{bmatrix} (T^i > 0) \wedge \left(v_{z,t}^i \le 2500\,ft/min\right) \wedge \left(\Delta_t^i \le 2500\,ft/min\right) \vee \\ (T^i < 0) \wedge \left(v_{z,t}^i \ge -2500\,ft/min\right) \wedge \left(\Delta_t^i \ge -2500\,ft/min\right) \end{bmatrix}. \qquad \textbf{Eq. 6-50}$$

Depending on the geometry of the encounter and whether the intruder is TCAS equipped or not, the interval in which an Increase RA can be issued, may vary. If the encounter is crossing and the intruder is not equipped, an Increase RA is only possible between 10 and more than 4 seconds before CPA. Provided the conditions for the reversal of the RA have not been fulfilled yet, the RA would change to an Increase RA, if the current altitude of own aircraft would be within 200 feet of the projected intruder's altitude at CPA, i.e.

$$\left(c_t^i > 0 \wedge m^k = 0 \wedge \tau_{h,t}^{ik} > 4\,s \wedge \tau_{h,t}^{ik} \leq 10\,s\right) \wedge$$
$$\left\{\begin{matrix} \left[(T^i > 0) \wedge \left(0\,ft \leq x_{z,t}^i - x_{z,t}^k - v_{z,t}^k \cdot \tau_{h,t}^{ik} \leq 200\,ft\right)\right] \vee \\ \left[(T^i < 0) \wedge \left(-200\,ft \leq x_{z,t}^i - x_{z,t}^k - v_{z,t}^k \cdot \tau_{h,t}^{ik} \leq 0\,ft\right)\right] \end{matrix}\right\}. \qquad \textbf{Eq. 6-51}$$

Otherwise, if either the encounter is non-crossing or the intruder is TCAS equipped, the Increase RA can be issued between a time threshold $INCR\_THR$ according Table 6-6, which depends on the Sensibility Level, and 6 seconds from CPA, which is the latest point the RA could be modified to an Increase RA in this case. Additionally, the separation, which can be achieved at CPA with the current RA, is projected to be less than 200 feet vertically. This separation $x_{z,t+\tau_{h,t}^{ik}}^{ik}$ is evaluated in the same way as described in the previous section for the *Nominal Separation* [95]:

$$\left\{\begin{matrix} \left[\left(c_t^i = 0 \vee m^k > 0\right) \wedge \tau_{h,t}^{ik} \geq 6\,s \wedge \tau_{h,t}^{ik} \leq INCR\_THR\right] \wedge \\ x_{z,t+\tau_{h,t}^{ik}}^{ik} < 200\,ft \end{matrix}\right\}. \qquad \textbf{Eq. 6-52}$$

Table 6-6 Time threshold for Increase RAs [103]

Sensitivity Level (SL)	**3**	**4**	**5**	**6**	**7**
INCR_THR (s)	13	18	20	24	26

Conditions for a Strengthening of Negative RAs

If during the encounter on any cycle the conditions for a Vertical Speed Limit according to Eq. 6-28 to Eq. 6-36 are not fulfilled anymore, the RA has to be strengthened to a Positive RA. However, this is only allowed up to a point which is more than 2.5 seconds before the CPA [95].

Weakening RAs and Clear of Conflict

Weakening RAs are an important element of the TCAS logic, as they prevent further traffic conflicts due to the limitation of the deviation of the cleared altitude. Weakening RAs are delayed to ensure that enough separation has been achieved. For the current encounter they indicate whether the separation is sufficient, and therefore, the risk of collision is at an acceptable level.

Whether the required separation has been achieved before CPA or not, the RA will not be cancelled before the horizontal trajectories are still converging towards each other, i.e. the RA will not be cancelled before the CPA. However, if a horizontal maneuver during the encounter leads to diverging trajectories, the RA will be cancelled, as no CPA exists anymore. Cancellation of the RA is announced by "Clear of conflict", and the display of the alert will be cancelled.

In summary, the following assumptions are made for the modification of RAs:

- **The reversal logic is based on TCAS Version 7.0, the CP112 feature is not considered in the presented model**
- **Weakening RAs are not considered**
- **Horizontally diverging trajectories before the CPA are not considered**

6.4 Pilot Model

The pilot model, which models the pilot response to the Resolution Advisory, is the other element to determine the environmental conditions. The pilot response influences the achieved separation at CPA significantly. Even the most advanced algorithms cannot prevent a midair collision completely, if the pilot does not respond in accordance with the trajectory which is expected by the system logic.

The expected response, also called the 'standard' pilot response, is used for the trajectory projection by the collision avoidance logic of TCAS for the selection of the respective advisory sense and strength. For initial TCAS RAs, a short delay of 5 seconds followed by a trajectory change with a change in vertical speed by 480 feet per minute each second (8 feet per second squared, this equals approximately 0.25 g) towards the target vertical rate is assumed. Once this target vertical rate is established, it has to be maintained until either the termination of the RA, or any modification of the RA [95].

If a sense reversal or strengthening RA is issued, the expected delay is shorter, and the trajectory change is more severe. In this case, the delay is reduced to a value of 2.5 seconds, and the change in vertical rate is increased to a value of 672 feet per minute each second (11.2 feet per second squared), which equals a vertical acceleration of approximately 0.35 g's. Prompt and accurate compliance with the advised rates is expected from the pilots in all airspaces and all phases of flight [100].

However, several studies showed a deviation from the 'standard' pilot response in actual TCAS RA maneuvers within the real air traffic environment [87,102]. Besides events, where pilots did not follow the advisory at all, a great variety of responses has been observed.

In order to evaluate the risk level of a certain TCAS event, both, the pilot responses of the intruder aircraft as well as the own aircraft (in case of a modified RA), have to be modelled. This modelled response can be derived from actual pilot response in real air traffic environment. Otherwise, if the 'standard' pilot response would be assumed, the resulting risk level by the model would differ from the actual risk level. However, modelling of the response to the initial

RA of the own aircraft is not required, as the actual response can be derived from the flight data directly, as this data is available in Flight Data Analysis.

A detailed pilot response model has been developed during the Eurocontrol ACAS Safety Analysis post-RVSM Project (ASARP), a study commissioned by EUROCONTROL to investigate the safety of ACAS, before introduction of RVSM in Europe [87]. For the evaluation of this model, also called ASARP 'typical pilot' model, on-board recorded flight data of several contributing European airlines has been analyzed through a period from 2001 to 2004. In total, 80 corrective RAs have been analyzed. To enable a comparison with the 'standard' pilot response, the actual responses have been quantified in terms of:

- Delay between the issuance of the RA and start of the maneuver,
- Vertical acceleration used to change the trajectory towards the target vertical rate,
- Vertical speed achieved by the maneuver.

Based on the conducted flight data analysis, 33 different combinations of several elementary pilot responses could be identified, including a portion of 10 percent of non-responding pilots [87]. These pilot responses combine four different typical pilot reaction times between 3 and 8 seconds with four different typical vertical rates in response to Positive RAs, ranging from 730 feet per minute up to 3900 feet per minute, and four different vertical accelerations ranging from 0.09 g to 0.30 g. The focus of the analysis was on corrective RAs, i.e. Positive RAs ("Climb" and "Descent") as well as Negative RAs ("Adjust Vertical Speed", which was the predecessor of "Level-off"). 10 percent of the analyzed responses referred to Preventive RAs, where in all cases pilots did react as expected, i.e. disengaged the autopilot, but did not deviate in response to the RA [104]. Within this analysis, no inappropriate reactions were observed in the case of a Positive RA, i.e. aircraft climbing instead of descending, and only few inappropriate reactions were identified in case of Negative corrective RAs, which lasted only a few seconds and were corrected by the pilots thereafter.

Above model was refined during the Safety Issue Rectification studies (SIR, SIRE and SIRE+), which had been commissioned by EUROCONTROL as a follow-up project in order to improve the TCAS safety performance [102]. Two major changes were implemented in this enhanced model: First, the proportion of non-responding pilots was increased to a value of 20 percent. Second, opposite pilot reactions were incorporated, which had not been considered in the former model [102]. In a few percent of cases, commercial airline monitoring had identified opposite responses in the aftermath of the first study. To reflect this behavior, the recent 'typical pilot' response model includes a 2 percent proportion of opposite reactions to initial RAs. According to an email conversation with the authors of the study, this is modelled by using the complementary value (i.e. negative value) of the respective vertical speed with the same amount of delay and vertical acceleration [102,105]. The resulting distribution can be seen in Figure 6-14, and forms the basis of the pilot response model used within this thesis.

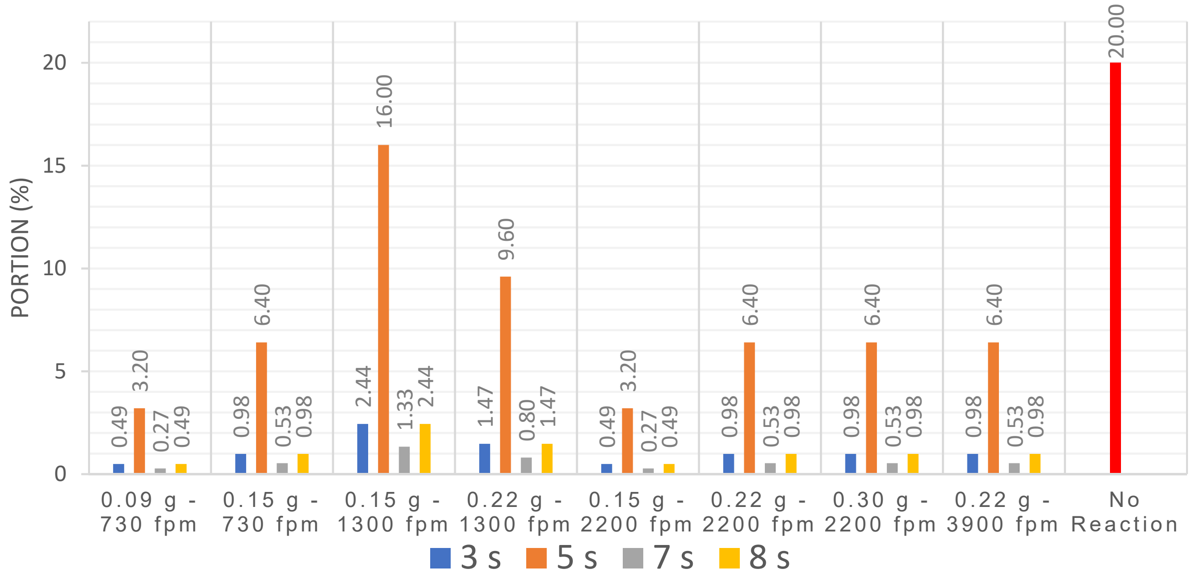

Figure 6-14 'Typical pilot' responses gathered during the ASARP project in 2001, 2002 and 2004, enhanced in 2008 during the SIRE+ study [87,102]**. Additionally, there is a 2 percent-chance, that the response is opposite to the advised rate**

As mentioned before, the vertical rates of the different pilot responses refer to a Positive RA, i.e. "Climb" or "Descent", where the absolute target vertical rate is 1500 feet per minute. The highest probability (16 percent) was observed for the combination 5 seconds delay, followed by a trajectory change with a vertical acceleration of 0.15 g, and continued with a vertical rate of 1300 feet per minute, which is very close to the 'standard' pilot response, but slightly weaker.

According to the conversation with the authors of this study, in case of a Negative Corrective RA the pilot response is identically distributed as for Positive RAs in terms of delay and acceleration, thus only the vertical rate differs [105]. To reflect the same behavior during Negative Corrective RAs as for Positive RAs, within the scope of the risk model in this thesis, the vertical rate for Negative Corrective RAs is modelled with a comparable proportion of trajectory change as used for Positive RAs. E.g., an actual vertical rate of 730 feet per minute during a "Climb"-RA equals a compliance proportion of $730fpm/1500fpm = 0.49$. Using the same compliance proportion during a Negative RA, where the aircraft shall level off during a climb maneuver of e.g. initially 2000 feet per minute, the resulting vertical rate during the maneuver would be $(1 - 0.49) \cdot 2000fpm = 1020fpm$. Thus, in general, the different vertical rates in Figure 6-14 are converted into the target rate during a Negative RA in the following way:

$$v_{s\_n} = \left(1 - \frac{v_{s\_p}}{1500ft/min}\right) \cdot v_{z,0}\,, \qquad \textbf{Eq. 6-53}$$

with v_{s_n} being the target vertical rate during the Negative Correcting RA, v_{s_p} being the vertical rate from Figure 6-14 for the respective response type, and $v_{z,0}$ being the vertical rate at start of the RA.

Besides during the Negative Corrective RAs, flight data also show weak or even opposite reactions during Positive RAs, where the target vertical rate is already achieved at the start of the RA, i.e. "Maintain Vertical Speed"-RAs, see also chapter 6.3, *initial strength selection*. To reflect this behavior, the different vertical rates shown in Figure 6-14 can also be adapted to this kind of RAs in the following way:

$$v_{s\_m} = \left(\frac{v_{s\_p}}{1500ft/min}\right) \cdot v_{z,0}\ , \qquad \textbf{Eq. 6-54}$$

with v_{s_m} being the target vertical rate during the "Maintain Vertical Speed"-RA.

The above pilot response model applies to the initial response to RAs. For responses to any subsequent RAs, a significant trend could not be identified during the studies, since the number of RAs was not significant enough and the pilot reactions varied considerably [87]. However, since all types ranging from aggressive, weak to even opposite reactions can be observed in flight data during subsequent RAs, the above pilot response model will also be applied to these RAs in the same manner as to initial RAs.

Moreover, since the required acceleration during trajectory change for strengthening and reversal RAs is higher than for initial Positive RAs, it is assumed that the pilot response is stronger in the same proportion as the required vertical accelerations between increase or reversal RA in relation to initial Positive RAs, i.e. a proportion of $\frac{0.35g}{0.25g} = 1.4$. The same applies to the target vertical rate during strengthening RAs, which is higher than the target vertical rate during initial Positive RAs with the proportion of $\frac{2500ft/min}{1500ft/min} = 1.67$. In this case, all vertical accelerations and vertical rates from Figure 6-14 will be adapted accordingly within the pilot response model of this thesis.

To verify whether the 'typical pilot' response model reflects the behavior of a wide range of participants, the model can be compared with data from a different source, e.g. by means of radar data. From March to November 2009, radar data from 16 radar stations within the UK and France was collected and analyzed by EUROCONTROL with the purpose of analyzing RA downlink data. The radar data covered also parts of other countries, e.g. Germany, Italy, Spain, Belgium, Netherlands and Luxembourg. Hence, the gathered data represents vital parts of the central European airspace. Approximately 3.4 Million hours of flight data has been collected, with a total of 1268 contained RAs, from which approximately 396 RAs were corrective RAs [106].

As Eurocontrol conducted a detailed analysis of the responses to the RAs, this data can be used to validate the ASARP 'typical pilot' response model. When compared to the analysis of on-board data, the RA downlink data is missing some details regarding specific type of RA, especially the advised rate of negative RAs. At the time of the data collection, TCAS version 7.0 was still in use, which provided four different target rates for negative RAs, and which have not been broadcasted via the RA downlink. Hence, an analysis for the response of this type of RA is not possible in detail and therefore the results are comparable only in a qualitative way.

When focusing on positive RAs only, the results can be compared with the ASARP 'typical pilot' response model. However, the classification definition within the RA downlink analysis is slightly different. EUROCONTROL distinguishes in this analysis 3 different reactions of RA responses: Weak, complied and over reaction. In case the RA was not followed correctly, the reaction was classified as either no reaction or even opposite reaction.

In this classification, a 'complied' response is being considered for vertical rates between 750 feet per minute and 2500 feet per minute, while a 'weak reaction' is being considered, if the vertical rate is below 750 feet per minute, and an 'over reaction' is being considered, if the vertical rate is greater than 2500 feet per minute. Additionally, if the current vertical rate is being maintained (e.g. continues to descend with a "Climb"-RA), the reaction is considered to be a 'no reaction'. Finally, the reaction is considered to be an 'opposite reaction', if the vertical rate was changed in the wrong sense.

As a result, which can be seen in Table 6-7, the proportions of the ASARP 'typical pilot' response are within a comparable range with the Eurocontrol monitoring data.

Table 6-7 Comparison between the pilot response of ASARP model [87,102] **and observed response (Eurocontrol RA monitoring data)** [106]

Target vertical rate acc. ASARP [87,102]	**Reaction type acc. RA monitoring** [106]	**ASARP 'typical pilot' response model** [87,102]	**RA monitoring** [106]
730 ft/min	Weak reaction	13.3 %	7.8 %
1300 ft/min – 2200 ft/min	Complied	57.8 %	58.6 %
3900 ft/min	Over reaction	8.9 %	11.9 %
No reaction	No Reaction	20.0 %	18.7 %
Opposite reaction	Opposite reaction	2.0 %	3.0 %

6.5 Combined Risk Model of TCAS

Both, the TCAS system model as well as the pilot model, which have been described in the previous sections, are components of the environmental conditions of the risk model. In this chapter, the environmental conditions will be combined with the aircraft state in order to obtain the combined risk model of a TCAS induced midair collision.

The aim of the TCAS risk model is to evaluate the event severity of a particular TCAS RA event, which has been observed in Flight Data Analysis. The risk of such an event is significantly influenced by the pilot responses in the vertical plane. The overall risk within an organization regarding TCAS is significantly influenced by the initial reactions of its own crews. This initial reaction represents the aircraft state and can be derived from the flight data. The resulting event risk levels of each FDA event combined with the frequency of such events will eventually provide the overall risk level of TCAS induced collisions.

The TCAS risk model in a first step evaluates the collision probability in the vertical plane. This step represents the main part of the combined model. This probability will then be combined with the collision probability in the horizontal plane in a second step, which is solely based on a distribution observed by radar data. As those aspects are airline independent, the risk levels of the various TCAS events for a particular airline mainly differ due to the different pilot responses of the own aircraft in the vertical plane.

The vertical collision probability is evaluated by means of a Monte Carlo method, which in a first step determines possible initial intruder data vectors by means of the TCAS system model and the pilot model for the intruder aircraft.

The initial intruder data vectors represent the environmental conditions. They are generated randomly and consist of initial relative altitude and vertical rate of the intruder. Further information about whether the intruder is TCAS equipped and the respective Mode S address of the intruder's transponder will be added to this intruder data vector, as this data also influences the risk level of the event. Also, the type of pilot response of the intruder aircraft is part of this data vector.

Only those initial intruder data vectors will be considered, which would lead to a TCAS alert of the same type as the observed TCAS RA with regard to the own aircraft position and the alert thresholds of the Collision Avoidance logic. If due to a certain encounter geometry an RA would be generated by the intruder first, the issuance of a TCAS RA on the own aircraft depends mainly on the pilot reaction of the intruder aircraft to its issued RA. Thus, for a certain initial encounter geometry, a TCAS RA might or might not be generated for the own aircraft, depending on the pilot response of the intruder aircraft on its RA.

A defined number of such randomly generated intruder data vectors will then be combined with the aircraft state, i.e. the trajectory of the own aircraft, as observed in flight data, to evaluate the collision probability.

6.5.1 Encounter Model

A special feature of the aircraft state with regard to the discussed risk category is the fact that the aircraft state can change during the development of the encounter. This change might also have an influence on the environmental conditions in terms of a possible modification of the RA. Therefore, it is not sufficient to consider only a single moment in time within the encounter. Rather, a simulation of the development of the vertical encounter geometry must be conducted over the entire period of the TCAS RA.

Figure 6-15 shows the general methodology. Several combinations of initial intruder data are generated randomly, until TCAS would generate a TCAS RA T^i for the own aircraft, which is equal to the TCAS RA type T^u of the FDA event. The generated vector of initial intruder data is therefore one possible combination, which could have caused the TCAS RA T^i of the own aircraft. This sub-process is called *Threat Detection* in Figure 6-15.

Once a valid combination has been found, the trajectories of both intruder and the own aircraft are modelled through the whole duration of the encounter until the termination of the RA at CPA. This is conducted by using the initial pilot response measured from flight data for the own aircraft, and a modelled trajectory for the intruder aircraft, based on the randomly selected pilot response from the pilot model. Based on these vertical trajectories, the development of the encounter geometry is evaluated for each cycle until CPA. If the modification part of the collision avoidance logic, as described in chapter 6.3, requires a modification of the RA during the simulation per simulated system logic, the initial RA type of either the own aircraft, T^i, or of the intruder aircraft, T^k, is modified. In this case, the respective trajectory has to be adapted accordingly. This will be done with the same pilot response as used for the initial response for the intruder aircraft, and a randomly selected pilot response from the pilot model for the own aircraft.

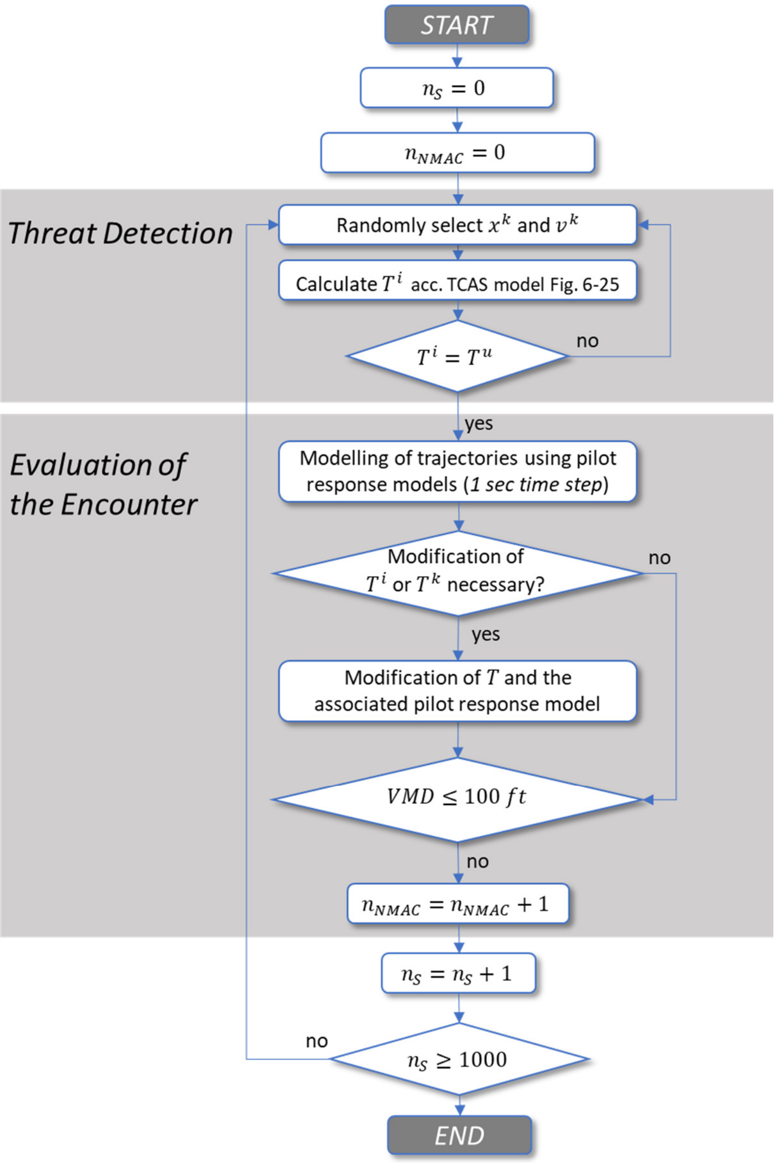
START
$n_S = 0$
$n_{NMAC} = 0$
Threat Detection
Randomly select x^k and v^k
Calculate T^i acc. TCAS model Fig. 6-25
$T^i = T^u$
no
yes
Evaluation of the Encounter
Modelling of trajectories using pilot response models (1 sec time step)
Modification of T^i or T^k necessary?
no
yes
Modification of T and the associated pilot response model
$VMD \leq 100\,ft$
no
$n_{NMAC} = n_{NMAC} + 1$
$n_S = n_S + 1$
no
$n_S \geq 1000$
END

Figure 6-15 General methodology of the simulation

In the last step of the method, the projected vertical miss distance at the end of each simulation has to be calculated at CPA. If it falls below the vertical threshold of a near midair collision, i.e. 100 feet vertically, the respective counter for the expected number of vertical NMACs, n_{NMAC}, is increased.

The above procedure will be repeated until a significant number of simulations n_S (here $n_s = 1000$) has been processed. The number of vertical NMACs n_{NMAC}, divided by the overall number of simulations, provides an adequate estimation of the probability of a near midair collision in the vertical plane, provided the number of simulations is high enough:

$$p\left(NMAC_z | T^i = T^u, P, X, V\right) = \lim_{n_S \to \infty} \frac{n_{NMAC}}{n_S}. \qquad \textbf{Eq. 6-55}$$

The resulting probability is a conditional probability of a vertical NMAC for a certain type of RA T^u. It depends on both, the pilot response model P as well as the used distributions of the values of each intruder vector, i.e. the relative altitudes X and vertical rates V between both aircraft as well as whether or not the intruder is TCAS equipped.

The variety of possible relative altitudes, vertical rates and, as a consequence, different RA types generated for the intruder is the basis of the risk model. These initial conditions at the start of the encounter, combined with the pilot reaction, form the variations of the environmental conditions as described in chapter 2.6.1. The variation of the environmental conditions will potentially lead to the midair collision. This variation covers all possible intruder scenarios which could have been encountered during the observed type of RA on the own aircraft. The combination of virtually all possible scenarios, combined with the pilot response model for the intruder aircraft, and the observed trajectory of the own aircraft, will finally provide the NMAC-probability in the vertical plane for the respective scenario. In other words, the risk model evaluates how likely a collision might be, if a similar event would reoccur in the future under slightly different environmental conditions.

One feature of the TCAS design makes the development of an adequate risk model extremely difficult: The possibility of a delayed alert threshold of the RA of one or both of the involved aircraft, which depends on the vertical rate of the respective aircraft. This might generate a TCAS RA on the aircraft with a higher vertical rate first. The pilot reaction on this RA has an influence on whether a TCAS RA will be issued for the other aircraft at all. The reaction might otherwise lead to a delayed RA for the other aircraft and influences the type of this RA.

Thus, the presented model incorporates **four different scenarios**, which are possible in a TCAS encounter:

Scenario 1: The intruder's RA will be issued first, and it will only be taken into consideration, if the modelled pilot response will lead to the issuance of an own RA equivalent to the RA type of the FDA event.

Scenario 2: The intruder's RA and the own RA will be issued at the same time. However, in this case the master aircraft will rule the sense of the RA and has to be evaluated first, as it will influence the RA of the other aircraft.

Scenario 3: The intruder's RA will be issued after the own RA.

Scenario 4: For the intruder, no RA will be issued at all, either, because the intruder is unequipped, or because the pilot of the own aircraft reacted efficiently enough on the issued RA to prevent the generation of a TCAS RA on the intruder aircraft.

In this context, it is important to discuss the possible time thresholds τ_{RA}, where the TCAS alert is generated. In an ideal encounter, this time threshold will be equal to a nominal alert threshold at TAU or $TVTHR$ before the CPA, respectively. However, horizontal trajectory changes can influence the intruder geometry and suddenly fulfill the threat conditions which might not have been fulfilled before due to either diverging trajectories or a horizontal projection being outside of the boundaries of the HMD filter. These accelerated horizontal trajectories might result in a reduced alert threshold below the nominal alert thresholds.

This also applies to the vertical plane, where a threat might have been suppressed by the *altitude separation test* well within the nominal alert thresholds TAU or even $TVTHR$. Due to continuing altitude convergence, the *altitude separation test* suddenly fails, and a TCAS RA is generated. In both cases described above, the warning time will be less than usual, and thus, the risk may increase due to a shorter available maneuver interval.

Thus, in general, the time to CPA at the start of the RA, τ_{RA}, can vary from a few seconds up to a maximum value of TAU, which is the earliest possibility for an RA to be issued.

Assuming an ideal encounter at the same Sensitivity Level, a different starting point of the respective RA at the nominal alert threshold would only be possible if one aircraft generates its RA at TAU, and the other aircraft generates its RA at its delayed threshold $TVTHR$ before CPA. Since the majority of encounters are expected to be close to an ideal encounter, the distribution of the time to CPA, τ_{RA}, should aggregate around those nominal alert thresholds, while other trigger points besides these prominent thresholds are expected to be observed more rarely. An analysis of flight data from actual TCAS encounters shows that approximately 95 percent of all encounters can be considered to be ideal. Thus, it is assumed that 95 percent of all aircraft generate their RA at one of the two possible nominal thresholds.

In **scenario 1**, where the intruder generates an RA earlier than the own aircraft, in the ideal encounter the nominal threshold for the intruder would be at TAU. Thus, according to the mentioned circumstances, the probability of the intruder's time threshold τ_{RA}^{k} at TAU is considered to be 0.95. In all other cases, τ_{RA} is equally distributed at lower values down to a minimum time threshold of min_thr, which is considered at 15 seconds. This minimum time threshold is incorporated in the model, since conflicts closer to the CPA are difficult to process and therefore are not considered. As in the first scenario the starting point of the intruder's RA has to be earlier than that of the own aircraft, the lower threshold for the intruder aircraft is at one cycle before min_thr. This schematic can be seen in Figure 6-16.

For the own aircraft, in this scenario the nominal trigger threshold would be at the delayed threshold $TVTHR$. For this reason, the majority of the alert thresholds of the own aircraft, τ_{RA}^{i}, are expected to accumulate around the value of $TVTHR$ with a probability of 0.95, while the rest ranges equally distributed between the lower value of TAU^{i} and $(TAU^{k} - 1)$.

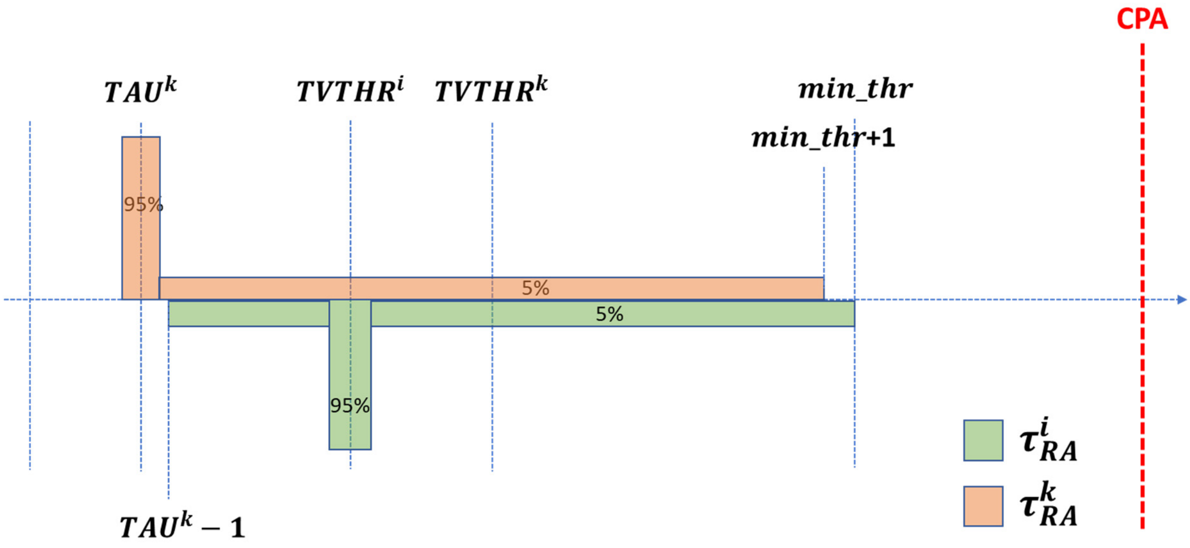

Figure 6-16 Schematic of the alert thresholds for scenario 1

For the evaluation of whether a certain initial encounter geometry could lead to the observed TCAS RA type of the own aircraft, the procedure according to the flowchart in Figure 6-17 is used. First, a random selection of the initial intruder data is conducted. This includes the altitude and vertical rate of the intruder, the question of whether the intruder is TCAS equipped, which of the two aircraft is master, and finally, the pilot response type p^k of the intruder. Once an initial intruder data set is defined to be valid, the pilot response type, selected at this point, will also be used if a modification becomes necessary during the further progression of the simulated encounter. A discussion on the required distributions of this initial intruder data will be provided in chapter 6.5.3.3.

The evaluation of a possible scenario 1, where the intruder's RA is generated earlier than the RA of the own aircraft, starts with the selection of the respective trigger times τ_{RA}^i and τ_{RA}^k of both TCAS RAs. The possible distributions of both trigger times are selected according to the schematic shown in Figure 6-16, where the timepoint of τ_{RA}^i must be closer to the CPA than that of τ_{RA}^k. The current time step t will then be set to the trigger time of the intruder, $t(\tau_{RA}^k)$, which is the timepoint at the CPA minus the duration of τ_{RA}^k.

Then, the altitude and vertical rate of the own aircraft at time τ_{RA}^k, i.e. earlier than the starting point of the own TCAS RA, is processed in the *TCAS_Sim* function together with the initial intruder data. The *TCAS_Sim* function basically is the system model of the Collision Avoidance Logic as described in chapter 6.3 and will be discussed in more detail later on.

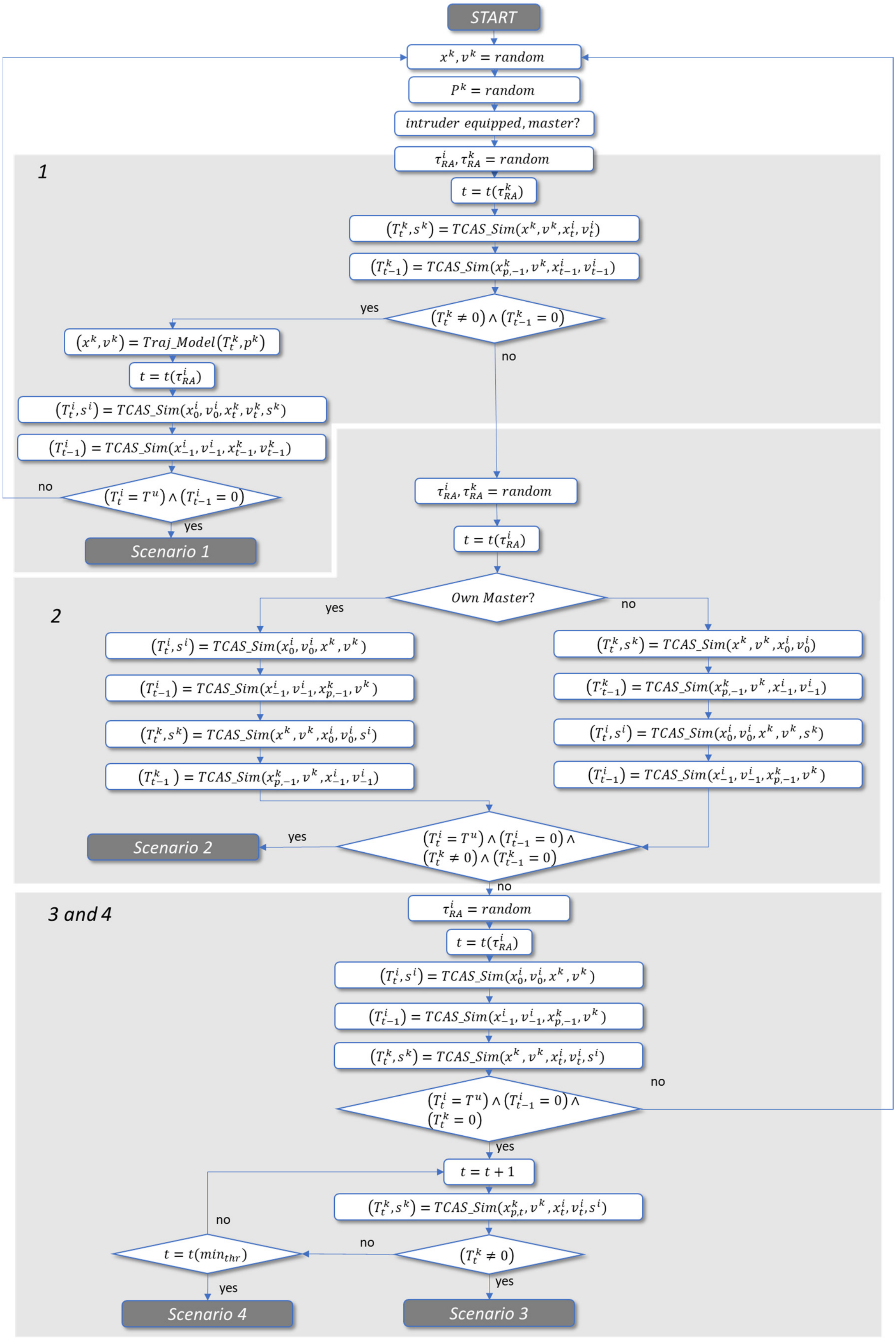
START
$x^k, v^k = random$
$P^k = random$
$intruder\ equipped, master?$
1
$\tau_{RA}^i, \tau_{RA}^k = random$
$t = t(\tau_{RA}^k)$
$(T_t^k, s^k) = TCAS\_Sim(x^k, v^k, x_t^i, v_t^i)$
$(T_{t-1}^k) = TCAS\_Sim(x_{p,-1}^k, v^k, x_{t-1}^i, v_{t-1}^i)$
$(T_t^k \neq 0) \wedge (T_{t-1}^k = 0)$
yes
no
$(x^k, v^k) = Traj\_Model(T_t^k, p^k)$
$t = t(\tau_{RA}^i)$
$(T_t^i, s^i) = TCAS\_Sim(x_0^i, v_0^i, x_t^k, v_t^k, s^k)$
$(T_{t-1}^i) = TCAS\_Sim(x_{-1}^i, v_{-1}^i, x_{t-1}^k, v_{t-1}^k)$
no
$(T_t^i = T^u) \wedge (T_{t-1}^i = 0)$
yes
Scenario 1
$\tau_{RA}^i, \tau_{RA}^k = random$
$t = t(\tau_{RA}^i)$
2
$Own\ Master?$
yes
no
$(T_t^i, s^i) = TCAS\_Sim(x_0^i, v_0^i, x^k, v^k)$
$(T_{t-1}^i) = TCAS\_Sim(x_{-1}^i, v_{-1}^i, x_{p,-1}^k, v^k)$
$(T_t^k, s^k) = TCAS\_Sim(x^k, v^k, x_0^i, v_0^i, s^i)$
$(T_{t-1}^k) = TCAS\_Sim(x_{p,-1}^k, v^k, x_{-1}^i, v_{-1}^i)$
$(T_t^k, s^k) = TCAS\_Sim(x^k, v^k, x_0^i, v_0^i)$
$(T_{t-1}^k) = TCAS\_Sim(x_{p,-1}^k, v^k, x_{-1}^i, v_{-1}^i)$
$(T_t^i, s^i) = TCAS\_Sim(x_0^i, v_0^i, x^k, v^k, s^k)$
$(T_{t-1}^i) = TCAS\_Sim(x_{-1}^i, v_{-1}^i, x_{p,-1}^k, v^k)$
Scenario 2
yes
$(T_t^i = T^u) \wedge (T_{t-1}^i = 0) \wedge$
$(T_t^k \neq 0) \wedge (T_{t-1}^k = 0)$
no
3 and 4
$\tau_{RA}^i = random$
$t = t(\tau_{RA}^i)$
$(T_t^i, s^i) = TCAS\_Sim(x_0^i, v_0^i, x^k, v^k)$
$(T_{t-1}^i) = TCAS\_Sim(x_{-1}^i, v_{-1}^i, x_{p,-1}^k, v^k)$
$(T_t^k, s^k) = TCAS\_Sim(x^k, v^k, x_t^i, v_t^i, s^i)$
no
$(T_t^i = T^u) \wedge (T_{t-1}^i = 0) \wedge$
$(T_t^k = 0)$
yes
$t = t + 1$
$(T_t^k, s^k) = TCAS\_Sim(x_{p,t}^k, v^k, x_t^i, v_t^i, s^i)$
no
no
$t = t(min_{thr})$
$(T_t^k \neq 0)$
yes
yes
Scenario 4
Scenario 3

Figure 6-17 Flowchart of the selection of the initial intruder data and the resulting scenario of the TCAS risk model

If this function returns any TCAS RA type T_t^k for the intruder aircraft at the timepoint of τ_{RA}^k, a TCAS RA is active for the intruder. To make sure that it was generated exactly at this timepoint, the *TCAS_Sim* function has to be additionally processed one cycle before, with the result of no RA active, i.e. $T_{t-1}^k = 0$. The necessary altitude and vertical rate of the own aircraft at this earlier timepoint $(t-1)$ is available in the flight data. For the intruder, the data has to be projected back in time by one step, i.e. one second. This is conducted by the use of a simple backwards extrapolation, i.e. the projected altitude one cycle earlier is $x_{p,-1}^k = x^k - v^k$.

Scenario 1 is possible, if both above conditions are fulfilled and the own aircraft generates a TCAS RA exactly at the timepoint τ_{RA}^i. Moreover, the type of RA T^i has to be the same as detected in FDA, T^u. While the altitude and vertical rate of the own aircraft at the trigger timepoint is available from flight data, these values have to be modelled for the intruder aircraft. This modelled intruder trajectory is based on the RA type T^k and the pilot response p^k. The function *Traj_Model* calculates the altitude and the vertical rate for each cycle, based on the type of RA and the type of pilot response, which consists of the parameters delay, the vertical acceleration, and the target vertical rate. It will be maintained until either the RA is modified during the further simulation of the encounter, or the CPA has been reached and the RA has been cancelled.

If all above conditions are fulfilled, the evaluated initial encounter geometry is saved and will be forwarded to the next step, which is the simulation of the progress of the encounter, including possible modifications of the initial RA.

If the first scenario does not evolve, **scenario 2** will be considered. In this scenario, the trigger thresholds of both aircraft occur at the same time, i.e. $\tau_{RA}^i = \tau_{RA}^k$. As before, it is more likely for the trigger points of the RAs to be around the nominal alert thresholds TAU and $TVTHR$. The overall probability of the trigger threshold being at those points is considered to be again 0.95, which in this case is equally divided between TAU and $TVTHR$, as shown in Figure 6-18. The remainder is considered to be equally distributed up to the minimum time threshold min_thr.

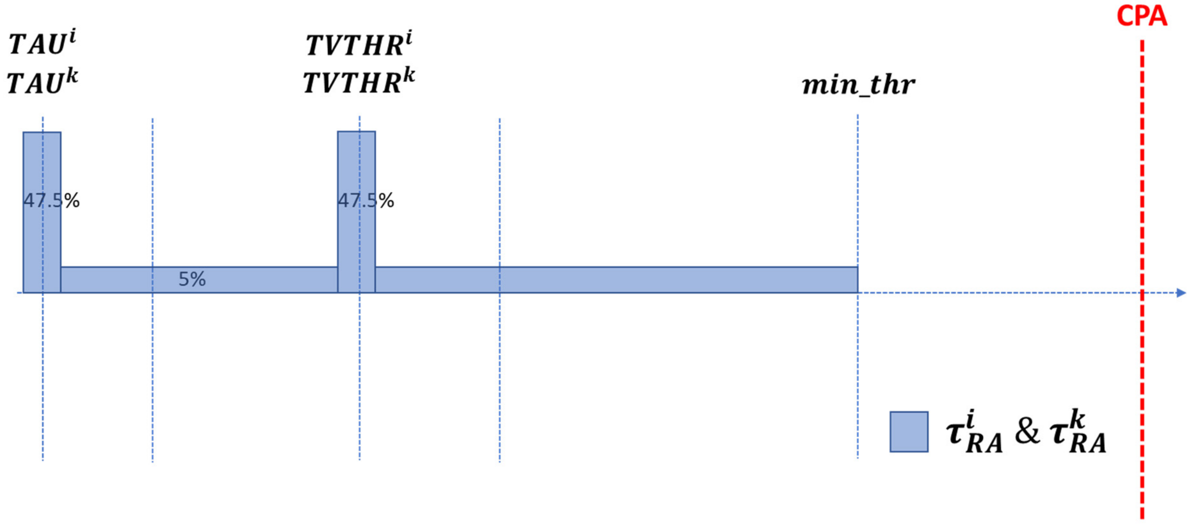

Figure 6-18 Schematic of the alert thresholds for scenario 2 in case of identical Sensitivity Levels

In case the Sensitivity Levels of both aircraft is not the same, the nominal alert thresholds will differ between both aircraft. In this case, the alert trigger τ_{RA} is not located at the nominal thresholds for both aircraft. Since the considered scenario is based on a simultaneous generation of the RAs on both aircraft, the alert trigger τ_{RA} is assumed to be equally distributed between the TAU, which is closest to CPA, and the minimum time threshold, min_thr. This schematic can be seen in Figure 6-19.

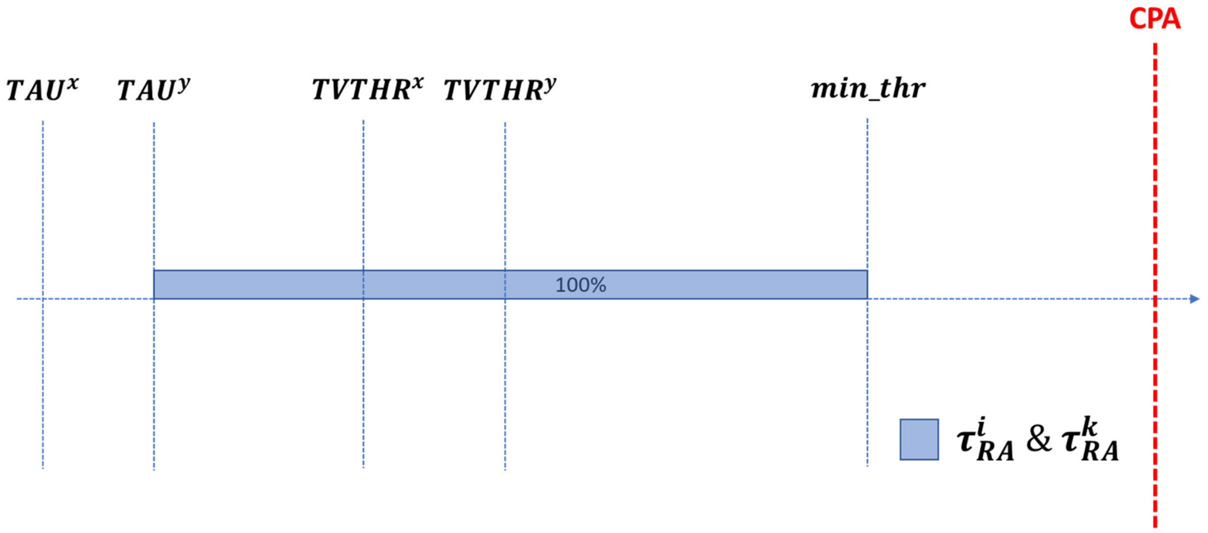

Figure 6-19 Schematic of the alert thresholds for scenario 2 in case of different Sensitivity Levels

Depending on which of the two aircraft is master, i.e. the transponder with the lower Mode S address, this TCAS RA is evaluated first. Normally, both aircraft select their RAs independently from each other. If the senses are not complementary, the master aircraft can initiate a tiebreak reversal within the first few seconds of the encounter, which forces the other aircraft to reverse its RA. As this mechanism is highly complex, the master aircraft will issue its RA first within the scope of this risk model. It is assumed that the slave aircraft receives the resolution advisory complement message in a timely manner to coordinate with the master aircraft without the necessity of a reversal. Thus, a distinction between both versions has to be made.

The master aircraft is processed first with the *TCAS_Sim* function by using the initial intruder data and the own flight data at τ_{RA} as well as the data one cycle before. The resulting sense s is used in a complementary direction for the other aircraft's RA in order to get a coordinated RA. As before, the RA of the own aircraft at time τ_{RA} must be the same type as observed in FDA, i.e. $T^i = T^u$. The intruder's RA must be of any type, and one cycle before no RA at either aircraft shall be active.

In case the second scenario has not evolved, **scenario 3** will be considered. In this scenario, an own RA is generated before the intruder's RA. The distributions of the alert trigger time τ_{RA}^i of the own RA is now inverse to the first scenario, as shown in Figure 6-20. The alert trigger time τ_{RA}^k solely depends on τ_{RA}^i. It may in general range between TAU^k and min_thr, but the earliest possible start is at least one cycle after τ_{RA}^i.

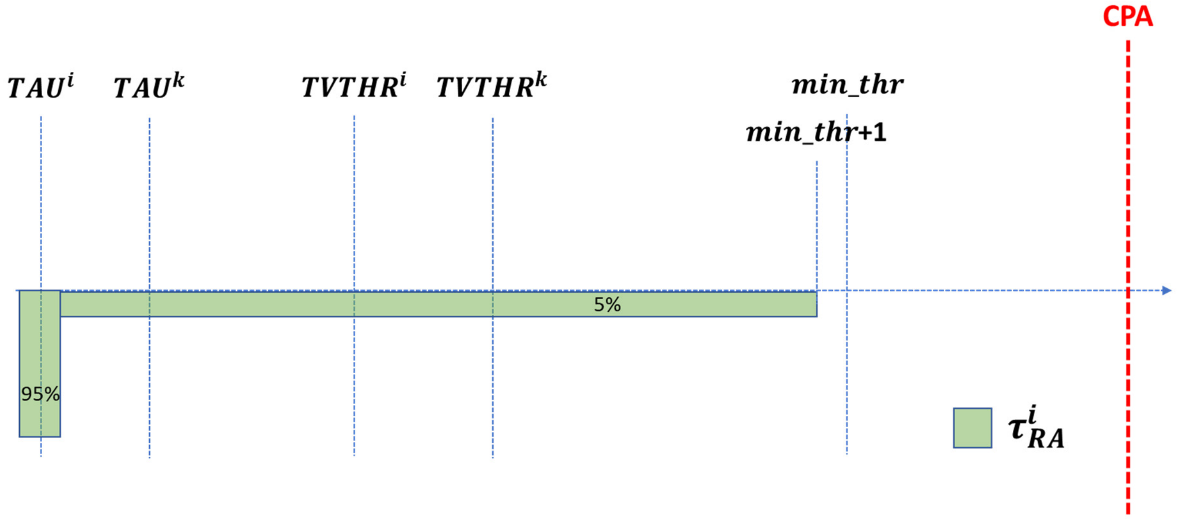

Figure 6-20 Schematic of the alert thresholds for scenario 3 and 4

As before, the type of RA for both aircraft have to be evaluated at time τ_{RA}^i, and for the own aircraft also at one cycle earlier. The difference to the former scenario is, that now the intruder aircraft shall not have generated any RA at τ_{RA}^i, and thus, T^k at time τ_{RA}^i has to be equal to 0. Then, the current time will be increased by one cycle, and the evaluation whether a TCAS RA would be generated for the intruder, will be repeated for this new point in time. The altitude and vertical rate of the own aircraft can be taken from the actual flight data. The altitude of the intruder will be forward projected by one cycle, analogous to the backwards projection in the first and second scenario, while the vertical rate of the intruder is considered to be constant.

If any RA type is generated by the intruder, i.e. $T^k \neq 0$, scenario 3 has evolved. Otherwise, the current time will be increased again by one cycle, until the minimum alert trigger threshold min_thr will be reached. As this threshold is the last point in time, at which a TCAS RA is considered for the intruder, it is assumed, that the intruder has not generated any RA. Hence, this corresponds to **scenario 4**. This is also true, if the intruder is not TCAS equipped at all. In this case, the vertical trajectory of the intruder will be considered to be maintained during the whole TCAS encounter.

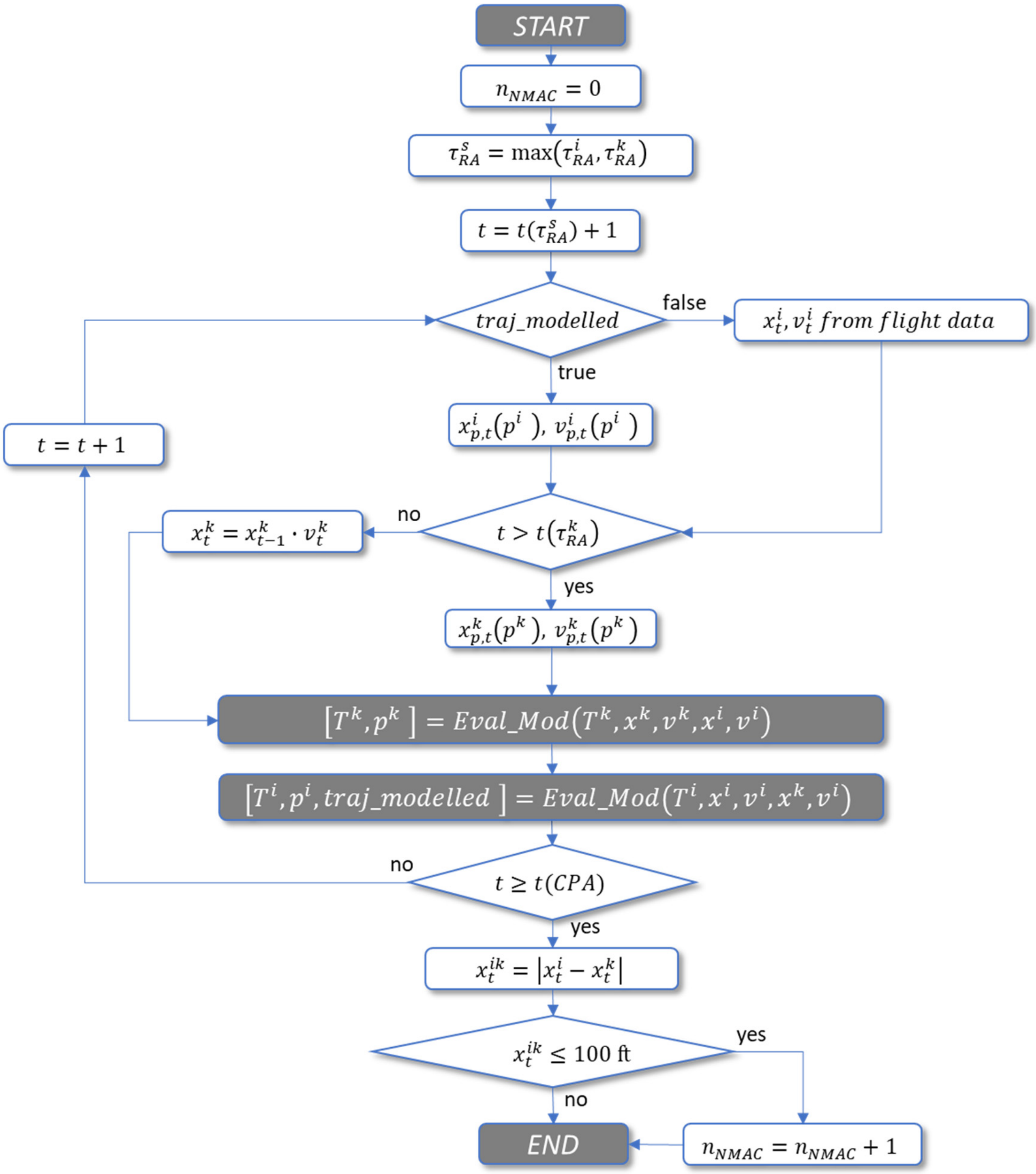
START
$n_{NMAC} = 0$
$\tau^s_{RA} = \max(\tau^i_{RA}, \tau^k_{RA})$
$t = t(\tau^s_{RA}) + 1$
$traj\_modelled$
false
$x^i_t, v^i_t\ from\ flight\ data$
true
$x^i_{p,t}(p^i), v^i_{p,t}(p^i)$
$t = t + 1$
no
$x^k_t = x^k_{t-1} \cdot v^k_t$
$t > t(\tau^k_{RA})$
yes
$x^k_{p,t}(p^k), v^k_{p,t}(p^k)$
$[T^k, p^k] = Eval\_Mod(T^k, x^k, v^k, x^i, v^i)$
$[T^i, p^i, traj\_modelled] = Eval\_Mod(T^i, x^i, v^i, x^k, v^i)$
no
$t \geq t(CPA)$
yes
$x^{ik}_t = |x^i_t - x^k_t|$
$x^{ik}_t \leq 100$ ft
yes
no
END
$n_{NMAC} = n_{NMAC} + 1$

Figure 6-21 Flowchart of the simulation of the progression of the encounter

If none of the scenarios evolves from the randomly selected intruder data, another set of intruder data will be generated, and the whole procedure will be repeated for this newly generated set of intruder data, until a valid set has been found.

On the other hand, if any of the four scenarios has evolved, the resulting encounter will be simulated through the whole progression of the encounter interval up to the CPA in order to calculate the vertical miss distance VMD at CPA. The principle of this simulation can be seen in Figure 6-21.

The simulation of the encounter starts at the first cycle after the start of the first RA of the involved aircraft. In general, an evaluation is conducted for each cycle to determine whether the RA of each aircraft should be modified in order to provide the necessary separation at CPA according to chapter 6.3, *Modification of the RA*. Modification is only taken into consideration, if the RA has to be either reversed or strengthened.

For the vertical trajectory simulation during the encounter, the intruder is assumed to continue with the initial vertical rate up to the start of its RA. As soon as the RA starts, the intruder's vertical trajectory is modelled according to the pilot response model as described below. As soon as a modification of the intruder's RA is necessary, the trajectory is being modelled accordingly.

For the vertical trajectory of the own aircraft, during the whole encounter the recorded vertical rates and altitudes will be taken from actual flight data to incorporate the actual pilot response into the risk model.

However, two problems could arise with that method. First, if the simulation results in a modification of the RA, this might not have been the case in the actual FDA event. Hence, the actual response in the flight data does not correspond with the simulated type of modification of the RA. Therefore, as soon as a modification is required in the simulation, the pilot response of the own aircraft will be modelled according to the pilot response p^i as described below, and the flag $traj\_modelled$ is set to true. An example can be seen in Figure 6-22. In the actual flight data, the response to a "Climb"-RA was a vertical rate v_t^i of around 1,700 feet per minute after a slight delay, indicated by the blue line. After 12 seconds, a reversal RA is required in the simulation. As this differs from the real FDA event, where no reversal RA has been observed, the pilot response for the further simulation is modelled instead of using the real flight data. This is indicated by the dotted orange line. The modelled data is referred to as $x_{p,t}^i(p^i)$ and $v_{p,t}^i(p^i)$ in the flowchart in Figure 6-21.

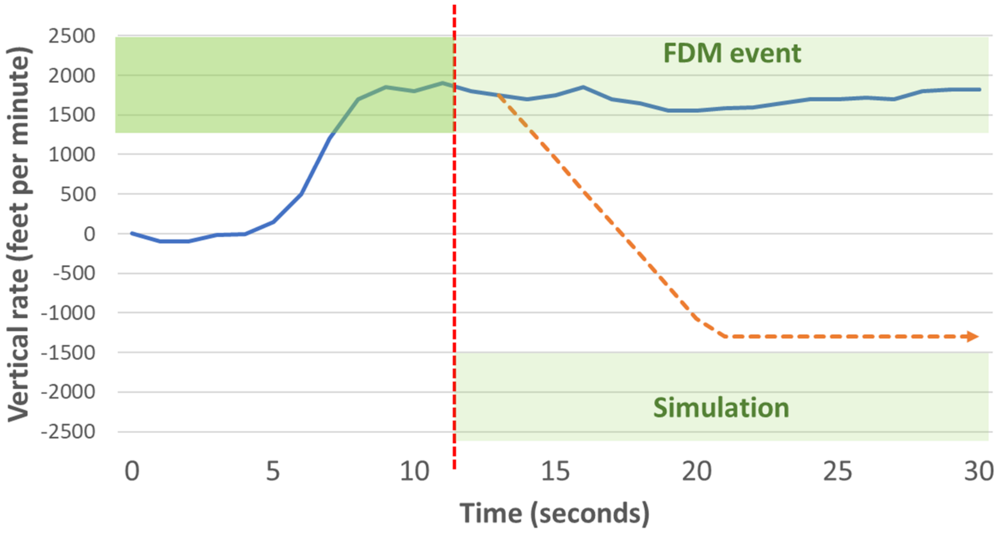

Figure 6-22 Example of a correction of the own trajectory due to a simulated reversal RA

On the other hand, since only the initial RA type of the FDA event is used as a reference for the initial part of the simulation, in the real FDA event an actual modification of the RA could have occurred during the encounter, which would result in an actual change of the trajectory. If this flight data would flow into the simulation, it would result in an incorrect trajectory. Thus, the last measured vertical rate just before the change is being memorized and extrapolated. The latter applies either until CPA or until a further modification of the RA during the respective simulation, which might be required.

An example is shown in Figure 6-23, where during the FDA event a reversal RA occurred. Therefore, the actual trajectory changes after 12 seconds towards a negative vertical rate (blue line). However, the simulation might differ due to a different behavior of the intruder, when compared to the actual event. Hence, from the timepoint where the RA has been modified, the trajectory of the own aircraft will be modelled (dotted orange line), using the last observed vertical rate at the timepoint where the RA was modified.

An analysis of actual flight data during different TCAS RAs shows that in the majority of all observed modifications the vertical rate has already reached steady values at the point of the modification. Hence, it can be assumed that this vertical rate would have been maintained, if no modification would have taken place, whether the rate was compliant or not.

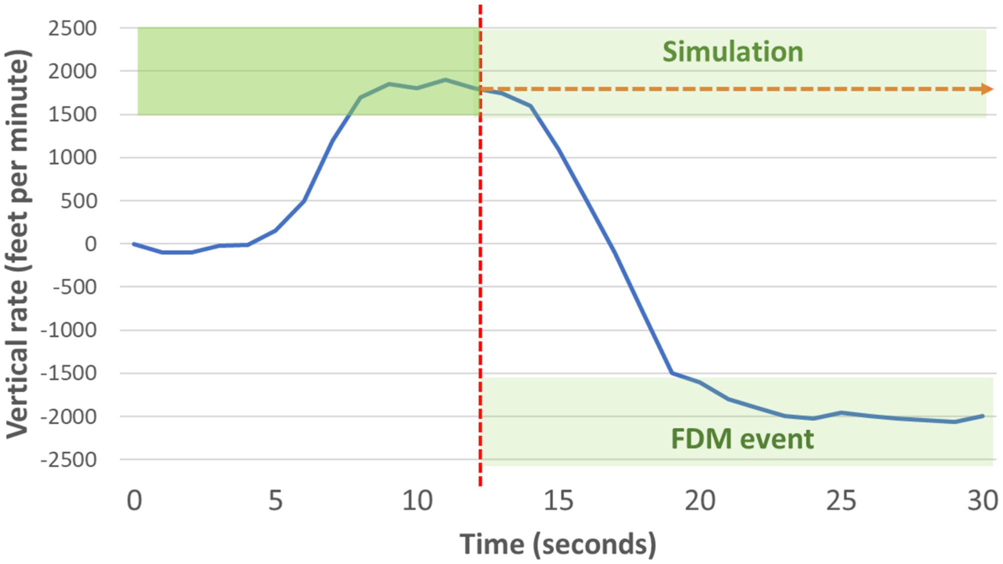

Figure 6-23 Example of a correction of the own trajectory due to an actual reversal RA

The principle for the check of the required modification, which is repeated during each cycle of the encounter for both involved aircraft, is called *Eval_Mod*. The principle is shown in Figure 6-24.

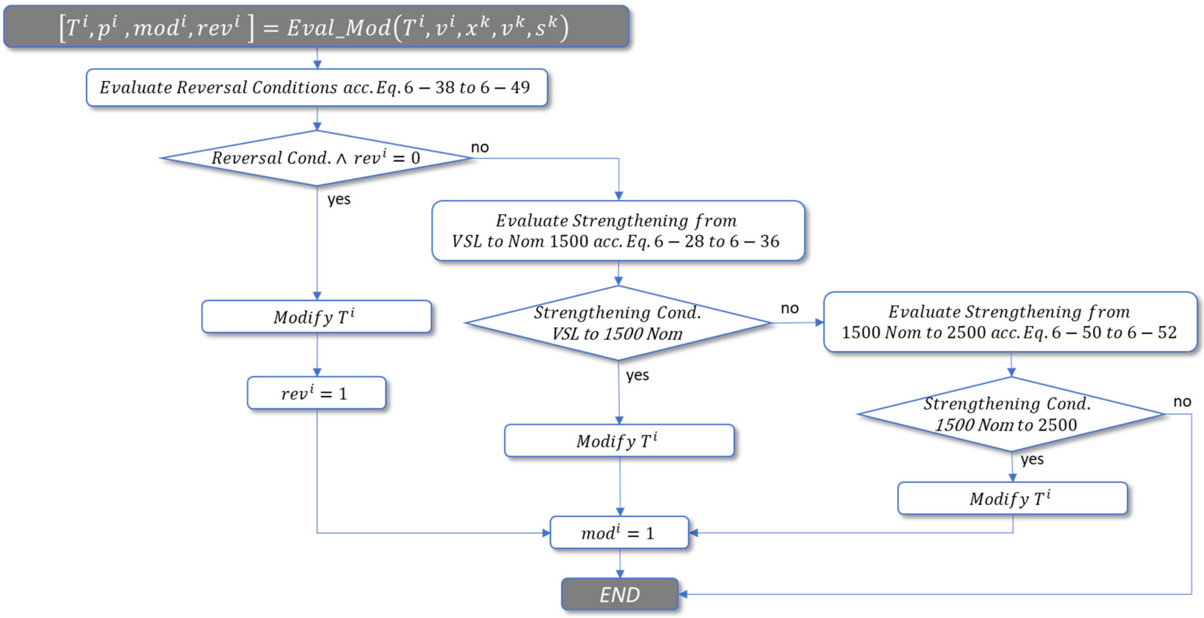
$[T^i, p^i, mod^i, rev^i] = Eval\_Mod(T^i, v^i, x^k, v^k, s^k)$
$Evaluate\ Reversal\ Conditions\ acc.\ Eq. 6-38\ to\ 6-49$
$Reversal\ Cond. \wedge rev^i = 0$
no
yes
$Evaluate\ Strengthening\ from\ VSL\ to\ Nom\ 1500\ acc.\ Eq. 6-28\ to\ 6-36$
$Modify\ T^i$
$Strengthening\ Cond.\ VSL\ to\ 1500\ Nom$
no
$Evaluate\ Strengthening\ from\ 1500\ Nom\ to\ 2500\ acc.\ Eq. 6-50\ to\ 6-52$
$rev^i = 1$
yes
$Strengthening\ Cond.\ 1500\ Nom\ to\ 2500$
no
$Modify\ T^i$
yes
$Modify\ T^i$
$mod^i = 1$
END

Figure 6-24 Flowchart for the evaluation of a modification of the RA (*Eval_Mod*)

If the reversal conditions according to chapter 6.3, *Conditions for a Reversal RA*, are fulfilled, the TCAS RA will be modified accordingly. In this case, the sense of the other aircraft, if equipped with TCAS, will also be reversed.

Otherwise, if the RA is currently Negative, either corrective or preventive, a strengthening to a Nominal-1500-type is considered ("Climb", "Descent" or "Maintain Vertical Speed"). If the RA is

Positive already, a strengthening RA is considered ("Increase Climb/Descent"). The flag mod^i indicates whether any modification took place during the actual simulation.

Finally, the principle of the *TCAS_Sim* function is shown in Figure 6-25. In general, this function evaluates whether a TCAS RA is generated for a certain conflict geometry, based on the altitudes and vertical rates of the involved aircraft, the time to CPA, and the equipment status of the intruder. If the conflict geometry is such that no threat exists, the simulation ends, and the RA type T^i is equal to 0. Otherwise, the type of RA T^i will be defined according to Table 6-4.

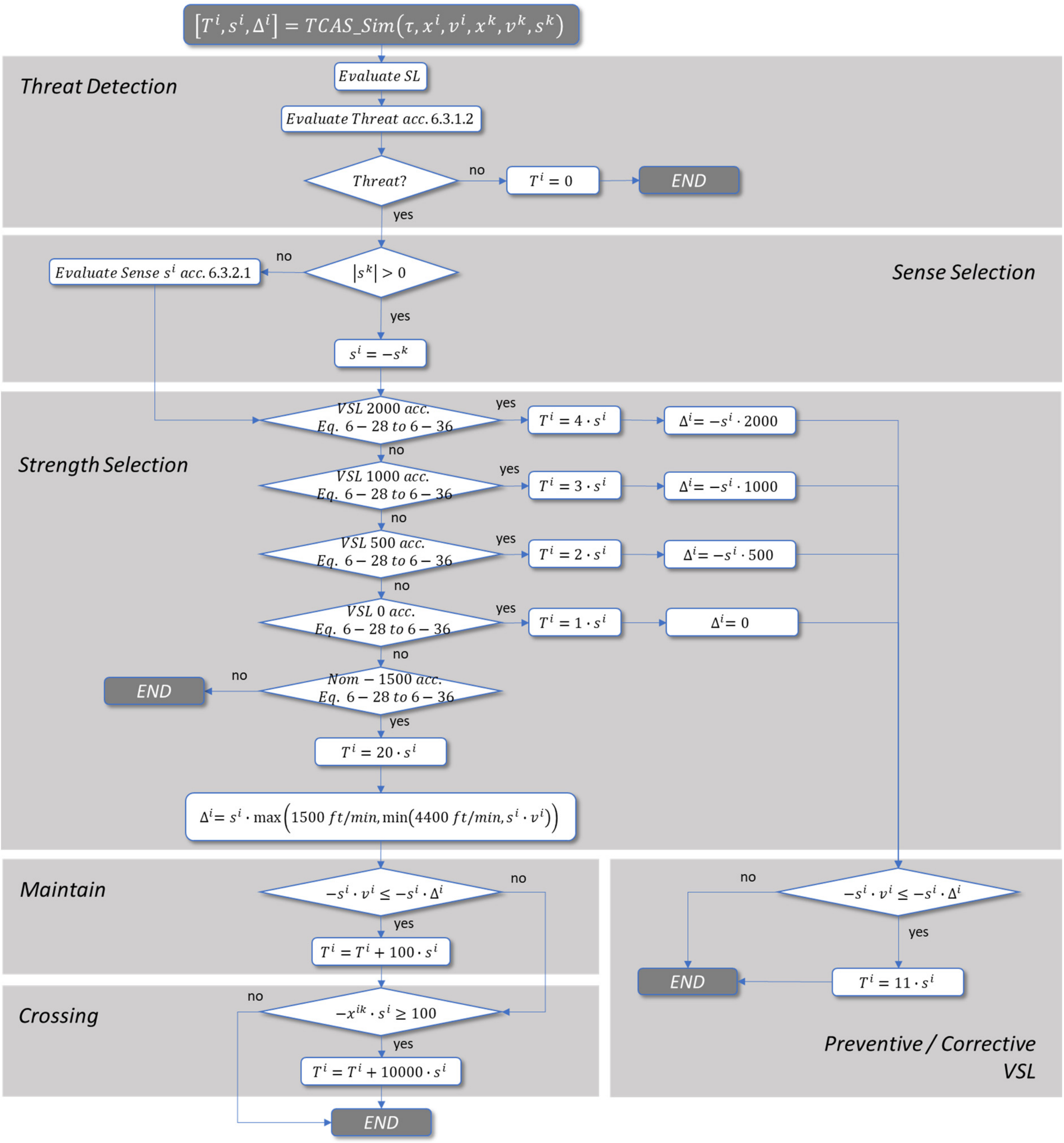

$[T^i, s^i, \Delta^i] = TCAS\_Sim(\tau, x^i, v^i, x^k, v^k, s^k)$
Threat Detection
Evaluate SL
Evaluate Threat acc. 6.3.1.2
Threat?
no
$T^i = 0$
END
yes
Sense Selection
no
Evaluate Sense s^i acc. 6.3.2.1
$|s^k| > 0$
yes
$s^i = -s^k$
Strength Selection
VSL 2000 acc. Eq. 6 – 28 to 6 – 36
yes
$T^i = 4 \cdot s^i$
$\Delta^i = -s^i \cdot 2000$
no
VSL 1000 acc. Eq. 6 – 28 to 6 – 36
yes
$T^i = 3 \cdot s^i$
$\Delta^i = -s^i \cdot 1000$
no
VSL 500 acc. Eq. 6 – 28 to 6 – 36
yes
$T^i = 2 \cdot s^i$
$\Delta^i = -s^i \cdot 500$
no
VSL 0 acc. Eq. 6 – 28 to 6 – 36
yes
$T^i = 1 \cdot s^i$
$\Delta^i = 0$
no
END
no
Nom – 1500 acc. Eq. 6 – 28 to 6 – 36
yes
$T^i = 20 \cdot s^i$
$\Delta^i = s^i \cdot \max\left(1500\ ft/min, \min\left(4400\ ft/min, s^i \cdot v^i\right)\right)$
Maintain
$-s^i \cdot v^i \leq -s^i \cdot \Delta^i$
no
yes
$T^i = T^i + 100 \cdot s^i$
Crossing
no
$-x^{ik} \cdot s^i \geq 100$
yes
$T^i = T^i + 10000 \cdot s^i$
END
no
$-s^i \cdot v^i \leq -s^i \cdot \Delta^i$
yes
END
$T^i = 11 \cdot s^i$
Preventive / Corrective VSL

Figure 6-25 Flowchart of the *TCAS_Sim* function

If a threat was identified according to *Threat detection* in chapter 6.3, the initial sense s^i is calculated, as described in section *Initial sense selection*. This initial sense selection is only conducted, if the sense has not yet been selected by the other aircraft, i.e. $s^k \neq 0$. Otherwise, the complementary sense will be used.

In the next step, the strength is selected, as described in *Initial strength selection* in chapter 6.3, where initially the use of a vertical speed limit VSL is evaluated in order to limit the trajectory change as much as possible. If the current vertical rate is already sufficient, i.e. in the target area, the RA is declared to be Preventive ("Monitor Vertical Speed"), otherwise it is declared to be Corrective, and the vertical speed limit is defined at 0 feet per minute ("Level Off").

In case no VSL is sufficient, a Positive RA has to be issued (Nominal 1500 feet per minute). It has to be distinguished whether the own vertical rate is currently less than or above 1500 feet per minute in the respective direction. If the own vertical rate is above this value in the respective sense, the current rate represents the target rate r, up to a maximum of 4400 feet per minute in the respective direction. In the latter case, a "Maintain Vertical Speed"-type RA is issued. Otherwise, the RA is a standard Nominal-1500-feet-per-minute-RA, i.e. "Climb" or "Descent", respectively.

Finally, it is evaluated whether the encounter is altitude crossing. This applies to Positive RAs only. In this case, the aural warning would be extended by the phrase "Crossing".

6.5.2 Implementation of the Pilot Model

If the pilot response for a particular simulation has not yet been defined for either the own aircraft or the intruder aircraft, an equally distributed random number is generated, ranging from 0 to 100. Then, both values for the delay d_s and the incremental load factor a_s are taken from Table 6-8, depending on the randomly selected response r. The table is derived from the 'typical pilot' responses gathered during the ASARP project, as shown in Figure 6-14.

Depending on the type of RA, the respective target rate will be looked up. For Nominal-1500-feet-per-minute RAs, v_{s_p} will be used. If the type of RA is a "Maintain Vertical Speed"-RA, v_{s_m} will be used, and in case of a Negative RA, v_{s_n} will be used.

The direction, in which the target rate points to, is defined by the sense of the RA, s.

In order to reflect the 2 percent probability of an opposite pilot reaction in the ASARP pilot response model, another random number is generated, which converts the target rate in the opposite direction with a 2 percent chance.

After the three parameters d_s, a_s and v_s have been defined, the altitude x and vertical rate v of the respective aircraft can be calculated for every timepoint during the encounter. For this calculation, the same method is used as shown in chapter 6.3, *Initial sense selection*, using Eq. 6-19 in combination with Eq. 6-17 and Eq. 6-18.

Table 6-8 Distribution of the used pilot response model, source: own research

$r = random[0;1] \cdot 100$	Delay d_s (s)	Incremental load factor a_s	Target rate v_{s_p} Positive RA (feet/min)	Target rate v_{s_n} Negative RA (feet/min)	Target Rate v_{s_m} Maintain (feet/min)
≤ 0.49	3	0.09	730	$0.51 \cdot v_{z,0}$	$0.49 \cdot v_{z,0}$
0.49 < r ≤ 3.69	5	0.09	730	$0.51 \cdot v_{z,0}$	$0.49 \cdot v_{z,0}$
3.69 < r ≤ 3.96	7	0.09	730	$0.51 \cdot v_{z,0}$	$0.49 \cdot v_{z,0}$
3.96 < r ≤ 4.45	8	0.09	730	$0.51 \cdot v_{z,0}$	$0.49 \cdot v_{z,0}$
4.45 < r ≤ 5.43	3	0.15	730	$0.51 \cdot v_{z,0}$	$0.49 \cdot v_{z,0}$
5.43 < r ≤ 11.83	5	0.15	730	$0.51 \cdot v_{z,0}$	$0.49 \cdot v_{z,0}$
11.83 < r ≤ 12.36	7	0.15	730	$0.51 \cdot v_{z,0}$	$0.49 \cdot v_{z,0}$
12.36 < r ≤ 13.34	8	0.15	730	$0.51 \cdot v_{z,0}$	$0.49 \cdot v_{z,0}$
13.34 < r ≤ 15.78	3	0.15	1300	$0.13 \cdot v_{z,0}$	$0.87 \cdot v_{z,0}$
15.78 < r ≤ 31.78	5	0.15	1300	$0.13 \cdot v_{z,0}$	$0.87 \cdot v_{z,0}$
31.78 < r ≤ 33.11	7	0.15	1300	$0.13 \cdot v_{z,0}$	$0.87 \cdot v_{z,0}$
33.11 < r ≤ 35.55	8	0.15	1300	$0.13 \cdot v_{z,0}$	$0.87 \cdot v_{z,0}$
35.55 < r ≤ 37.02	3	0.22	1300	$0.13 \cdot v_{z,0}$	$0.87 \cdot v_{z,0}$
37.02 < r ≤ 46.62	5	0.22	1300	$0.13 \cdot v_{z,0}$	$0.87 \cdot v_{z,0}$
46.62 < r ≤ 47.42	7	0.22	1300	$0.13 \cdot v_{z,0}$	$0.87 \cdot v_{z,0}$
47.42 < r ≤ 48.89	8	0.22	1300	$0.13 \cdot v_{z,0}$	$0.87 \cdot v_{z,0}$
48.89 < r ≤ 49.38	3	0.15	2200	$-0.47 \cdot v_{z,0}$	$1.47 \cdot v_{z,0}$
49.38 < r ≤ 52.58	5	0.15	2200	$-0.47 \cdot v_{z,0}$	$1.47 \cdot v_{z,0}$
52.58 < r ≤ 52.85	7	0.15	2200	$-0.47 \cdot v_{z,0}$	$1.47 \cdot v_{z,0}$
52.85 < r ≤ 53.34	8	0.15	2200	$-0.47 \cdot v_{z,0}$	$1.47 \cdot v_{z,0}$
53.34 < r ≤ 54.32	3	0.22	2200	$-0.47 \cdot v_{z,0}$	$1.47 \cdot v_{z,0}$
54.32 < r ≤ 60.72	5	0.22	2200	$-0.47 \cdot v_{z,0}$	$1.47 \cdot v_{z,0}$
60.72 < r ≤ 61.25	7	0.22	2200	$-0.47 \cdot v_{z,0}$	$1.47 \cdot v_{z,0}$
61.25 < r ≤ 62.23	8	0.22	2200	$-0.47 \cdot v_{z,0}$	$1.47 \cdot v_{z,0}$
62.23 < r ≤ 63.21	3	0.30	2200	$-0.47 \cdot v_{z,0}$	$1.47 \cdot v_{z,0}$
63.21 < r ≤ 69.61	5	0.30	2200	$-0.47 \cdot v_{z,0}$	$1.47 \cdot v_{z,0}$
69.61 < r ≤ 70.14	7	0.30	2200	$-0.47 \cdot v_{z,0}$	$1.47 \cdot v_{z,0}$
70.14 < r ≤ 71.12	8	0.30	2200	$-0.47 \cdot v_{z,0}$	$1.47 \cdot v_{z,0}$
71.12 < r ≤ 72.10	3	0.22	3900	$-1.6 \cdot v_{z,0}$	$2.6 \cdot v_{z,0}$
72.10 < r ≤ 78.50	5	0.22	3900	$-1.6 \cdot v_{z,0}$	$2.6 \cdot v_{z,0}$
78.50 < r ≤ 79.03	7	0.22	3900	$-1.6 \cdot v_{z,0}$	$2.6 \cdot v_{z,0}$
79.03 < r ≤ 80.01	8	0.22	3900	$-1.6 \cdot v_{z,0}$	$2.6 \cdot v_{z,0}$
> 80.01	0	0	$v_{z,0}$	$v_{z,0}$	$v_{z,0}$

6.5.3 Event Risk

For the evaluation of the overall event risk, both, the severity as well as the probability have to be evaluated.

6.5.3.1 Severity

The most credible accident scenario of a midair collision is a hull loss, which is usually not survivable. This scenario could be observed in the past several times [90,107,108]. As the risk model is focused on midair collisions, the severity is assumed to be a catastrophic outcome, i.e. the highest Severity Level *A5*.

6.5.3.2 Probability

The NMAC probability is the product of the vertical and horizontal NMAC-probability, as long as both components are independent from each other. According to a series of flight test in three different airspaces within the United States in 1981, generating 153 TCAS RAs, any dependence between both components could be strongly rejected. The correlation coefficient was evaluated at 0.0177 for the Spearman rank-order statistic, where 0 implies no correlation, +1 implies perfect positive correlation, and -1 implies perfect negative correlation [109].

The vertical NMAC probability $p(NMAC_z|T^i = T^u, P, X, V)$ of a certain TCAS RA type T^u depends on the encounter geometry (altitudes X and vertical rates V) and the pilot responses of both involved aircraft.

The midair collision probability $p(MAC|T^i = T^u, P, X, V)$ can then be evaluated by the product of the NMAC probability and the conditional probability of a midair collision from a near midair collision, $p(MAC|NMAC)$, which is usually assumed to be at a value of 0.1 [87]:

$$p(MAC|T^i = T^u, P, X, V) = p(NMAC_z|T^i = T^u, P, X, V) \cdot p(NMAC_h) \cdot p(MAC|NMAC)\,. \qquad \textbf{Eq. 6-56}$$

As the evaluation of NMAC probability described above is based on the vertical plane only, and information about the horizontal geometry of the encounter is not available except the fact, that the horizontal miss distance during the RA is equal to or less than DMOD, the horizontal NMAC-probability $p(NMAC_h)$ has to be estimated by using the HMD-distribution. Two possibilities exist to get these distributions.

The first possibility is the assumption of a uniform distribution of HMD values, as described in [110]. The other possibility is the use of real data from external data sources.

In case of a uniform distribution, the respective probability of a horizontal NMAC can be calculated in the following way:

$$p_u(NMAC_h) = \frac{500\text{ feet}}{DMOD}\,. \qquad \textbf{Eq. 6-57}$$

For the evaluation of the horizontal NMAC-probability with real data, $p_o(NMAC_h)$, e.g. radar data can be used. Lincoln Laboratory has collected two sets of radar data from TCAS events in the U.S., including 133 close encounters between two aircraft. This data covers approximately 2 years of data in the Boston airspace, approximately 2 months of data in the New York airspace, and 51 days of data in the Philadelphia airspace [110]. The data, which can be seen in Figure 6-26, show a non-uniform distribution of horizontal miss distances at CPA, with a higher probability towards greater miss distances. A similar distribution was observed by a second analysis, covering 21,615 close encounters with and without TCAS RAs, collected during 9 months with 130 radar sensors across the U.S. [110]. However, this second set of data only covers HMDs up to a value of 0.35 NM, but the distribution of this smaller section shows a relationship between horizontal miss distances below 500 feet and up to 0.35 NM. This is comparable to the same relationship in the first data set.

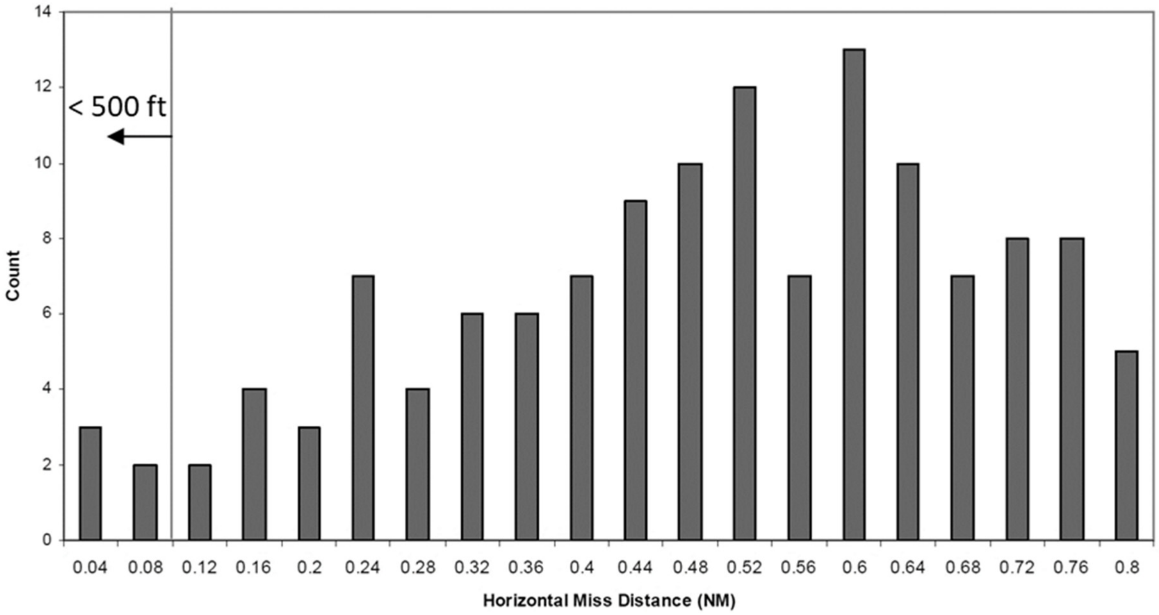

Figure 6-26 Distribution of Horizontal Miss Distances during different encounters [110]

For altitudes up to 20,000 feet, the probability of a horizontal NMAC can be directly derived from the data shown in Figure 6-26, since the DMOD values for the respective Sensitivity Levels are equal to or less than 0.8 NM. For an extrapolation beyond 0.8 NM up to 1.1 NM, it is assumed that the distribution of the Horizontal Miss Distances is equivalent to the average values of HMDs in the interval between 0.55 NM and 0.8 NM. By extrapolating the mean value of these horizontal miss distances, the probability can therefore also be estimated for horizontal NMACs, where the DMOD value is 1.1 NM.

As a result, the following values can be used for $p(NMAC_h)$:

Table 6-9 Probabilities of horizontal NMACs during TCAS RA at CPA, external data p_o and uniformly distributed p_u, source: own research

SL	DMOD	Altitude	$p_o(NMAC_h)\ lwr95\%$	$p_o(NMAC_h)$	$p_o(NMAC_h)\ upr95\%$	$p_u(NMAC_h)$
5	0.55 NM	FL50 - FL100	0.022	0.067	0.149	0.150
6	0.80 NM	FL100 – FL200	0.012	0.038	0.086	0.103
7	1.10 NM	FL 200 and above	0.008	0.025	0.057	0.075

Table 6-9 also indicates the lower and upper bounds of the 95 percent confidence interval of $p_o(NMAC_h)$ for real data, taking into account the number of considered TCAS RAs. For the uniformly distributed HMDs no confidence interval exists.

The data in Table 6-9 shows an approximately 3 times higher probability for the assumption of uniformly distributed HMDs. For the application of the model, both values will be used.

6.5.3.3 Distribution of Intruder Data Vectors

The probability of a vertical NMAC is influenced by the used distributions of the randomly generated intruder data. This applies to the distributions of the relative altitude x^{ik} between the intruder and the own aircraft, the vertical rate v^k of the intruder, as well as the TCAS equipment of the intruder.

For every type of the own RA in combination with the current vertical rate of own aircraft at the start of the RA, all possible initial intruder data can be displayed in an intruder's initial data graph, showing the relative altitude and the vertical rate of the intruder at the start of the own RA, as well as the type of RA of the intruder. An example can be seen in Figure 6-27, displaying a "Climb"-RA for the own aircraft, generated during a level flight at Sensitivity Level 6 (e.g. FL150), including 3,000 simulations. Basically, the graph displays all possible initial intruder data combinations, which could lead to a "Climb"-RA. Therefore, the graph reflects the filtering algorithm of the TCAS collision avoidance logic. The only missing information is the selected pilot response of the intruder. The intruder's response may influence the type of RA, which is generated for the own aircraft. Outliers in the graph are usually generated by extreme pilot responses, either in the right or wrong direction.

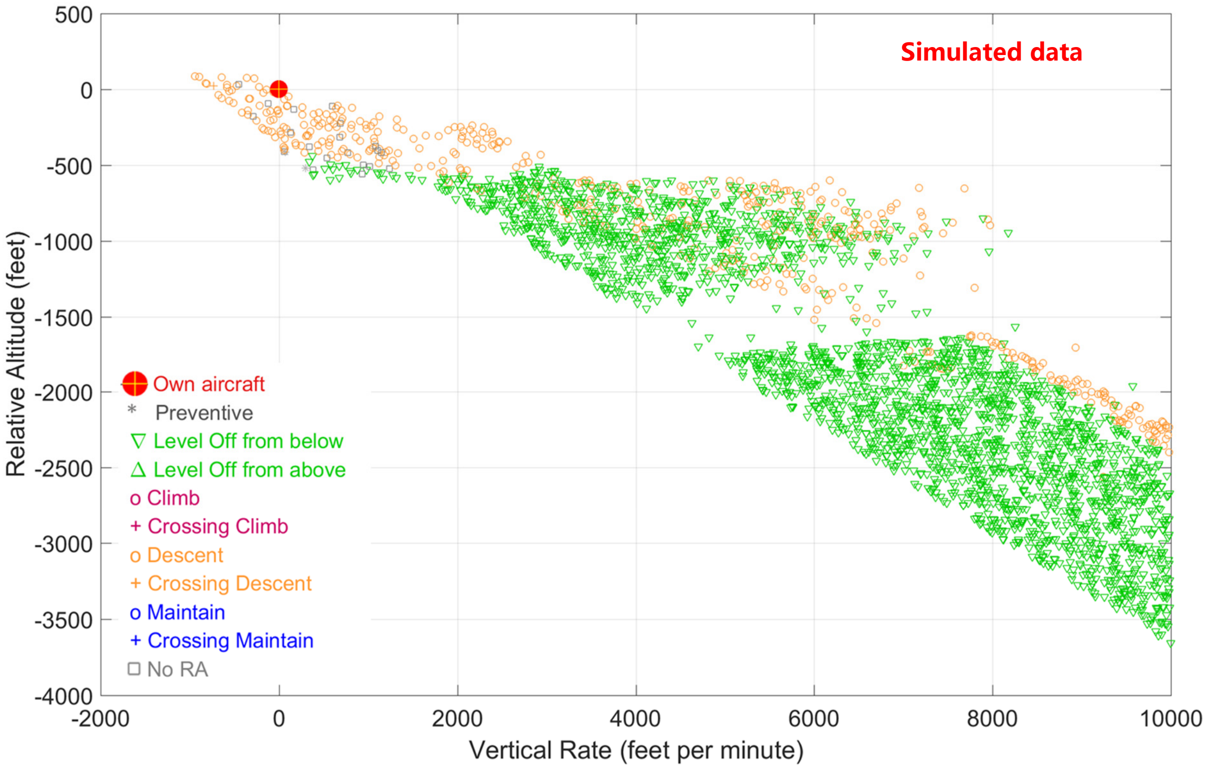

Figure 6-27 Distributions of simulated intruder data vectors, with own aircraft generating a "Climb"-RA, source: own research

Since this simulation contains a significant number of encounter geometries with very high intruder vertical rates, the probability of a vertical NMAC is relatively high, i.e. 0.055.

However, the vertical rates of the intruder, as shown in Figure 6-27, are different from actually observed rates, since the intruder's vertical rates are equally distributed in this graph. In actual flight data, vertical rates of more than 6,000 feet per minute are very rare due to performance limits of the involved aircraft.

To reflect a more realistic distribution of vertical rates, the actual distribution of vertical rates observed in FDA at the start of a TCAS RA event is used instead. An analysis of the vertical rates at the start of 1077 TCAS RA events results in a normal distribution with a mean value near 0 feet per minute, and a standard deviation of approximately 1260 feet per minute. Using this distribution, the initial data graph of the intruder changes towards a more condensed representation of relative altitudes and vertical rates around the altitude and the vertical rate of the own aircraft, as shown in Figure 6-28. The probability of a vertical NMAC reduces significantly to a value of 0.009. This reduction in probability results from a less dynamic encounter geometry.

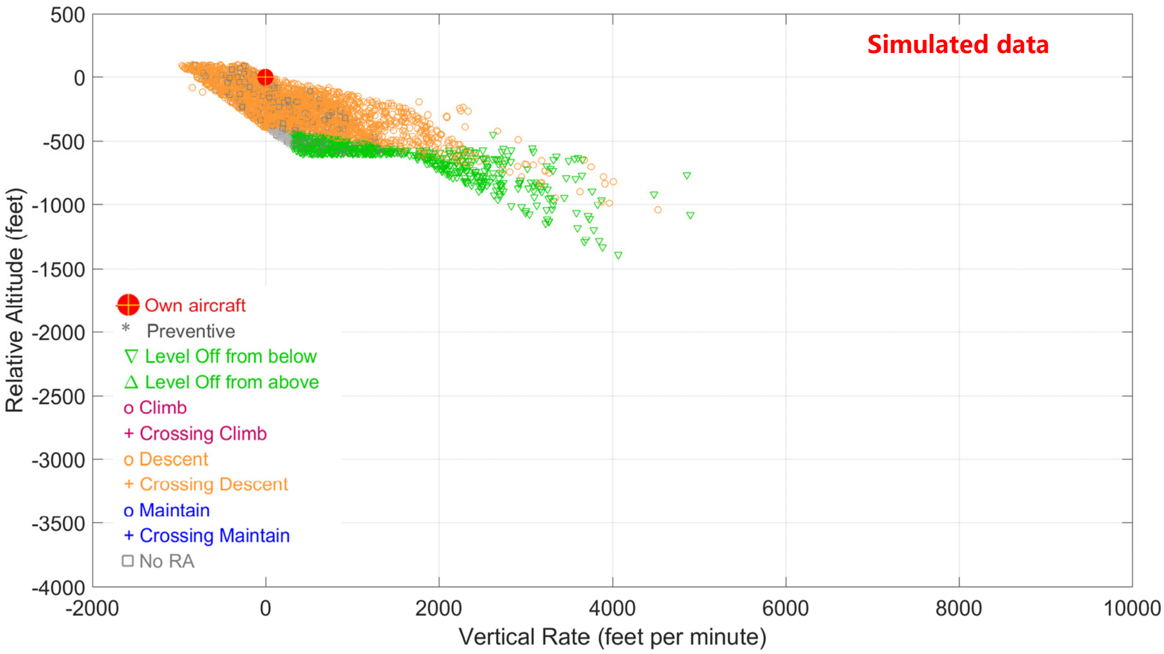

Figure 6-28 Distributions of simulated intruder data vectors, with own aircraft generating a "Climb"-RA. The distribution of intruder vertical rates was adapted to observed values, source: own research

The intruder altitudes are assumed to be equally distributed around the own altitude. Since an intruder is only taken into consideration if the absolute vertical rate is equal to or less than 10,000 feet per minute, and the maximum possible time to CPA is 35 seconds at the start of the RA, the maximum possible relative altitude of the intruder is limited to an absolute value of 5,833 feet. In addition, the maximum vertical alert threshold $ZTHR$ of 700 feet must be considered, resulting in a maximum possible relative altitude of the intruder of approximately 6,500 feet. Taking this fact into account, the number of iterations to find a valid initial intruder data vector can significantly be reduced.

However, for certain encounter geometries, a specific altitude distribution is more probable. According to an analysis of TCAS monitoring data in the U.S. airspace, conducted in 2008 and 2009 during the TCAS Operational Performance Assessment (TOPA), containing 36,689 RA encounters recorded in the Boston, Philadelphia, New York, Southern California and Dallas terminal areas, a significant clustering at vertical miss distances of 500 feet and 1000 feet could be observed at CPA. This clustering indicates that a substantial number of TCAS RAs have been likely related to the standard separation used between an aircraft flying under IFR, and either another IFR aircraft (1000 feet), or an aircraft flying under Visual Flight Rules (VFR, 500 feet) [101], see Figure 6-29. A similar observation could be made in the European airspace [106]. Most of those encounters with 500 feet or 1000 feet separation are in accordance with safe air traffic regulations but fall within the TCAS alerting criteria. Therefore, these TCAS RAs may be considered as 'nuisance' or 'unnecessary' in hindsight, but still have the potential of a false reaction and thus, contain the probability of an induced collision.

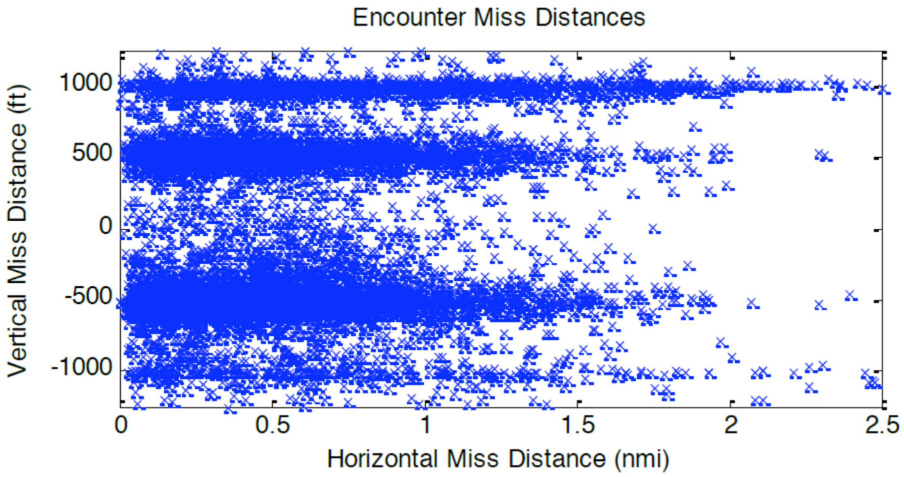

Figure 6-29 TCAS RA vertical and horizontal separation [101]

The encounters with a vertical miss distance at CPA of 1000 feet are usually generated by two IFR traffics, where at least one is levelling off at a level, which is 1000 feet above or below the level of the other IFR traffic, or both aircraft levelling off with a 1000 feet separation. This applies especially to threats induced by high vertical rates of the own aircraft, followed by a 'Level off'-RA. According to the TOPA analysis, approximately 56 percent of the RAs, where at least one aircraft is levelling off, are associated with a 1000 feet separation, while the rest results in vertical miss distances below 500 feet [101]. Thus, in the presented risk model it is proposed to maintain a level, which is 1000 feet above or below the intended level off altitude of the own aircraft, if the current altitude of the own aircraft is within 3000 feet of the selected altitude, and the absolute vertical rate of the own aircraft is at least 1000 feet per minute for 56 percent of all initial intruder data vectors. According to flight data analysis for level flying aircraft the initial vertical rate follows a Normal distribution with a mean value of 0 feet per minute, and a standard deviation of 224 feet per minute. The altitude follows a Normal distribution, with a mean value at 1000 feet above the selected altitude of the own aircraft, if the own aircraft is climbing, and 1000 feet below the selected altitude, if the own aircraft is descending, respectively. For both cases, the standard deviation is 80 feet.

For a 'Level off'-RA during climb with a vertical rate of 3,600 feet per minute at 500 feet below the selected altitude, where the level off is intended, the respective intruder's initial data graph is shown in Figure 6-30. Note that the majority of intruders in this scenario maintains the level 1000 feet above the level off altitude, and due to the response of the own aircraft on the RA, more than 20 percent of the intruders will not receive any RA.

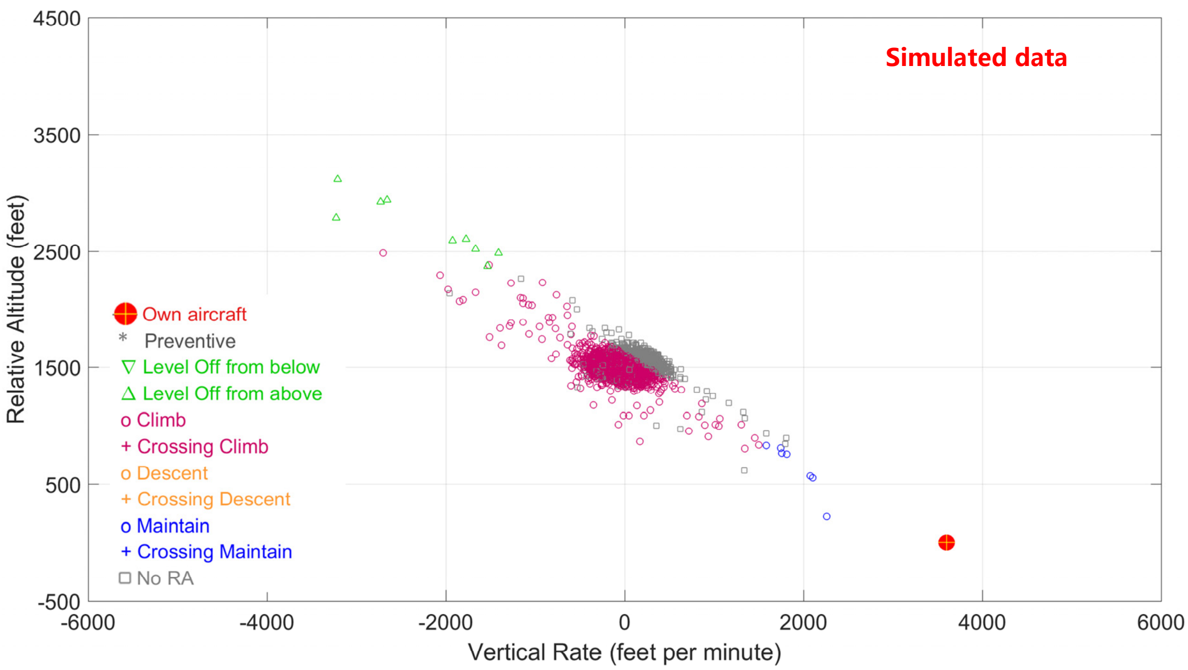

Figure 6-30 Distributions of simulated intruder data vectors, with own aircraft generating a "Level off"-RA during climb. The distribution of intruder vertical rates was adapted to observed values, source: own research

If this special distribution of initial vertical rate and altitude of the intruder would not be considered, the intruder's initial data graph would be completely different, as shown in Figure 6-31. However, the probability of an induced collision is not significantly affected in this case.

The TCAS equipment status is another element which may affect the risk level of a TCAS event. It is assumed that in the upper airspace (above 10,000 feet) only military traffic is not yet TCAS equipped. This portion is assumed to be 5 percent [87,111].

For the lower airspace, the portion of TCAS unequipped traffic is much higher, since VFR traffic usually is not equipped with TCAS. This portion is assumed to be 50 percent [87].

If an intruder is TCAS equipped, the probability that the own aircraft is the master, is 50 percent.

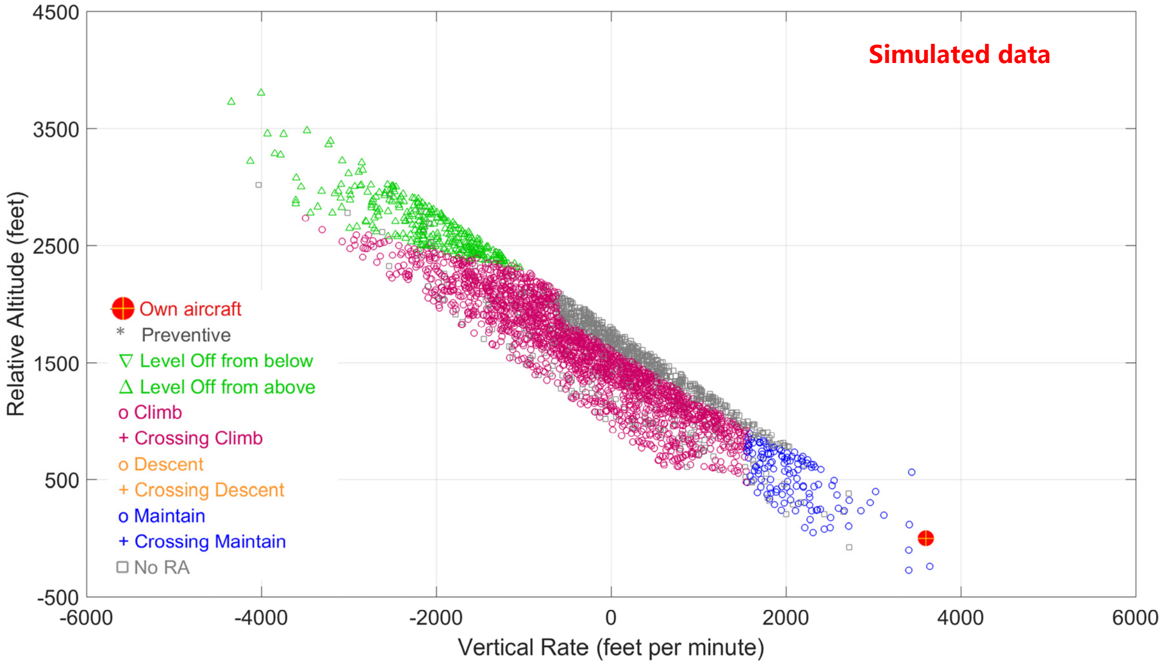

Figure 6-31 Distributions of simulated intruder data vectors, with own aircraft generating a "Level off"-RA during climb, source: own research

6.6 Application of the Method

The risk model was applied on actual TCAS RA events, which occurred during a 24-month period in a major European airline. The events were filtered for altitude and flight phase. Since the risk model cannot be applied for encounters caused by close encounters (DMOD), TCAS RAs which occurred during the approach phase were not taken into consideration. The reason is, that TCAS RAs during approach are often caused by DMOD, especially during closely spaced parallel approaches in the U.S. airspace.

Since the encounter geometry is more distinct at higher altitudes, an altitude filter was applied. Only RAs generated above 9,000 feet pressure altitude have been used. A further advantage of this filter is that it enforces the elimination of RAs which have been triggered during the approach phase, even on high elevation airports like Denver.

The above filter resulted in 91 TCAS RA events. The analyzed RAs occurred mainly in the European and U.S. airspace (more than 90 percent). For some of the involved aircraft types, intruder data was available in the flight data. However, since the risk model is based on the consideration of the same event with slightly different environmental conditions regarding the intruder, this data has not been used.

Flight data from the own aircraft has been used in one-second samples in an interval from 40 seconds before the own RA until 40 seconds after the generation of the RA. For the risk analysis, only the TCAS parameters, the pressure altitude, and the vertical rate have been used.

6.6.1 Number of Iterations Required for the Simulation

Since the described method for risk evaluation is based on a Monte Carlo method, the number of simulations is essential for the precision of the resulting probability value. The estimated probability of a vertical NMAC $\hat{p}_{NMAC,z}$, which is the result of a simulation, can be calculated by the quotient between the number of vertical NMACs $n_{NMAC,z}$, which have been counted in the simulation, and the number of simulations n_i. The precision of this value should be high enough to avoid an incorrect risk classification.

From the perspective of a safety management, the risk level of an event should not be underestimated. The risk index of the event should therefore not fall into the next lower risk index. On the probability scale of the risk matrix in Figure 2-12, the next lower risk index is $\sqrt{10} = 3.16$ times lower for all probabilities due to its logarithmic design. Thus, it is reasonable to ensure that the estimated probability $\hat{p}_{NMAC,z}$ does not deviate from the expected probability $p_{NMAC,z}$ by more than a factor of 3.16 with a confidence of 95 percent. This prevents an inadvertent shift to the adjacent risk level due to improper precision of the probability.

For the calculation of the required number of simulations n_{req}, the *coefficient of variation* CV can be used, which is a standardized measure for the variability of the estimated probability. The *coefficient of variation* CV is the relationship between the standard deviation of the estimated probability $\hat{p}_{NMAC,z}$ and the expectation of the probability $p_{NMAC,z}$ [112,113]:

$$CV = \frac{\sqrt{var\left[\hat{p}_{NMAC,z}\right]}}{p_{NMAC,z}}. \qquad \textbf{Eq. 6-58}$$

The difference between the estimated and the expected probability $(\hat{p}_{NMAC,z} - p_{NMAC,z})$ usually follows a Normal distribution. Thus, the coefficient of variation indicates the standard deviation of the relative estimation error, which is $(\hat{p}_{NMAC,z} - p_{NMAC,z})/p_{NMAC,z}$. In other words, the estimated probability is within the interval of $p_{NMAC,z} \cdot (1 \pm 1.96 \cdot CV)$ with a confidence of 95 percent.

Since the relationship between the expected probability $p_{NMAC,z}$ and the lower boundary of the 95-percent confidence interval $p_{NMAC,z} \cdot (1 - 1.96 \cdot CV)$ should be lower than 3.16, the required coefficient of variation CV_{req} can be calculated as follows:

$$\frac{1}{\left(1 - 1.96 \cdot CV_{req}\right)} \leq 3.16\,. \qquad \textbf{Eq. 6-59}$$

Therefore, the required coefficient of variation CV_{req} should not exceed the value of 0.349 for all probabilities.

As a rule of thumb, for every application of the Monte Carlo method, the number of vertical NMACs $n_{NMAC,z}$ should be at least 10, i.e. the number of required simulations n_{req} is approximately $10/p_{NMAC,z}$. Depending on the probability, the number of required simulations n_{req} can be calculated as follows [113]:

$$n_{req} = \frac{1 - p_{NMAC,z}}{p_{NMAC,z} \cdot {CV_{req}}^2}. \qquad \textbf{Eq. 6-60}$$

Since the probability of a vertical NMAC in Eq. 6-60 has to be known beforehand, in a first iteration, the Monte Carlo method has been applied to the 91 TCAS RA events. For each event 30,000 simulations have been applied to estimate the required probability of a vertical NMAC. The number of resulting vertical NMACs can be seen in Figure 6-32. Also, the number of required simulations n_{req} according Eq. 6-60 is indicated in the graph for different magnitudes of vertical NMACs.

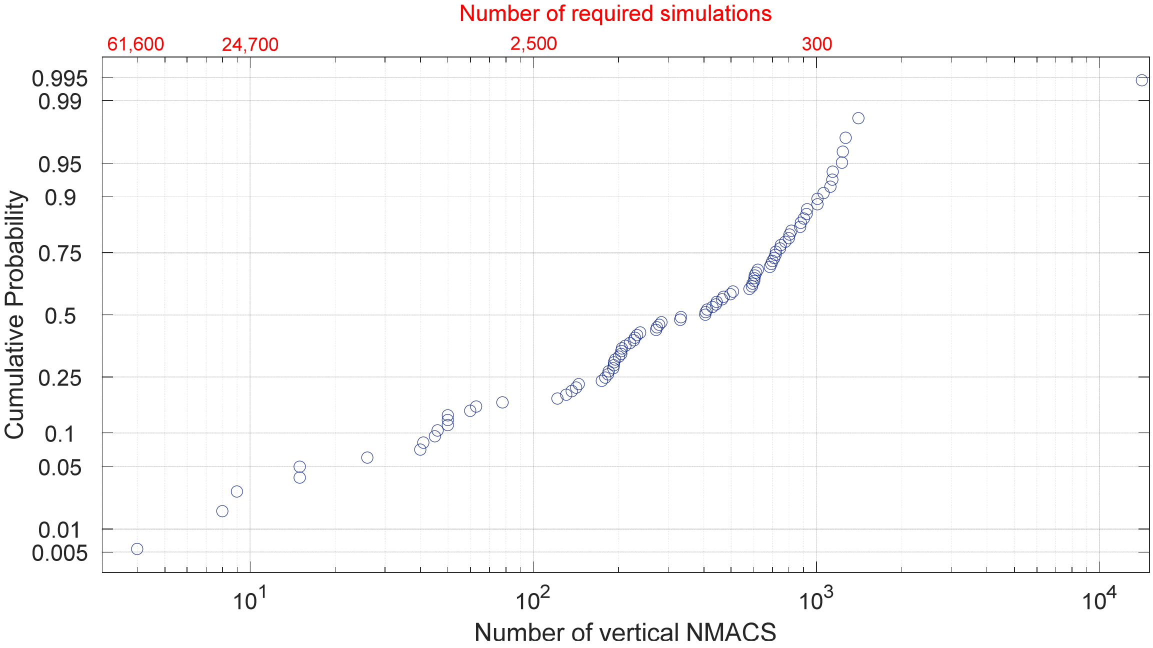

Figure 6-32 Number of required simulations depending on the number of vertical NMACs, source: own research

While for 95 percent of all events 25,000 simulations would be sufficient to reach the required precision, for the 3 events with the lowest probability, the number of vertical NMACs is below ten, which is not enough according to the rule of thumb. Thus, the number of required simulations needs to be higher. For the event with the lowest probability, the required number of simulations is 61,600 (rounded to the next higher 100).

2,500 simulations are sufficient to save computing power for most events (more than 80 percent). Depending on the estimated probability, the number of simulations per event is increased in order to reach the required precision for those events, which have a lower probability, up to a value of 61,600 simulations.

It may be discussed whether the additional computing power is justified for events with a very low probability, since those events do not contribute significantly to the overall risk. By applying 2,500 simulations, for the majority of events the achieved precision is significantly higher than required. This applies in particular to those events that contribute most to the overall risk.

6.6.2 Results

For each TCAS RA event, at least 2,500 randomly selected initial intruder data sets have been generated and used for the respective simulation. Different initial RA types in combination with a certain initial vertical rate of the own aircraft either may encourage or even impede the detection of valid initial intruder data, thus, both the processing times and number of loops, which are necessary to find such a valid data set, might differ significantly. In case of the analyzed events, the processing times ranged between 3 seconds up to 40 minutes per event[23], depending on the number of simulations as well as on the conflict geometry in combination with the type of RA. The number of iterations, required to find a valid initial data set as described in Figure 6-15 and Figure 6-17, ranged from 43,000 up to 9.5 million iterations with an average of approximately 992,000 loops, i.e. for one valid data set detection, in average 120 iterations were necessary.

The results can be seen in Figure 6-33. The symbols depicted in this diagram refer to the type of RA, which was observed in the own aircraft. The probability of the TCAS induced midair collision is marked on the horizontal axis. This value refers to the observed pilot reaction of the own aircraft.

On the vertical axis, the probability of an induced collision is indicated, under the assumption that the pilot would have reacted according to the 'standard' pilot response. For the evaluation of this standard response, the vertical trajectory is not taken from actual flight data as above. Instead, the altitude and vertical rate is modelled according the 'standard' pilot response from start of the RA. This enables a comparison between the risk level resulting from the observed reaction with the hypothetical 'standard' response. The graph therefore suggests by what factor the risk would have been reduced if the crew had followed the RA according to the 'standard' response.

[23] Since the processing times depend on the used hardware, the absolute values are less important than the relative numbers between the processing times of different events

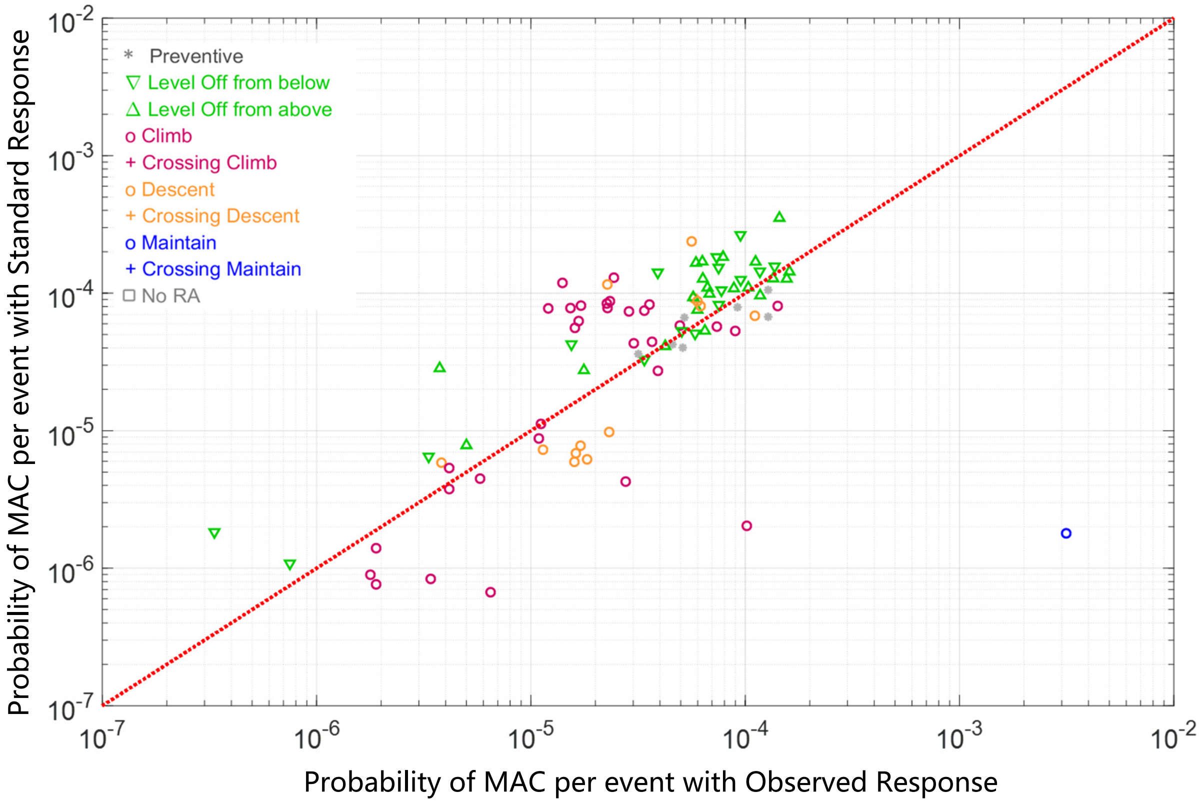

Figure 6-33 MAC probabilities for HMDs distributed as observed in radar data, observed response versus standard response, source: own research

The displayed probabilities in Figure 6-33 are based on the assumption of the observed distribution of horizontal miss distances, as discussed in chapter 6.5.3.2. This is the preferred distribution for the evaluation of the overall MAC probability of a TCAS RA within the scope of this thesis.

The shown graph can be used for a clustering of different observed pilot responses, since it directly compares the actual response with the standard response, as indicated in Figure 6-34. Results, which are located around the red dotted 45 degree-intersection-line, are associated with a 'standard' reaction. Results below the intersection line are associated with a weak reaction, and the risk is higher when compared to the 'standard' response. This is due to a weaker than expected reaction in response to the RA, and thus, a higher probability of not to reach the required separation at CPA. Results above the intersection line are an indication of overreaction.

According to the used risk model, stronger reactions are associated with less risk. This would also be true for real air traffic environment, if no other traffic than the intruder aircraft was present. However, since a stronger reaction on an RA leads to a higher probability to reach an adjacent flight level. This increases the probability for a follow-up RA against another aircraft, which has not been involved before. This effect is not considered by the risk model of this thesis.

Instead, the risk level is based solely on the one intruder aircraft, which has been taken into consideration for the particular simulation.

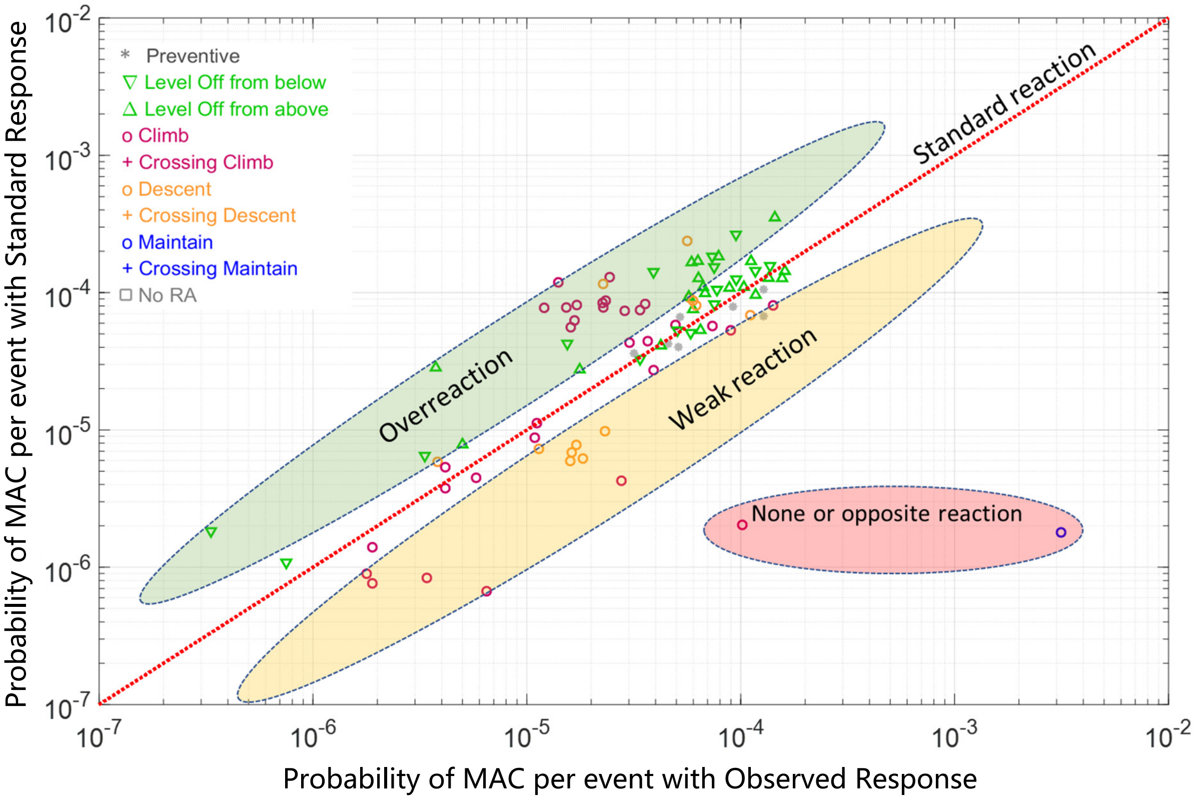

Figure 6-34 Classification of responses, source: own research

Outliers are associated with no or even opposite reactions and lead to a significantly higher risk level when compared to the 'standard' response.

Looking at the vertical axis, the range of risk levels is approximately 3 orders of magnitude, which indicates that even with a 'standard' response, different risk levels exist. Since the different types of RAs are widely distributed without any order, the differences in risk levels evolve due to different encounter geometries as well as airspaces, i.e. Sensitivity Levels with different HMD filters as well as different TCAS equipment rates, depending on the airspace.

On the horizontal axis, the range of risk levels is even higher, i.e. approximately 4 orders of magnitude. The reason for the greater variation lies in the different observed responses to the RA. The outlier on the right side, a "Maintain Vertical Speed"-RA, was an event where the flight crew reacted in the opposite direction, which results in a high probability of a vertical NMAC. Additionally, the event took place below 10,000 feet, i.e. Sensitivity Level 5, where the HMD filter is at 0.55 Nautical Miles. Therefore, the probability of a horizontal NMAC increases by a factor of 2 when compared to the upper airspace, where the HMD filter is at 1.1 Nautical Miles.

The variation of risk levels of the different TCAS events demonstrates, that it may be useful to evaluate the risk level of such events, as just counting the number of RAs does not indicate the risk, which is associated with the event. Instead, when having the risk levels of the different events, the investigation and possible mitigation work can focus on those events, which dominate the contribution to the overall risk.

From the perspective of safety management, there are different means in reducing the risk. First, the number of TCAS RAs per time unit should be reduced. Second, the risk level of each TCAS RA event should be reduced by adequate measures to follow an RA correctly. For the latter, the diagram in Figure 6-33 and Figure 6-34 can be used as a monitoring tool. TCAS RAs, which are located below the red dotted 45-degrees line shall be shifted horizontally to the left to finally reach this line. As long as the risk is higher than needed, possible measures should be taken, including:

- **Technical:** Enhancement of TCAS with technical features to automatically follow the RA (Autopilot/Flight Director TCAS) or even avoid the RA entirely (TCAS Alert Prevention TCAP) [84]
- **Human Factors:** Initial and recurrent training of flight crews regarding TCAS maneuvers
- **Organizational:** Enhancement of Flight procedures regarding TCAS.

6.7 Verification of the Results

According to a safety study of EUROCONTROL, the expected probability of an induced midair collision is $2.7 \cdot 10^{-8}$ per flight hour for aircraft equipped with TCAS Version 7.0 [102]. This probability is based on the assumption that approximately one TCAS RA is generated during 2,680 flight hours. This relationship was evaluated using European radar data, where 1269 TCAS RAs have been observed during a total of approximately 3.4 million flight hours. This results in an average induced collision risk per TCAS RA of $7.2 \cdot 10^{-5}$ [106]. This probability can be taken as a reference to compare with the evaluated induced collision risk within the risk model of this thesis.

The induced collision probability derived from the 91 analyzed TCAS RAs ranges between $3.33 \cdot 10^{-7}$ and $3.2 \cdot 10^{-3}$ per event for the observed distribution of horizontal miss distances, while the average of these values is $8.52 \cdot 10^{-5}$ per event (see Figure 6-35). This average is nearly the same as the prediction of the EUROCONTROL study.

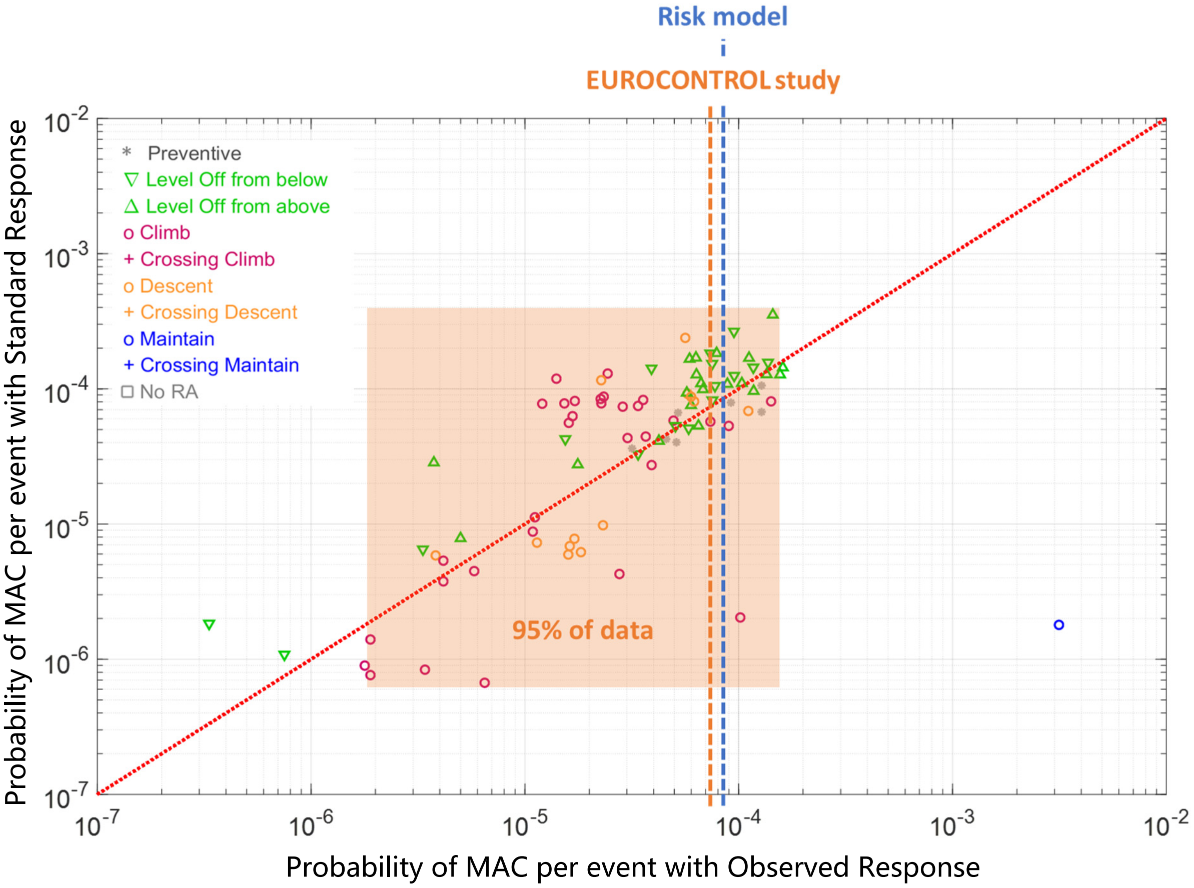

Figure 6-35 MAC probabilities for HMDs distributed as observed in radar data, observed response versus standard response, source: own research

For the uniformly distributed horizontal miss distances (see chapter 6.5.3.2), the induced collision probability ranges between $1{\cdot}10^{-6}$ and $7.1{\cdot}10^{-3}$ per event, while the average of these values is $2.16{\cdot}10^{-4}$ per event (see Figure 6-36). This value is 3 times higher than the predicted mean value of the EUROCONTROL study.

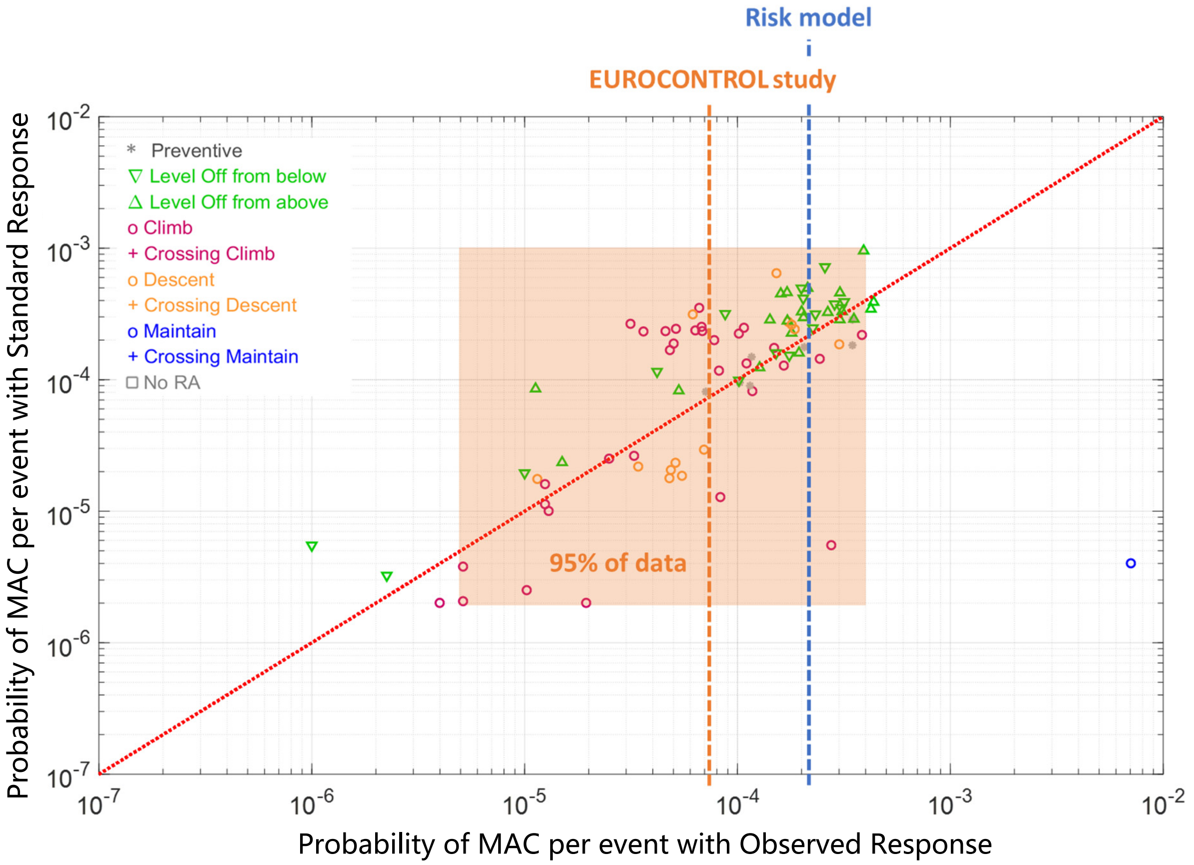

Figure 6-36 MAC probabilities for uniformly distributed HMDs, observed response versus standard response, source: own research

The results of the presented risk model show a high degree of consistency with the assumptions of the EUROCONTROL study. This shows that the risk model of this thesis is suitable to assess the risk of TCAS RA events.

7 The Risk Level of Turbulence-Induced Injuries

In this chapter, the risk of turbulence-induced injury is evaluated. The risk of turbulence has been addressed in several Safety Reports by the International Air Transportation Association (IATA) [23–25].

Turbulence is one of the major causes of injuries to passengers and cabin crew [114]. In non-fatal accidents, turbulence is the leading cause of serious and minor injury of passengers and flight attendants [115]. During the period of April 1980 to December 1997, the NTSB reported a total of 423 injuries to passengers and 186 injuries to flight attendants with even 3 passenger fatalities in that period.

The United States Federal Aviation Administration (FAA) estimates the worldwide cost of turbulence injuries is over US$100 million per year [116]. One major U.S. airline estimates their damage to be "tens of millions" dollars for customer injuries, and approximately 7,000 days of injury-related disabilities of employees each year [117].

For the evaluation of turbulence-induced injuries, not all information about the environmental conditions is contained in the flight data. Additional information from other sources is necessary, e.g. investigation data or reports. This information has to be correlated with certain measurements derived from the flight data. Therefore, in this dissertation the underlying model is referred to as a **correlation model**.

While the state of the aircraft with regard to turbulence can be defined by a certain amount of vertical acceleration, the environmental conditions, which is the probability of injury depending on the turbulence intensity, can only be evaluated with the use of additional information, such as safety reports or investigation data of incidents or accidents.

The analysis of previous flights is performed to determine the probability distribution of both, the vertical acceleration due to turbulence and the correlation between acceleration and reported injuries.

7.1 Correlation Model

Turbulence is caused by irregular movement of air, due to colliding air masses with different speeds, direction or temperature. If an aircraft flies through these varying currents of air, the aircraft starts accelerating into different directions and the smooth flight path will be disturbed. The changing accelerations during the flight are a typical indications of turbulence [115].

There are four different scenarios which can cause turbulence:

- Thunderstorm turbulence near convective weather. This type of turbulence can usually be avoided by use of weather radar.
- Clear air turbulence typically caused by jet streams in high altitudes. As this type of turbulence occurs in clear air without the presence of clouds, it is difficult to forecast and not possible to detect by means of onboard radar.
- Mountain wave turbulence caused by air which blows over a mountain range and therefore causing up- and downdrafts.
- Aircraft wake vortex turbulence caused by the aerodynamics of a preceding aircraft.

According to NTSB, approximately half of all turbulence accidents and incidents are caused by convective weather. The other half is caused by clear air turbulence [114]. The other two scenarios have no significant influence on the overall number of accidents or incidents.

Turbulence is a larger threat to passengers and cabin crew rather than to controllability of the aircraft or possible damage to the airframe. If an accident[24] or incident occurs, normally the majority of people on board receive no injuries. Typical indications of turbulence would be accelerations inflight, mainly vertical accelerations, which cause unfastened bodies and unsecured objects within the aircraft to move around uncontrolled. This typically causes injuries, when either persons are tossed around or objects fall onto persons [116]. Exposure to flight attendants is disproportionally higher than to all other occupants. According to [118] flight attendants represent about 4 percent of aircraft occupants but experienced about 52 percent of turbulence-induced serious injuries or even fatal injuries.

Basically, even light turbulences can lead to injuries depending on the overall situation in the cabin. The probability that a cabin attendant or passenger gets injured due to turbulence depends on the circumstances and therefore cannot exactly be predicted. Even though there is a certain correlation between the magnitude of turbulence and the probability of injuries on board of the aircraft, the relationship is difficult to quantify.

Some of the circumstances which influence the probability are merely by chance. On the other hand, some clearly defined recovery measures exist, which can reduce this probability when used before entering the turbulence area. This results in a vague correlation.

[24] According to ICAO Annex 13, an incident resulting in fatal or serious injury is referred to as an accident, see also page 16 [31].

Since there is a lack of systematic acquisition of injury data caused by turbulence, a risk model is developed within the scope of this thesis, which correlates accident and incident data with flight data of a major European airline [115].

7.1.1 Bow Tie Model

Based on the above facts, a bow tie model can be developed, which is shown in Figure 7-1. Possible threats, which are the cause of the turbulence, have been mentioned before. These threats are entirely environmental caused. Either the turbulence is weather related, caused by convective clouds (thunderstorm), strong high-level winds (clear air turbulence) or geographic obstacles (mountain waves). Additionally, turbulence can be caused by preceding aircraft (wave vortex).

Possible control measures, which could prevent the turbulence event, are the weather radar as well as pilot reports from preceding aircraft on a tactical basis, and weather charts on a strategical basis. The strategic planning includes re-routings, planned by flight dispatch before or during the flight, based on weather charts. This applies especially to clear air turbulence and mountain waves, as they are not possible to detect on-board [115]. Regarding wake turbulence of preceding aircraft, adequate ATC separation is the most efficient control measure [115].

The hazard in the bow tie model is the turbulence event itself, which in general causes large fluctuations in acceleration within a short timeframe.

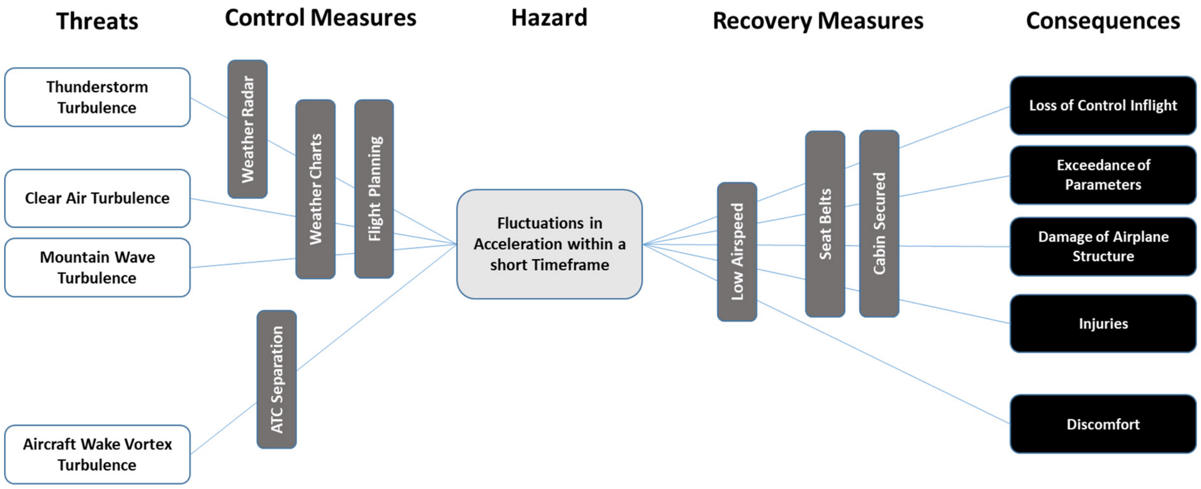

Figure 7-1 Bow tie model of turbulence, source: own research

The most important recovery measure is to fasten the seat belts during the turbulence event. This requires to switch on the seat belt signs in time, which is not always possible. However, even though the seat belt signs have been switched on, probably the cabin attendants are still working in the cabin, which rises the probability of an injury for the cabin staff. Depending on the urgency of the situation, the cabin crew may be advised to be seated. Even in this case, at least the most important tasks like securing loose cabin equipment have to be done, before the cabin crew fasten their seat belts [115]. This delay is sufficient to enhance the probability of injury to cabin staff.

Reduction of airspeed results in lower acceleration forces and thus, reduces the impact of the turbulence to the passengers and crew [119]. The position of the occupants within the airplane has an influence on injury probability. The normal acceleration at the rear part of the aircraft due to the angular acceleration is superimposed to the normal acceleration in the center of gravity. Thus, a higher probability of injury exists in the rear of the aircraft [115].

Possible outcomes of the turbulence events are at least a discomfort situation for all occupants. From the perspective of pilots, turbulence induces additional stress, the cabin crew is not able to conduct the service to the passengers, and passengers are feeling uncomfortable due to the bumpiness of the ride, which may lead to the impression that air travel is unsafe [117].

The most severe outcome is a loss of control inflight, which is very rare. More frequent are precursors of this scenario, like exceedance of aircraft parameters (fluctuating speeds causing overspeed) or damages to aircraft structure, most probably due to side effects like hail in thunderstorms etc.

However, the focus in this thesis is on injury of occupants, i.e. in most cases flight attendants or unrestrained passengers. The severity ranges from minor injuries or discomfort like falling on the ground up to fatality, which is very unlikely.

7.1.2 Definition of the Hazard

There are two requirements for the definition of the turbulence hazard. First, typical attributes of turbulence have to be identified, and second, a metric of the turbulence intensity should be incorporated, which allows a classification of the turbulence level.

The main cause for injuries and damages to aircraft related to turbulence events are the changing accelerations impacting the aircraft [120]. Accelerations are not only a typical attribute of turbulence, but also adequate for the estimation of the turbulence level.

Historically, turbulence intensity was described as either "light", "moderate", "severe" or "extreme", and was based on occupant experiences and aircraft loads, i.e. aircraft dependent [117]. An overview of this classification can be seen in Table 7-1.

Table 7-1 Classification of turbulence intensities [117]

Description	Aircraft reaction	Reaction inside aircraft	Peak of normal incremental g	RMS of normal incremental g
Light	Turbulence that momentarily causes slight, erratic changes in altitude and/or attitude (pitch, roll, yaw). Report as **Light Turbulence** or Turbulence that causes slight, rapid and somewhat rhythmic bumpiness without appreciable changes in altitude or attitude. Report as **Light Chop**.	Occupants may feel a slight strain against belts or shoulder straps. Unsecured objects may be displaced slightly. Food service may be conducted and little or no difficulty is encountered in walking.	0.2 - 0.5	0.1 - 0.2
Moderate	Turbulence that is similar to Light Turbulence but of greater intensity. Changes in altitude and/or attitude occur but the aircraft remains in positive control at all times. It usually causes variation in indicated speed. Report as **Moderate Turbulence**; or Turbulence that is similar to Light Chop but of greater intensity. It causes rapid bumps or jolts without appreciable change in aircraft or attitude. Report as **Moderate Chop**.	Occupants feel definite strains against seat belts or shoulder straps. Unsecured objects are dislodged. Food service and walking are difficult.	0.5 - 1.0	0.2 - 0.3
Severe	Turbulence that causes large, abrupt changes in altitude and/or attitude. It usually causes large variations in indicated airspeed. Aircraft may be momentarily out of control. Report as **Severe Turbulence**.	Occupants are forced violently against seat belts or shoulder straps. Unsecured objects are tossed about. Food service and walking are impossible.	1.0 - 2.0	0.3 - 0.6
Extreme	Turbulence in which the aircraft is violently tossed about and is practically impossible to control. It may causes structural damage. Report as **Extreme Turbulence**.	*[Not specified]*	≥ 2.0	≥ 0.6

Additionally, a corresponding value for the peak of normal incremental g and root mean square (RMS) of normal incremental g are provided in the table, as discussed in a NASA study [119]. Both values are based on aircraft loads. However, the RMS value is the root mean square of the normal incremental g during a 5 second sliding-window, i.e. the resulting values are of lower magnitude than the values of the peak value method. The values of both methods show a strong correlation with each other for typical commercial passenger aircraft.

A NASA study concludes, that especially the peak values of acceleration cause injuries to the aircraft occupant, if the seat belts are not used. The changes in high vertical accelerations may cause the most severe injuries, when during negative g-loads the unrestrained passengers or flight attendants will be thrown towards the ceiling of the aircraft, and thereafter they fall back on the ground during the positive g-loads, where they potentially suffer their injuries [120]. In most cases, moderate or severe turbulence is of short duration, however, the magnitude of the peaks may play a more important role than the duration of the overall turbulence event.

An example can be seen in Figure 7-2 and Figure 7-3. The very short wake vortex turbulence in Figure 7-2 has caused the same injuries as the more extensive convective turbulence from Figure 7-3. Note that the difference between the positive and negative peaks is approximately 1.5 g for both examples. The probability of such extreme turbulence levels is less than 10^{-3} per flight, using all turbulence classified events as a reference.

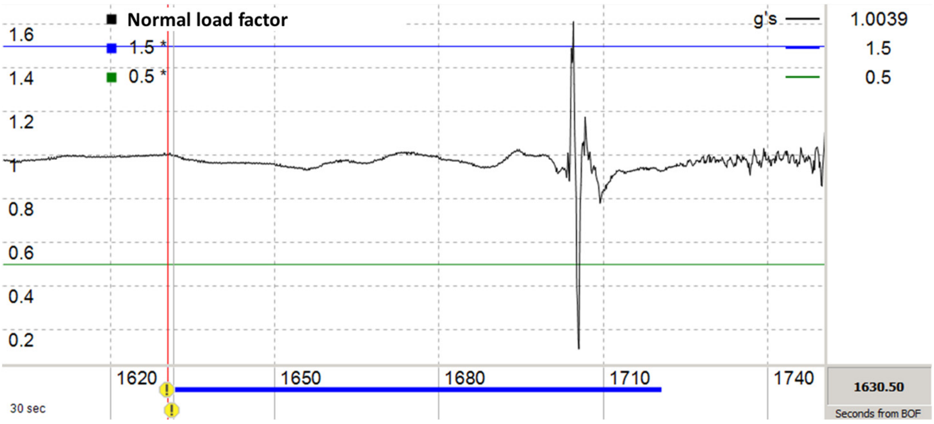

Figure 7-2 Example of load factor during a turbulence encounter (wake vortex turbulence), source: FDA

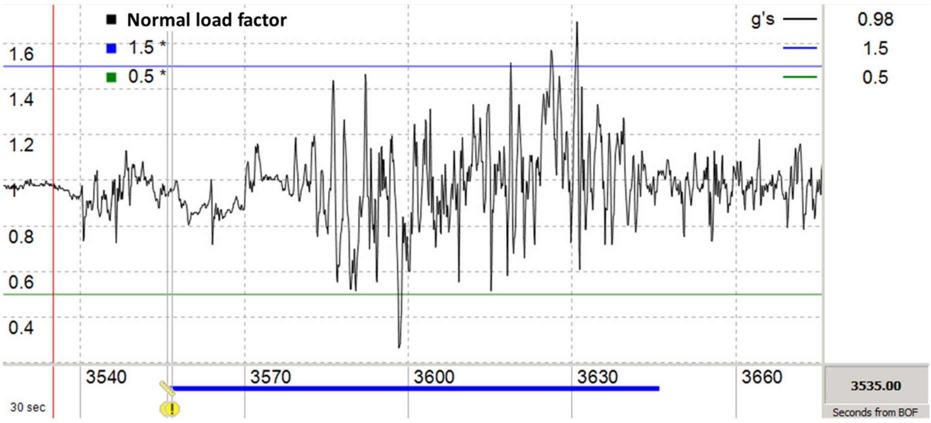

Figure 7-3 Example of load factor during a turbulence encounter (convective turbulence), source: FDA

More recent studies are focusing on an aircraft independent metric of turbulence level, the *Eddy Dissipation Rate* metric. Even though this metric also includes aircraft accelerations, it eliminates influence factors from the respective aircraft. This aircraft independent metric might be beneficial for objective turbulence reports to other aircraft, since turbulence impact on aircraft depends among others on aircraft size, speed and altitude. An aircraft independent metric is therefore better suited for turbulence reports to other aircraft.

However, for the risk of injury, the accelerations experienced on board of a specific aircraft might be more influencing. Thus, for the risk model in this thesis, the definition of the hazard is defined by the measured aircraft acceleration in the center of gravity. An appropriate measurement for the turbulence level could be the amount of change of the vertical acceleration within a defined timeframe.

A sliding window with a duration of 60 seconds is chosen to cover a higher bandwidth of acceleration peaks. The window is moved through the flight data, starting from 60 seconds after the aircraft is airborne t_{a0} to 60 seconds prior last touchdown t_{a1}. The 60 seconds delay from takeoff and landing is used to avoid a disturbance of the data by ground effects, e.g. undetected ground contact during balked landings causing an acceleration peak. The influence of turbulence on potential injury is negligible during these intervals, since all occupants are normally restrained in these phases.

The difference between the maximum and minimum value of the load factor within this sliding window is calculated in the following manner:

$$n_{z,diff}(t) = \left(\max_{[t,t+60]}(n_z) - \min_{[t,t+60]}(n_z)\right) \forall \; t \in [t_{a0}; t_{a1}]\,. \qquad \textbf{Eq. 7-1}$$

For each flight, the turbulence level $n_{z,dmax}$ will then be evaluated by using the maximum value $n_{z,diff}$ of all possible timepoints in the airborne interval described above:

$$n_{z,dmax} = \max_{t=[t_{ao},t_{a1}]} n_{z,diff}\,(t). \qquad \textbf{Eq. 7-2}$$

Figure 7-4 visualizes this method, applied on an example, where $\max_{[t,t+60]}(n_z) - \min_{[t,t+60]}(n_z) = 1.91$.

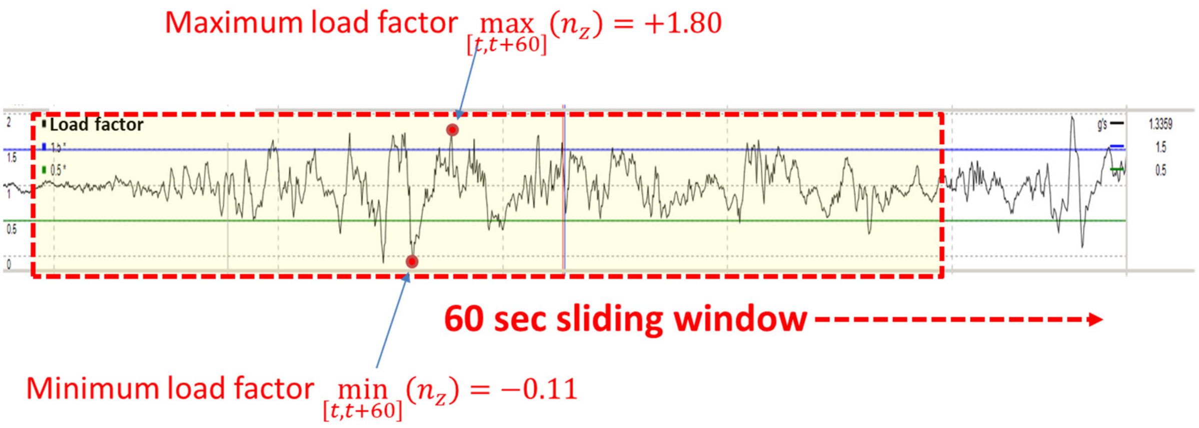

Figure 7-4 Maximum load factor difference $n_{z,diff}$ is 1.91, source: FDA, own research

The maximum difference of the load factor $n_{z,dmax}$ of each flight is from now on called the *turbulence intensity* within the scope of this thesis. The value of $n_{z,dmax}$ combined with the location within the flight defines the FDA event, on which the evaluated risk level is based.

7.2 Evaluation of the Event Risk Level

The method shown in this thesis is based on the correlation between incidents or accidents and flight data. Depending on the severity, the incidents or accidents may have been either reported by Air Safety Reports or investigated internally or by the respective authority. Most of the turbulence encounters may not have any significant impact on the occupants of the aircraft. The majority of injuries result from the failure to wear seat belts [115]. However, the probability of injury increases with higher turbulence intensities.

7.2.1 Reference Data

Reference data, i.e. the number of flights of a certain turbulence intensity, irrespective whether or not an injury occurred on the respective flight, is necessary to calculate the risk level of a turbulence event. The number of actual damages or injuries in relation to the number of reference flights for a certain turbulence intensity leads to the probability that such an injury will occur.

For the reference set of the analysis, the flight data of a major European airline has been used. 57 month of flight data (i.e. 4.75 years), containing more than 1.74 million flights, have been used for the analysis.

A normal flight, containing no turbulence, reaches a turbulence intensity of slightly above 0.3. Aircraft loads within this regime are caused by vertical trajectory changes and turns. Hence, a "turbulence intensity" in this size range is usually caused by normal flight maneuvers and is not really an indication of turbulence. The vast majority of all flights is not exceeding values above 0.4. A turbulence event is assumed to start at turbulence intensity values above 0.5, which is still very light turbulence. Approximately 17.4 percent of all flights encounter at least such turbulence.

The highest turbulence intensity value in the analyzed flight data was 2.41, which actually seriously injured one passenger and one flight attendant. Two accidents have been investigated, which occurred outside of the analyzed period, where the turbulence intensity was even higher, up to a value of 3.19.

Since especially the higher values of turbulence intensities may be generated by erroneous spikes in the flight data (example see Figure 7-5), a validation of the flight data is required.

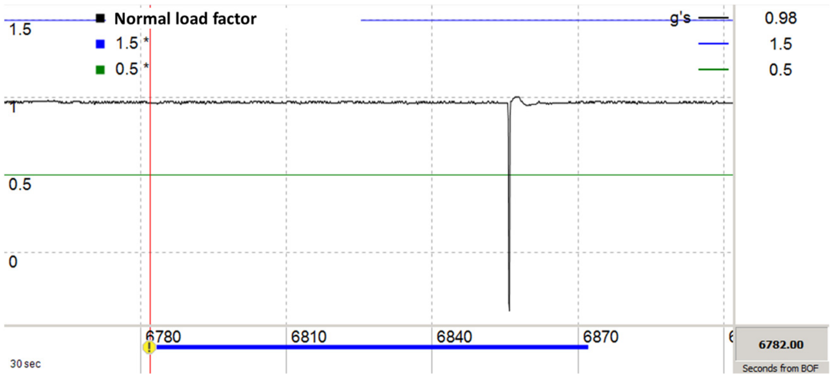

Figure 7-5 False positive due to flight data error, source: FDA

The false positive rate decreases with lower values of turbulence intensity. Therefore, all flights with a turbulence intensity of 1.25 and above have been reviewed and validated, since due to the relatively low number of events the cost benefit ratio of manual review is still acceptable. For lower values of turbulence intensity, a manual review of the data is not possible due to the high number of events. Instead, the false positive rate is estimated by the use of a random sample of 200 events for each turbulence intensity interval.

Since the relationship between incidents or accidents and a certain turbulence intensity has to be evaluated in a later stage of the analysis, the turbulence intensities have to be broken down in adequate intervals to indicate the influence of different turbulence intensities on the accident or incident probability or risk. The size of each interval of 0.25 is assumed to be a good trade-off between a sufficient number of accidents or incidents per interval, and a clear distinction between different turbulence intensities.

The respective false positive rate is then applied to the corresponding data in order to estimate the number of reference values per interval of the turbulence intensity reference set. The results can be seen in Table 7-2. Note that the estimated false positive rate is not indicated for turbulence intensities of more than 1.25, since all events were reviewed individually. Thus, the *number of valid events* in the right-hand column of the table is the result of either the application of the estimated false positive rate on the non-validated number of events, or the result of a complete review of the flight data for values greater than 1.25.

Table 7-2 False positive rate of *turbulence intensity*, source: own research

Turbulence intensity	Number of events	(Estimated) false positive rate*	Number of valid events
0.50 – 0.75	272,046	(< 1 %)	269,326
0.75 – 1.00	26,562	(2.0 %)	26,031
1.00 – 1.25	7,316	(7.0 %)	6,804
1.25 – 1.50	1274	9.5 %	1153
1.50 – 1.75	208	17.8 %	171
1.75 – 2.00	41	26.8 %	30
2.00 – 2.25	20	55.0 %	9
2.25 – 2.50	7	28.6 %	5
above 2.50	27	100.0 %	0

* Estimated values in brackets

The resulting reference set, consisting of all flights, where turbulence was encountered, can now be used for the correlation between actual injury and turbulence intensity.

Even though a large number of Air Safety Reports and incident investigations concerning turbulence are related to exceedance of flight parameters, which cause a certain amount of damage due to required maintenance actions, the focus of the analysis in this thesis is solely on injury of occupants.

Without distinguishing between different severities of the respective injuries, the probability of injury increases with higher turbulence intensities. While for low turbulence intensity, the probability of injury is less than 10^{-4} per flight, in the area of severe turbulence (turbulence intensity above a value of 2), the probability reaches values of more than 0.4 per flight. The respective correlation including the 95 percent confidence interval, based on the number of occurrences, can be seen in Figure 7-6.

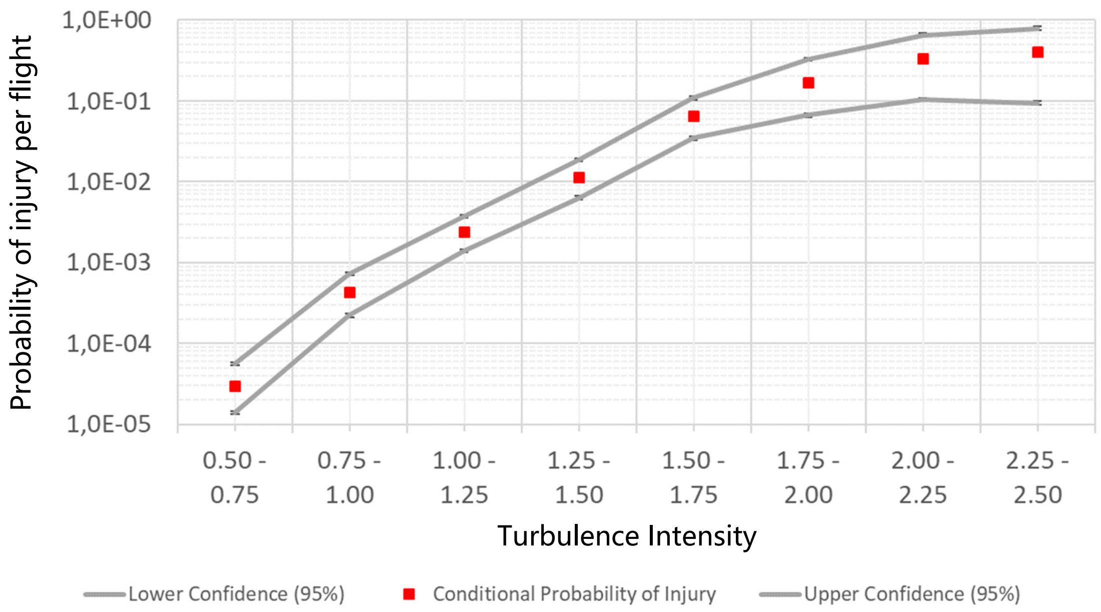

Figure 7-6 Probability of injury per flight, depending on the turbulence intensity, source: own research

However, accident data shows that not only the probability of injury increases with higher turbulence intensity, but also the severity of the injuries increases. While in the region of lower turbulence intensities only minor injuries occurred, at turbulence levels above a turbulence intensity of 1.75, also serious injuries were documented. In order to evaluate an event risk level, a differentiation between the possible accident scenarios (severities) has to be conducted.

7.2.2 Severity

The turbulence-related accident with the highest severity in the considered airline occurred in 2003 on an Airbus A340 in the U.S. airspace due to convective clouds. The accident was an outlier regarding the turbulence intensity, which was at a value of 3.19. Two passengers suffered from serious injuries, and 26 occupants were slightly injured, including 3 flight attendants [121]. The accident was classified as serious incident by the Bundesstelle für Flugunfalluntersuchung (BFU)[25] [122]. Due to the high severity, the accident meets the criteria of a ***serious incident with injuries*** according the ESC risk matrix, i.e. accident scenario *A2* [17].

Even though accident scenarios with higher severities, i.e. turbulence encounters with fatalities, have occurred in worldwide air traffic, it is assumed that the *most credible accident scenario* for the considered airline is the mentioned accident, which has been observed once in 15 years. This assumption is made, since the airline conducted 5.4 Million flights in this period without encountering any more severe accident.

[25] German investigation authority

The described accident accounts for one risk unit (1 RU). Figure 7-7 indicates other observed accident scenarios of lower severity in relation to the described accident.

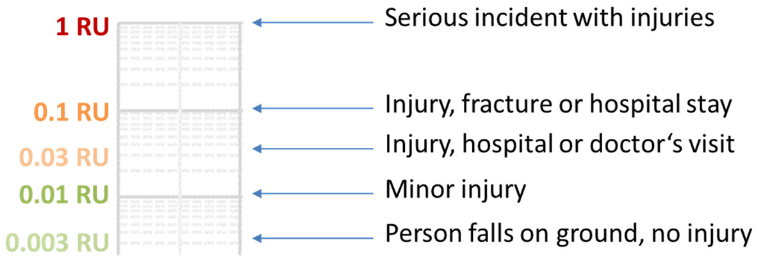
1 RU
0.1 RU
0.03 RU
0.01 RU
0.003 RU
Serious incident with injuries
Injury, fracture or hospital stay
Injury, hospital or doctor‘s visit
Minor injury
Person falls on ground, no injury

Figure 7-7 Differentiation between possible accident scenarios, logarithmic scale, source: own research

Most of the incidents and accidents are of lower severity with slight injuries, in most cases flight attendants, who are working in the cabin or securing the cabin equipment as soon as they are informed about possible turbulences by the cockpit crew. Typical descriptions about injuries are "*a passenger … minor injured*", "*one flight attendant slightly hurt*", "*3 flight attendants slightly injured*", "*one crewmember reported minor injury*", "*flight attendants complaining about minor aches*", or "*one flight attendant got injured in the hip area and burns from hot liquids*". These scenarios correspond to a ***minor injuries or damage*** scenario, *A0*, and accounts for 0.01 risk units, which is 100 times lower than the *most credible accident scenario*, *A2*. If a flight attendant is affected, usually these scenarios do not lead to a disability, and he or she is able to continue their work. If a doctor or hospital is consulted as a consequence of the injury, e.g. "*one injured flight attendant consulted a doctor*", the accident scenario is upgraded by a half accident category to *A0-A1* (0.03 RUs). In contrast, if no injury was encountered, but the situation went beyond a solely discomfort, e.g. the affected person fell to the ground without further injury, the accident scenario is downgraded by a half accident category to *An-A0* (0.003 RUs), see also Figure 7-7.

Furthermore, some incidents or even accidents happened, where the severity is in-between of above described scenarios. In these accidents, typically one passenger or flight attendant is seriously injured according the accident definition of ICAO, i.e. fractures or extended hospital stays [31]. However, in comparison to the *most credible accident scenario*, the overall impact for the airline is less severe, as the number of injured persons is limited, e.g. "*one crewmember and one passenger seriously injured. Several interior panels damaged*". This accident scenario can be described as ***incident with injuries and/or damage to aircraft***, resulting in accident scenario *A1* (0.1 RUs).

7.2.3 Probability

For the evaluation of the probability, Air Safety Reports and flight data from the same period, as mentioned above, have been analyzed and correlated to the respective flight data. In this period, 69 reports about injured occupants were filed. Due to possible insurance claims resulting from an accident at work, it can be assumed that all scenarios with at least *minor injuries* have been reported. However, for incident scenarios with lower severity, where the level of discomfort was exceeded, but no injury occurred, a significant number of unreported events exists, see also [7]. Therefore, this level is not taken into consideration.

The classification of the incident reports according Figure 7-7 results in the following scheme (see Table 7-3). For turbulence intensities below a value of 1.0, only minor or even lower injuries have been observed. Serious injuries have been observed only in the higher region of turbulence intensities, starting from a value of 1.75.

Table 7-3 Conditional probabilities of injuries, depending on turbulence level, source: own research

Turbulence intensity	Number of injury reports				Aggregated risk units (RUs)	RUs per turbulence event
	discomfort, no injury	minor	minor, hospital or doctor's visit	serious		
	(0.003 RUs)	0.01 RUs	0.03 RUs	0.1 RUs		
0.50 – 0.75	(1)	7			0.07	$2.60 \cdot 10^{-7}$
0.75 – 1.00		11			0.11	$4.23 \cdot 10^{-6}$
1.00 – 1.25		15	1		0.18	$2.64 \cdot 10^{-5}$
1.25 – 1.50	(1)	8	4		0.20	$1.73 \cdot 10^{-4}$
1.50 – 1.75		9	2		0.15	$8.77 \cdot 10^{-4}$
1.75 – 2.00		3	1	1	0.16	$5.33 \cdot 10^{-3}$
2.00 – 2.25		2	1		0.05	$5.56 \cdot 10^{-3}$
2.25 – 2.50			1	1	0.13	$2.60 \cdot 10^{-2}$

Since the event risk level does not only consists of the probability of injury, but also incorporates the severity of the injury, a transformation of the different severities towards a common metric for all different injury severities has to be conducted. An incident with an *A0* outcome can be transferred to a higher severity, using the ESC matrix. However, to ensure that the risk level is maintained through this transformation, the probability has to be lowered accordingly. The common severity for all turbulence-related injury cases is the highest possible severity, i.e. the *most credible accident scenario*.

For the turbulence-related injury, the *most credible accident scenario* was defined as *A2*. Hence, the common severity for all turbulence-related injury cases is at accident scenario A2. Therefore, the reference scenario, to which all lower severities have to be transformed, is the scenario *A2* in the ESC matrix. This ensures that all turbulence-related injuries could potentially end up at risk level *c* in the worst case.

Even though it would be sufficient for lower severities to use any lower accident scenario in the matrix, a common metric has to be used for the evaluation of an average risk level per turbulence intensity. An example can be seen in Figure 7-8, where for a particular flight a minor injury occurred, i.e. accident scenario *A0* with probability *E0*, resulting in risk level *e*. This event risk can be upgraded in terms of severity by 2 steps, and thus, the probability has to be lowered accordingly without changing the risk level.

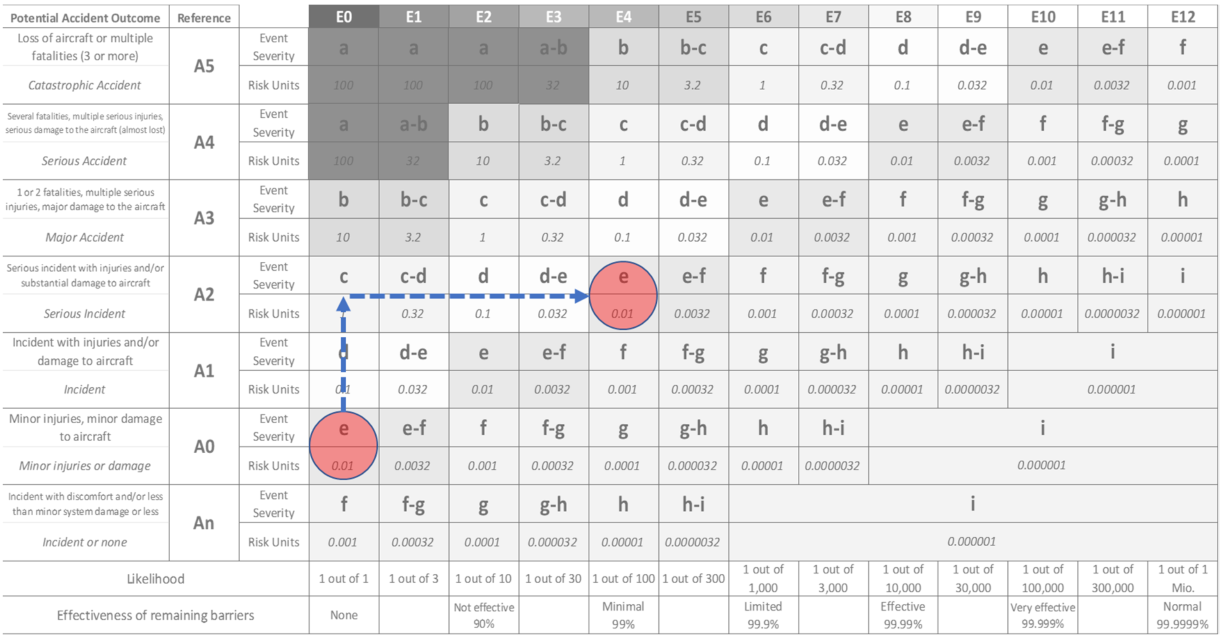

Potential Accident Outcome	Reference		E0	E1	E2	E3	E4	E5	E6	E7	E8	E9	E10	E11	E12
Loss of aircraft or multiple fatalities (3 or more)	A5	Event Severity	a	a	a	a-b	b	b-c	c	c-d	d	d-e	e	e-f	f
Catastrophic Accident		Risk Units	*100*	*100*	*100*	*32*	*10*	*3.2*	*1*	*0.32*	*0.1*	*0.032*	*0.01*	*0.0032*	*0.001*
Several fatalities, multiple serious injuries, serious damage to the aircraft (almost lost)	A4	Event Severity	a	a-b	b	b-c	c	c-d	d	d-e	e	e-f	f	f-g	g
Serious Accident		Risk Units	*100*	*32*	*10*	*3.2*	*1*	*0.32*	*0.1*	*0.032*	*0.01*	*0.0032*	*0.001*	*0.00032*	*0.0001*
1 or 2 fatalities, multiple serious injuries, major damage to the aircraft	A3	Event Severity	b	b-c	c	c-d	d	d-e	e	e-f	f	f-g	g	g-h	h
Major Accident		Risk Units	*10*	*3.2*	*1*	*0.32*	*0.1*	*0.032*	*0.01*	*0.0032*	*0.001*	*0.00032*	*0.0001*	*0.000032*	*0.00001*
Serious incident with injuries and/or substantial damage to aircraft	A2	Event Severity	c	c-d	d	d-e	e	e-f	f	f-g	g	g-h	h	h-i	i
Serious Incident		Risk Units	*1*	*0.32*	*0.1*	*0.032*	*0.01*	*0.0032*	*0.001*	*0.00032*	*0.0001*	*0.000032*	*0.00001*	*0.0000032*	*0.000001*
Incident with injuries and/or damage to aircraft	A1	Event Severity	d	d-e	e	e-f	f	f-g	g	g-h	h	h-i	i		
Incident		Risk Units	*0.1*	*0.032*	*0.01*	*0.0032*	*0.001*	*0.00032*	*0.0001*	*0.000032*	*0.00001*	*0.0000032*	*0.000001*		
Minor injuries, minor damage to aircraft	A0	Event Severity	e	e-f	f	f-g	g	g-h	h	h-i	i				
Minor injuries or damage		Risk Units	*0.01*	*0.0032*	*0.001*	*0.00032*	*0.0001*	*0.000032*	*0.00001*	*0.0000032*	*0.000001*				
Incident with discomfort and/or less than minor system damage or less	An	Event Severity	f	f-g	g	g-h	h	h-i	i						
Incident or none		Risk Units	*0.001*	*0.00032*	*0.0001*	*0.000032*	*0.00001*	*0.0000032*	*0.000001*						
Likelihood			1 out of 1	1 out of 3	1 out of 10	1 out of 30	1 out of 100	1 out of 300	1 out of 1,000	1 out of 3,000	1 out of 10,000	1 out of 30,000	1 out of 100,000	1 out of 300,000	1 out of 1 Mio.
Effectiveness of remaining barriers			None		Not effective 90%		Minimal 99%		Limited 99.9%		Effective 99.99%		Very effective 99.999%		Normal 99.9999%

Figure 7-8 Transformation of severity in the ESC matrix from chapter 2.6.3, source: own research

For each step of severity upgrade, the probability has to be decreased by a factor of 10 in order to maintain the respective risk level. In an ideally constructed risk matrix, the relationship between the numbers of events with the respective risk levels shall be the same as the relationship between the corresponding probabilities, i.e. for 1 event with risk level *c*, approximately 100 events with risk level *e* are expected to occur. Using the numbers of Table 7-3, extrapolated to the amount of different injuries, which can be expected after a period of 15 years, for the one serious incident with injuries (*A2*), which occurred in the considered airline in this period, approximately 6 injuries (*A1*) and 174 minor injuries (*A0*) can be expected (see Figure 7-9).

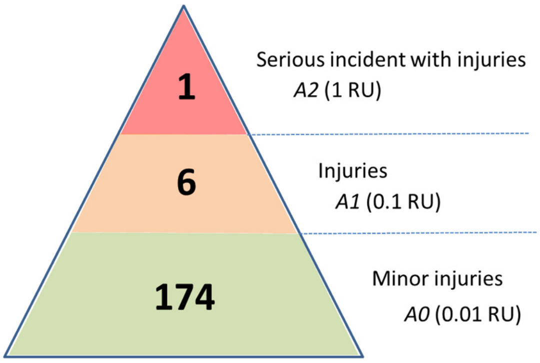

Figure 7-9 Heinrich pyramid showing the relationship between different severities

The same effect as a shift in severity is the use of the respective risk units (RUs), which is an adequate common metric, as discussed in chapter 2.6. The respective risk units, depending on the different injury severities, can be aggregated for each turbulence intensity segment, as shown in Table 7-3. This aggregated number of risk units, when divided by the number of reference flights, indicates the average amount of risk units, which can be expected per turbulence event, depending on the turbulence intensity. This equals the conditional probability of the *most credible accident scenario*, i.e. conditional probability of an *A2* accident. These average amounts of risk units per turbulence events can be seen in Table 7-4 for the analyzed data set. In Figure 7-10, this tabular data can be seen in a graph. This graph also includes the 95-percent confidence intervals of the risk units per turbulence event for different turbulence intensities in steps of 0.25 each. The confidence intervals are based on the overall number of injury reports per segment of turbulence intensity. However, the distribution of the different severities within a certain segment of turbulence intensity is assumed to be equal as the distribution contained in Table 7-4 for the respective turbulence intensity segment.

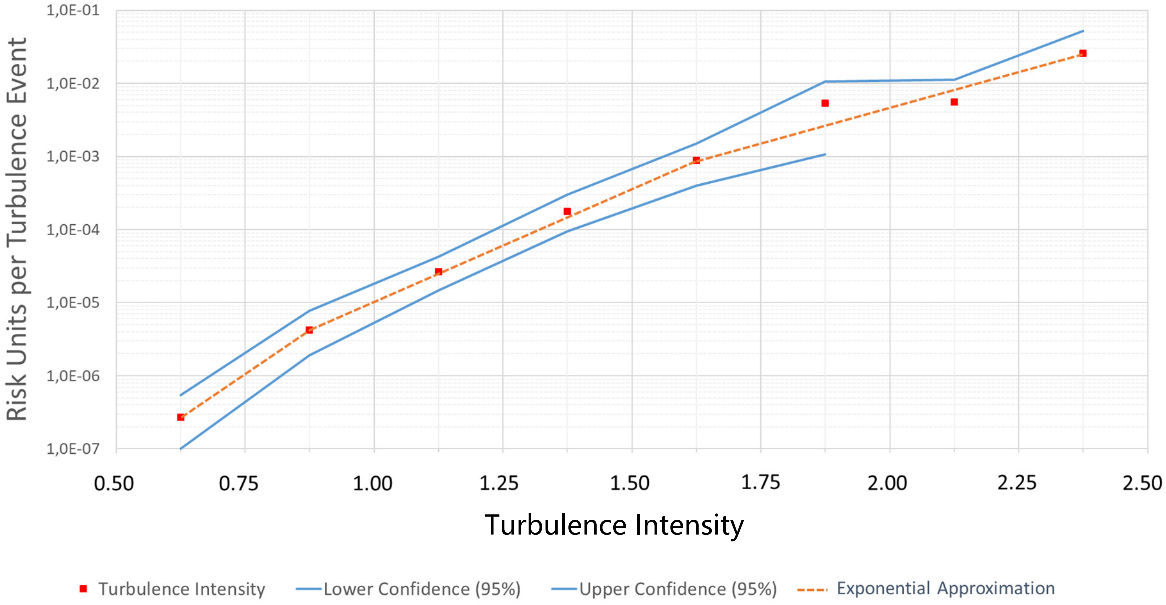

Figure 7-10 Risk Units per turbulence event, depending on turbulence intensity, source: own research

Note, that the lower confidence levels for turbulence intensities above 2.0 are not indicated, since these levels are at 0 due to the low number of injury reports. Nevertheless, the exponential approximation, as indicated in the graph, is located within the confidence bounds.

The risk units per turbulence events, which per definition are indicating the conditional probability of a serious incident scenario *A2*, can be described by an exponential trend line. Since the gradient becomes smaller with higher turbulence intensities, it is useful to segment the trendline in order to reduce the average error. A segmentation into 3 different parts results in the following equations:

$$p(A2) = \begin{cases} 1.7 \cdot 10^{-8} \cdot e^{2.7467 \cdot \left(\frac{n_{z,dmax}-0.375}{0.25}\right)}, \text{if } n_{z,dmax} < 0.875,\ R^2 = 1 \\ 1.2 \cdot 10^{-7} \cdot e^{1.7902 \cdot \left(\frac{n_{z,dmax}-0.375}{0.25}\right)}, \text{if } (n_{z,dmax} \geq 0.875) \wedge (n_{z,dmax} < 1.625),\ R^2 = 0.999 \\ 3.1 \cdot 10^{-6} \cdot e^{1.1279 \cdot \left(\frac{n_{z,dmax}-0.375}{0.25}\right)}, \text{if } n_{z,dmax} \geq 1.625,\ R^2 = 0.978\,. \end{cases} \tag{Eq. 7-3}$$

with a coefficient of determination, R^2, ranging between 1 and 0.978, depending on the respective segment. By means of this parametrization, it becomes possible to calculate the conditional probability of an *A2*-outcome for every turbulence intensity.

However, due to the limited analysis period, the risk model is not yet complete, since no incident fell into this period with a severity above *A1*. Also, reference data with turbulence intensities beyond 2.5 is lacking. Since serious incidents or accidents are normally documented very well, incidents with higher severities, which fall into an extended period beyond the analyzed data, can be used.

One accident report has been taken into consideration, falling into a 10 years-period, i.e. extending the period containing the reference flight data. This accident was a serious injury of a flight attendant, occurring during a turbulence intensity of 2.61, i.e. a turbulence intensity which was not yet observed in the analysis period described before.

Moreover, the most credible accident scenario, which has been described before, was an accident, which falls into a 15 years-period and is thereby extending the period, where reference flight data is available.

However, for both the 10-years period as well as for the 15-years period, no reference flights are available. Obviously, some flights must have exceeded a turbulence intensity of 2.5 in this extended period, as indicated by the described accidents. The number of reference flights for turbulence intensities above 2.5 has therefore to be estimated.

For this estimation, the peak over threshold (POT) method can be used. The respective threshold value is selected at a turbulence intensity of 1.75, the distribution of the observed values above this threshold in the analyzed reference data set is displayed in Figure 7-11.

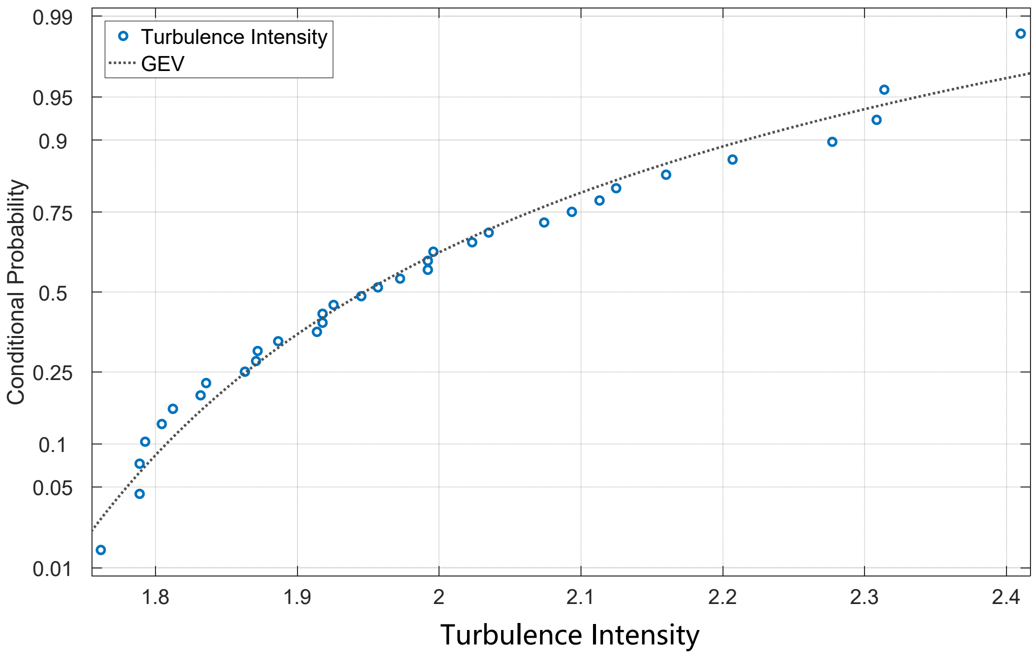

Figure 7-11 Conditional probability of different turbulence intensities, source: own research

For the extrapolation of this data, a parametrization of the data is required. For the POT method, a Generalized Extreme Value distribution (GEV) can be used, consisting of location parameter μ, scale parameter σ, and shape parameter k [82]:

$$p(n_{z,dmax}|n_{z,dmax} \geq 1.75\ ) = \left(\frac{1}{\sigma}\right) \cdot exp\left(-\left(1+k\frac{(n_{z,dmax}-\mu)}{\sigma}\right)^{-\frac{1}{k}}\right) \cdot \left(1+k\frac{(n_{z,dmax}-\mu)}{\sigma}\right)^{-1-\frac{1}{k}}, \qquad \textbf{Eq. 7-4}$$

with parameters $k = 0.131$, $\sigma = 0.120$ and $\mu = 1.902$. The Kolmogorov-Smirnov hypothesis test results in a p-value of 0.996, which indicates an adequate fit of Eq. 7-4 to the data of a turbulence intensity beyond 1.75.

The extrapolation of the data, based on above Equation, up to a value of 3.5, is provided in Table 7-4. The value of 3.5 is used as the upper limit of consideration, since this value is the design limit of an average passenger aircraft [68].

The probability of $n_{z,dmax}$ equal to or greater than 1.75 can be calculated by the relationship between number of reference flights with a turbulence intensity of at least 1.75 by the total number of reference flights, resulting in a value of $2.53 \cdot 10^{-5}$ per flight.

Table 7-4 Extrapolation of reference flights per turbulence intensity class, source: own research

Turbulence intensity greater than	Conditional probability	Probability	Events expected per year*	Events expected every *x* years*
2.00	0.3691	$9.34 \cdot 10^{-6}$	3.362	0.3
2.25	0.0818	$2.07 \cdot 10^{-6}$	0.745	1.3
2.50	0.0212	$5.36 \cdot 10^{-7}$	0.193	5.2
2.75	0.0067	$1.70 \cdot 10^{-7}$	0.061	16.4
3.00	0.0024	$6.07 \cdot 10^{-8}$	0.022	45.7
3.25	$9.91 \cdot 10^{-4}$	$2.51 \cdot 10^{-8}$	0.009	110.8
3.50	$4.45 \cdot 10^{-4}$	$1.13 \cdot 10^{-8}$	0.004	246.7

* with 360,000 flights per year

The data in Table 7-4 indicates, that a turbulence intensity of 3.19 is a significant outlier, which is expected to occur less than once every 45 years in average. Since the occurrence of such a high level of turbulence intensity is a very rare event, it is assumed, that the one experienced incident was the only occurrence of such a turbulence intensity. As this turbulence lead to a serious incident *A2*, it is assumed that the conditional probability of *A2* at this turbulence intensity is at 100 percent (see marker ② in Figure 7-12).

According to Table 7-4, a turbulence intensity between 2.50 and 2.75 is expected to occur 0.132 times per year, assuming 360,000 flights in total per year. Thus, in a 10-years period, this level of turbulence intensity is expected only 1.3 times. In this 10-years period, one accident with accident scenario *A1* (0.1 RUs) occurred, so an average risk level of 0.1 RUs per 1.3 occurrences of the respective turbulence intensity, i.e. 0.077 RUs per occurrence, is expected in average (see marker ① in Figure 7-12), without considering any confidential intervals. This equals a probability of 0.077 for accident scenario A2 per turbulence event in the range between 2.5 and 2.75.

However, since the number of reference flights are based on an average estimate, the confidence interval is difficult to obtain for the high-risk levels. The values are based on average values only. Also, in some cases it is difficult to estimate a precise accident scenario in terms of severity, since the respective accident may be difficult to categorize. Thus, the estimation of a distinct risk level for higher turbulence intensities comes to a certain limit.

Nevertheless, an extrapolation of the upper part of Eq. 7-3 fits very well both accidents, which have been described above. The respective coefficient of determination is $R^2 = 0.978$.

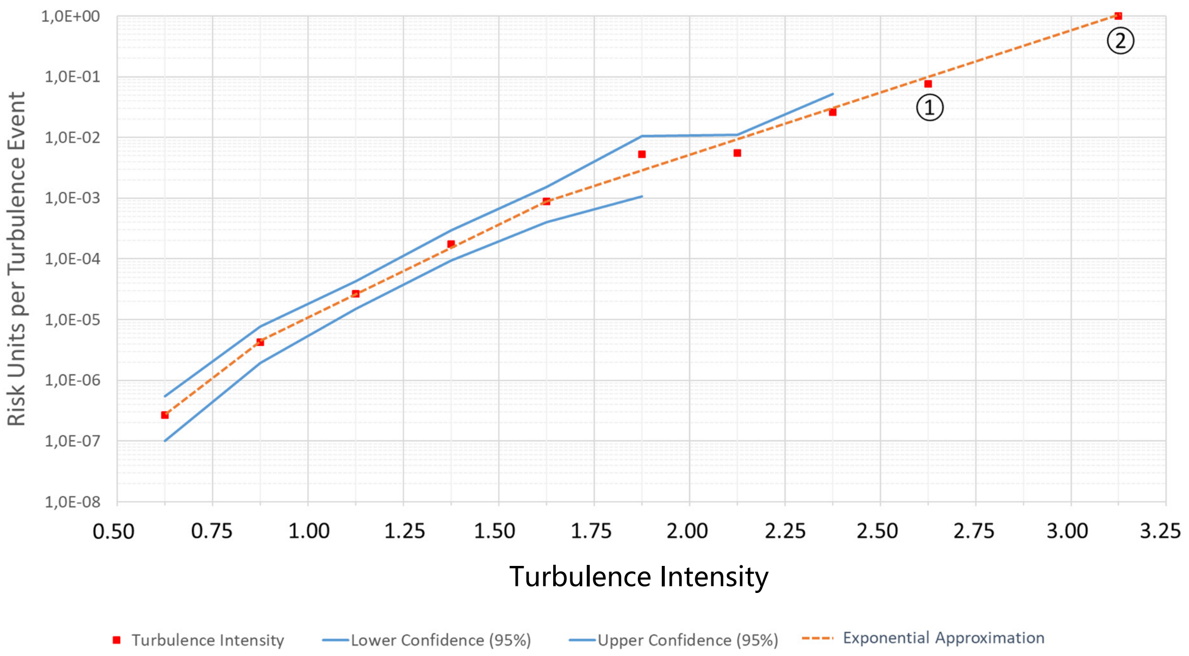

Figure 7-12 Risk Units per flight, depending on turbulence intensity, source: own research

The parametrization of the correlation between risk units per turbulence event and turbulence intensity enables the precise evaluation of the risk level of any turbulence encounter event in FDA. The results from Figure 7-12, thus, allow an event risk classification, based on injury probability, without knowing any details about the outcome of a particular flight. In fact, even if the seatbelt signs have been switched on, there is still the probability of injury, since flight attendants may still finish their cabin preparation, or passengers may disregard the seatbelt signs. This unpredictable correlation is reflected by equal treatment of all events with the same turbulence intensity.

The aggregated risk units of all turbulence events, whether or not an actual injury occurred, reflects therefore the sum of all actual incidents.

For selected risk levels, the average turbulence intensities which lead to these risk levels are provided in Table 7-5.

Table 7-5 Definition of the different event risk levels, depending on turbulence intensity

probability **risk level**	10^{-4} g	$3.3 \cdot 10^{-4}$ f-g	10^{-3} f	$3.3 \cdot 10^{-3}$ e-f	10^{-2} e	$3.3 \cdot 10^{-2}$ d-e	10^{-1} d	$3.3 \cdot 10^{-1}$ c-d	1 c
Turbulence intensity	1.32	1.48	1.67	1.91	2.17	2.42	2.68	2.85	≥ 3.06

If the turbulence intensity of a certain flight is around 1.67, the probability of an *A2* outcome, i.e. serious incident with injuries, is 10^{-3} per flight in average. This corresponds to a probability of 1:10 ending up in a minor injury.

8 Conclusion and Outlook

8.1 Conclusion

The objective of the present work was to enable a data-driven and thus objective quantification of risks of defined safety events in aviation based on Flight Data Analysis. In this context, it should not only be possible to make a statistical prediction, but rather to determine the risk level for each individual flight in a retrospective analysis.

The idea was to look at the state of the aircraft in the context of the environmental conditions. While the aircraft state can be derived directly from the flight data, it is not possible to provide a common approach for modeling the environmental conditions due to the diversity of different aviation risks and the associated data availability.

The different types of these models were exemplarily developed using three highly relevant accident risk categories: runway overrun, TCAS-induced midair collision and turbulence-induced injuries.

The comparison of the obtained results of these models with real accident data results in a high degree of consistency, which clearly demonstrates the practical relevance of the new method.

For the first example, the runway overrun, the required friction for the landing was compared with the statistically available friction and thus the probability of an overrun was determined. The required friction could be determined from the aircraft state, while the available friction could be statistically determined from the observation of past landings. Since the available friction cannot be measured directly, two novel methods were developed in the context of this dissertation to determine the distribution of this friction: The region of high coefficients of friction could be modelled by correlation between BPD and deceleration. For the low friction region, landings were considered where autobrake was used and the target deceleration could not be achieved. By means of a POT method, the corresponding distribution could be calculated.

In the second example the risk of a TCAS-induced midair collision could be determined for the first time by using the flight trajectory of the own aircraft in combination with a statistical model of the state of the intruder, which represents the environmental conditions. This model was based on both a system model of TCAS and a pilot model, which represents the behavior of the flight crew of the intruder. By this means it has become possible to determine the corresponding collision risk for each TCAS RA.

In the third example, the risk of turbulence-induced injuries was determined. The aircraft state in terms of acceleration was correlated with a large number of air safety reports and accident reports on injuries. From these correlations a model of the environmental conditions was developed. This method allows the risk of injury to be predicted at certain turbulence intensities.

The new data-driven method allows each flight to be evaluated independently of the estimated level of risk and therefore enables a comprehensive risk picture. In contrast, the existing methods, which were primarily based on expert estimation, were limited by the available resources. The novel method of objective risk assessment enables the measurement of an organization's safety performance by aggregating the individual risks, which is required by the ICAO and EASA within the framework of a matured SMS. This dissertation thus represents a significant contribution to achieving this goal.

8.2 Outlook

The examples presented here represent only a small excerpt of the possible accident categories to which the new method can be applied.

The physical model of the runway overrun can be extended to other aircraft types. The results may be refined by using the actual aerodynamic parameters, provided that they are made available by the manufacturer or can otherwise be obtained. The physical model of the environmental conditions can also be extended to other aspects of a runway excursion. This has been successfully accomplished in the area of runway overrun during takeoff as part of an operational risk analysis [123]. A suitable physical model can also be applied to the hard landing and tail strike categories to determine the associated risks.

The system model of the TCAS presented in this paper can be extended by the modified Reversal Logic of the new version 7.1. In combination with a suitable pilot model, a system model can also be developed for other last line of defense warning systems, for example for the Ground Proximity Warning System.

The correlation model could also be used for other accident categories, for example by correlating landing impacts with maintenance actions performed to determine the risks in the hard landing category.

The method presented here has a high practical relevance. I have used the results of this new method in practical safety management. Due to the now possible objective risk determination of safety events in aviation, the subjective component could in future be limited to the development of the underlying risk models. I would very much appreciate if this work could contribute a part to that.

Bibliography

*Note: Sources marked with an asterisk * are not publicly available.*

[1] Boeing Commercial Airplanes, *Statistical Summary of Commercial Jet Airplane Accidents - Worldwide Operations 1959-2016*, Seattle, WA, USA, 2017. Available: https://www.skybrary.aero/bookshelf/books/4239.pdf. [Accessed December 18, 2017].

[2] International Civil Aviation Organization (ICAO), *Doc 9859, Safety Management Manual (SMM)*, 3rd ed., Montréal, Canada, 2013. Available: https://www.icao.int/safety/SafetyManagement/Documents/Doc.9859.3rd Edition.alltext.en.pdf. [Accessed February 16, 2016].

[3] International Civil Aviation Organization (ICAO), *Doc 9859, Safety Management Manual (SMM)*, 2nd ed., Montréal, Canada, 2009. Available: https://www.icao.int/safety/fsix/Library/DOC_9859_FULL_EN.pdf. [Accessed February 19, 2016].

[4] European Aviation Safety Agency (EASA), *Annual Safety Review 2017*, Cologne, Germany, 2017. Available: https://www.easa.europa.eu/sites/default/files/dfu/209735_EASA_ASR_MAIN_REPORT_3.0.pdf. [Accessed December 18, 2017].

[5] European Commission, *Flightpath 2050*, Luxembourg, 2011. Available: http://ec.europa.eu/transport/modes/air/doc/flightpath2050.pdf. [Accessed January 28, 2018].

[6] R. Bowen, *Do more regulations equal less safety?* Arlington, USA: Mercatus Center at George Mason University, 2013. Available: https://www.mercatus.org/system/files/More-Regulations-Less-Safety.pdf. [Accessed February 21, 2016].

[7] J. Mickel, *Bewertung operationeller Flugrisiken*, Dissertation (Johann Wolfgang Goethe-Universität Frankfurt am Main), Aachen, Germany: Shaker Verlag, 2011.

[8] International Civil Aviation Organization (ICAO), *Global Aviation Safety Plan*, Montréal, Canada, 2007. Available: https://www.icao.int/safety/afiplan/Documents/Documents/Global Aviation Safety Plan.pdf. [Accessed February 19, 2016].

[9] European Commission, “Commission Regulation (EC) No 965/2012 of 5 October 2012,” *Official Journal of the European Union*, issue L 296, pp. 1–148, 2012. Available: https://eur-lex.europa.eu/LexUriServ/LexUriServ.do?uri=OJ:L:2012:296:0001:0148:EN:PDF. [Accessed January 28, 2018].

[10] J. Nisula, “From Safety Indicators to Measuring Risk – the Risk-Guided Transport Safety Agency,” In Proc. Int. Conf. Human-Computer Interact. Aerosp., 2014. Available: https://arkisto.trafi.fi/filebank/a/1434456797/19018fa995da55930a03c3af8bc4f1ed/17872-Nisula_From_Safety_Indicators_to_Measuring_Risk.pdf. [Accessed October 7, 2016].

[11] European Authorities coordination group on Flight Data Monitoring (EAFDM), *Developing Standardised FDM-Based Indicators*, Cologne, Germany, 2016. Available: https://www.easa.europa.eu/sites/default/files/dfu/EAFDM__standardised_FDM-based_indicators_v2_Ed2017.pdf. [Accessed February 16, 2018].

[12] European Aviation Safety Agency (EASA), *Report - European Aviation Safety Plan 2012-2015*, Cologne, Germany, 2012. Available: https://www.easa.europa.eu/sites/default/files/dfu/sms-docs-European-Aviation-Safety-Plan-(EASp)-2012-2015--v1.0-FINAL.pdf. [Accessed February 1, 2018].

[13] Civil Aviation Authority (CAA), *CAP 739 Flight Data Monitoring*, Gatwick Airport South, UK,

2013. Available: https://publicapps.caa.co.uk/docs/33/CAP739.pdf. [Accessed February 12, 2018].

[14] G. van Es, K. Tritschler, M. Tauss, *Development of a Landing Overrun Risk Index*, 2009. [Online]. Available: https://reports.nlr.nl/xmlui/bitstream/handle/10921/235/TP-2009-280.pdf?sequence=1&isAllowed=y. [Accessed February 16, 2016].

[15] * Austin Digital, *Event Measurement System (EMS)*. [Software program]. Austin, TX, USA: Austin Digital, Inc., 2000.

[16] Aviation Risk Management Solutions (ARMS) Working Group, *The ARMS Methodology for Operational Risk Assessment in Aviation Organisations*, 2010. [Online]. Available: https://skybrary.aero/bookshelf/books/1141.pdf. [Accessed February 16, 2016].

[17] * J. Mickel, S. Krämer, *Single Event / Incident Severity Classification for FODA and AII-Team*, Frankfurt, Germany, 2016.

[18] G. van Es, “Running Out of Runway - Analysis of 35 Years of Landing Overrun Accidents,” 2005. [Online]. Available: https://reports.nlr.nl/xmlui/bitstream/handle/10921/549/TP-2005-498.pdf?sequence=1&isAllowed=y. [Accessed February 16, 2016].

[19] L. Drees, *Predictive Analysis: Quantifying Operational Airline Risks*, Dissertation (Technische Universität München TUM), Munich, Germany: Verlag Dr. Hut, 2017.

[20] * C. Wang, “Visualisierung und Analyse von FODA-Daten am Beispiel Tailstrike,” Unpublished Bachelor’s Thesis (Technische Universität München TUM), Munich, Germany, 2011.

[21] C. Wang, L. Drees, F. Holzapfel, “Extracting measurements from operational flight data using the flare example,” In Proc. AIAA Model. Simul. Technol. Conf., 2016.

[22] * M. Butter, J. Mickel, “Die Wahrscheinlichkeit eines Landeunfalls,” *CF-Information*, issue 1, pp. 3–14, 2007.

[23] International Air Transport Association (IATA), *Safety Report 2016*, Montréal, Canada, 2017.

[24] International Air Transport Association (IATA), *Safety Report 2014*, Montréal, Canada, 2015.

[25] International Air Transport Association (IATA), *Safety Report 2015*, Montréal, Canada, 2016.

[26] Federal Aviation Administration (FAA), “Safety Management System Basis,” 2017. [Online]. Available: https://www.faa.gov/about/initiatives/sms/explained/basis/. [Accessed December 22, 2017].

[27] A. Roelen, *Causal risk models of air transport - Comparison of user needs and model capabilities.*, Amsterdam, Netherlands: IOS Press, 2008.

[28] A. Roelen, M.B. Klompstra, “The challenges in defining aviation safety performance indicators,” 2012. [Online]. Available: http://www.proceedings.com/16286.html. [Accessed February 16, 2016].

[29] International Traffic Safety Data and Analysis Group (IRTAD), *Road Safety Annual Report 2015 Summary*, Paris, France, 2015.

[30] European Organisation for the Safety of Air Navigation (Eurocontrol), *ACAS II Bulletin No 18*, Brussels, Belgium, 2015. Available: https://www.skybrary.aero/bookshelf/books/3166.pdf. [Accessed November 10, 2016].

[31] International Civil Aviation Organization (ICAO), *Annex 13 Aircraft Accident and Incident Investigation*, Montréal, Canada, 2010.

[32] H.W. Heinrich, *Industrial Accident Prevention*, New York, USA: McGraw-Hill, 1931.

[33] Global Aviation Safety Network, *Operator’s Flight Safety Handbook*, 2001. [Online]. Available: https://flightsafety.org/wp-content/uploads/2016/09/OFSH_english.pdf. [Accessed September 11, 2016].

[34] Z. Nazeri, G. Donohue, L. Sherry, “Analyzing Relationships Between Aircraft Accidents and Incidents,” In Proc. Int. Conf. Res. Air Transp., 2008. Available: https://pdfs.semanticscholar.org/d392/018b8fa28140800fe88cdcf6cf1d09869c4b.pdf. [Accessed October 16, 2016].

[35] International Civil Aviation Organization (ICAO), *Doc 9859, Safety Management Manual (SMM)*, 1st ed., Montréal, Canada, 2006.

[36] J. Reason, *Human Error*, 19th ed., New York, USA: Cambridge University Press, 2008.

[37] J. Reason, “Human Error: Models and Management.,” *BMJ (Clinical research ed.)*, vol. 320, issue 7237, pp. 768–70, 2000. Available: https://www.ncbi.nlm.nih.gov/pmc/articles/PMC1117770/?tool=pmcentrez&report=abstract. [Accessed February 20, 2016].

[38] Australian Transport Safety Bureau, *In-flight uncontained engine failure A380-842, VH-OQA*, Canberra, Australia, 2013. Available: https://www.atsb.gov.au/media/4173625/ao-2010-089_final.pdf. [Accessed January 16, 2018].

[39] European Commercial Aviation Safety Team (ECAST), *Guidance on Hazards Identification*, 2009. [Online]. Available: https://www.easa.europa.eu/sites/default/files/dfu/ECASTSMSWG-GuidanceonHazardIdentification1.pdf. [Accessed January 16, 2018].

[40] S.S. Alizadeh, P. Moshashaei, “The Bowtie method in safety management system : A literature review,” *Scientific Journal of Review*, vol. 4, pp. 133–138, 2015.

[41] J. Franklin, “European Risk Classification Scheme Development - Taxonomy Update,” In Proc. 7th IORS Work., 2017.

[42] B. Bottomley, *OCCUPATIONAL HEALTH & SAFETY MANAGEMENT SYSTEMS : STRATEGIC ISSUES REPORT*, Sydney, Australia: National Occupational Health and Safety Commission, 1999.

[43] M. Thomas, *A systematic review of the effectiveness of safety management systems*, Canberra, Australia, 2012. Available: http://www.atsb.gov.au/media/4053559/xr2011002_final.pdf. [Accessed February 16, 2016].

[44] Environment Protection Authority, *Becoming a harms-based regulator – developing a problem-solving culture*. Adelaide, Australia: 2013. Available: https://www.epa.sa.gov.au/files/4771767_change_harms.pdf. [Accessed February 18, 2016].

[45] European Aviation Safety Agency (EASA), *Acceptable Means of Compliance (AMC) and Guidance Material (GM) to Part-ORO*, Cologne, Germany, 2013. Available: https://www.easa.europa.eu/sites/default/files/dfu/04 Part-ORO %28AMC-GM%29_Amdt2-Supplementary document to ED Decision 2013-019-R.pdf. [Accessed February 18, 2016].

[46] J. Verstraeten, A. Roelen, L. Speijker, “Safety Performance Indicators for System of Organizations in Aviation,” In Proc. ASCOS — Aviat. Saf. Certif. New Oper. Syst., 2014. Available: https://www.ascos-project.eu/downloads/ascos_paper_verstraeten.pdf. [Accessed February 19, 2016].

[47] Safety Management International Collaboration Group (SMICG), *Measuring Safety Performance Guidelines for Service Providers*, 2013. [Online]. Available: https://www.skybrary.aero/bookshelf/books/2395.pdf. [Accessed February 19, 2016].

[48] ATR Training Center, *Flight Data Monitoring on ATR Aircraft*, Blagnac cedex, France, 2016. Available: https://www.easa.europa.eu/sites/default/files/dfu/16T0153_ATR_FDM_2016.pdf. [Accessed March 17, 2018].

[49] International Civil Aviation Organization (ICAO), *Flight Data Analysis Programme Manual*, Montréal, Canada, 2013.

[50] European Commission, “Commission Regulation (EC) No 859/2008 of 20 August 2008,” *Official Journal of the European Union*, issue L 254, pp. 1–238, 2008. Available: https://eur-lex.europa.eu/legal-content/EN/TXT/PDF/?uri=CELEX:32008R0859&from=DE. [Accessed March 21, 2018].

[51] Skybrary, “Flight Data Recorder (FDR),” *skybrary.aero*, December 13, 2017. [Online]. Available: https://www.skybrary.aero/index.php/Flight_Data_Recorder_(FDR). [Accessed March 24, 2018].

[52] N.A.H. Campbell, “The Evolution of Flight Data Analysis,” 2007. [Online]. Available: https://asasi.org/papers/2007/The_Evolution_of_Flight_Data_Analysis_Neil_Campbell.pdf. [Accessed March 21, 2018].

[53] Civil Aviation Authority (CAA), *CAP 731 Approval, Operational Serviceability and Readout of Flight Data Recorder Systems and Cockpit Voice Recorders*, Gatwick Airport South, UK, 2011. Available: https://publicapps.caa.co.uk/docs/33/CAP731.PDF. [Accessed April 1, 2018].

[54] * M. Jäger, “FODA und das 1000 ft - Gate,” *CF-Information*, issue 01, pp. 6–13, 2003.

[55] M. Butter, “Evaluation of the risk of runway overrun using flight data monitoring,” In Proc. Eur. Saf. Reliab. Conf., 2017.

[56] International Civil Aviation Organization (ICAO), *Safety Report 2014*, Montreal, Canada, 2014. Available: http://www.icao.int/safety/Documents/ICAO_2014 Safety Report_final_02042014_web.pdf. [Accessed February 16, 2016].

[57] D. Bateman, “A Review of Some Technological Aids to Support - The Flight Safety Foundation Runway Safety Initiative (RSI),” In Proc. 61st Annu. IASS, 2008. Available: https://asasi.org/papers/2007/The_Evolution_of_Flight_Data_Analysis_Neil_Campbell.pdf. [Accessed May 14, 2016].

[58] G. van Es, *A Study of Runway Excursions From a European Perspective*, 2010. [Online]. Available: https://skybrary.aero/bookshelf/books/2069.pdf. [Accessed February 16, 2016].

[59] M. Menestrot, “Landing Risk Reduction,” In Proc. Third Meet. Asia Pacific Reg. Aviat. Saf. Team, 2013. Available: https://www.icao.int/APAC/Meetings/2013_APRAST3/6.Landing Risk Reduction[Airbus].pdf. [Accessed September 10, 2016].

[60] J.N.M. van Eekeren, *Estimated Cost–Benefit analysis of runway severity reduction based on actual arrestments*, Nendaz, Switzerland: Safe-Runway GmbH, 2016.

[61] I.D.L. Kirkland, “The risk assessment of aircraft runway overrun accidents and incidents,” Dissertation (Loughborough University), Loughborough, UK, 2001. Available: https://dspace.lboro.ac.uk/dspace-jspui/bitstream/2134/13270/1/Thesis-2001-Kirkland.pdf. [Accessed August 9, 2016].

[62] M. Jenkins, R.F. Aaron, “Reducing Runway Landing Overruns,” *Aero*, vol. Q3 2012, pp. 15–19, 2012. Available: http://www.boeing.com/commercial/aeromagazine/articles/2012_q3/3/. [Accessed May 14, 2016].

[63] K. Zwirglmaier, D. Straub, L. Drees, F. Holzapfel, “Reliability analysis for runway overrun using subset simulation,” In Proc. Eur. Saf. Reliab. Conf., 2014.

[64] Transportation Safety Board of Canada, *Aviation Investigation Report Air France Airbus A340-313 F-GLZQ Toronto, Ontario*. Gatineau, Canada: 2007. Available: http://www.tsb.gc.ca/eng/rapports-reports/aviation/2005/a05h0002/a05h0002.pdf. [Accessed April 3, 2016].

[65] J. Gerthoffert, C. Grosjean, V. Cerezo, M. Do, “Modelling of Aircraft Braking Coefficient from IMAG Friction Measurements,” In Proc. Airports in Urban Networks (AUN), 2014. Available: https://www.stac.aviation-civile.gouv.fr/sites/default/files/stac/manifestation/tra2014/presentations/8-aircraft_breaking.pdf.

[Accessed March 17, 2016].

[66] Flight Safety Foundation (FSF), "FSF ALAR Briefing Note 8.5 - Wet or Contaminated Runways," *Flight Safety Digest*, issue 08-11, pp. 179–184, 2000. Available: https://flightsafety.org/files/alar_bn8-5-wetrwy.pdf. [Accessed August 9, 2016].

[67] T. Leland, G. Taylor, *An investigation of the influence of aircraft tire-tread wear on wet-runway braking*, Washington D.C., USA: National Aeronautics and Space Administration (NASA), 1965.

[68] * Airbus Industries, *A320 Flight Crew Operations Manual (FCOM)*, Toulouse, France: Airbus Industries, 2000.

[69] International Civil Aviation Organization (ICAO), *Airport Services Manual Part 2*, Montréal, Canada, 2002.

[70] N.S. Currey, *Aircraft Landing Gear Design: Principles and Practices*, Washington D.C., USA: American Institute of Aeronautics and Astronautics, Inc., 1988.

[71] Airbus Industries, *Takeoff Safety Training Aid (Appendix)*. Toulouse, France: Airbus Flight Operations Support & Services, 2005.

[72] * Lufthansa Systems LIDO, *Lido Route Manual - Frankfurt/Main AOI Chart 1-10*, Frankfurt, Germany, 2016.

[73] Flight Safety Foundation (FSF), "ALAR Toolkit - FSF ALAR Briefing Note 8.7 - Crosswind Landings," *Flight Safety Digest*, issue 8–11, pp. 189–196, 2000. Available: https://skybrary.aero/bookshelf/books/871.pdf. [Accessed May 15, 2017].

[74] European Organisation for the Safety of Air Navigation (Eurocontrol), "BADA," 2018. [Online]. Available: https://www.eurocontrol.int/eec/public/standard_page/ETN_2009_1_BADA.html. [Accessed August 4, 2018].

[75] * T. Drasky, "Vorstellung und prototypische Umsetzung einer Methode zur Quantifizierung von Unfallwahrscheinlichkeiten im Flugbetrieb einer Fluggesellschaft," Unpublished Master Thesis (Technische Universität München TUM), Munich, Germany, 2010.

[76] Federal Aviation Administration (FAA), *Takeoff Safety Training Aid*. Washington D.C., USA: U.S. Department of Transportation, 1994.

[77] * Lufthansa Systems LIDO, *Lido Route Manual - Moscow Vnukovo ILS DME 01 Chart 7-10*, Frankfurt, Germany, 2017.

[78] T.J. Yager, W.A. Vogler, P. Baldasare, *Evaluation of Two Transport Aircraft and Several Ground Test Vehicle Friction Measurements Obtained for Various Runway Surface Types and Conditions*, Hampton, VA, USA: NASA Langley Research Center, 1990.

[79] T.J. Yager, "How Best to Determine Runway / Highway Pavement Surface Friction Performance," In Proc. 10th ALACPA Airpt. Pavement Semin., 2013. Available: https://www.icao.int/NACC/Documents/Meetings/2013/ALACPA10/ALACPA10-P22.pdf. [Accessed March 31, 2016].

[80] C. Zhang, "Improving Airport Runway Braking Analysis through Innovative Modeling," Master Thesis (University of Waterloo), Waterloo, Ontario, Canada, 2014.

[81] W.L. Martinez, A.R. Martinez, *Computational Statistics Handbook With Matlab*, 3rd ed., Chapman and Hall/CRC, 2002.

[82] Matlab, *Statistics and Machine Learning Toolbox*, Natick, MA, USA: MathWorks, Inc., 2015.

[83] P. Friederichs, "An Introduction to Extreme Value Theory Applications of EVT," In Proc. COPS Summer Sch., 2007.

[84] European Organisation for the Safety of Air Navigation (Eurocontrol), *ACAS Guide*, Brussels,

Belgium, 2016.

[85] L. Weigang, A. de Barros, I.R. de Oliveira, *Computational Models, Software Engineering, and Advanced Technologies in Air Transportation*, Hershey, PA, USA: IGI Global, 2010.

[86] J.K. Kuchar, A.C. Drumm, “The traffic alert and collision avoidance system,” *Lincoln Laboratory Journal*, vol. 16, issue 2, pp. 277–296, 2007. Available: https://pdfs.semanticscholar.org/c35e/0023e8c2ae4e14a8aed2c996f21ffcbcbaf9.pdf. [Accessed April 8, 2016].

[87] B. Raynaud, T. Arino, *Final report on the safety of ACAS II in the European RVSM environment*. Brussels, Belgium: European Organisation for the Safety of Air Navigation (Eurocontrol), 2006. Available: https://www.eurocontrol.int/sites/default/files/content/documents/nm/safety/ACAS/acas-finalreportonthesafetyofscasiiintheeuropeanrvsmenvironmentv1.1-2006.pdf. [Accessed February 19, 2016].

[88] Flight Safety Foundation (FSF) Editorial Staff, “Bracing the Last Line of Defense Against Midair Collisions,” *Flight Safety Digest*, vol. 23, issue 3, pp. 1–28, 2004. Available: https://flightsafety.org/fsd/fsd_mar04.pdf. [Accessed April 21, 2017].

[89] P.B. Ladkin, “Causal Analysis of the ACAS/TCAS Sociotechnical System,” In Proc. 9th Aust. Work. Saf. Relat. Program. Syst., 2004., pp. 3–12 Available: http://dl.acm.org/citation.cfm?id=1082339. [Accessed April 22, 2017].90] Bundesstelle für Flugunfalluntersuchung (BFU), *Investigation Report AX001-1-2/02 Ueberlingen*, Braunschweig, Germany, 2004. Available: https://www.bfu-web.de/EN/Publications/Investigation Report/2002/Report_02_AX001-1-2_Ueberlingen_Report.pdf?__blob=publicationFile. [Accessed January 29, 2017].

[91] L.P. Espindle, J.D. Griffith, J.K. Kuchar, *Safety Analysis of Upgrading to TCAS Version 7.1 Using the 2008 U.S. Correlated Encounter Model*. Washington D.C., USA: Federal Aviation Administration (FAA), 2009. Available: http://citeseerx.ist.psu.edu/viewdoc/download?doi=10.1.1.435.404&rep=rep1&type=pdf. [Accessed April 13, 2016].

[92] European Organisation for the Safety of Air Navigation (Eurocontrol), *European ACAS Operational Monitoring 2003 Report*, Brussels, Belgium, 2005.

[93] M.J. Kochenderfer, J.P. Chryssanthacopoulos, L.P. Kaelbling, T. Lozano-Perez, *Model-Based Optimization of Airborne Collision Avoidance Logic*. Washington D.C., USA: Federal Aviation Administration (FAA), 2010. Available: http://citeseerx.ist.psu.edu/viewdoc/download?doi=10.1.1.1034.6366&rep=rep1&type=pdf. [Accessed May 13, 2016].

[94] H. Tomita, “Accident investigation into a near mid-air collision,” In Proc. ASASI Reg. Semin., 2005. Available: https://www.asasi.org/papers/2005/Hiroaki Tomita - near collision in Japan.pdf. [Accessed November 10, 2016].

[95] European Organization for Civil Aviation Equipment (EUROCAE), *TCAS II Collision Avoidance System (CAS) Requirements Specification Volume II*, Malakoff, France: European Organization for Civil Aviation Equipment (EUROCAE), 2008.

[96] C. Livadas, J. Lygeros, N.A. Lynch, “High-Level Modeling and Analysis of TCAS,” In Proc. 20th IEEE Real-Time Syst. Symp., 1999., pp. 115–125.

[97] F. Netjasov, A. Vidosavljevic, V. Tosic, H. Blom, “Systematic Validation of a Mathematical Model of ACAS Operations for Safety Assessment Purposes,” In Proc. Ninth USA/Europe Air Traffic Manag. Res. Dev. Semin., 2011., pp. 1–12.

[98] F. Netjasov, “Risk Analysis and Safety Assessment of Air Traffic Control System,” Dissertation (University of Belgrade), Belgrade, Serbia, 2010.

[99] C. Munoz, A. Narkawicz, J. Chamberlain, “A TCAS-II Resolution Advisory Detection Algorithm,” *AIAA Guidance, Navigation, and Control (GNC) Conference*, 2013. Available: http://arc.aiaa.org/doi/abs/10.2514/6.2013-4622. [Accessed April 8, 2016].

[100] International Civil Aviation Organization (ICAO), *Doc 9863, Airborne Collision Avoidance System (ACAS) Manual*, Montréal, Canada, 2006. Available: https://www.icao.int/Meetings/anconf12/Document Archive/9863_cons_en.pdf. [Accessed April 13, 2016].

[101] J.E. Olszta, W.A. Olson, “Characterization and Analysis of Traffic Alert and Collision Avoidance Resolution Advisories Resulting from 500’ and 1,000’ Vertical Separation,” *Ninth USA/Europe Air Traffic Management Research and Development Seminar (ATM2011)*, 2011.

[102] S. Chabert, H. Drévillon, T. Arino, *Decision criteria for regulatory measures on TCAS II version 7.1 - Safety Issue Rectification Extension Plus Project (SIRE+ Project)*. Brussels, Belgium: European Organisation for the Safety of Air Navigation (Eurocontrol), 2008. Available: https://www.eurocontrol.int/sites/default/files/content/documents/nm/safety/ACAS/safety-acas-sire-decision-criteria-for-regulatory-measures-on-tcas-v-7.1-20080725.pdf. [Accessed April 8, 2016].

[103] International Civil Aviation Organization (ICAO), *Doc 9863, Airborne Collision Avoidance System (ACAS) Manual*, Montréal, Canada, 2012.

[104] C. Aveneau, “Outcomes of ACAS / RVSM operational data analysis,” In Proc. ACAS Saf. Anal. Post-RVSM Proj. Semin., 2006.

[105] * T. Arino (Skill Unit Director System Definition & Performance Egis Avia). “WG: Pilot response model” Personal email (June 11, 2017).

[106] S. Chabert, T. Arino, *Collision risk due to TCAS safety issues - Investigation and analysis of TCAS II safety issues in the European airspace*. Brussels, Belgium: European Organisation for the Safety of Air Navigation (Eurocontrol), 2010. Available: https://www.eurocontrol.int/sites/default/files/content/documents/nm/safety/ACAS/safety-acas-collision-risk-due-to-tcas-safety-issues-20100510.pdf. [Accessed April 8, 2016].

[107] National Transportation Safety Board (NTSB), *Aircraft Accident Report Pacific Southwest Airlines B-727 and Cessna 172 San Diego, California*. Washington D.C., USA: 1979. Available: https://www.ntsb.gov/investigations/AccidentReports/Reports/AAR7905.pdf. [Accessed June 30, 2017].

[108] Centro de Investigação e Prevenção de Acidentes Aeronáuticos (CENIPA), *Final Report A-00X/CENIPA/2008*, Brasília, Brazil, 2008. Available: https://reports.aviation-safety.net/2006/20060929-0_B738_PR-GTD.pdf. [Accessed June 30, 2017].

[109] The MITRE Corporation, *System Safety Study of Minimum TCAS II*, McLean, VA, USA, 1983. Available: https://apps.dtic.mil/dtic/tr/fulltext/u2/a138674.pdf. [Accessed December 18, 2017].

[110] J. Kuchar, *White Paper on SA01 Near Mid-Air Collision Risk Modeling*. Lexington, MA, USA: Lincoln Laboratory (MIT), 2008. Available: http://hub.easa.europa.eu/crt/docs/viewcrdattachment/cid_41243/aid_463/fmd_d1b0040c50899175938dfa38daf01c79. [Accessed April 8, 2016].

[111] M. Kochenderfer, J. Kuchar, L. Espindle, J. Griffith, “Uncorrelated Encounter Model of the National Airspace System, Version 1.0,” 2008. Available: https://www.ll.mit.edu/sites/default/files/publication/doc/2018-12/Kochenderfer_2008_ATC-345_WW-18178.pdf. [Accessed April 13, 2016].

[112] M.D. Byrne, “How many times should a stochastic model be run? An approach based on confidence intervals,” *Proceedings of the 12th International Conference on Cognitive Modeling*, pp. 445–450, 2013.

[113] S.-K. Au, Y. Wang, *Engineering Risk Assessment with Subset Simulation*, Hoboken, NJ, USA: Wiley-Blackwell, 2014.

[114] R.L. Frantz, “Turbulence Injury Reduction - A Systems Approach,” In Proc. Fed. Aviat. Adm. Int. Fire Cabin Saf. Res. Conf., 1998. Available: https://www.fire.tc.faa.gov/1998Conference/presentations/RobertFrantz.pdf. [Accessed May 8, 2016].

[115] Boeing Commercial Airplanes, *Turbulence Education and Training Aid*, Seattle, WA, USA, 1998.

[116] Australian Transport Safety Bureau, *Staying safe against in-flight turbulence*. 2014. Available: https://www.atsb.gov.au/media/4718845/AR-2008-034 Turbulence FactSheet_v2.pdf. [Accessed August 5, 2016].

[117] R. Sharman, T. Lane, *Aviation Turbulence*, Basel, Switzerland: Springer International Publishing Switzerland, 2016.

[118] Flight Safety Foundation (FSF), “Strategies Target Turbulence-related Injuries To Flight Attendants and Passengers,” *FSF Cabin Crew Safety*, vol. 36, issue 1, pp. 1–11, 2001.

[119] R.L. Bowles, B.K. Buck, *A Methodology for Determining Statistical Performance Compliance for Airborne Doppler Radar with Forward-Looking Turbulence Detection Capability*, Hampton, VA, USA: National Aeronautics and Space Administration (NASA), 2009.

[120] E.C. Stewart, *Turbulence Hazard Metric Based on Peak Accelerations for Jetliner Passengers*, Hampton, VA, USA: National Aeronautics and Space Administration (NASA), 2005.

[121] * Lufthansa, *Unfalluntersuchungsbericht Einflug in extreme Turbulenz über Missouri , USA*. Frankfurt, Germany: Flight Safety Department, 2003.

[122] Bundesstelle für Flugunfalluntersuchung (BFU), *Jahresbericht 2003*, Braunschweig, Germany, 2003. Available: https://www.bfu-web.de/DE/Publikationen/Flugsicherheitsinformationen/Berichte/V164 - BFU Jahresbericht 2003.pdf?__blob=publicationFile. [Accessed January 14, 2018].

[123] * M. Butter, *Risk Assessment Takeoff Distance SJO (A340-300) Extreme Value Analysis Risk Assessment Takeoff Distance SJO (A340-300)*, Flight Safety Department, Frankfurt, Germany, 2018.

[124] Skybrary, “European Commercial Aviation Safety Team (ECAST),” *International Business Publications, USA*, 2016. [Online]. Available: https://www.skybrary.aero/index.php/European_Commercial_Aviation_Safety_Team_(ECAST). [Accessed January 16, 2018].

[125] European Organisation for the Safety of Air Navigation (Eurocontrol), *User Manual for the Base of Aircraft Data (BADA)*, Brussels, Belgium, 2004. Available: https://www.eurocontrol.int/eec/gallery/content/public/document/eec/report/2004/022_BADA_User_Manual.pdf. [Accessed July 8, 2018].

[126] European Organisation for the Safety of Air Navigation (Eurocontrol), *Base of Aircraft Data (BADA) Aircraft Performance Modelling Report*, Brussels, Belgium, 2009. Available: https://www.eurocontrol.int/sites/default/files/field_tabs/content/documents/sesar/bada-aircraft-performance-modelling.pdf. [Accessed January 18, 2017].